



The
University
Of
Sheffield.

**Bacterial-neuronal interaction: investigations into the
potential mechanisms of dental pain.**

By:

Aunwaya Kaewpitak

A thesis submitted in partial fulfilment of the requirements for the degree of
Doctor of Philosophy

The University of Sheffield
Faculty of Medicine, Dentistry and Health
School of Clinical Dentistry

June 2016

Acknowledgements

First of all I would like to express my deepest gratitude to both of my supervisors for giving me the great opportunity to do a PhD in this school. For my primary supervisor, Professor Charles William Ian Douglas, I am heartily thankful for his huge patience, unwavering support, excellent mentorship and his understanding overseas students like myself. Secondly, I would like to extend my appreciation to my second supervisor, Professor Fiona Boissonade for her useful suggestions and kind support that enable me to develop an understanding of the subject of my PhD study. I was fortunate to be their student, where I learnt a lot from them.

I would like to deeply thank Dr Elizabeth Seward for allowing me to use the calcium imaging microscope in the department of Biomedical Science. I am indebted to Dr Claudia Bauer who helped, taught and gave me a hand when I didn't know how to deal with an experiment. I also wish to say a big thank you to the neuroscience group members for their help with techniques in the lab. Thank you to Professor Mike Cutis, Dr Rangarajan, and Dr Potempa for their gift of Rgp and Kgp that made Chapter 6 possible for this thesis.

On a personal note, I would like to say thank you to a number of Thai students who have shared their love and support throughout my study in Sheffield. Special thanks to Supakchai Ponglertsukul who kept me sane during the past three years and for his moral support. Lastly, I thank the Faculty of Dentistry, Prince of Songkla University for giving me the opportunity to study abroad, and the Royal Thai government for the funding throughout my study in the UK.

Finally, I wish to thank my father who cultivated me to love maths, science and logical thinking, even if he cannot see me graduate. This thesis is dedicated to my mother for her mental strength that literally saves me from any difficulty. I could not have achieved this without her positive force throughout my life.

Abstract

Dental inflammatory pain is mainly caused by bacterial infection. Although the culprit bacteria vary from case-to-case, at least one species of black-pigmented, anaerobic bacteria is usually present. *Porphyromonas gingivalis* is one such species and which is known to possess a number of virulence factors that can contribute to the inflammatory process. However, the mechanisms involved in the pathogenesis of pain during bacterial infection of the dental pulp remain unclear. Therefore, using a trigeminal ganglion (TG) culture system as a model of bacterial infection provides the opportunity to analyse the effects of bacterial components on sensory neurones and the help identify the cellular receptors that could mediate pain.

The aim of these studies was to utilise mouse TG cultures to investigate the direct effects of *P. gingivalis* cells and two of its well-known virulence factors (lipopolysaccharide and gingipain proteases) in activation of neuronal responses.

Our findings provide the first evidence that *P. gingivalis*, LPS and gingipains can elicit a rapid excitatory response in sensory neurones. These effects appear to be mediated through Toll-like receptors (TLRs), transient receptor potential channels (TRPs), and protease-activated receptors (PARs). These responses were accompanied by an elevated release of the neuropeptide calcitonin-gene related peptide (CGRP) and NF- κ B nuclear translocation, both of which are known to regulate a range of pro-inflammatory effects.

Here, we also demonstrate for the first time that neuronal supporting cells are also sensitive to *P. gingivalis* and its components. This provides a further mechanism by which *P. gingivalis* and other Gram-negative pathogens may manipulate trigeminal sensory neurones and contribute to acute and chronic inflammatory pain.

In the light of these investigations, we lend weight to the argument that the neurones are being acted upon directly by the bacteria as well as by local host inflammatory mediators. Moreover, since TRPA1, TLR4, and PAR2 are involved in response to bacterial stimuli, these receptors could be potential targets for the control of dental inflammatory pain.

Abbreviations

ANOVA	Analysis of variance
ATP	Adenosine Tri-Phosphate
BSA	Bovine Serum Albumin
CA	Cinnamaldehyde
CAP	Capsaicin
CGRP	Calcitonin Gene-Related Peptide
DAPI	4',6-Diamidino-2-Phenylindole, Dihydrochloride
DIV	Day <i>In Vitro</i>
dH₂O	Distilled water
DMEM	Dulbecco's Modified Eagle Medium
DMSO	Dimethyl Sulphoxide
DNA	Deoxyribonucleic acid
EDTA	Ethylenediaminetetraacetic acid
ELISA	Enzyme linked immunosorbent assay
ERK	Extracellular signal regulated kinases
FBS	Foetal bovine serum
FITC	Fluorescein isothiocyanate
<i>g</i>	Acceleration of gravity
GFAP	Glial Fibrillary Acidic Protein
GJ	Gap junction
GPCR	G protein-coupled receptor
GS	Glutamine synthetase
H₂O₂	Hydrogen peroxide

HBSS	Hanks' balanced salt solution
HCl	Hydrochloric acid
HRP	Horseradish peroxidase
ICW	Intracellular calcium wave
IHC	Immunohistochemistry
IL	Interleukin
KCl	Potassium Chloride
kDa	Kilo-Daltons
Kgp	Lys-gingipain
LPS	Lipopolysaccharide
LDCV	Large Dense-Core Vesicle
MAb	Monoclonal antibody
MAPK	Mitogen-Activated Protein Kinase
mL	Milliliter
mm	Millimeter
MMP	Matrix metalloproteinase
NF-κB	Nuclear factor-Kappa light chain enhancer of activated B cells
ng	Nanogram
NGF	Nerve growth factor
<i>p</i>	<i>p</i> -value
PAMP	Pathogen-associated molecular pattern
PAR	Protease-activated receptor
PBS	Phosphate-buffered saline
PBT	Triton-X 100 in phosphate-buffered saline

PDL	Poly-D-Lysine hydrobromide
PFA	Paraformaldehyde
PH	Pleckstrin Homology
PI3-K	Phosphatidylinositol 3-kinase
PIP3	Phosphatidylinositol (3,4,5)-triphosphate
PKC	Protein kinase C
PLC	Phospholipase C
PNS	Peripheral nervous system
PRR	Pattern Recognition Receptor
Rgp	Arg-gingipain
RIPA buffer	Radioimmunoprecipitation assay buffer
RNA	Ribonucleic acid
rpm	Round per minute
ROI	Region of Interest
SDS-PAGE	Sodium dodecyl sulphate polyacrylamide gel electrophoresis
SGC	Satellite glial cell
SP	Substance P
TBST	Tris Buffered Saline with Tween® 20
TEMED	N,N,N',N'-Tetramethylethylene-1,2-diamine
TG	Trigeminal ganglia
TLR	Toll-like receptor
TNF	Tumor necrosis factor
Tris	Tris[hydroxymethyl]-aminomethane
TRP	Transient receptor potential channel

WT

Wild-type

Table of Contents

Acknowledgement	i
Abstract	ii
Abbreviations	iii
Table of Contents	vii
Figures index	xiii
Tables index	xvii
Chapter 1. Introduction	1
1.1 Pathophysiology of pulpodental infection	3
1.1.1 Dental pain pathway	3
1.1.2 Bacteriology of dental pulp infection	5
1.1.3 Symptomatic infection	9
1.2 Virulence factors of oral pathogenic bacteria	11
1.2.1 Gram negative oral pathogen	11
1.2.2 <i>Porphyromonas gingivalis</i>	12
1.2.3 Modification of <i>P. gingivalis</i> virulence factors – Role of Iron	17
1.3 Molecular basis of signal detection of inflammatory pain	19
1.3.1 Toll-like receptors (TLRs)	21
1.3.2 Transient receptor potential (TRPs)	23
1.3.3 Protein-activated receptors (PARs)	26
1.3.4 Interaction between PARs, TLRs, and TRPs	29
1.4 Consequences of sensory nerve response to inflammatory bacterial infection	33
1.4.1 Axonal reflexes	34
1.4.2 NF- κ B pathway	35
1.5 Roles of non-neuronal cells in responses to bacterial toxins	37
1.5.1 Intercellular calcium wave (ICW)	37
1.5.2 Bidirectional communication via paracrine functions	38
1.6 Methods used to study inflammatory pain	41
1.6.1 Inflammatory pain models	41
1.7 Summary	44
1.8 Hypotheses, aims and objectives	44
1.8.1 Hypothesis	44
1.8.2 Thesis aims	45
1.8.3 Objectives	45

Chapter 2. Materials and Methods	47
2.1 Materials	49
2.1.1 Chemicals	49
2.1.2 Reaction systems	51
2.1.3 Expendable materials	51
2.1.4 Buffer and solution formulae	51
2.2 Primary trigeminal ganglia culture	54
2.2.1 Animals and animal housing	54
2.2.2 Animal preparation and dissection	54
2.2.3 Coverslip preparation	55
2.2.4 TG culture	55
2.3 Bacterial culture	56
2.4 LPS extraction method	56
2.5 LPS analysis	57
2.5.1 Quantitative analysis; KDO assay	57
2.5.2 Qualitative analysis; LPS gel	57
2.5.3 Biological analysis	58
2.6 Determination of proteolytic activity using chromogenic substrates	59
2.6.1 N- α -benzoyl DL-arginine-p-nitroanilide (BAPNA)	59
2.6.2 N-(p-Tosyl)-Gly-Pro-Lys-4-nitroanilide acetate salt (GPK-NA)	59
2.7 Intracellular calcium measurements	60
2.7.1 Microscopic set up and imaging acquisition	61
2.7.2 Loading of cells with various dyes	64
2.7.3 Sequences of the treatment in calcium records	69
2.7.4 Calcium imaging analysis	69
2.8 Cultured TG stimulation protocols	71
2.9 Reagent blockers	71
2.10 Immunohistochemistry analysis	72
2.11 Immunohistochemistry imaging analysis	74
2.11.1 Cellular surface expression	74
2.11.2 PAR2 expression	75
2.11.3 Assessment of NF- κ B translocation	76
2.12 CGRP ELISA and the protocol development	78
2.13 Total protein analysis	79
2.14 Statistic analysis	79

<u>Chapter 3. Establishing optimal culture system from trigeminal ganglia</u>	81
3.1 Introduction	83
3.2 Conventional protocol for neuronal culture	85
3.2.1 Methods	85
3.2.2 Results	85
3.3 Neuronal cell purification	89
3.3.1 Methods (1): Continual feeding with antimitotic treatment	89
3.3.2 Methods (2): Single high dose	90
3.3.3 Methods (3): Differential centrifugation to separate the cells by size	90
3.3.4 Results	91
3.4 Characterisation of short-term TG cultures	96
3.4.1 Methods	96
3.4.2 Results	96
3.5 Discussion	99
3.5.1 Characterisation of trigeminal cell culture	99
3.5.2 Applications and limitations of the study	100
3.5.3 Conclusion	101
<u>Chapter 4. <i>P. gingivalis</i> infection and environmental cues in trigeminal cells</u>	103
4.1 Introduction	105
4.2 Results	107
4.2.1. <i>P. gingivalis</i> W50 activation of the calcium influx in TG neurones	107
4.2.2. Activation of CGRP release from neurone cultures by <i>P. gingivalis</i> W50	107
4.2.3. <i>P. gingivalis</i> induces NF- κ B nuclear translocation	110
4.2.4. Effect of haemin level on neuronal cell release of CGRP	112
4.3 Discussion	113
4.3.1 Overview	113
4.3.2. <i>P. gingivalis</i> strategies to manipulate host responses	115
4.3.3. Control of peripheral sensitisation by integration of environmental cues	116
4.3.4. Trigeminal neuronal supporting cell	117
4.3.5 Limitation, and future prospects	118

4.4 Conclusion	119
----------------	-----

Chapter 5. Possible role of TLRs, and TRPs in generation of pain

<u>associated with dental infection</u>	121
5.1 Introduction	123
5.2 Results	125
5.2.1 Expression of TLRs, TRPs in TG cultured cells	125
5.2.2 Functional characterisation of TG cells in response LPS	132
5.2.3 Consequent effects of LPS on TG neurones: CGRP release	143
5.2.3 Consequent effects of LPS on TG neurones: NF- κ B translocation	145
5.3 Discussions	150
5.3.1 Overview	150
5.3.2 Expression of potential LPS-interacting receptors in TG neurone cultures	152
5.3.3 Functional response of TG neurones to LPS	154
5.3.4 Limitations and future prospects	161
5.3.5 Clinical relevance	162
5.4 Conclusion	162

Chapter 6. Possible role of PARs in generation of pain associated with

<u>dental infection</u>	163
6.1 Introduction	165
6.2 Results	167
6.2.1 Presence of PAR2 in TG cultured cells	167
6.2.2 The reduction of PARs expression following gingipain exposures	167
6.2.3 Effect of proteolytic enzymes on the functional responses of TG cells	169
6.2.4 Rgp, and Kgp caused significantly release of CGRP	172
6.2.5 The ability of <i>P. gingivalis</i> gingipain mutant to stimulate CGRP release	173
6.2.6 The reduction of CGRP against Rgp and Kgp	174
6.3 Discussions	175
6.3.1 Overview	175
6.3.2 Both Rgp and Kgp could cleave PAR2	176
6.3.3 Possible neuronal PAR2 mechanisms	178

6.3.4	Consequences of neuronal activation following exposure to gingipains	180
6.3.5	Limitations and future prospects	181
6.3.6	Clinical relevance	182
6.4	Conclusion	182

Chapter 7. Neuronal-glia behaviour in response to sensory nerve activation 183

7.1	Introduction	185
7.2	Results	187
7.2.1	Characteristics of non-neuronal cells in TG	187
7.2.2	Non-neuronal cells respond to whole <i>P. gingivalis</i> W50 cells	191
7.2.3	Non-neuronal cells respond to <i>P. gingivalis</i> LPS	192
7.2.4	Non-neuronal cells respond to gingipains	195
7.2.5	Minocycline reduced the release of CGRP in response <i>P. gingivalis</i> , and its constituents	196
7.2.6	Minocycline inhibited the nuclear translocation of NF- κ B in both neurones and non-neuronal cells in response to <i>P. gingivalis</i>	198
7.3	Discussion	201
7.3.1	Overview	201
7.3.2	Characteristics of TG non-neuronal cell <i>in vitro</i>	202
7.3.3	Different patterns of neuro-glia interaction responded to LPS and gingipain exposures	203
7.3.4	Mechanisms of minocycline	205
7.3.5	Possible roles of non-neuronal cell in PNS	206
7.3.6	Limitation and future prospects	207
7.3.7	Clinical relevance	207
7.4	Conclusion	207

Chapter 8. General discussion 209

8.1	Rationale for study	211
8.2	The empirical findings and theoretical implication	214
8.2.1	Synergistic effects of LPS and gingipains	214
8.2.2	environmental cues control neuronal changes	216
8.2.2	Neuronal-glia interaction	217
8.3	Limitations of the study	218

8.3.1 Primary TG culture	218
8.3.2 Bacteria aspects	221
8.4 Future investigations arising from studies in this thesis	224
Bibliography	225

Figures index

Figure 1.1	Pulpal nerve plexus in the pulp and the location in the dentinal tubule.	3
Figure 1.2	Anatomy of dental pain pathway.	4
Figure 1.3	Relative abundance and diversity of bacterial detected in pulpal infection.	6
Figure 1.4	Stages of dental carious lesion and dental pulp infection.	8
Figure 1.5	The structure of LPS.	13
Figure 1.6	<i>P. gingivalis</i> virulence factors.	16
Figure 1.7	The heterogeneity of lipid A that can be modified under different growth condition.	18
Figure 1.8	Inflammatory mediators and their specific receptors on sensory neurones.	19
Figure 1.9	The potential mechanisms that can stimulate peripheral sensitisation involving bacterial infection.	20
Figure 1.10	This figure shows the possible downstream pathways via TLR4 activations.	21
Figure 1.11	Thermo-sensory properties of transient receptor potential channels (TRPs).	23
Figure 1.12	TRPV1 activation pathways.	24
Figure 1.13	Mechanisms of activation of protease-activated receptors.	27
Figure 1.14	PAR2-stimulated pathways.	28
Figure 1.15	Intracellular mechanisms cross talk of TLRs and TRPV1 activation.	29
Figure 1.16	Common pathway of TLRs and PARs.	30
Figure 1.17	Cross-talk pathways for TRPV1 and PAR2.	31
Figure 1.18	Regulation of neuropeptide release by a variety of mechanisms.	33
Figure 1.19	This figure shows calcium wave scheme between neurones and SGCs in respond to peripheral noxious stimuli.	38
Figure 1.20	Paracrine function interaction of neurone and SGC forms bi-directional talk signalling in response to neuronal activation in sensory ganglia.	39
Figure 2.1	The location of trigeminal ganglia in mice.	54
Figure 2.2	Calcium dye detection mechanisms.	60
Figure 2.3	Overall scheme of calcium image system configuration.	63
Figure 2.4	Fura-2 AM dye loaded in trigeminal cultured cells.	64
Figure 2.5	The TG cells loaded with Fura-2AM at the basal and excited stages.	65
Figure 2.6	Fluo-4 AM loaded in cultured trigeminal cells.	66
Figure 2.7	Expression of calcium concentration in trigeminal cells loaded with Cal-520 AM.	67

Figure 2.8	The basal and activated stages of cultured trigeminal cells loaded with Cal-520 AM.	68
Figure 2.9	The timeframe to challenge cultured TG cells with various tested materials.	70
Figure 2.10	The principle of quantification of response to tested materials and TRPA1 and TRPV1 agonists.	70
Figure 2.11	The principle of quantification of interesting protein occupancy.	74
Figure 2.12	The principle of quantification of neuronal PAR2 expressions.	75
Figure 2.13	Analysis of immunelabelling of NF- κ B location.	76
Figure 2.14	Principle of quantification of NF- κ B translocation in TG neurones.	77
Figure 2.15	Principle of quantification of NF- κ B translocation in TG non-neuronal cells.	77
Figure 2.16	Competitive CGRP ELISA used in this study.	79
Figure 3.1	Day 1, 3 and 5 of conventional method of trigeminal cells cultures visualised under light microscope.	86
Figure 3.2	Day 1, 3, and 5 of convention method of trigeminal cells cultures visualised by immunofluorescence.	87
Figure 3.3	Day 5 of conventional method culture of trigeminal cell cultures visualised by immunofluorescence stained various protein markers.	87
Figure 3.4	The mixture of dissociated cells was gradient separated into 2 layers of Large and small cells.	90
Figure 3.5	Trigeminal cells from day 1 to day 10 in maintaining media supplemented with recommended dose of antimetabolic agents.	92
Figure 3.6	Graph shows the number of total cell count (stained by DAPI) of independent samples from day 1 to day 14.	93
Figure 3.7	Graph shows the number of neurones from independent sample from day 1 to day 14.	93
Figure 3.8	Day 7 of trigeminal cells treated by single high dose of antimetabolic agents visualised by immunofluorescence	94
Figure 3.9	Images showing presence of SGCs in close proximity to neurones.	95
Figure 3.10	Day 2 of trigeminal cultured using the conventional method but higher cell seeding	96
Figure 3.11	Confirmation of neuronal viability in culture by response to high potassium	97
Figure 3.12	Trigeminal cultured neurones express the intracellular CGRP.	98
Figure 3.13	Trigeminal cultured neurones express the intracellular SP.	98

Figure 4.1	Analysis of intracellular calcium levels in primary trigeminal neurones in response to live <i>P. gingivalis</i> and high concentration of potassium chloride.	108
Figure 4.2	CGRP levels in live <i>P. gingivalis</i> -, and capsaicin-stimulated TG neurones from control (n=6).	109
Figure 4.3	Photomicrographs of p65 NF- κ B nuclear translocation in live <i>P. gingivalis</i> -treated TG neurones and non-neuronal cells.	111
Figure 4.4	CGRP level in haemin modified <i>P. gingivalis</i> -stimulated TG neurones.	112
Figure 4.5	Overall TG responses in the exposure of live <i>P. gingivalis</i> .	114
Figure 4.6	<i>P. gingivalis</i> virulence factors.	114
Figure 5.1	The expression of TLR4 in TG culture.	127
Figure 5.2	The expression of TLR7 in TG culture.	128
Figure 5.3	The expression of CD14 on cells of TG culture.	129
Figure 5.4	The expression of TRPV1 on cells of TG culture.	130
Figure 5.5	The expression of TRPA1 on cells of TG culture.	131
Figure 5.6	LPS loaded in SDS-PAGE with silver staining.	132
Figure 5.7	The secretion of TNF- α to <i>P. gingivalis</i> and <i>E. coli</i> LPS.	133
Figure 5.8	<i>P. gingivalis</i> W50 LPS-induced calcium signals in TG neurones.	135
Figure 5.9	Analysis of intracellular calcium influx in primary TG cell cultures.	137
Figure 5.10	Analysis of intracellular calcium influx in primary TG cell cultures. In the presence of CLI-095	140
Figure 5.11	Analysis of intracellular calcium influx in primary TG cell cultures. In the presence of HC-030031	141
Figure 5.12	The effects of LPS and TRPA1 and TLR4 signalling.	142
Figure 5.13	CGRP levels in LPS-, and capsaicin-stimulated TG neurones.	143
Figure 5.14	CGRP levels in TG neurone cultures in response to LPS in the presence of specific agonist inhibitors	144
Figure 5.15	Photomicrographs of p65-NF- κ B nuclear translocation in <i>P. gingivalis</i> LPS-treated TG neurones and non-neuronal cell.	146
Figure 5.16	Photomicrographs of p65-NF- κ B nuclear translocation in <i>P. gingivalis</i> LPS-treated TG neurones and non-neuronal cell In the presence of TLR4, TRPA1, and TRPV1 signalling inhibitors.	147
Figure 5.17	Percentages of p65-NF- κ B nuclear translocation in <i>P. gingivalis</i> LPS-Treated TG neurones in the presence of TLR4, TRPA1, and TRPV1	

	Signalling inhibitors.	149
Figure 5.18	Summary of the finding from this chapter.	151
Figure 5.19	The mechanisms of CLI-095 and HC-030031.	157
Figure 5.20	Model of functional interactions in PAR2, TRPA1, and TRPV1.	158
Figure 5.21	Proposed model for LPS stimulation of TG neurones	160
Figure 6.1	The reduction of PAR2 in trigeminal cells after stimulation with Rgp, and Kgp.	168
Figure 6.2	Analysis of intracellular calcium in primary trigeminal cell culture – effects of trypsin.	170
Figure 6.3	Effects of Rgp on trigeminal cell response.	171
Figure 6.4	CGRP levels in Rgp, Kgp, and capsaicin-stimulated TG neurones from control	172
Figure 6.5	Release CGRP in response to various <i>P. gingivalis</i> strains	173
Figure 6.6	CGRP concentration plots in the present of Rgp, and Kgp against no treatment CGRP in various concentrations.	174
Figure 6.7	Functional domain of PAR2.	177
Figure 6.8	PAR2 could internally sensitise TRPV1.	179
Figure 7.1	Cross section of TG shows the close contact of neurones (green), and satellite glial cells (red).	186
Figure 7.2	Non-neuronal cell characterised by satellite glial cell marker, GFAP, colocalisation with β -tubulin III, and DAPI in early day of the cultures.	189
Figure 7.3	Satellite glial cells characterised by glutamine synthetase (GS), co-localised with β -tubulin III, and DAPI in later day of the cultures.	190
Figure 7.4	Graphs trace the transient changes in calcium in individual cells over time following LPS application of TG 2-day in vitro.	193
Figure 7.5	Identification of responding SGCs to LPS in culture.	194
Figure 7.6	Graphs trace the transient changes in calcium in individual cells over time following Rgp application of TG 3-day in vitro cultures.	195
Figure 7.7	Effects of <i>P. gingivalis</i> , LPS and arg-gingipains in the presence and absence of minocycline.	197
Figure 7.8	NF- κ B nuclear translocation of non-neuronal cells in TG cultures induced by whole <i>P. gingivalis</i> cells and the effects of minocycline.	199
Figure 7.9	NF- κ B nuclear translocation of non-neuronal cells in TG cultures induced by <i>P. gingivalis</i> LPS and the effects of minocycline.	200

Figure 8.1	Schematic of TG sensitisation by <i>P. gingivalis</i> arising from this thesis.	213
Figure 8.2	Summary of the response of a TG nerve ending following encounter with <i>P. gingivalis</i> LPS, and gingipains.	215
Figure 8.3	Approximate concentration of LPS calculated from average bacterial load found in infected teeth	221

Tables Index

Table 1.1	Summary of products and/or mechanisms that promote oral pathogenic bacteria virulence.	11
Table 1.2	Proteolytic system of <i>P. gingivalis</i> .	14
Table 1.3	Summary of PAR activating protease and localisation.	26
Table 1.4	TRPs activities following PAR-2 mediated effects.	32
Table 1.5	Summary of pulpal neuropeptides, receptors, and functions.	36
Table 2.1	The solution formula for calcium imaging buffer used during record.	51
Table 2.2	Fixative and buffer used for immunofluorescence in this study.	52
Table 2.3	Brain heart infusion broth solution used in this study.	53
Table 2.4	List of reagents used for ELISA in this study.	53
Table 2.5	Blocking reagents and the administrations used in this study.	71
Table 2.6	Details of all primary antibodies and relevant according secondary fluorescent labels employed in study.	73
Table 5.1	Percentages of neurones and non-neuronal cells that respond to <i>E. coli</i> LPS and <i>P. gingivalis</i> LPS.	138
Table 7.1	Percentages of neurones and non-neuronal cells that respond to <i>E. coli</i> LPS and <i>P. gingivalis</i> LPS	192



Chapter 1

Introduction



1. Introduction

The dentine-pulp complex is a unique environment that is composed of a variety of tissue structures, including collagen fibres, cellular processes, networks of blood vessels and neuronal plexus. This neurovascular network is key in the regulation of inflammation of the dental pulp (Kim 1990; Abd-Elmeguid and Yu 2009; Byers et al. 2003).

1.1 Pathophysiology of pulpodental infection

This section describes our current knowledge of the potential routes of interaction of microorganisms with the sensory nervous system.

1.1.1 Dental pain pathway

Bacterial infection is the most common cause of dental pain, normally following the development of a deep carious lesion or trauma (Figure 1.1). Bacteria can invade the odontoblast layer and penetrate through the dentinal tubules into pulpal tissue (Fouad 2011; Pääkkönen et al. 2009).

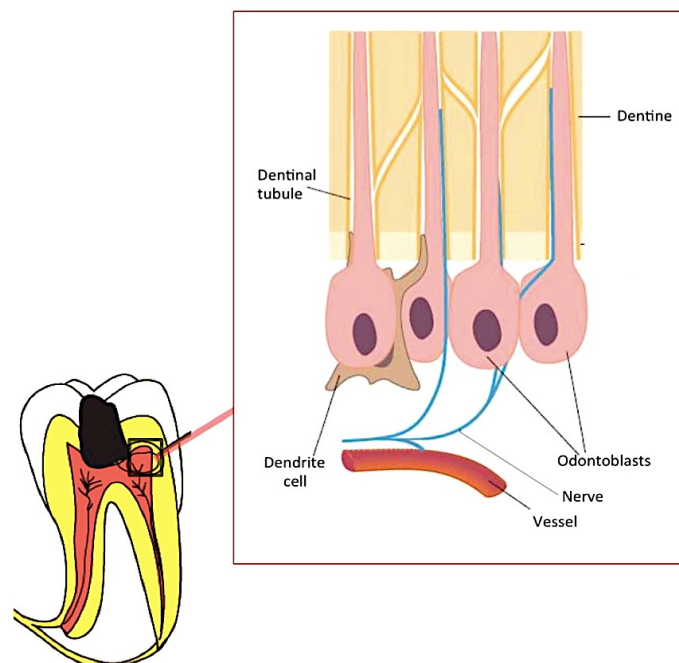


Figure 1.1 Pulpal nerve plexus in relation to the dentine.

This illustration shows the relationship between the various cellular components of the pulp and the dentine, i.e. odontoblasts, immune cells (dendrite cells), and sensory nerves that form the neurovascular complex.

Not surprisingly, the inflammatory orchestration is a highly complex process, but we can categorise the responses into 2 systems – the nervous system and the immune system (Austin and Gila 2010; Steinman 2004). This study focuses on the sensory nervous system involvement.

The pathology of dental pain and the associated pain pathway is depicted in Figure 1.2. When bacteria or their components interact with sensory nerve fibres, many inflammatory responses are triggered to eliminate the bacterial invader.

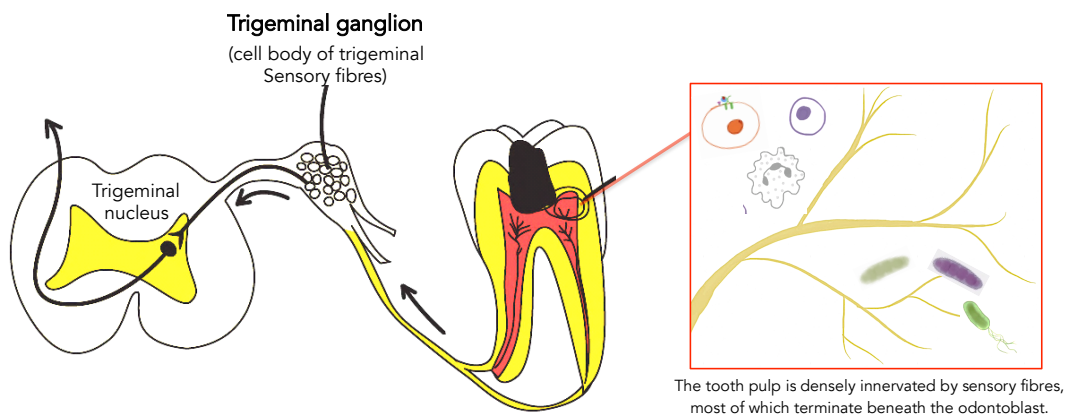


Figure 1.2 Anatomy of dental pain pathway.

Noxious information could be transduced by primary afferent nociceptors and the signal then conveyed to the dorsal horn of the trigeminal ganglia.

The peripheral nervous system plays a pivotal role in dental pain signalling, with the pulpal nerves converting any physical changes from noxious stimuli into biochemical and/or electrical signals. The signal is then transmitted to the neuronal cell bodies in trigeminal ganglia, and subsequently, it reaches the trigeminal which contains the second order neurones. Eventually, the signal reaches the higher brain for further signal encoding (Huang et al. 2006; Hahn and Liewehr 2007).

1.1.2 Bacteriology of dental pulp infection

Caries is the most common precursor of dental pulpal infection. The early stages of enamel demineralisation involve microbial production of organic acids by fermentation of carbohydrate. The major bacterial pathogens involved are commonly cited as the Gram-positive species, *Streptococcus mutans*, *Streptococcus sobrinus*, *Lactobacillus*, *Rothia dentocariosa* and *Actinomyces gerenseriae* species. However, more recent data (Nadkarni et al. 2010) indicate that a complex microbial community is present in an established carious lesion, including asaccharolytic, Gram-negative anaerobes that do not contribute directly to demineralisation, and that this population represents an imbalance of a community that is associated with sound enamel. Figure 1.3 shows the prevalence and diversity of pathogenic bacteria found in pulpal infection (Bergenholtz 1981). Moreover, more recent evidence of Sanghavi et al. in 2014 shows that the red complex bacteria are related to aetiology of symptomatic periradicular diseases. Taken together, this could sight into evidence that *P. gingivalis* is strongly associated with symptomatic pulpitis.

As caries develops through dentine the anaerobic bacteria can be “carried” down the dentinal tubules to reach the pulp by adhesion to other species (e.g. the streptococci) (Nishimura et al. 2004; Kansal et al. 2003; Nadkarni et al. 2010). Different bacterial species will dominate at different stages. Shifts in the composition of the microbiota are largely due to changes in environmental conditions, particularly with regards to oxygen tension and nutrient availability. Indeed, it is the anaerobic, proteolytic species that come to dominate in the protein-rich environment of the pulp.

The stages of bacterial infection can be classified by the degree of bacterial penetration (Figure 1.4) and the population of bacteria pathogen (Nadkarni et al. 2010; Hahn and Liewehr 2007; Bergenholtz 1981; Michaelson and Holland 2002).

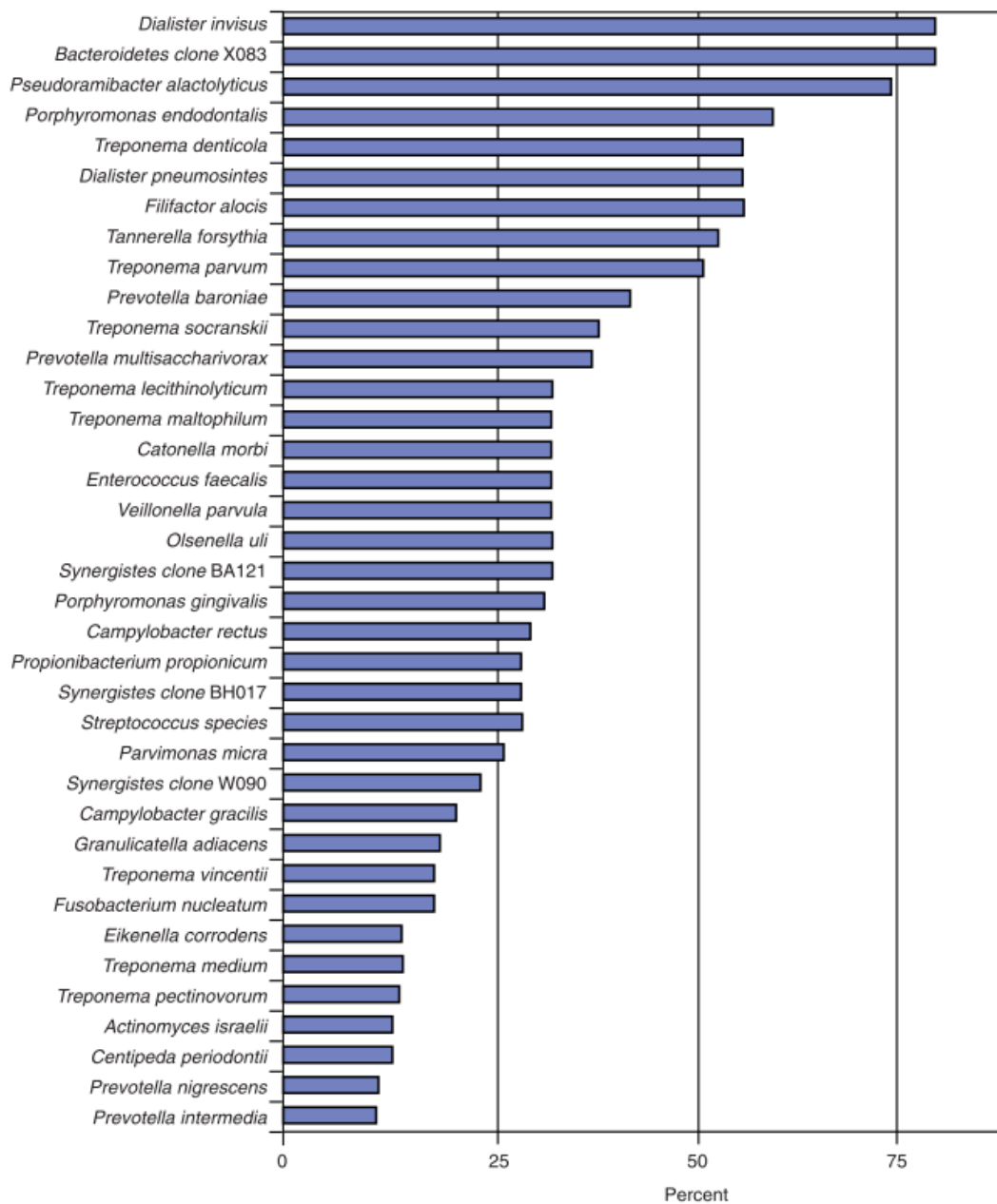


Figure 1.3 Relative abundance and diversity of bacterial detected in pulpal infection.

This figure shows diversity of oral bacteria in pulpal infection, as analysed by molecular microbiology methods (From Siqueira and Rôças 2011, permission granted to reproduce).

1.1.2.1 Limited stage

In the initial phases of the pulpal infectious (the limited stage), bacteria invade the odontoblast layer and penetrate deeply into pulpal tissue. The limited stage lesions show high densities and predominance of facultative bacteria such as α - and non-haemolytic streptococci and lactobacilli that are associated with a variety of tissue responses from undetectable to intense inflammatory reactions.

1.1.2.2 Established stage

The distinction between established and advanced phases of pulpal infection remain unclear, because clinical findings may not always correlate with histopathological reports (Nadkarni et al. 2010). The established stage is characterised by the presence of *Bacteroidetes*, *Fusobacteria*, *Lachnospiraceae*, and *Coriobacteriaceae* as the major microbial groups that invade the necrotic regions of the established stage.

1.1.2.3 Advanced stage

The advanced stage of infection is characterised by the presence of mixed anaerobic species, although *Coriobacteriaceae* and *Lachnospiraceae* are also among the major groups present. The so called "Red complex" bacteria, which includes *Tannarella forsythia*, *Porphyromonas gingivalis* and *Treponema denticola*, play an important role in root canal infection (Potempa et al. 2000), despite the fact that the name derives from studies of periodontal microbial communities (Socransky et al. 1998). The virulence factors of these pathogenic organisms include endotoxin release, cell surface toxic components and spreading factors, such as collagenase, hyaluronidase and other enzymes that are cytotoxic and can break down connective tissues (Kayaoglu and Ørstavik 2004).

1.1.2.4 End stage

In the end stage of inflammation, following a period of pulpal infection, oxygen is depleted within the root canal as a result of pulp necrosis and consumption by facultative bacteria. The necrotic tissue remains infected and becomes a reservoir for any infectious agent that may ultimately enter the periapical region. An interesting microorganism is *Enterococcus faecalis* that is frequently isolated from suppurative

pulp infections (Stuart et al. 2006; Plutzer 2009; Hedge 2009; Kayaoglu and Ørstavik 2004), albeit only present in small numbers in the oral cavity as it occupies a very narrow ecological niche. This microbial species grows well even in a harsh environment and is resistant to numerous antimicrobial agent (Hahn and Liewehr 2007).

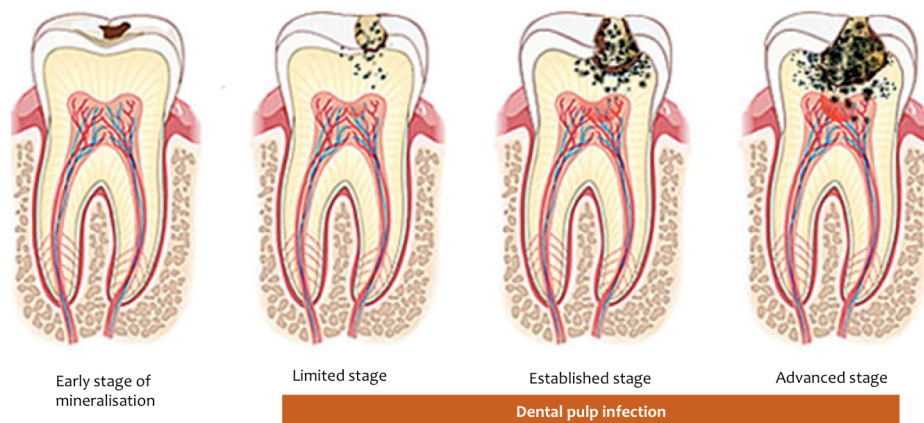


Figure 1.4 Stages of dental carious lesion and dental pulp infection.

This figure shows stages of dental pulp infection based on the depth of bacterial penetration. Each stage has a different major bacterial population. These dental pulp infection stages are the stage before oxygen is depleted in the root canal resulting in pulp necrosis (available from <http://stopcavity.com/caries/stages-of-dental-caries/>).

1.1.3 Symptomatic infection

From a clinical perspective, symptomatic endodontic infections can lead to pain and/or swelling and have the potential to develop into sinuses or other more serious complications. The microbiota involved in endodontic abscesses is mixed and dominated by anaerobic bacteria (see Figure 1.3) and there is no conclusive evidence that points to any single species involvement with any particular sign or symptom of apical periodontitis.

Having said that, accumulating evidence from a range of studies have all pointed to *Porphyromonas spp.*, as being particularly relevant. It was shown that all root canals affected by mixed infections were dominated by anaerobic bacteria with a high incidence of *Porphyromonas spp.*, particularly *P. gingivalis* (Jacinto et al. 2006). This genus and species produces a plethora of virulence factors (Jacinto et al. 2006; Rôças et al. 2002).

Some Gram-negative anaerobic bacteria have also been suggested to be involved with symptomatic lesions, but the same species may also be present in somewhat similar frequencies in asymptomatic cases. Therefore, factors other than the mere presence of a given putative pathogenic species may be important in the aetiology of symptomatic endodontic infections. Such factors include:-

1. Number of bacterial cells (load).
2. Virulence among strains of the same bacterial species.
3. Bacterial interactions resulting in additive or synergistic effects among species in mixed infections.
4. Environmental cues regulating the expression of virulence factors.
5. Host resistance.

These suggestions have led us to hypothesise that the environment of an infection can modulate bacterial virulence factors and this may explain why there is no direct relationship between bacteria identified as present and the presence of symptoms of pain.

Summary

This section is about the physiology and pathophysiology of dental pain caused by bacterial infection. Pathogenic bacteria play different roles in each stage, varying in the depth of the progression. There appears to be some specific bacterial species related to symptomatic pulpitis such as anaerobic bacteria of the 'Red complex'. However, the environment of the infection can also modify the virulence factors. Therefore, these environmental cues could influence pain sensitisation.

1.2 Virulence factors of oral pathogenic bacteria

1.2.1 Gram negative oral pathogens

The bacteriology of oral pathogens can be used to describe the stages of dental infection. In the early stage of carious lesion, the virulence factors of the bacterial pathogens involved in dental pulp infection are generally the molecules that aid colonisation, invasion, toxin production, enzyme activity, cytotoxic products, and cell structural constituents all of which can contribute to resistance to neutrophil killing and imbalance in the host response (Friso et al. 2010).

A list of oral bacterial products that can promote bacterial virulence is summarised as follows (Table 1.1).

Table 1.1 Summary of virulence products and/or mechanisms that promote oral pathogenic bacteria.

Factor/Product	Mechanism/Action
1. Peptide damage enzymes	
1.1 Elastases and other proteases.	Degrade extracellular matrix proteins
1.2 Nucleases	Degrade DNA released from host cells.
2. Bacterial attachment promoters	
2.1 Pili/fimbriae	Attachment mediators.
2.2 Non-fimbrial adhesins	Mediate tight binding to host cells.
3. Promote movement of bacteria	
3.1 Invasins	Allow entry into non-phagocytic cells.
4. Against phagocytosis by the host cells	
4.1 Polysaccharide capsules	Prevent phagocytic uptake, and reduce complement activation.
4.2 C5a peptidases	Interfere with chemotaxis signalling function of C5a.
4.3 Catalase and superoxide dismutase	Reduce the strength of the oxidative burst to allow survival in phagosome.
5. Toxic proteins	
5.1 Toxins	Kill phagocytes, reduce strength of oxidative burst, modify host cell signalling to dampen immune response, cause cell morphology changes and increase dissemination, and modify host cell processes to allow survival and replication.
6. Other virulence factors	
6.1 Other factors	Modulate LPS O-antigen structure can direct MAC formation, or iron binding proteins to replace iron-scavenging enzyme. (aid acquisition of this essential enzyme co-factor)

1.2.2 *Porphyromonas gingivalis*

In view of the high incidence of *Porphyromonas gingivalis* in pulpal infection and association with dental pain (Jacinto et al. 2006; Hajishengallis and Lamont 2014), we discuss its virulence factors that could contribute to the observed pathology (Sundqvist 1989).

1.2.2.1 Cell surface associated virulent factors

Gram-negative bacteria possess a lipid-rich outer membrane which is usually considered to possess proteins, phospholipids, and lipopolysaccharide (LPS). The major cell surface virulence factors include LPS, gingipain, haemagglutinin (Hag), fimbriae, capsule, and adherence activities (Okuda et al. 1991).

1.2.2.1.1 Lipopolysaccharide (LPS)

Lipopolysaccharides (LPS; Figure 1.5) are known as endotoxins and consist of lipid A and a polysaccharide core linked to a variable polysaccharide core. They are found in the outer membrane of Gram-negative bacteria, and elicit strong immune responses (Diya Zhang et al. 2008). Toll-like receptors (TLRs) are key receptors in the innate immune system that recognise bacterial components, such as lipoproteins, peptidoglycan, DNA, LPS (Acosta and Davies 2008), and HagB. TLRs would be reviewed in more detail in section 1.3.1. [Toll-like receptors (TLRs)].

1.2.2.1.2 Proteases

Bacterial proteases break down proteins to provide C- and N-sources for the bacteria that cause damage either directly to local host tissue or indirectly by disruptions to host systems (Ingmer and Brøndsted 2009). The best understood proteases of *P. gingivalis* are the gingipains; R and K gingipains (Arg-X-specific and Lys-X-protease respectively) which can hydrolyse endopeptides (Pike et al. 1994; Joseph et al. 2000; Stathopoulou et al. 2009). The bacterium also produces other proteases such as amino peptidases, collagenase, etc. (Table 1.2)

There are speculations that *P. gingivalis*, *T. forsythia*, and *T. denticola*, as a consortium of bacteria, releases multiple proteolytic enzymes, which overwhelm the host's local defences (Campos Lopes et al. 2012). They can mimic the action of host

endogenous proteinase and can even activate MMPs from their pro-enzyme form to their active form (Grayson et al. 2003). This has a deleterious effect on the host and provides nutrients for all the microbial organisms within the injury site (Ossovskaya and Bunnett 2004).

The proteases from *P. gingivalis* play important roles in interfering with host immunity. This is because gingipain proteases can degrade plasma proteins, cytokines, complement components and immunoglobulins. Interestingly, Arg-gingipain can cleave the protease activated receptor 2 (PAR2) which can then affect the function of neuronal and neuronal cells (Rothmeier and Ruf 2012; Potempa et al. 2000; Lourbakos et al. 1998). PARs will be reviewed in more detail in 1.3.3. [Proteinase-activated receptors (PARs)].

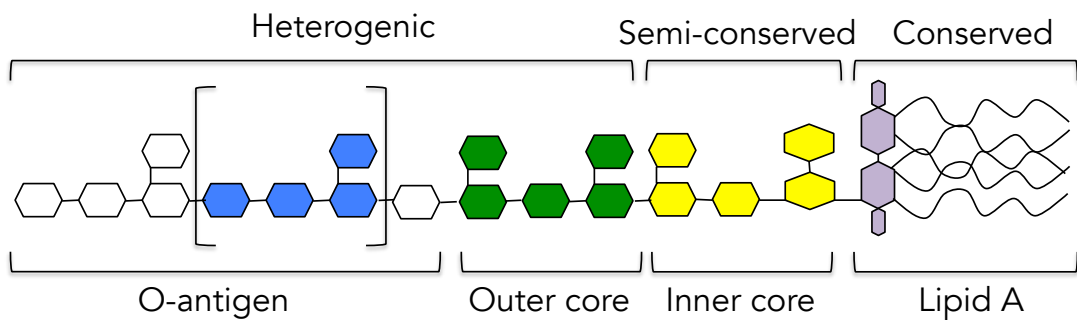


Figure 1.5 The structure of LPS.

LPS structure consists of lipid A embedded in the bacterial cell outer membrane and polysaccharide components of outer and inner cores, and highly variable O-antigen segment which protrudes into the external environment (Adapted from Dixon and Darveau 2005, permission granted to reproduce).

Table 1.2 Proteolytic system of *P. gingivalis*.

Proteinase	Related-genes	Description
Gingipain R	<i>rgpA</i> , <i>rgpB</i>	Arg-Xaa-specific cysteine endopeptidase
Gingipain K	<i>kgp</i>	Lys-Xaa-specific cysteine endopeptidase
Periodontain	(unfinished genomic database)	Cysteine endopeptidase
PrtT proteinase	Acc.no. S75942 gene structure	Not yet characterized at protein level
Tpr proteinase	<i>tpr</i> gene Acc.no. M84471, AF0204499	Endopeptidase
Collagenase	<i>prtC</i> gene Acc.no. M60404, AB006973	Cleavage of Pz-Pro-Leu-Gly-Pro peptide Soluble type I collagen
PtpA	(unfinished genomic database)	Serine exopeptidase Cleavage after Pro residues with the consensus sequence: H ₂ N-Xaa-Xaa-Pro- Yaa-(Xaa) _n
DPP IV	<i>dppIV</i> gene Acc.no. AF026511	Serine exopeptidase Prefer to cleave H ₂ N-Xaa-Pro- dipeptidases
DPP VI	Unknown gene structure	Cysteine peptidase
Amino-peptidase P	(unfinished genomic database)	Hydrolyses N-terminal Xaa-Pro-bonds
Oligo-peptidase O	(unfinished genomic database)	Metalloproteinases
True collagenase	(unfinished genomic database)	Cleavage all three α -chains near C-terminal
Gelatinase		Cysteine peptidase Hydrolyses Pz-peptide

Acc. No. – Accession Number (GeneBank)

1.2.2.1.3 Hemagglutinin

P. gingivalis produces at least five hemagglutinating molecules. These surface located hemagglutinin (Hag) proteins are important virulence factors for *P. gingivalis*, since they promote colonization by mediating the binding of bacteria to oligosaccharide receptors on human cells. This includes binding to erythrocytes which, along with the concerted action of other virulence factors, can provide *P. gingivalis* with vital heme for growth (Pandit et al. 2015). It is also been found that TLR4 can interact with HagB.

1.2.2.2 Secreted virulent factors (supernatant proteins)

Some virulent factors are released into the extracellular matrix through a mechanism involving cell wall turnover and the release of outer membrane vesicles (OMVs) as shown in Figure 1.6. These vesicles could consist of a subset of outer membrane components such as LPS and gingipain (Schwechheimer and Kuehn, 2015).

1.2.2.3 Invasion of cells

It has been established that *P. gingivalis* can invade epithelial and endothelial cells (Nisapakultorn et al. 2001). This pathogen can pass through the epithelial barriers and replicate within the intracellular environment. Such invasion is driven by bacterial fimbriae interacting with integrins on the surface of host epithelials. Signal activation is initiated when surface receptors occupied by *P. gingivalis* leads to mitogen-activated protein kinase pathways (MAPK). Subsequent internalisation results in epithelial cell signalling and the inhibition of transcription and secretion of IL-8 by neutrophils (Aruni et al. 2011). While it is known that *P. gingivalis* can invade a range of cell types, nothing is known whether it is capable of invading neuronal and glial cells in the pulp. Neurones are capable of Clathrin-independent endocytosis, which is thought to be a mechanisms for neurotransmitter receptor trafficking (Klein et al. 2015; Patwardhan et al. 2005; Soh et al. 2010), and this could provide a means for *P. ginigvalis* or its OMVs to gain direct entry to neurones. However, currently there is no information to support that conjecture.

1.2.2.4 Others

It has been suggested that *P. gingivalis* appears in the root canal because the local environment that allows this bacterium to thrive. The pathogen not only has a wide range of enzymes that degrade host tissues, but it also possesses fimbriae (Enersen et al. 2013) that allows bacteria to attach to host surfaces and to other bacteria in a 'piggy-back'-like manner.

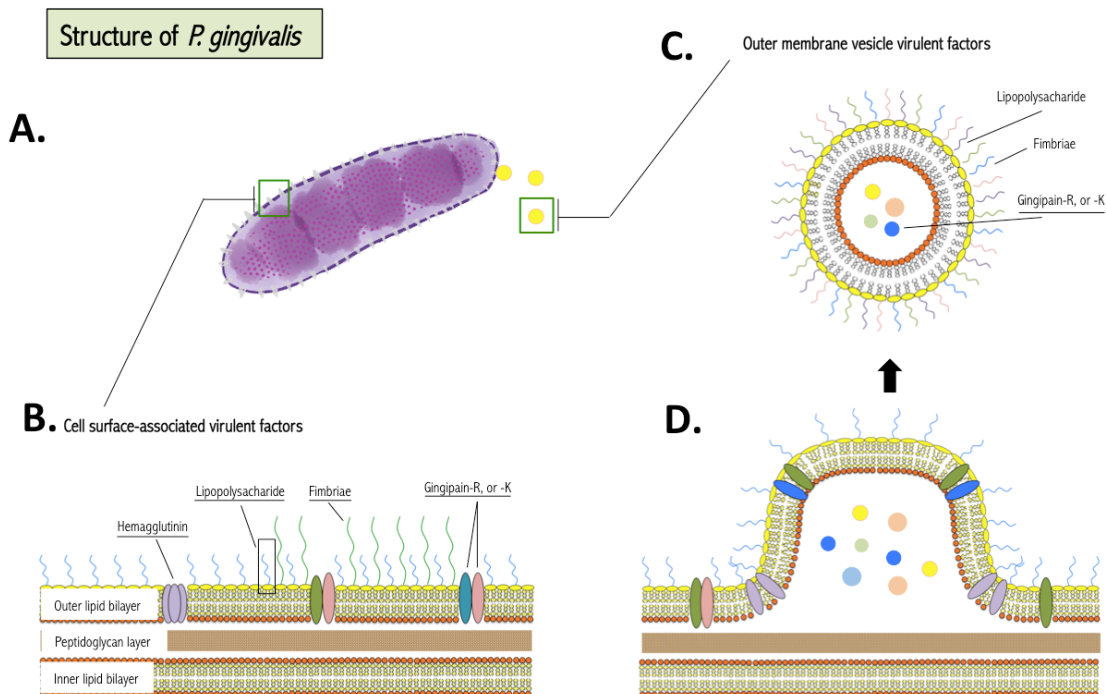


Figure 1.6 *P. gingivalis* virulence factors

(A) *P. gingivalis* is a rod-shaped, Gram-negative, anaerobic bacterium. The virulence factors of *P. gingivalis* could be into 2 forms; cell surface-associated form (B), and outer-membrane vesicle (C). Both forms could contain LPS, gingipain, fimbriae, and etc. In the process of outer-membrane vesicle biogenesis of *P. gingivalis*, many virulence factors could be included in the vesicle as well (D). (Modified from Schwechheimer and Kuehn, 2015, permission granted to reproduce).

1.2.3 Modification of *P. gingivalis* virulence factors – Role of Iron

1.2.3.1 LPS modification

A number of studies have shown that environmental changes can affect *P. gingivalis* lipid A. For instance, the activity of deacylase is modulated by the environment or at the genetic level (Hashimoto et al. 2004; Darveau and Hancock 1983; Dixon and Darveau 2005; Herath et al. 2013) as shown in Figure 1.7. This could modulate the host response and also influence the interaction of variant forms of *P. gingivalis* LPS with TLR4 and other receptors on neurones.

The host responses to LPS of enteric bacteria and oral bacteria are different. Gram-negative oral anaerobic bacteria do not elicit strong host responses when compared with that of enterobacteria such as *Escherichia coli*. An important explanation for the lower host response is the difference in the chemical make-up of lipid A between these various bacteria. *E. coli* Lipid A is hexa-acylated, four acyl chains being attached directly to the glucosamine sugars while the two additional acyl chains are attached to the beta hydroxy group. In contrast, *P. gingivalis* Lipid A has often been thought of as being penta-acylated but it has been shown to also exist in tri- or tetra-acylated forms. The latter Lipid A displays a relatively low endotoxic activity compared with the penta-acylated and hexa-acylated forms of lipid A (Herath et al. 2013)

These variations in the structure of *P. gingivalis* LPS can be brought about by changes in its growth conditions, e.g. haemin concentration, pH, and temperature. *In vitro* study has shown that growing *P. gingivalis* in limited-haemin concentration, mainly produced LPS penta-acylated lipid A. Under conditions where haemin is present in excess, multiple-tetra- and penta-acylated lipid A are synthesised. These changes can have an impact on host inflammatory response to the bacterium because penta-acylated lipid structures can act as TLR4 agonists, whereas tetra-acylated structures can conversely serve as TLR4 antagonists (Al-Qutub et al. 2006). Consequently, it is possible that the degree of excess haemin in the pulp will result in variation in interaction of *P. gingivalis* LPS with neuronal TLR4 and so influence the resultant inflammatory pain transduction.

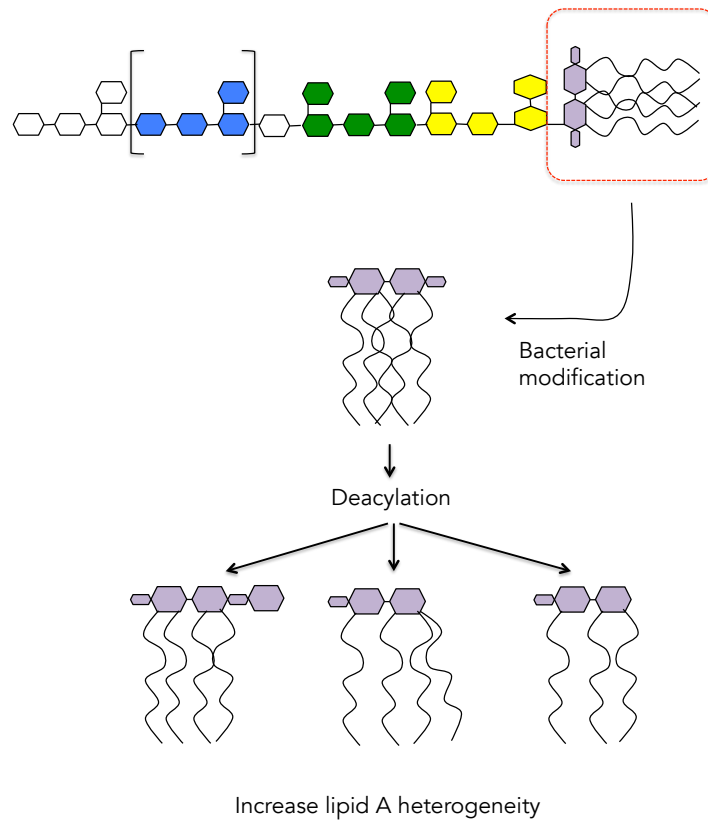


Figure 1.7 The heterogeneity of lipid A that can be modified under different growth condition.

Either by number or length of acyl chains, phosphorylation pattern or overall chemical symmetry of the lipid A structure; resulted in intermediate or low biologic activity (Adapted from Dixon and Darveau 2005, permission granted to reproduce).

1.2.3.2 Gingipain modification

In the previous section, we have discussed how the growth conditions can alter LPS structure and consequently affect the pathogenicity of LPS. To add to this, it has been shown that there is greater proteolytic activity, and a higher concentration of metabolic enzymes when environmental haemin is in excess (Pike et al. 1994; Marsh et al. 1994). The presence of excess free haemin is closely linked to higher virulence (Marsh et al. 1994) because bacterial cells grown in the absence of haemin need more resources to be devoted to anabolic reactions thus limiting the energy and nutrients available for their virulence capability.

1.3 Molecular basis of signal detection of inflammatory pain

Sensory neurones are responsible for the conversion of noxious stimuli into molecular messages. This property allows the nervous system to detect a wide range of chemical irritants, mechanical and thermal stimuli (Fischer et al. 2010; Li et al. 2008). Peripheral mediators of inflammation are the best-studied examples among the many factors that can directly act on the nociceptors (through binding to the cell surface receptors and triggering peripheral sensitisation).

The sensory neurones are very sensitive to inflammatory molecules, such as pro-inflammatory cytokines. There are many types of receptors that can detect a wide range of cytokines as shown in .

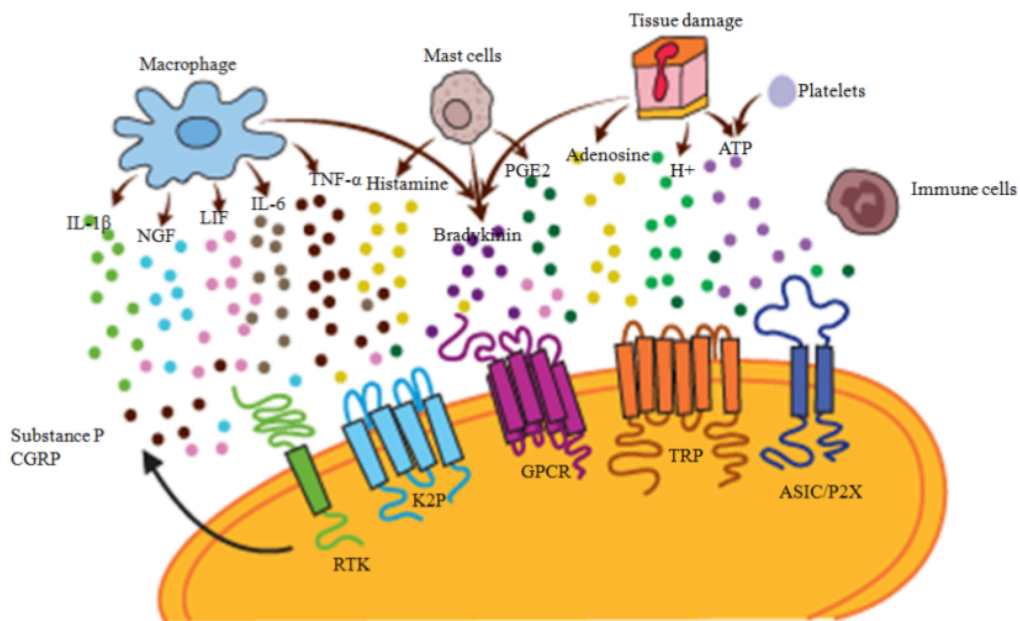


Figure 1.8 Inflammatory mediators and their specific receptors on sensory neurones.

This diagram depicts the peripheral sensitisation triggered by inflammatory mediators from various sources such as released cytokines from immune cells, mediators from tissue damage, and/or neuropeptides released by sensory neurones. These mediators could potentially activate their specific receptors on sensory neurones (Modified from Basbaum et al. 2009, permission granted to reproduce).

Abbreviations used: Interleukin 6 (IL-6), Interleukin 1 beta (IL-1β), Nerve growth factor (NGF), Leukemia inhibitory factor (LIF), Tumour necrotic factor alpha (TNF-α), Prostaglandin 2 (PGE2), Adenosine triphosphate (ATP), Receptor tyrosine kinases (RTK), Two-pore domain potassium channels (K2P), G-protein-coupled receptors (GPCR), Transient receptor potential (TRP), and Acid-Sensing Ion Channel (ASIC).

It is important to note that the focus of this study is the direct affect of bacterial components interacting with surface receptors on trigeminal sensory neurones. There are various categories of mechanism that can potentially convert bacterial components into neural signals and stimulate peripheral sensitisation. Figure 1.9 illustrates the surface receptors that can potentially stimulate neuronal activities.

Based on the bacterial virulence factors, LPS and gingipain, here we list three major categories of molecular receptors that may directly activate sensory neurones. They are pattern recognition receptors (PRRs) (Goethals et al. 2010; Ochoa-Cortes et al. 2010; Frenkel et al. 2010), transient receptor potential channels (TRPs) (Geppetti et al. 2008; Santoni et al. 2015), and protease-activated receptors (PARs) (Wang et al. 2012).

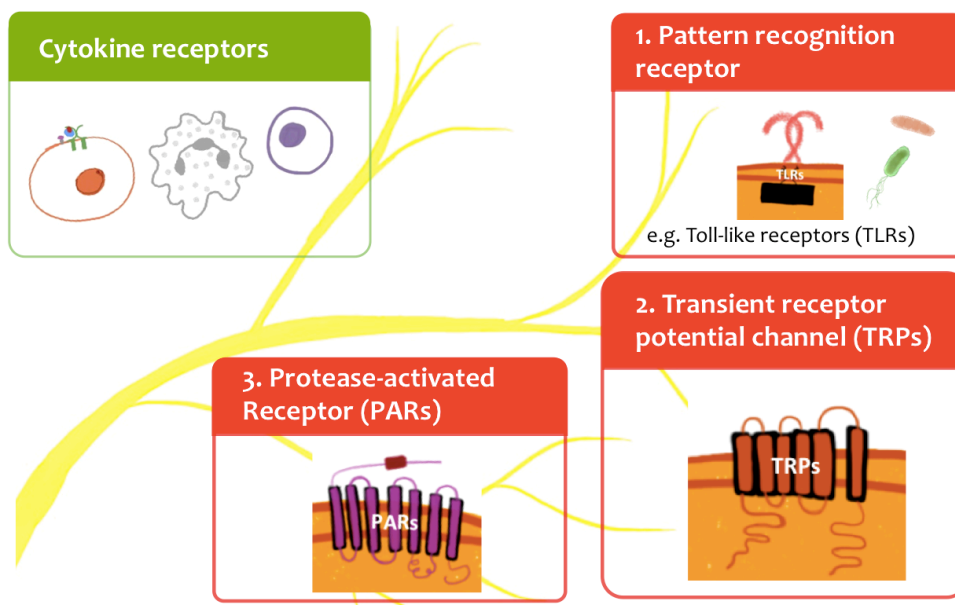


Figure 1.9 The potential mechanisms that can stimulate peripheral sensitisation involving bacterial infection.

Peripheral sensitisation has been shown to be activated by pro-inflammatory mediators such as cytokines via the specific receptors. There are 3 potential receptor families that can be directly activated by bacteria and their components, namely TLRs, TRPs, and PARs.

1.3.1 Toll-like receptors (TLRs)

Toll-like receptors (TLRs) are a family of evolutionarily conserved pattern recognition receptors that act as a first line of defence in the innate immune system (Tsan and Gao 2004; Goethals et al. 2010). Upon stimulation with microbial ligands, they orchestrate the induction of a host defence response by activating different signalling cascades.

The innate immune system can respond to common shared structures called pathogen associated molecular patterns (PAMPs) that can be recognised by TLRs (Santoni et al. 2015; Liu et al. 2012). TLRs are transmembrane proteins expressed by many cells that recognise invaders and activate signalling pathways in response to the presence of invaders. Different TLRs recognise different ligands, such as bacterial cell wall components, viral RNA, or immunomodulatory compounds. The result of TLR activation involves two major intra-cellular signalling pathways (Vaisid and Kosower 2013; Tsan and Gao 2004). The core pathway is the activation of Nuclear Factor- κ B (NF- κ B) via the Mitogen-Activated Protein kinase (MAPKs) p38 and c-Jun N-terminal kinase (JNK). The second pathway involves TLR3 and TLR4 which can lead to the activation of both NF- κ B, and the transcription factor Interferon Regulatory Factor-3 (IRF3) (Watanabe et al. 2013; Nhu et al. 2010; Figure 1.10).

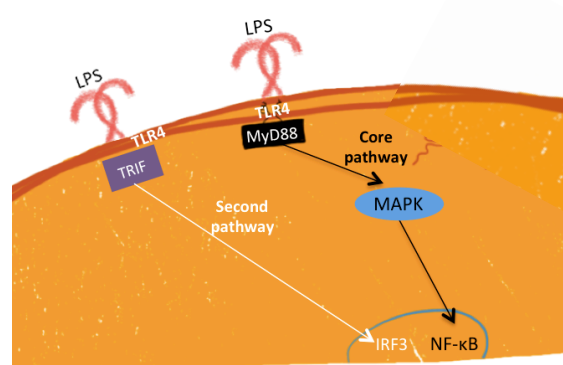


Figure 1.10 This figure shows the possible downstream pathways via TLR4 activation.

Following TLR4 activation, neurons can be stimulated by two possible pathways: a core pathway that includes MyD88, MAPK, and NF- κ B, and second pathway involving TRIF, and IRF3.

TLR signalling may lead to different responses in distinctive cell types through an interaction with MyD88 unique variants (Liaunardy-jopeace and Gay 2014). Not every cell expresses the same set of adaptors. For example, it is becoming clear that selective expression of the MyD88-independent pathway found in neurones (for a review see Frenkel et al. 2010), renders these cells uniquely sensitive to TLR-mediated activation of the JNK pathway to apoptosis, instead of the NF- κ B pathway towards inflammatory response, as in glial cells. In this way, selective expression of adaptors strongly influences the quality of the response mounted by different types of cells to a given TLR agonist.

1.3.1.1 TLR4

Recent data reports the expression of various TLRs in the central nervous system (CNS) and peripheral nervous system (PNS) (Al-Qutub et al. 2006; Okun et al. 2011; Ferraz et al. 2011; Diogenes et al. 2011). In the central nervous system, TLR2 and TLR4 appears to play defensive roles in acute neurodegeneration (Okun et al. 2011; Leow-dyke et al. 2012). Interestingly, they appear to detect the presence of endogenous signals of danger as well, and as such, neurodegeneration is thought to trigger an immune response by binding to TLRs (Goethals et al. 2010; Frenkel et al. 2010).

The TLRs that are expressed in PNS are TLR2, TLR3, and TLR4, which are mainly on Schwann cells, while only TLR4 has been found in dorsal root ganglia and trigeminal ganglia neurones (Tsan and Gao 2004; Qi et al. 2011). While the stimulation with TLR ligands can induce NF- κ B dependent signalling in immune cells, a similar cascade has not yet been identified in the PNS.

There is a suggestion that the LPS receptor complex on neurones may be expressed differently from that on cells of the immune system. Previous work has demonstrated that LPS could induce release of the neuropeptide, CGRP, in dissociated dorsal root ganglia cultures (Hou et al. 2003; Hiruma et al. 2000). However, it is still unclear whether LPS directly acts on the neurones or affects non-neuronal cells that were also present in the cultures (Hou et al. 2003) and which could then indirectly affect

neurones. Furthermore of relevance to pulpitis pain, it is highly likely that the pulpal growth environment could influence the degree of acylation of LPS and this would impact on its interaction with TLRs (Coats et al. 2005; Herath et al. 2013; Al-Qutub et al. 2006).

1.3.2 Transient receptor potential (TRPs)

An important target of inflammatory pain mediators is the TRP channel, expressed particularly on subsets of C and A δ nociceptors (Thakur et al. 2014; Smith and Lewin 2009). TRP channels have many different physiological roles, mediating their roles in thermo- and chemo-sensation. Figure 1.11 shows how different temperatures could involve the action of different subsets of TRP channels.

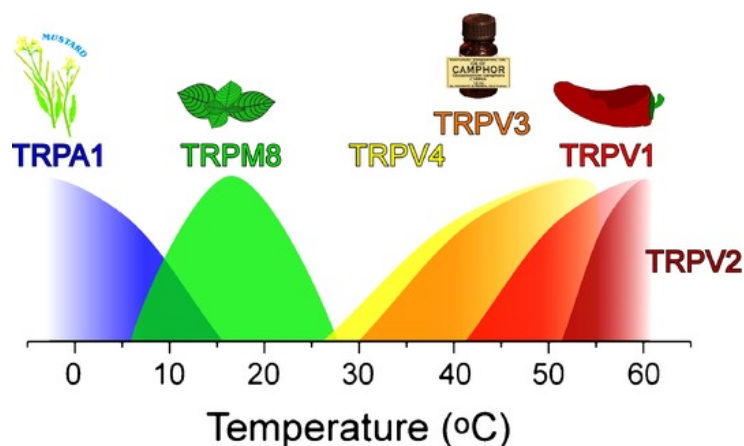


Figure 1.11 Thermo-sensory properties of transient receptor potential channels (TRPs).

The thermo-sensory properties of TRPs that have the potential to transduce a range of thermal stimulation from cold to hot. Additionally, the TRPs can be specifically activated by chemical compounds.

TRPV1 and TRPA1 are of particular relevance to pain and neurogenic inflammation as they are activated by a variety of noxious stimuli, with TRPV1 being co-expressed on the vast majority of TRPA1-expressing sensory nerves (Fernandes et al. 2012; Lapointe and Altier 2011). Consequently we have focussed on two types of TRP channels; TRPV1, and TRPA1. TRPV1 is a physiological target of noxious heat stimulants (>43°C), capsaicin (pungent compound of hot chilli pepper), and other chemicals, including anadamide and euginol (Huang et al. 2006; Gibbs et al. 2011;

Tóth et al. 2011). In contrast, TRPA1 is a target for cold stimulation ($<15^{\circ}\text{C}$) and chemical toxicants including mustard (Chen et al. 2011; Basbaum et al. 2009). These thermal and mechanical signals are transduced by the nociceptors, the receptor potential activates the voltage-gated ion channels (Fehrenbacher et al. 2009).

1.3.2.1 TRPV1

The sensitisation of TRPV1 is influenced by various intracellular signalling pathways. TRPV1-mediated cation influx initiated by the application of noxious chemical or temperatures is further enhanced by low pH. Activation of TRPV1 results in an influx of mainly Ca^{2+} but also other cations such as Na^{+} , K^{+} , and Mg^{2+} , which can enter the cell through this channel (Figure 1.12). Such cation influx invokes membrane depolarisation, and subsequently generates the nociceptor sensitisation.

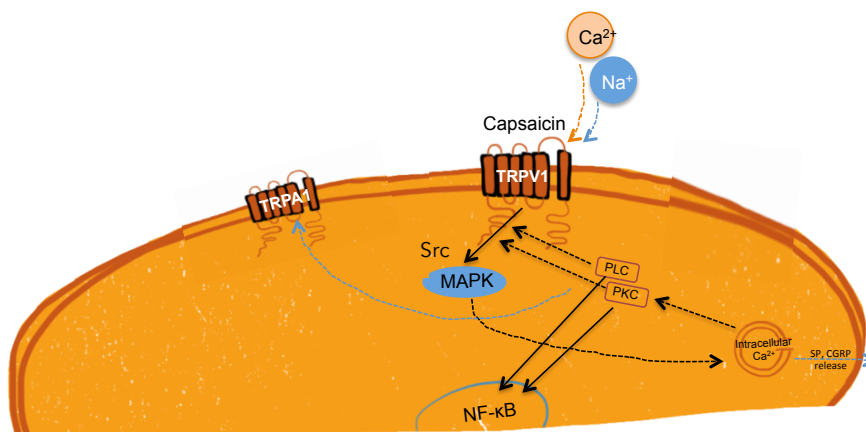


Figure 1.12 TRPV1 activation pathways.

This figure shows the signal transduction in primary nociceptive neurons by the, TRPV1 agonist, capsaicin. Activation of TRPV1 mobilises intracellular Ca^{2+} by the MAPK pathway and increased Ca^{2+} can trigger release of neuropeptides. TRPV1 is sensitised through multiple phospholipase C-coupled receptor pathways and phosphorylation through PKC also affects TRP channel activity during inflammation.

There are potential target sites on TRPV1 for phosphorylation by protein kinases, namely protein kinase C (PKC) (Bhave et al. 2003; Vellani et al. 2010; Aksoy et al. 2004) and protein kinase A (PKA) (Chen et al. 2011). In addition, tyrosine kinase Src can modulate the trafficking of TRPV1 to the neuronal membrane (Igwe 2003; Huang et al. 2006). These kinases sensitise the channel by increasing the probability of the open gate, and increasing the expression on the neurone membrane channel

by regulated exocytosis through the action of Src (White et al. 2011; Basbaum et al. 2009), as outlined in Figure 1.12.

1.3.2.2 TRPA1

TRPA1 channels respond to multiple irritant sensors, such as chemical irritants and environmental toxicants. Some chemical compounds, such as mustard oil can bind to TRPA1 through ligand-receptor interaction and induce sensory neural excitation. The regulation of TRPA1 can lead to ion channel activation, the pathways for which include phosphorylation cascades similar to TRPV1 and the regulation of intracellular Ca^{2+} (Guimaraes and Jordt 2007).

1.3.3 Protease-activated receptors (PARs)

Another important target for pain signalling in the G-protein coupled receptor (GPCR) family are the PARs that are expressed on some afferent sensory neurones. The GPCR family is a group of transmembrane receptors that binds signalling molecules and leads to outside-in transduction for cellular responses (Fehder et al. 1998; Patwardhan et al. 2006; Ossovskaya and Bunnett 2004).

The family comprises 4 PARs for which there are a wide ranges of protease activators (Macfarlane et al. 2001). Such receptor activation can modulate signalling events in many cell types from haemostasis to pain transmission (Ossovskaya and Bunnett 2004). The list of PAR1-4 activators and the types of cells involved are shown in the Table 1.3.

Table 1.3 Summary of PAR activating proteases and the cell involved.

	PAR1	PAR2	PAR3	PAR4
Activating protease	Thrombin FXa APC Granzyme A Gingipain-R Trypsin	Tryptase FVIIa FXa Proteinase-3 Gingipain-R Trypsin	Thrombin	Thrombin Gingipain-R Trypsin Cathesin G
Localisation	Platelets, endothelium, epithelium, fibroblasts, myocytes, neurones, astrocytes	endothelium, epithelium, fibroblasts, myocytes, neurones, astrocytes	Platelets, endothelium, myocytes, astrocytes	Platelets, endothelium, myocytes, astrocytes

The PAR-stimulated signalling pathways include PLC-dependent PIP_2 hydrolysis to form diacylglycerol (DAG) so leading to PKC phosphorylation, and the IP_3 pathway that triggers Ca^{2+} mobilisation (from intracellular store) as shown in Figure 1.13.

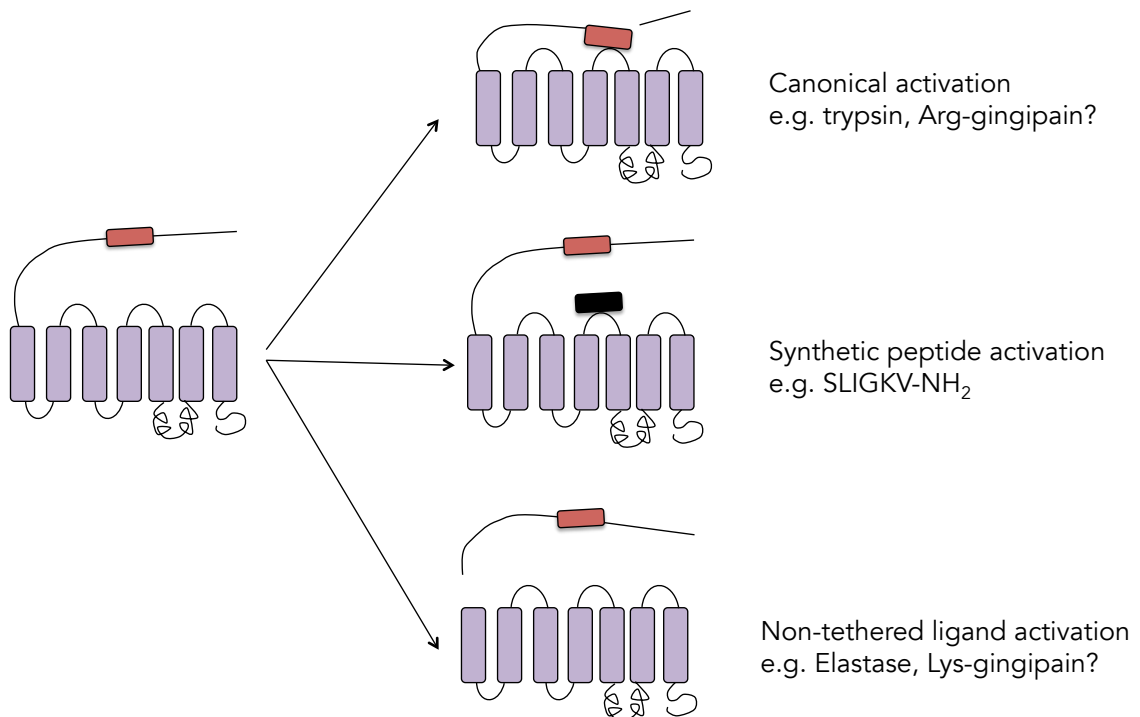


Figure 1.13 Mechanisms of activation of protease-activated receptors.

This figure shows PAR2 regulation by various types of stimuli and the activation mechanisms; canonical, synthetic peptide, and non-tethered ligand activations (Modified from Zhao et al. 2014).

Although, there are several PAR cleavage mechanisms mediated by various types of proteases (Figure 1.13), one of those is the bacterial protease mechanism that can disarm the tethered ligand-derived peptides of PAR. The consequences of PAR activation are the induction of downstream signalling cascade that is similar to canonical activation. Both *P. gingivalis* Arg-, and Lys- gingipains are potential factors that could activate PARs on neurones during pulpal infection. However, the mechanisms are potentially complex because Arg-, and Lys-gingipain could activate other pathways because of the different target sites of each enzyme and these effects in turn could involve activation of PARs (Figure 1.14).

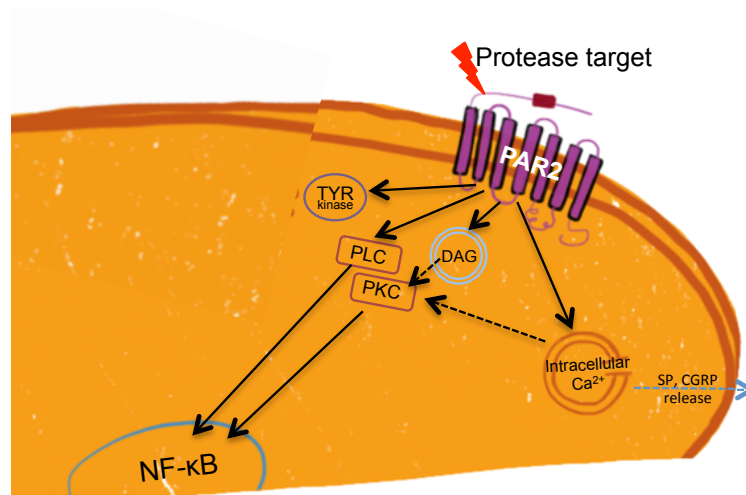


Figure 1.14 PAR2-stimulated pathways.

This diagram shows the intracellular signalling pathway following protease cleavage of PARs on sensory neurones. Cleavage of PAR2 can lead to the phosphorylation of PKC and PLC pathways. This stimulation pathway can induce the release of neuropeptides and multiple physiological responses.

1.3.4 Interaction between PARs, TLRs, and TRPs

1.3.4.1 TLRs-TRPs

There is evidence to support the interactions between the innate immune system and the peripheral nervous system. The crosstalk of TLR ligands with neurones up-regulates the expression of TRPV1, and this suggests that TLRs play an important role in peripheral neurone responses to their environment (Diogenes et al. 2006; Wadachi and Hargreaves 2006). Several studies have supported a direct activation pathway involving TLRs in peripheral nociceptive transduction (Qi et al. 2011; Ochoa-Cortes et al. 2010; Ferraz et al. 2011). Although TRPV1 and TLR4 co-expression has been demonstrated (Diogenes et al. 2011), a complete picture of the crosstalk with other receptors and the actual pathways that these receptors feed into has not been elucidated.

The proposed crosstalk between TLR and TRP is illustrated in Figure 1.15. LPS appears to activate an intracellular signalling cascade through MyD88 leading to the downstream activation of MAPK and NF- κ B (Lin et al. 2015). LPS can additionally activate PKC which can potentially bind to TRPV1. Moreover, Ca^{2+} from the activation influx can activate PKC for further modulations (Assas et al. 2014).

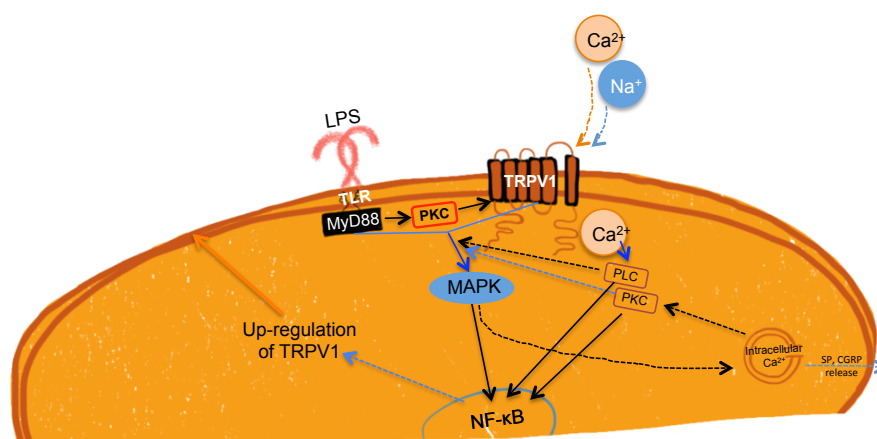


Figure 1.15 Intracellular activation mechanisms involving crosstalk of TLRs with TRPV1.

LPS activates TLR4 which stimulates MyD88 leading to MAPK activation and NF- κ B nuclear translocation. PKC and other protein kinases can potentially bind to TRPV1 for further modulation.

1.3.4.2 TLRs-PARs

PARs can serve as the sensors for bacterial proteases through PAR1-4 (Ossovskaya and Bunnett 2004; Soh et al. 2010; Vellani et al. 2010). As shown in Figure 1.16, PARs can interact with TLRs and induce neuronal activity via MAPK, subsequently stimulating hypersensitivity and neurogenic inflammatory processes (Moretti et al. 2008; Nhu et al. 2010).

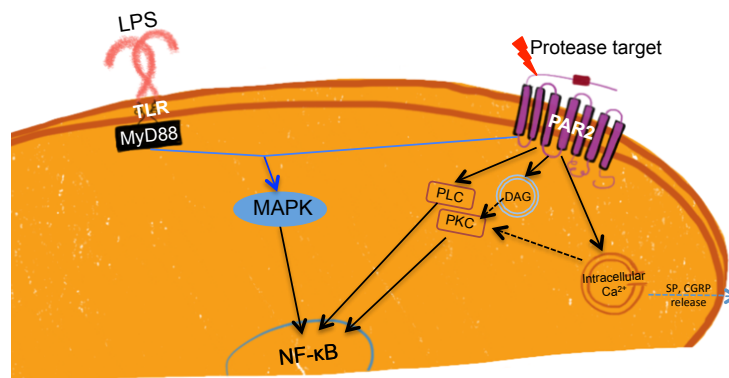


Figure 1.16 Common pathway of TLRs and PARs.

This figure shows interaction of TLRs and PAR2, both receptors could induce MAPK, and induce translocation of NF-κB.

Although the crosstalk of TLR with PAR signalling has not been completely elucidated in the nervous system, there is evidence that demonstrates TLR-4-mediated enhancement of PAR2 signalling in a MyD88-dependent pathway in PAR2 and TLR4 transfected cells. (Krysko et al. 2011; Watanabe et al. 2013).

1.3.4.3 PARs-TRPs

There is evidence to suggest that PAR2 activation can decrease the threshold of TRP ion channels through direct crosstalk between the two receptors and which, therefore, leads to hyperalgesia of inflammatory pain and allodynia (Vellani et al. 2010; Dai et al. 2004).

The signalling pathway from activated PAR2 can lead to activation of PLC-PKC pathways. The ability to develop crosstalk with other nociceptive receptors, such as TRPV1 and TRPV4, is made possible by the participation of TYR kinase (Vellani et al. 2010). In addition, by increasing phosphorylation of MAPK, activated PAR2 may functionally interact with ion channels and cause depolarisation. Consequentially, the activation of PAR2 could lead to the sensitisation or potentiation of TRPV1 activity; Figure 1.17 (Vellani et al. 2010; Chen et al. 2011; Dai et al. 2004). In addition, TRP channel activity is thought to be an important component of a number of PAR2-mediated effects and these are listed in Table 1.4.

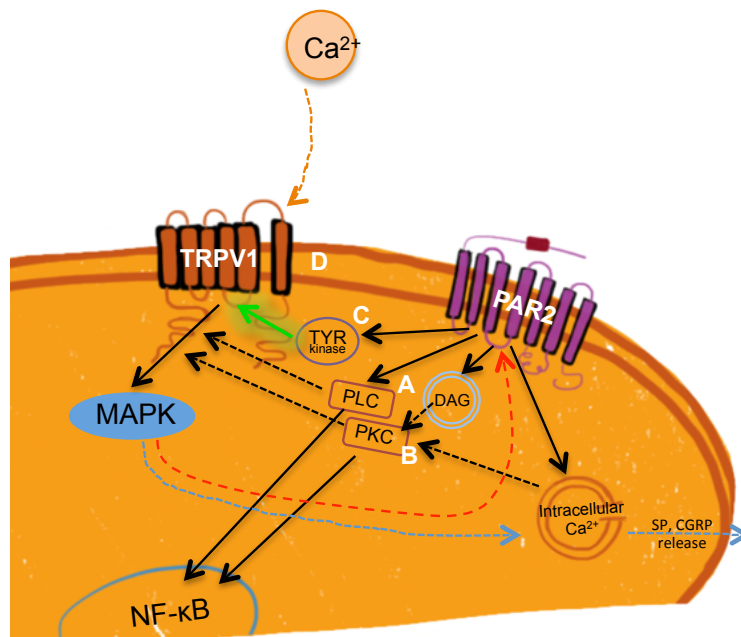


Figure 1.17 Crosstalk pathways for TRPV1 and PAR2.

PAR2 cleavage leads to the TRPV1 activation by TYR kinase, which in turn promotes phosphorylation of intracellular molecules by MAPK.

Table 1.4 TRPs activities following PAR-2 mediated effects.

TRP channel	Activity
TRPV1	PAR2 reduces temperature threshold for TRPV1 activation in DRG.
	PAR2 stimulates PKC, PLC, sensitising TRPV1 to cause thermal hyperplasia.
	PAR2 activation of PKC sensitises TRPV1 for SP and CGRP release.
TRPA1	TRPA1 potentiated effects of PAR2 activation in DRG neurones via PLC-mediated PIP2 hydrolysis.
	PAR2 induces hyperplasia requires TRPA1 expression in sensory neurones.
TRPV4	PAR2 activation of PKC, PKA, PKC and protein kinase D sensitise TRPV4 induce releasing of SP and CGRP
TRPV1, TRPA1, TRPV4	Drug induced PAR2 signalling sensitises all three channels to induce neuropathic pain.

Abbreviation used; substance P (SP), calcitonin-gene related peptide (CGRP), Phospholypase C (PLC), Protein kinase C (PKC), Protein kinase A (PKA), and Phosphatidylinositol (4,5)-bisphosphate (PIP2).

Summary

This section has described the molecular basis of the potential mechanisms for peripheral nerve activation via TLRs, TRPs, and PARs. The capability of nociceptors to transduce noxious stimuli may not be accomplished by single cellular receptors but might require the actions of multiple receptor stimuli to sufficiently amplify the signals for peripheral sensitisation. The consequences of neuronal activation will be discussed in the next section.

1.4 Consequences of sensory nerve response to inflammatory bacterial infection

Reaction to pathogens can lead to the activation of sensory neurones, causing the release of a range of neuropeptides and pro-inflammatory mediators which contribute to the onset of pathological pain. Pulpal sensory nerve fibres sprout significantly in response to injury and subsequently increase SP and CGRP release (Byers et al. 2003; Lundy and Linden 2004). Sensory neuropeptides such as SP and CGRP have been considered as neuroimmunomodulators that regulate the immune cells against invaders via specific receptors (Figure 1.18) (Metz-Boutigue et al. 2003; Hiruma et al. 2000; Assas et al. 2014). The molecular basis of peripheral sensitisation by activation of potential cellular receptors was described in the previous section.

The effects of resultant neuropeptide release (SP and CGRP) not only can activate inflammatory processes aiming to eliminate pathogens, but also can influence the interaction of other cells in the pulpal tissue.

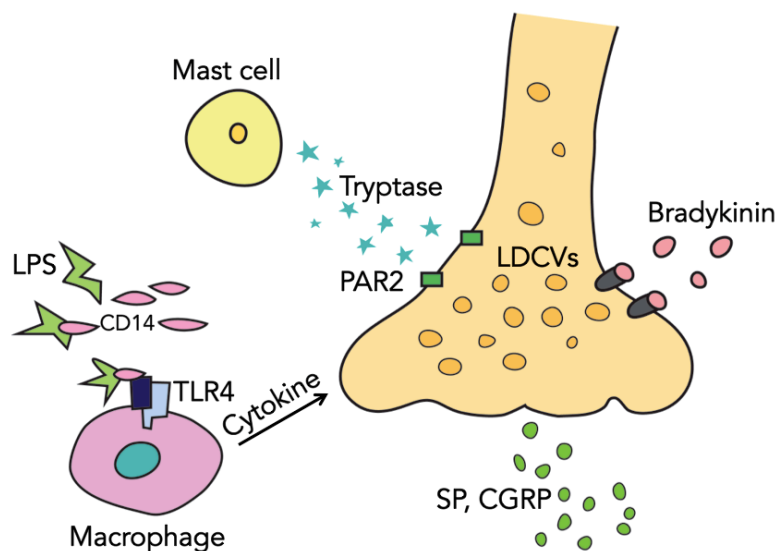


Figure 1.18 Regulation of neuropeptide release by a variety of mechanisms.

Following inflammation or injury, primary nerve terminals can release neuropeptides. These peptides can contribute to neurogenic inflammation and multiple localised physiological responses (Modified from Lundy and Linden 2004, permission granted to reproduce).

1.4.1 Axonal reflexes

Activation of some sensory nerve causes the release of pro-inflammatory mediators, including ATP and neuropeptides from their peripheral endings (Matsuka et al. 2001; Rang et al. 1991). These mediators then act on the tissue of innervation to initiate neurogenic inflammation (Kristiansen and Edvinsson 2010). This peripheral release of mediator from the sensory nerve collaterals and the resulting end-organ effects is known as the axon reflex (Hagains et al. 2010).

Many afferent nerve endings, including trigeminal neurones, contain potent pro-inflammatory peptides, such as substance P and CGRP. When administered exogenously, these neuropeptides have profound effects in inflammatory cell recruitment (Maltos et al. 2004; Ellis and Bennett 2013). In addition, neuropeptides are known to be multifunctional molecules, which act as neurotransmitters, growth factors and immune system signalling molecules amongst others (Roosterman et al. 2006)

1.4.1.1 Release mechanisms of neuropeptides

Similar to other secreted protein products, the neuropeptides are cleaved from precursor pre-propeptide molecules. Prepropeptides are cleaved to become propeptides in the endoplasmic reticulum (ER) by the action of specific enzymes to produce large quantities of propeptides and subsequently neuropeptides. Following their synthesis, neuropeptides are stored in large dense-core vesicles (LDCVs) in neurones (Sobota et al. 2010). As illustrated in Figure 1.18, CGRP is released through synaptic clefts in response to calcium-dependent polarisation of intracellular stores by triggering the exocytosis of the LDCVs. Subsequently, the recruited LDCVs are then activated to bring about "store-regulated" release (Meng et al. 2007).

1.4.1.2 Neuropeptide functions in response to pathogenic bacteria

Dental pulp tissue is highly innervated by sensory neurones and there are many types of neuropeptides that can be released from pulpal sensory neurones (Table 1.5). Substance P was the first neuropeptide that was found in dental tissue and this functions as a chemo-attractant enhancing phagocytosis by macrophages but it also

augments cytokine and arachidonic acid production in the inflammatory processes. Substance P was found increasing in pulpal inflammatory and pain (Rodd and Boissonade 2000). In addition, CGRP can intercept T lymphocyte proliferation by inhibiting their mitogen conduction, block antigen presenting cells and reduce superoxide production from macrophages (Caviedes-Bucheli et al. 2006). These effects are summarised in Table 1.5.

1.4.2 NF- κ B pathway

NF- κ B is normally held in the cytoplasm in an inactivated state by the inhibitor protein I κ B- α , in a NF- κ B/I κ B- α complex form. Upon activation, free NF- κ B translocates to the nucleus (Grimm and Baeuerle, 1993). It has been found that activation of the NF- κ B pathways in DRG neurones can increase the transcription of TNF- α and IL-1 β , stimulate the secretion of TNF- α (Ochoa-Cortes et al. 2010). The activation of NF- κ B can also induce CGRP synthesis (Hou et al. 2003). This may support the immune activity of sensory neurones via the release of cytokines to contribute to innate immune system.

Table 1.5 Summary of dental pulpal neuropeptides, receptors, and functions.

Origin	Neuropeptides	Cell receptor	Cell responding	Biological effects
Trigeminal ganglion	Substance P	NK 1	Mast cells Macrophages Mesenchymal cells Odontoblasts Fibroblasts Lymphocytes	Vasodilation Plasma extravasation Chemotaxis Enhances macrophages activity Mitogen for lymphocyte
Trigeminal ganglion	Neurokinin A	NK 2	Mast cells Macrophages Mesenchymal cells Lymphocytes	Vasodilation Plasma extravasation Chemotaxis
Trigeminal ganglion	CGRP	CGRP 1, CGRP 2	Mast cells Macrophages Mesenchymal cells Ameloblasts Fibroblasts Lymphocytes	Vasodilation Plasma extravasation Chemotaxis Mitogen for odontoblasts
Parasympathetic ganglion	VIP	VPAC 1, VPAC 2	Mast cells Macrophages Lymphocytes Osteoblasts Osteoclasts	Vasodilation Immunomodulator Regulate inflammation

Summary

Following neuronal excitation, the effects of peripheral sensitisation of sensory neurones includes the axonal reflex i.e. release of ATP, neuropeptides, and nuclear factor translocation. Both effects can lead to neurogenic inflammation and the consequent amplification of pain signalling.

1.5 Roles of non-neuronal cells in responses to bacterial toxins

Another key step in nociceptive processing is the communication between sensory neurones and glial cells, such as satellite glial cells (SGCs), and Schwann cells. However, the role of SGCs in physiological pain is less clear since studies on the satellite glial cell have not been well established, unlike astrocytes. Satellite glial cells share many properties with astrocytes of the central nervous system, e.g. the expression of glutamine synthetase (Belzer et al. 2010), and various types of neurotransmitter transport. The possible roles of SGCs are:

1. Release of bioactive molecules and cytokines that potentiate neuronal transmission (Villa et al. 2010).
2. Maintain ionic homeostasis (Kristiansen and Edvinsson 2010).
3. Respond to release of neuronally active molecules, e.g. bradykinin, P2X7, P2Y (Suadicani et al. 2010), and neuropeptides (Takeda et al. 2009).

SGCs are thought to play key roles in the modulation of neuronal activity, through their abilities to communicate with neighbouring neurones by intercellular calcium waves (ICW) (Scemes and Giaume 2006), and by bi-directional communication in a paracrine fashion with neurones (Costa and Neto 2015).

1.5.1 Intercellular calcium wave (ICW)

SGCs and neurones in trigeminal ganglia can communicate through transmission of calcium signals. The activations of ICW between neurones and SGCs are thought to involve two mechanisms — ATP release and gap junction mechanisms.

Peripheral nerve sensitisation causes the release of ATP, which in turn stimulates SGCs via purinergic receptors, resulting in an increase of Ca^{2+} levels in the cells. The propagation of calcium waves from neurones to SGCs can also occur through gap junctions. As the calcium waves activates neighbouring cells, so the overall effects translate into a greater neuronal excitation (see Figure 1.19).

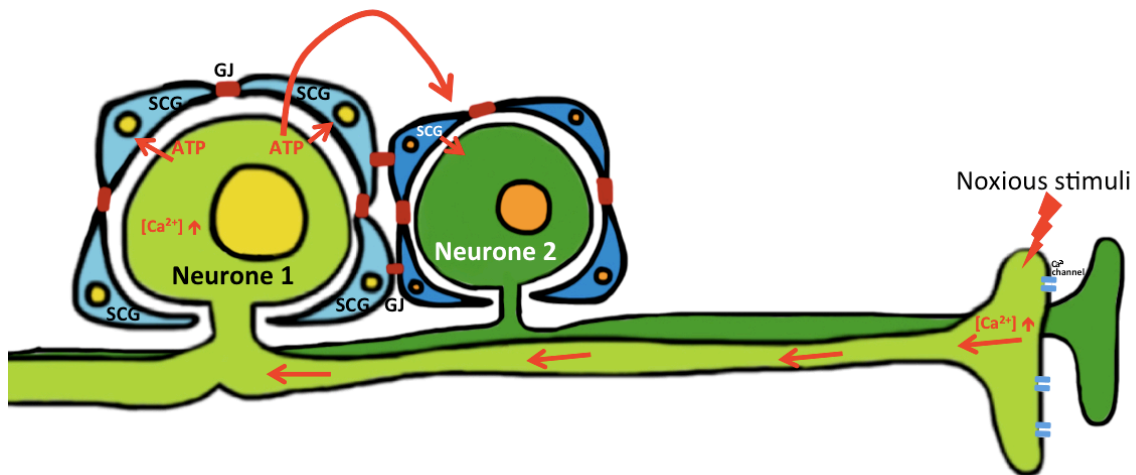


Figure 1.19 This figure shows the relationship between neurones and SGCs and the calcium wave in response to peripheral noxious stimuli.

This model shows the interaction between neurones and SGCs in response to peripheral stimuli. Peripheral sensitisation directs calcium wave movements from the terminal end to neuronal cell bodies. The neuronal calcium waves lead to the spread of ATP to their own SGCs and the neighbouring SGCs through gap junctions (Modified from Hanani 2015)

1.5.2 Bidirectional communication via paracrine functions

Activated SGCs are known to release cytokines, such as IL-1 β and tumour necrosis factor- α (TNF- α), which can potentially excite neuronal activities (Poulsen et al. 2014). All these can lead to the auto-amplification of the loop of neuronal sensitisation. As shown in Figure 1.20, there is bi-directional crosstalk between neurones and non-neuronal cells i.e. SGCs via a variety of channels (Suadicani et al. 2010; Ren and Dubner 2008).

The potential roles of SGCs include the clearance of extracellular potassium from active neurones. However, SGCs differ from astrocytes in some respects, e.g. their tight entrapment of neuronal cell bodies (Poulsen et al. 2014). This character enables SGCs to be highly responsive to ATP released from the neurones (Wang et al. 2012; Villa et al. 2010).

This cross-communication between neurones and non-neuronal cells can increase the excitability of primary afferents and centrally projecting neurones. This may suggest the supportive roles of satellite glial cells in the development of hyperalgesia and allodynia (Ren and Dubner 2008; Watkins and Maier 2002).

In order to explore how SGCs could orchestrate the inflammatory system and/or stimulate neurones in pain generation, an *in vitro* model of trigeminal ganglia cells represents one opportunity for studying the potential roles of receptors that are known to be involved in cell-to-cell communication. However, such a system will lack a co-ordinated immune system because no immune cells are present even though foetal calf serum is included in the culture medium. Also, the effects of laboratory culture conditions should be considered when interpreting the data. For example, the medium would lack local specific growth factors and the initial disruption of the TG would not necessarily result in cell re-association.

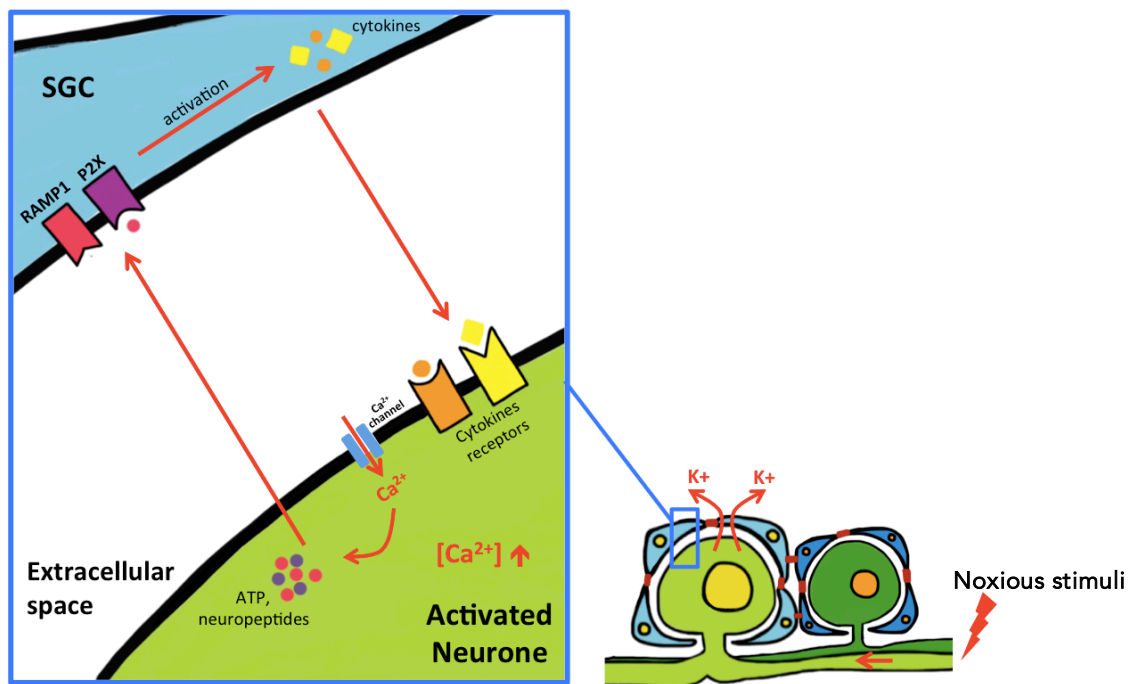


Figure 1.20 Paracrine-like interaction between neurone and SGC – examples of bi-directional talk signalling.

This figure summarises neurone-SGCs communication. The activated neurone exchanges Ca^{2+} and K^{+} ions, consequently releasing neurotransmitters such as neuropeptides, and ATP. These neurotransmitters can activate specific receptors on SGC. The activated SGC responds by releasing cytokines that can potentially stimulate neuronal excitation. These processes of extracellular communication perpetuate and form signalling amplification (Modified from Suadicani et al. 2010, permission granted to reproduce).

Summary

The bi-directional communication between neurones and SGCs in DRG and TG are unique to PNS. The communication of both types of cells is a crucial step in the transmission of pain signals. Such communication can be made through the calcium wave from cell-to-cell to maintain homeostasis of ions, and the neurotransmitters subsequently released can induce SGC activities. These characteristics may suggest the supportive roles of SGCs in pain development and possibly presents novel therapeutic targets for control of pain involving the PNS.

1.6 Methods used to study inflammatory pain

The main purpose of models to study pain is to gain new insights and to ultimately manage acute and chronic pain in humans. Although they aim to mimic the clinical conditions in humans, due to scientific and ethical considerations, the animal pain assessment has been developed. Animal and cellular models are the two most common models used.

1.6.1 Inflammatory pain model

1.6.1.1 *In vivo*

Using animal models, scientists can study the animal nocifensive behaviour e.g. the paw withdrawal that can be used to infer pain. Models to study orofacial pain mechanisms initiated in 1989 by Claveolou et al. They observed the rat's reaction after formalin injections and observed the nocifensive behaviour. Moreover, there are many reports shown that LPS from bacteria can cause death of CNS neurones *in vivo* (Kim et al., 2000; Eklind et al., 2001; Nguyen et al., 2002). Although, this method has been shown to be reliable for assessing pain in trigeminal area, there are many limitations of the models such as

- Animals can produce systemic therapeutic administration by themselves.
- The animal models could be confounded by providing the animal analgesic agents.
- Any deviation from normal behaviour can also suggest the pain in the animal, which could lead to misinterpretation.

1.6.1.2 *Ex vivo*

There are a number of reports that have shown the responses of neurones using *ex vivo* material. One such study showed neuronal activity in response to LPS (Donovan and Grundy 2012). However, most *ex vivo* work has mostly involved thermal stimuli, mechanical sensitivity, and measurements of behavioural output. *Ex vivo* skin-nerve recordings have been most informative in matching stimulus properties (such as intensity, frequency, speed, and adaptation) to specific fibre subtypes. However, there are a number of disadvantages of this model to be considered such as the limitation in the identification of the specific target cell response.

1.6.1.3 Primary sensory neurone cultures

Neurone culture is an integral part of contemporary study in neurobiology because this technique can be used to overcome difficulties associated with animal/organ models, in particular the study of detailed neurophysiology of nociceptors. Consequently the primary cultures of neurones provide unique insight into the neuronal cell body and axonal component independent of other cells (Higgins 1998).

Trigeminal ganglion sensory neurones in culture exhibit certain characteristics of those *in vivo* in the orofacial region. Sensory neurones conduct action potentials, following activation of the cells, which can then be observed using calcium imaging. Moreover, non-neuronal cells can be readily studied on the co-culture system as well since cell behaviour can be studied on a single cell basis (Higgins and Banker 1998). However, the cell culture systems that are commonly used do have some major limitations. These include the purity of the neuronal cell population, difficulty of long-term culture maintenance, and low cell numbers. Moreover, there are no immune cells or other elements of neuronal circuitry that may modulate responses. So, it is thought to be relevant to *in vivo* physiology, however, neurones in culture are not 'normal'.

1.6.1.4 Cell lines

Cell lines are another useful approach that offers a homogeneous population of neurones, uncontaminated by glia. This model may mimic certain aspects of *in vivo* signal transduction between the cells or within the cell. However, the cells are originally derived from neural tumour, the cell lines presently available for neurobiological research do not express some key aspects of neuronal differentiation (Banker and Goslin 1998). Therefore, cell lines may not reflect normal neuronal physiology or the complexity of this pain mechanisms.

In this study of the peripheral pain signalling, involving the pathological changes of trigeminal pain pathway at the peripheral level, primary cell culture is deemed the most promising model over *in vivo* or cell line culture, because it can replicate the

underpinning molecular pathways influencing bacterial interactions with neuronal cells. In addition, trigeminal cells culture may also exhibit certain characteristics specific to the orofacial region. We expect that this model to reflect mechanisms relevant to inflammatory pain originating from the orofacial area.

Summary

This section discusses the advantages and disadvantages of methods available for the study of inflammatory pain. While there are pros and cons for all experimental systems, it was considered that primary neuronal cell culture offered the best opportunity to study the cellular mechanisms of inflammatory pain activated by bacteria components.

1.7 Summary

This review of the literature aimed to define the gaps in the knowledge of peripheral mechanisms of pain that could be mediated by 3 neuronal cellular receptors, TLRs, TRPs, and PARs. The gaps in knowledge that could be raised from this literature review are an understanding of the mechanisms of bacterial stimulation of trigeminal nerves leading to symptomatic pulpitis and how environmental changes modify pathogenicity of bacteria that may alter neuronal activities. Because of the complexity of inflammatory processes, the mechanisms of pain due to odontogenic infections remain unclear.

Dental pain is generally thought to be caused by bacterial components indirectly activating nociceptors via the host responses (e.g. the release of cytokines triggering cytokine receptors). However, because TLRs, TRPs, and PARs are expressed on trigeminal neurone cell surfaces, it seems likely that bacteria or their components (e.g. LPS and gingipains) could directly activate sensory neurones through these receptors.

1.8 Hypotheses, aims and objectives

1.8.1 Hypothesis

Peripheral sensory neuronal cells (nociceptors) can be directly sensitised by bacterial LPS and other products, especially constituents of *Porphyromonas gingivalis*. This is based on two sub-hypotheses:

1. Trigeminal nociceptive neurones are directly sensitised by the structural element of a bacterial cell, e.g. LPS via the innate immune receptors (TLRs) on neurones. Also, the different structures of LPS formed under different growth conditions are known to interact with TLRs differently and it is expected that these will affect the neuronal pain pathway differently.
2. Bacterial proteases generated locally to the neurones in diseased pulp act directly through PARs, and this will impact on the pain pathways of neurones.

1.8.2 Thesis aims

This study aims to (1) determine whether cellular products of *P. gingivalis* can directly activate trigeminal neurones and (2) whether these can lead to the activation of neurones, as evidenced by the increased secretion of the neuropeptide CGRP and the translocation of NF- κ B.

1.8.3 Objectives

The specific objectives of this study were:

1.8.3.1 To develop a neuronal culture system from trigeminal ganglion.

- Optimise the culture protocol for use in a bacteria-challenge assay while investigating the conditions for CGRP-release assay.
- Characterise the cells present in the trigeminal cell culture obtained under each of the culture modifications.

1.8.3.2 To demonstrate the expression of TLRs, TRPs, and PARs on the trigeminal neurones and non-neuronal cells.

- Observe the changes in cellular receptor expression following incubation with *P. gingivalis*, and its components.

1.8.3.3 To study the functional characteristics of trigeminal cells, in particular calcium behaviour, in response to oral pathogenic bacteria, their components, and neuronal receptor agonists.

- Optimise the calcium-imaging techniques to observe a trigeminal cell culture.
- Develop the protocol to get a time-lapse record of cell response to various types of products and neuronal receptor agonists/antagonists.

1.8.3.4 To investigate the consequences of oral pathogenic bacteria and their components on neurones and non-neuronal cells e.g. CGRP release, NF- κ B expression.

- Quantify the levels of secreted CGRP in response to *P. gingivalis*, and its components.
- Observe the changes in NF- κ B expression following incubation with *P. gingivalis*, and its components

1.8.3.5 To investigate the potential influence of non-neuronal cells on neuronal activity.

- Observe the latency of non-neuronal cell responses, in particular the calcium flow activity in neuronal and non-neuronal cells.
- Quantify the levels of secreted CGRP in response to *P. gingivalis*, and its components in the presence of blockers of satellite glial cell activity.
- Observe the changes in NF- κ B expression following incubation with *P. gingivalis*, and its components in the presence of glial blockers.



Chapter 2

Materials and Methods



2. Methods

2.1 Materials

2.1.1 Chemicals

Acetic acid (glacial)	Fisher Chemical, UK
40% acrylamide/bis-acrylamide solution	Fisher Chemical, UK
Ammonium sulphate	Fisher Scientific, UK
Bovine serum albumin	Sigma-Aldrich, UK
Brain Heart Infusion Broth	Fisher Scientific, UK
Chloroform	Fisher Chemical, UK
Collagenase (type IV)	Sigma-Aldrich, UK
Cytosine β -D-arabinofuranoside	Sigma-Aldrich, UK
Dextrose	Sigma-Aldrich, UK
Dimethyl sulfoxide	Sigma-Aldrich, UK
DMEM/F12	Sigma-Aldrich, UK
DNAse	Qiagen, UK
Endotoxin-free water	Sigma-Aldrich, UK
Ethanol	Fisher Chemical, UK
Fastidious Anaerobic Agar	Lab M, UK
Fetal Bovine Serum (FBS)	Sigma-Aldrich, UK
5-Fluoro-5-deoxyuridine	Sigma-Aldrich, UK
Formaldehyde	Sigma-Aldrich, UK
Fungizone	Gibco, UK
Hanks' Balanced Salt Solution	Invitrogen, UK
Heamin	Sigma-Aldrich, UK
HEPES	Sigma-Aldrich, UK
Horse blood (oxalated)	Oxoid
36.23% Hydrogen Chloride	Sigma-Aldrich, UK
Isopropanol	Fisher Chemical, UK
Keto-3-deoxyoctonate	Sigma-Aldrich, UK
L-Cysteine	Sigma-Aldrich, UK

Laminin	Sigma-Aldrich, UK
LPS extraction kit	iNtron Biotechnology
N2 supplement	Invitrogen, UK
N- α -benzoyl-arginine 4-nitroanilide hydrochloride	Sigma-Aldrich, UK
Neural growth factor	Sigma-Aldrich, UK
Normal donkey serum	Sigma-Aldrich, UK
Penicillin (10 ⁴ U)/Streptomycin (10 ⁴ μ g/mL)	Gibco, UK
Periodate	Sigma-Aldrich, UK
Phosphate buffered saline (PBS); 0,1 M	Sigma-Aldrich, UK
Phosphate citrate buffer tablet	Sigma-Aldrich, UK
Poly-L-lysine	Sigma-Aldrich, UK
Poly-D-lysine	Sigma-Aldrich, UK
Proteinase K	Qiagen, UK
RMPI	Sigma-Aldrich, UK
RNAse	Qiagen, UK
Silver Stain Plus kits	Life Science Research, UK
Sodium Arsenite	Sigma-Aldrich, UK
Sodium bicarbonate	Sigma-Aldrich, UK
Sodium dodecyl sulphate	Fisher Chemical, UK
Sucrose	Sigma-Aldrich, UK
Sulphuric acid	Sigma-Aldrich, UK
3,3',5,5'-tetramethylbenzidine (TMB)	Sigma-Aldrich, UK
Thiobarbituric acid	Sigma-Aldrich, UK
Triton-X 100	Sigma-Aldrich, UK
TRIzol reagent	Life technologies
Trypsin	Sigma-Aldrich, UK
Tween-20	Sigma-Aldrich, UK
Urea	Fisher Chemical, UK
Uridine	Sigma-Aldrich, UK
Vectashield	Vectashield, UK
Vectashield with DAPI	Vectashield, UK

Vitamin K	Sigma-Aldrich, UK
Yeast extraction	Fisher Scientific, UK

2.1.2 Reaction systems

Bio-Rad protein assay	Bio-Rad Laboratories, UK
Human TNF- α ELISA Kit	eBioscience, UK

2.1.3 Expendable materials

11 mm diameter round glass cover slip	VWR international
12 well plates cell culture flasks	BDBioscience, UK
24 well plates cell culture flasks	BDBioscience, UK
96 well plates for ELISA	BDBioscience, UK

2.1.4 Buffer and solution formulae

2.1.4.1 Calcium imaging buffer

Table 2.1 The solution formula for calcium imaging buffer used during record.

Chemical	Calcium imaging solution (mM)	Potassium Chloride solution (mM)
NaCl	142	15
NaHCO ₃	5	5
HEPES	10	10
Glucose	16	16
KCl	2	60
CaCl ₂	2	2
MgCl ₂	1	1
BSA	0.1%	0.1%
pH 7.3 (adjust with HCl, or NaOH)		

2.1.4.2 Immunofluorescence assay

Table 2.2 Fixative and buffer used for immunofluorescence in this study.

Buffer and Solutions	Reagent	Amount or Volume
0.2M PB buffer pH 7.2	Na ₂ HPO ₄	21.8 g
	NaH ₂ PO ₄	6.4 g
	Distilled water	900 mL
	Stir until it is dissolved completely, adjust pH with HCl, then add dH ₂ O to 1L.	
4% paraformaldehyde (PFA)	Paraformaldehyde	40 g
	Distilled water	500 mL
	NaOH	10 µL
	Made fixative up on a hotplate with stirring bar until it dissolves completely, then adjust pH to 7.2.	
	0.2M PB buffer, pH 7.2	500 mL
0.1M PBS-Triton X	Na ₂ HPO ₄	1.16 g
	KCl	0.1 g
	K ₃ PO ₄	0.1 g
	NaCl	4 g
	Distilled water	500 mL
	Adjust pH with 1M HCl.	
	Triton-X	50 µL
Blocking solution (10% NDS in PBS-T)	Normal donkey serum	200 µL
	PBS-Triton	1800 µL
Diluent buffer (1% BSA in PBS)	BSA	0.5 g
	PBS-Triton	50 mL

2.1.4.3 Bacterial culture materials

Table 2.3 Brain heart infusion broth solution used in this study.

Buffer and Solutions	Reagent	Amount or Volume
Haemin	1M NaOH	100 μ L
	Haemin powder	5 g
	Distilled water	4900 μ L
	Stirred until dissolved.	
Cysteine	Cysteine powder	1.25 g
	Distilled water	5 mL
Vitamin K	Menadione sodium bisulphite	5 mg
	Distilled water	500 μ L
Brain Heart Infusion broth	Brain Heart Infusion	18.5 g
	Yeast extraction	2.5 g
	Distilled water	500 mL
	Autoclaved and supplements (haemin, cysteine, and vitamin K) then added after cooling.	

2.1.4.4 ELISA

Table 2.4 List of reagents used for ELISA in this study.

Buffer and Solutions	Reagent	Amount or Volume
Bicarbonate/carbonate coating buffer pH 9.5	Na ₂ CO ₄	3.03 g
	NaHCO ₃	6 g
	Distilled water	900 mL
PBS	Na ₂ HPO ₄	1.16 g
	KCl	0.1 g
	K ₃ PO ₄	0.1 g
	NaCl	4 g
	Distilled water	500 mL
	Blocking solution	
Blocking solution	BSA	2.5 g
	PBS	50 mL
Washing buffer (PBS-T)	Tween-20	150 μ L
	PBS	300 mL
Phosphate-citrate buffer pH 5.0	Phosphate-citrate buffer tablet	1 tablet
	Distilled water	100 mL
TMB solution	Phosphate-citrate buffer	10 mL
	TMB tablet	1 tablet
	H ₂ O ₂	2 μ L
Stop solution	Conc. HCl (36.23%)	20.13 mL
	Distilled water	100 mL

2.2 Primary trigeminal ganglia culture

2.2.1 Animals and animal housing

C57BL/6 wild type adult mice were used in this study. All animals were maintained on a 12-hour light/dark cycle in a temperature-controlled environment and given food and water *ad libitum*. All animal procedures were conducted in accordance with the Animal Surgical Procedure Act (ASPA) and approved by the UK Home Office. All procedures were carried out under the supervision of the Home Office licence holder, Professor F Boissonade.

2.2.2 Animal preparation and dissection

Mice were sacrificed by an overdose of isoflurane anaesthetic and cervical dislocation and the trigeminal ganglia (TG) surgically removed immediately. The ganglia are located at the base of the skull, as shown in the Figure 2.1.

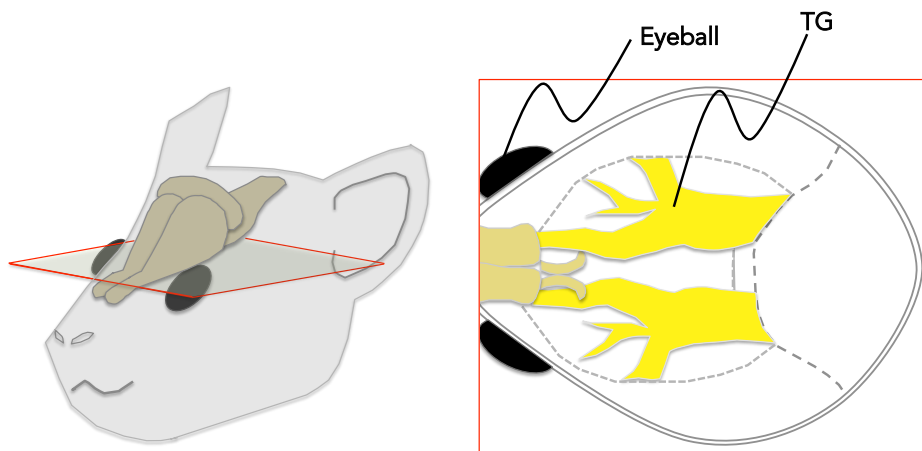


Figure 2.1 The location of trigeminal ganglia in mice.

The left figure shows the plane that is the location of trigeminal ganglia in the mouse at the surgical level. The right figure is the cross-sectional image of the base of the skull where the trigeminal ganglia (TG) are located.

2.2.3 Coverslip preparation

12-mm.-thickness number 1 glass coverslips (VWR) were washed in a 70% ethanol solution before being washed copiously with dH₂O and left to dry on filter paper in glass Petri dishes. Coverslips were then sterilised by autoclaving. Before use, the sterile coverslips were coated by 1% poly-L-lysine (PLL) in dH₂O for 30 min at the room temperature, then washed twice, and dried in a hood. The dried coverslips were coated by 20-50 µg/mL laminin-diluted in DMEM/F12 media for 1 h, then washed twice with culture media. The laminin-coated coverslips were protected from desiccation prior to the cell plating step.

2.2.4 TG culture

The ganglia were digested with 1.25% w/v Type IV collagenase twice for 60 min and 45 min, and 1.25% w/v of trypsin for 15 min at 37°C. After digestion, the TG were homogenised mechanically by pipetting up and down, and centrifuged at 1,500 × g for 3 min, and resuspended in Bottenstain and Sato medium (DMEM/F12 media, 1% w/v BSA, 1% N2 supplement, 1% PS). The mixtures were transferred to poly-L-lysine and laminin-coated coverslips that were placed at the bottom of 24-well tissue culture trays and cultured for 2 – 3 days with media change once after 24 h. All experiments on cultured cells were performed on day 2 – 3. The developments of protocols for neuronal cell culture will be described in Chapter 3: Culture system of trigeminal ganglia.

2.3 Bacterial culture

Freeze dried wild type (W50) *Porphyromonas gingivalis* was cultured anaerobically on Fastidious Anaerobe agar (FAA, LabM Ltd) supplemented with yeast extract (1 g/L) and 5% (v/v) horse blood for a week. *P. gingivalis* was then sub-cultured anaerobically in Brain Heart Infusion (BHI) broth supplemented with haemin 10 mg/mL, cysteine 250 µg/mL, and vitamin K 1 mg/mL at 37°C for 48 hours. Low haemin comprised BHI medium was supplemented with haemin 1 mg/mL, cysteine 250 µg/mL, and vitamin K 1 mg/mL.

Bacterial cells were harvested by centrifugation at 9000 rpm at 4°C for 20 min, and the pellet washed twice with PBS (centrifuged at 9000 rpm, 20 min, 4°C). The LPS was extracted from the bacterial cells using the following protocols.

2.4 LPS extraction method

In this study, the LPS from *P. gingivalis* was extracted using a commercial kit (iNtRON biotechnology). Briefly, whole bacterial cells (100 mg) were suspended in 1 mL of lysis buffer. The cell suspension was then incubated for complete cell homogenization before 200 µL of chloroform was added to create a phase separation. The mixture was then vigorously vortexed and incubated at room temperature for 10 minutes. The resulting mixture was centrifuged at 13,000 × g to separate the aqueous and organic phases and the aqueous phase was transferred into a new 1.5 mL microfuge tube, then 800 µL purification buffer was added to the organic phase. Subsequently, it was incubated at –20°C for 15 minutes, then the mixture was vortexed and centrifuged at 13,000 × g for 15 min. The LPS crude extract was washed in 70% ethanol and dried. 50 – 70 µL Tris-HCl buffer pH 8.0 was then added prior to sonication and storage at –20°C.

2.5 LPS analysis

2.5.1 Quantitative analysis; 2-Keto-3-deoxy-octonate (KDO) assay

Fifty microlitres of 2-Keto-3-deoxy-octonate (KDO) standards (0, 40, 80, 120, and 160 $\mu\text{g}/\text{mL}$), *E. coli* LPS (0.8, 8, 80, 800 $\mu\text{g}/\text{ml}$) and the *P. gingivalis* LPS extract were prepared. The LPS samples were carefully hydrolysed in 50 μL 0.5 N H_2SO_4 and incubated at 100 °C for 8 min. Then, KDO reacts successively with 50 μL of 22.8 mg/mL periodic acid, 200 μL of 40 mg/mL sodium arsenite and 800 μL of 6 mg/mL thiobarbituric acid to form a chromophore. The samples were centrifuged and the supernatants used for the determination of KDO by measuring the resultant colour at 550 nm,

2.5.2 Qualitative analysis; LPS gel

2.5.2.1 SDS-urea PAGE procedure

The LPS preparation was analysed by gel electrophoresis using a 15% resolving gel (3.75 mL of 40% acrylamide and 7 M urea in 1.5 M Tris-HCl buffer, pH 8.8). Polymerisation was initiated by adding 5 μL TEMED and 350 μL of 5% ammonium persulphate. Then, electrophoresis was performed at constant voltage (220V) and was stopped when the dye front reached the bottom of the gels.

2.5.2.2 Silver staining

After electrophoresis, the gels were fixed overnight in a solution containing 40% ethanol, 5% acetic acid. They were then soaked for 5 min in periodic acid solution (0.7% periodic acid, 40% isopropanol, 5% acetic acid) to oxidise the LPS. The gels were then rinsed in running distilled water for 2 hours, before silver staining (Silver Stain Plus; BioRad®) for 10 min with agitation according to the manufacture's protocol. After the gels were developed, they were rinsed and washed 3 times in distilled water (15 min/wash). To stop the staining reaction, they were washed with 0.35% acetic acid and fixed in this solution for at least one hour. Samples resolved on polyacrylamide gels were stained with coomassie blue in parallel to detect presence of contaminating protein bands.

2.5.3 Biological analysis

2.5.3.1 Stimulation protocol

THP-1 cells are human monocyte cells that can differentiate into macrophages. THP-1 cells in 6 well plates were fed with macrophage-serum free medium. The cells were then incubated with 200 ng/mL of phorbol myristate acetate (PMA) for 24 h to differentiate the THP-1s into macrophages. After incubation, non-attached cells were removed and attached cells were washed with RPMI 3 times. The cells were then stimulated for 4 h with 1, 5, and 10 µg/mL of extracted *P. gingivalis* LPS and 2 and 5 µg/mL of commercial *E. coli* LPS strain 055:B5 (Sigma) in fresh C-RPMI with 2% heat inactivated human AB serum. The supernatant was assayed for TNF- α release from the macrophages by ELISA.

2.5.3.2 TNF- α analysis

Human TNF- α was quantified by ELISA using a commercial kit (eBioscience, UK) and according to the manufacture's protocol. Briefly, samples and biotin-conjugated buffer were added to 96-well plates coated with anti-TNF- α and incubated for 2 h. Consequently, streptavidin-HRP buffer was then added and incubated for 1 h. Wells were then developed using the chromogen, tetraethyl benzidine (TMB) for 30 min. The reaction was stopped by the addition of stop solution and the absorbance read at 450 nm.

2.6 Determination of *P. gingivalis* Arg- and Lys-gingipain proteolytic activity using chromogenic substrates.

These analyses were performed in sterile 96-well microtiter plates. The Arg-gingipain proteolytic activity was assessed by its ability to breakdown N- α -benzoyl DL-arginine-p-nitroanilide (BAPNA), while, Lys-gingipain activity was determined by release of nitroanilide from N-(p-Tosyl)-Gly-Pro-Lys-4-nitroanilide acetate (GPK-NA).

2.6.1 N- α -benzoyl DL-arginine-p-nitroanilide (BAPNA)

0.5 mg/mL N- α -benzoyl DL-arginine-p-nitroanilide (BAPNA) was dissolved in DMSO and diluted in 50 mM Tris buffer pH 8.0. The BAPNA solution was incubated with the test preparation, or positive control (50, 100 μ g/mL trypsin) at 37 °C for 15, 30, 60, 90, 120, 180 min time points. The absorbance was read at 410 nm. For 96-well plate, 200 μ L of BAPNA substrate were incubated with 50 μ L of sample per well. A graph was plotted with absorbance (y-axis) versus concentration of trypsin (x-axis) to determine unknown proteolytic activities of Rgp.

2.6.2 N-(p-Tosyl)-Gly-Pro-Lys-4-nitroanilide acetate salt (GPK-NA)

0.5 mg/mL N-(p-Tosyl)-Gly-Pro-Lys-4-nitroanilide acetate salt (GPK-NA) was dissolved in DMSO and diluted in 400 mM Tris buffer pH 8.0. The GPK-NA solution was then incubated with the test preparations or positive control (50, 100 μ g/mL trypsin) at 37 °C at 15, 30, 60, 90, 120, 180 min time points. The absorbance was read at 410 nm. For 96-well plate, 200 μ L of GPK-NA substrate were incubated with 50 μ L of sample per well. A graph was plotted with absorbance (y-axis) versus concentration of trypsin (x-axis) to determine unknown proteolytic activities of Kgp.

2.7 Intracellular calcium measurements

Calcium imaging is a useful technique for measuring individual cell responses and in this context of the activities of cultured neurones. This technique benefits from the behaviour of calcium dyes that change with the flux of intracellular calcium. The dyes can be grouped into 2 types: ratio-metric and single wavelength.

Two of the single wavelength calcium indicators are Fluo-4 AM, and Cal-520 AM, ester dyes, can be passively loaded into cells. Upon entry into the cell, the ester is cleaved by esterases and the dye becomes membrane impermeable, this allows non-invasive measurement of intracellular calcium activity. Fluo-4AM, and Cal-520AM have a single emission peak of 488nm but dual calcium dependant excitation peaks (340nm and 380nm). One of the most common calcium indicators is Fura-2AM which has an emission peak at 505 nm, and a shift in its excitation peak from 340nm to 380 nm in response to calcium binding (Barreto-Chang and Dolmetsch 2009). This is the representative mechanisms for detecting the emission wavelength of calcium dye, as shown in Figure 2.2 Cal-520 AM calcium detection mechanisms.

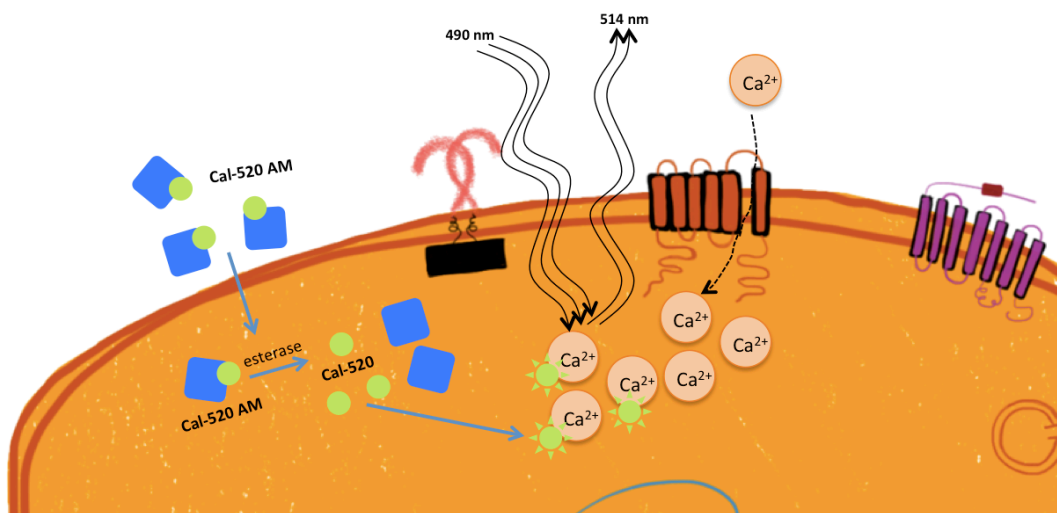


Figure 2.2 Calcium dye detection mechanisms.

This is an example of calcium dye, Cal-520 AM, that can cross cell membrane, and can be cleaved by intracellular esterases, resulting in the negative charges of the fluorescence molecules. The fluorescence can be enhanced upon binding to calcium ions. Stimulated neurones increase intracellular calcium. Consequently, there will be an increase in the fluorescence of Cal-520. For calcium probing, Cal-520 can be excited by the wavelength at 490 nm, and the fluorescence can be detected via the emission wavelength at 514 nm.

2.7.1 Microscopic set up and imaging acquisition

Coverslips were placed into a Warner recording chamber (bath dimensions (l × W × H) 24 × 13 × 4.1 mm, volume by depth 133 μ L/mm) (RC-25F, Warner instruments) and perfused with calcium imaging buffer from a syringe. The time taken for the solution to reach the recording chamber was 20s, determined by monitoring the flow of a dye into the recording chamber, the flow rate being 5mL/min. Vehicle control were tested in parallel as negative control. Obtained images have been adjusted accordingly. Syringes present on a perfusion rack were used to apply additional solutions when required. Each syringe was aligned at the same height and stoppers with tubing were placed into the syringes to ensure a constant flow rate. The outflow of the recording chamber was a bevelled needle connected to a length of silicone tubing, with a suction pump (Watson Marlow SciQ 323) being used to draw the fluid into a waste bottle. Figure 2.3 shows a diagram of the recording set up used.

Coverslips were mounted onto a Zeiss Axiovert S100TV inverted microscope and viewed using a 40 \times objective (NA1.3, Zeiss), which enabled the visualisation of individual cells. Cells were subsequently illuminated at 488nm and images taken at 6s intervals. The excitation wavelength was specifically selected via the excitation filter. While the emitted light was passed through an emission (510 – 540 nm band-pass) filter before detection and detected using a cascade 512B CCD camera (Roper scientific, Photometrics UK). Timelapse images were recorded using WinFlour[®] software. Meanwhile, the fluorescence values, background subtracted, corresponding to each frame of each cell could be exported for further analysis. The graph plotting and analysis was performed using Prism software (GraphPad).

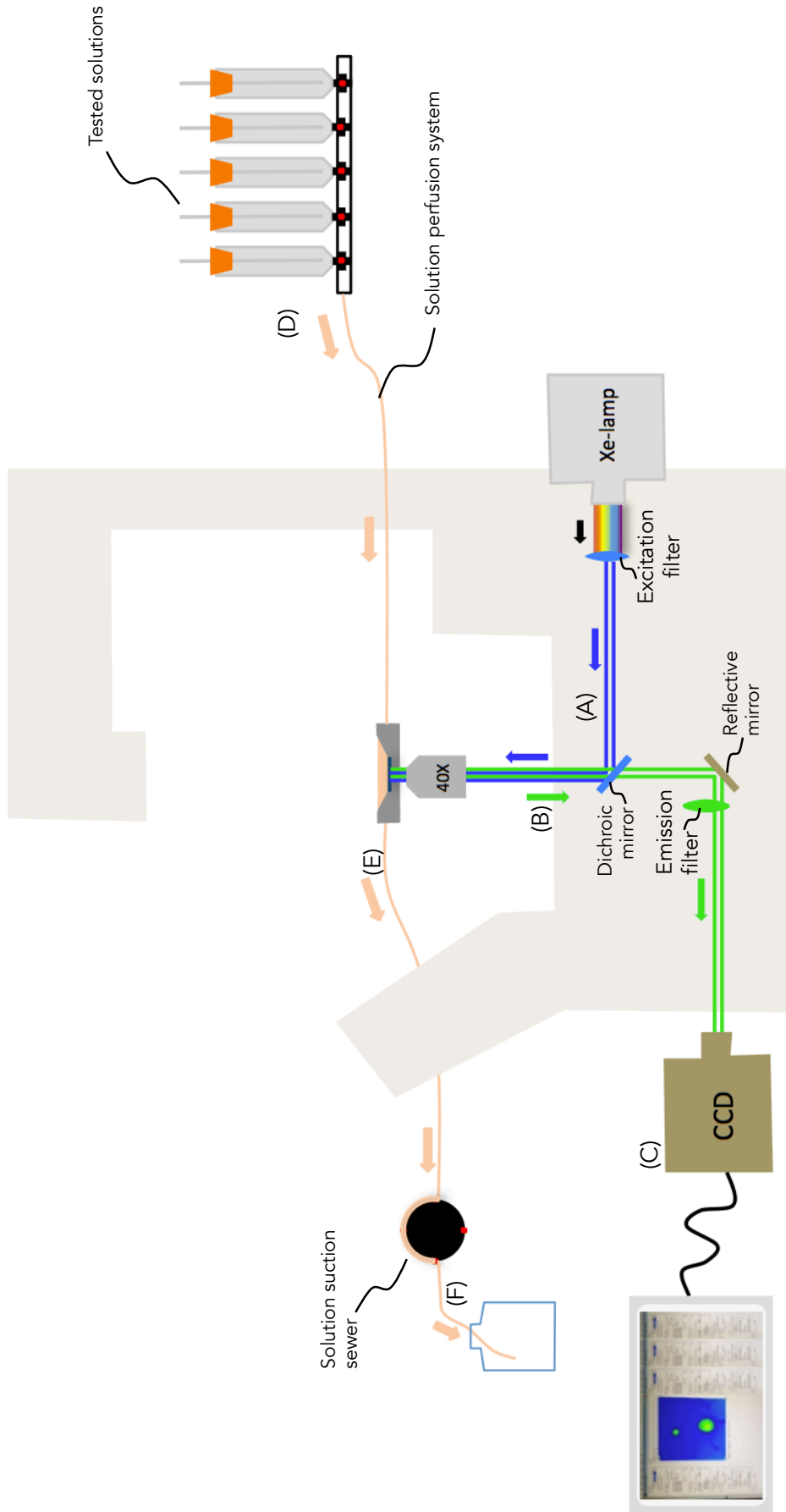


Figure 2.3 Overall scheme of calcium image system configuration.

This shows the inverted microscope apparatus with light source to create excitation wavelength. Coverslips were mounted onto an inverted microscope which enabled the visualisation of individual cells. Cells were illuminated at 488nm. The excitation wavelength was produced via the excitation filter (A), while the emitted light was passed through an emission (510 – 540 nm band-pass) filter (B) before detection using a cascade 512B CCD camera (C). Coverslips were placed into a Warner recording chamber and perfused with external imaging solution from a solution syringe. The calcium levels were determined by monitoring the flow of a dye into the recording chamber. The obtained images have been adjusted accordingly. For the perfusion system, each syringe was aligned at the same height and stoppers with tubing were placed into the syringes to ensure a constant flow rate (D). The outflow of the recording chamber (E) was a bevelled needle connected to a length of silicone tubing, with a suction pump being used to draw the fluid into a waste bottle (F).

2.7.2 Loading of cells with dyes

TG (2 day) cultured cells on coverslips were washed with culture medium and flooded with loading medium containing 5 μM of either Fura-2AM, Fluo-4AM, or Cal-520AM (1 mM stock in DMSO) in DMEM/F12, and placed in a 5% CO_2 humidified atmosphere at 37°C for 60 min. Coverslips were protected from light at all stages. A range of loading solutions and conditions for trigeminal neurones were tested.

2.7.2.1 Fura-2 AM

Fura-2 AM can diffuse across the cell membrane and the dye is then de-esterified by cellular esterases to yield Fura-2 free acid. Following a 1-hour incubation of dye loading, the coverslip were removed from the loading solution and placed in the fresh DMEM/F12 for 30 min before the coverslip was mounted on the imaging chamber (Barreto-Chang and Dolmetsch 2009). Figure 2.4 shows the fluorescence of trigeminal cell calcium images labelling by Fura-2 AM. However, upon binding to calcium, the excitation spectrum of Fura-2 AM would shift to shorter wavelength from 380 nm to 350 nm as shown in Figure 2.5. Because the intensity of the wavelength is increased proportionally, the calcium level could be represented by the ratio of wavelength intensity of 340nm/380nm.

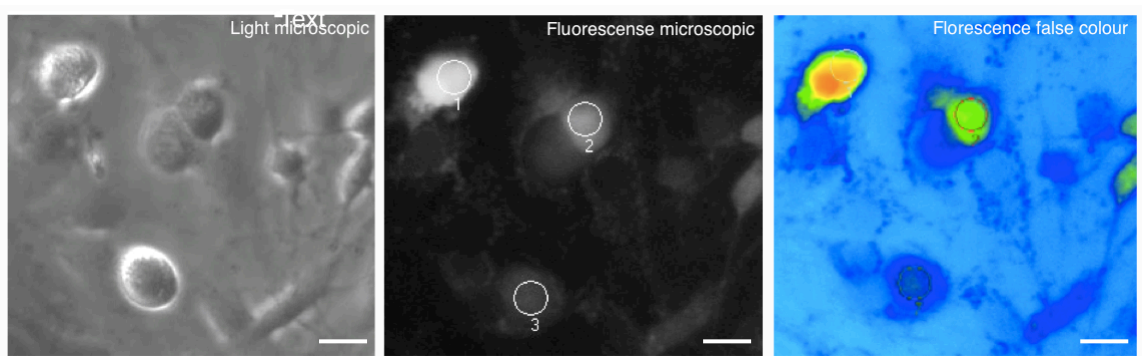


Figure 2.4 Fura-2 AM dye loaded in trigeminal cultured cells.

These are the images of trigeminal cultures loaded by Fura-2 AM at the basal level of intracellular calcium concentration. The left panel is phase-contrast, middle is the fluorescence image at 340 nm, the fluorescence can be converted to false colour as shown in right panel. Scale bar = 30 μm .

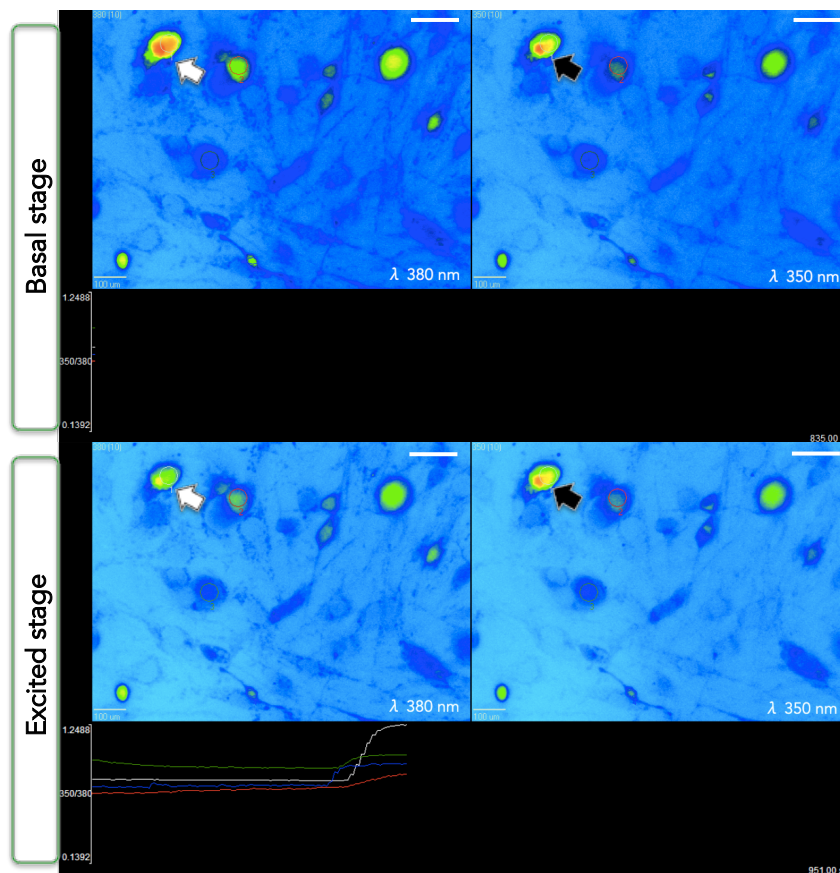


Figure 2.5 The TG cells loaded with Fura-2AM at the basal and excited stages.

Ca²⁺ levels were measured by loading cells with the ratiometric fluorescent dye Fura-2AM. Ca²⁺ levels were represented as the intensity of the fluorescence emitted at 380 nm and 350 nm after the excitation with 505 nm. Upper 2 panels are TG cells at the basal stage viewed at wavelength 380 nm (A) and 350 nm (B). Lower 2 panels are TG cells at the activated stage in presence of 60 nM KCl viewed at wavelength 380 nm (C) and 350 nm (D). Fura-2 ratios (350/380 nm) of representative cells in the presence of KCl (C, D) were traced as shown in panels C and D. Once the cells were activated, the intensity of 380 nm wavelength decreased (white arrows), while the intensity of 350 nm wavelength slightly increased (black arrows). Scale bar = 60 μm.

2.7.2.2 Fluo-4 AM

Fluo-4 is a high calcium ion affinity dye that has a large dynamic range of visible fluorescence upon binding cytosolic calcium. This dye has, therefore, gained widespread acceptance as an intracellular calcium probe (Gee et al. 2000). The dye can diffuse across the cellular membrane, and cellular esterase can cleave Fluo-4 AM to release Fluo-4 which can bind intracellular calcium and show visible wavelength at 514 nm (Barreto-Chang and Dolmetsch 2009). Ca^{2+} levels can be represented as the intensity of the fluorescence emitted at 520 nm after the excitation with 488 nm. Similar to the Fura-2 AM method above, after 1-hour of dye loading, the coverslips were removed from the loading solution and placed in fresh DMEM/F12 for 60 min before being placed in the imaging chamber. Typical images labelling by Fluo-4 AM are shown in Figure 2.6. Because this dye showed a poor signal-to-noise ratio, background/basal calcium detection was relatively low. Therefore, we have tried another single wavelength dye loading such as Cal-520AM as outlined in the following section.

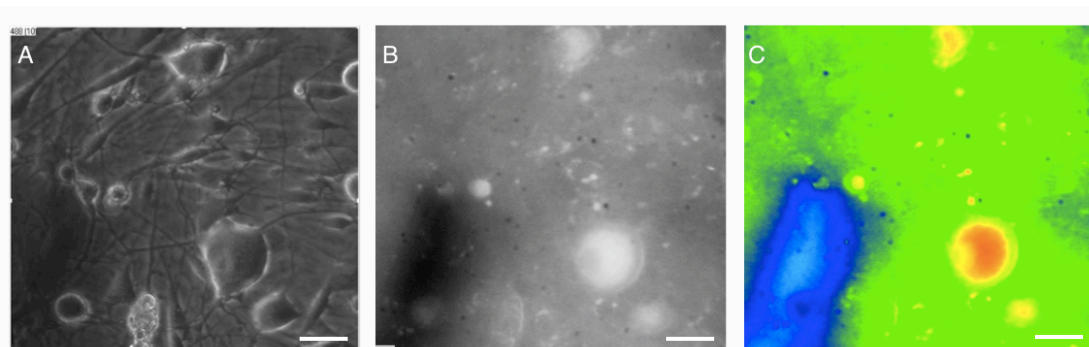


Figure 2.6 Fluo-4 AM loaded in cultured trigeminal cells.

Images of trigeminal cultured cells at the basal stage of calcium levels. The left panel is a phase contrast microscopical image, while the middle and right panels show grey and false colour fluorescence images of the cells at wavelength 488 nm, respectively. Scale bar = 30 μm .

2.7.2.3 Cal-520 AM

TG (2 day) cultured cells on coverslips were washed with culture medium and flooded loading medium, 5 μ M of Cal-520 AM (1 mM stock in DMSO) in DMEM/F12, and placed in a 5% CO₂ humidified atmosphere at 37°C for 60 min. Coverslips were protected from light at all stages. Cal-520 AM is a single wavelength calcium dye that can pass through the cellular membrane and the AM group is cleaved by esterase. Ca²⁺ levels can be represented as the intensity of the fluorescence emitted at 520 nm after the excitation with 488 nm. However, Cal-520 AM shows very good signal-to-noise ratio as shown in the Figure 2.7. Following an hour incubation of Cal-520 AM dye loading, the coverslip could be mounted on the imaging chamber straight away without a washing step. Upon binding to calcium, at excitation wavelength 488 nm the fluorescence signal increased (Figure 2.8).

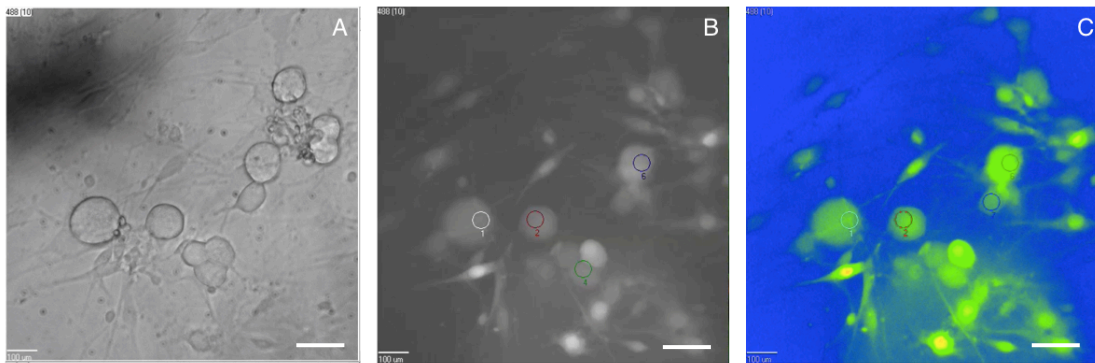


Figure 2.7 Expression of calcium concentration in trigeminal cultured cells loaded with Cal-520 AM.

Images of basal stage trigeminal cells, phase-contrast (A), fluorescence image (B), and false colour of calcium intensity (C). Scale bar = 30 μ m.

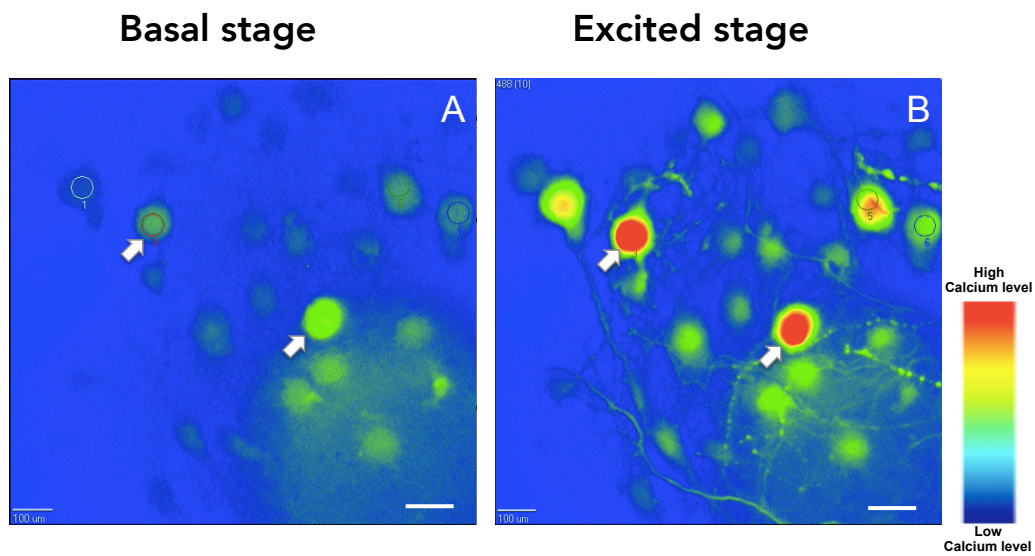


Figure 2.8 The basal and activated stages of cultured trigeminal cells loaded with Cal-520 AM.

Representative images show fluorescence intensity at (A) basal stage, and (B) a time-lapse calcium image during KCl application. The calcium image colour range is shown on the right. Intracellular calcium shifted from green (arrows in panel A) to red (arrows in panel B) which represents medium to high calcium levels in response to the stimulus. ($\lambda_{ex} = 488 \text{ nm}$, $\lambda_{em} = 520 \text{ nm}$). Scale bar = $40 \mu\text{m}$.

2.7.3 Sequences of the treatment in calcium records

The sequence of placement of the materials to be on the TG cultures was crucial as it could affect the behaviour of the TG neurones. Upon the recognition by cellular membrane receptors, cellular signalling would result in the alteration of the levels of key surface proteins and disturbance to the intracellular concentrations of calcium. Therefore, it was important to consider the treatment time and resting interval to allow calcium to be restored to the basal level before application of another agonist. The optimal sequence in our experiment is outlined in Figure 2.9. The tested bacteria and bacterial product, either LPS, or gingipain, were applied for 2 min after the basal calcium level was recorded. This was followed by 1-minute application of TRPA1 agonist (200 μ M cinnamaldehyde), and TRPV1 agonist (2 μ M capsaicin). Finally, to determine the viability of the neurones present, 60 mM potassium chloride solutions were applied.

2.7.4 Calcium imaging analysis

Images were analysed by regions of interest surrounding the individual cells by using WinFlour (Fluorescence image software). The background fluorescence corresponding to each frame was digitally subtracted from the fluorescence value for each cell at each wavelength.

Cells were classified as 'responding' to a particular stimulus when fluorescence, measured as a region of interest (ROI) placed over the whole cell, increased by more than 10 standard deviations over the baseline fluorescence. Baseline fluorescence was measured as the average of the last 10 frames before application of tested products or agonists. Data is presented as the changes in intensity of fluorescence between the baseline and peak of the activated curve. This calculation was used to account for variations in the starting fluorescence of individual cells. Moreover, the responding cells to a particular stimulus could be scored by eye, as the calcium trace was transiently elevated according with stimuli exposures (Figure 2.10).

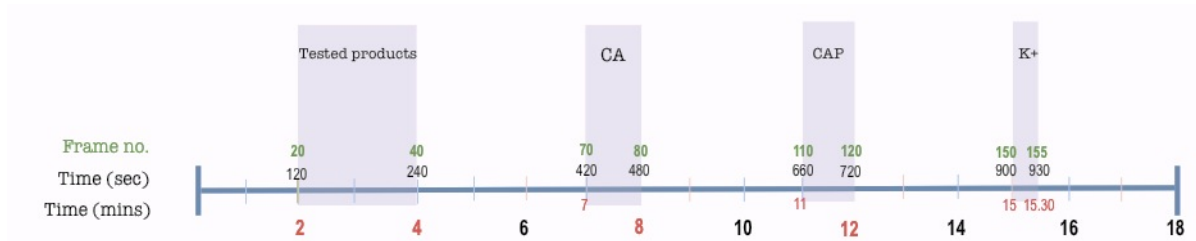


Figure 2.9 The timeframe to challenge cultured TG cells with various test materials.

The cultured cells were exposed to bacterial products for 2 min, followed by cinnamaldehyde (CA), capsaicin (CAP) for 1 min each, and 60 mM potassium chloride (KCl) for 30 s. The TG cells were allowed to rest after each application by application of fresh wash solution.

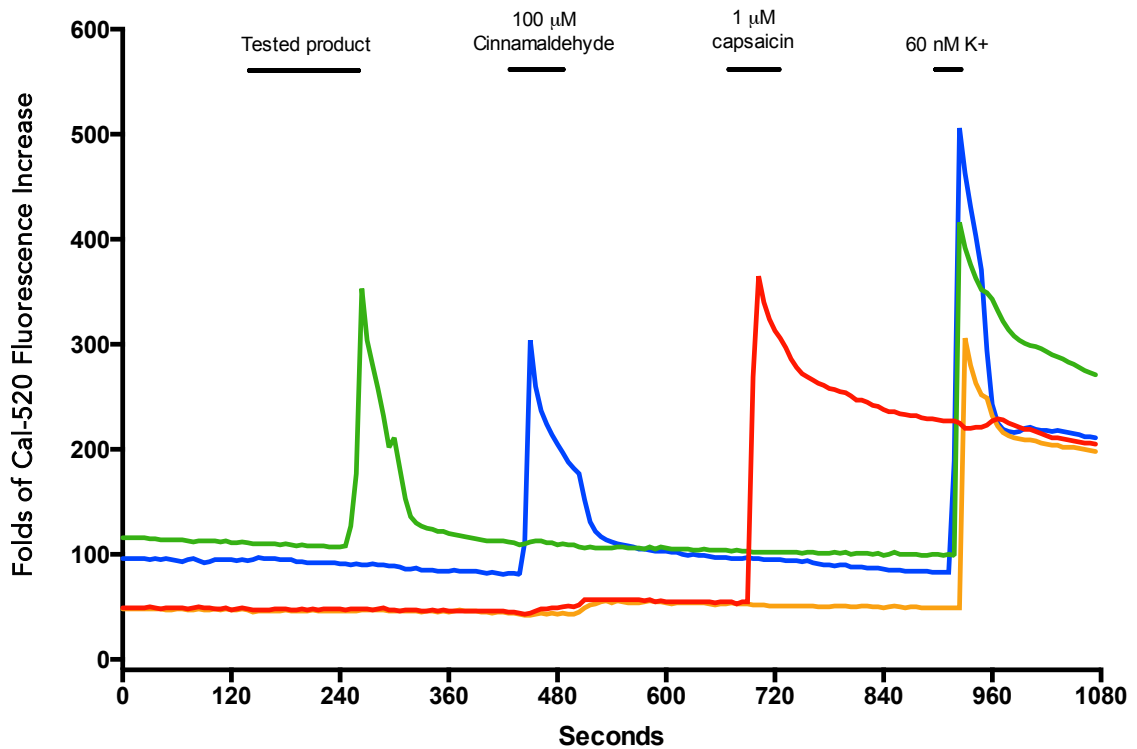


Figure 2.10 The principle of quantification of response to test materials and TRPA1 and TRPV1 agonists.

Calcium traces of individual cells could be obtained from fluorescent intensities of Cal-520 AM. Each cell was analysed by regions of interest surrounding the individual cells. Responding cells to each product/agonist could also be scored and each cell in each representative trace is the calcium level that was recorded overtime. In this example the green trace would represent the cell that responded to test material while the blue, red, and orange traces would represent the cells that responded to cinnamaldehyde, capsaicin, and 60 mM K⁺, respectively.

2.8 Cultured TG stimulation protocols – for CGRP quantification, and IHC analysis

To analyse the consequences of activated TG cells following activation by bacteria or their constituents, we determined the release of the neuropeptide calcitonin gene related peptide (CGRP) into the culture supernatant, and determined the nuclear translocation of NF- κ B in the cells. The cell experiments were performed on day 2–3 of culture, at 37°C, using modified HBSS (Invitrogen) (10.9 mM HEPES, 4.2 mM sodium bicarbonate, 10 mM dextrose, and 0.1% bovine serum albumin in 1× HBSS). After 2 initial washes with PBS buffer, the cells were exposed to the test materials such as LPS, gingipains or whole bacteria (10^8 bacteria/mL) in PBS. The supernatants and attached cells were harvested after 15 or 30 minutes treatment to detect CGRP by ELISA, and/or analysis of particular molecules by immunofluorescence.

2.9 Reagent blockers

CLI-095, HC-030031, and minocycline are thought to specifically inhibit TLR4, TRPA1, and glial cell activity, respectively as shown in Table 2.5.

Table 2.5 Blocking reagents and the administrations used in this study.

Reagents	Targets	Concentrations	Administrations
CLI-095	TLR4-mediated signalling	1 μ M	1 h. prior to the exposure and co-treatment with tested products as described in Tse et al. 2014.
HC-030031	TRPA1	3 μ M	2 min prior to the exposure and co-treatment with tested products as described in Eid et al. 2008.
Minocycline	p38 MAPK pathway of glial cells	30 μ M	1 h. prior to the exposure and co-treatment with tested products as described in Gong et al. 2010.
Capsazepine	TRPV1	10 μ M	2 min prior to the exposure and co-treatment with tested products as described in Henrich and Buckler 2009.

2.10 Immunohistochemical analysis

For the immunofluorescence microscopy experiments, TG neurones were cultured on coverslips in culture wells, washed twice with 0.1 M PBS and fixed in 4% paraformaldehyde (PFA) for 40 min. Non-specific antibody-binding sites were blocked with 10% Normal Donkey Serum (NDS) and 0.5% Triton X-100 in PBS for 1h at room temperature. The cell-coated coverslips were then incubated in primary antibodies (Table 2.6) in 1% NDS with 0.5% Triton X-100 solution at room temperature for 1h. Cultures were washed twice in PBS with 0.5% Triton X-100 and incubated with according secondary antibodies (Table 2.6) in 1% NDS with 0.5% Triton X-100 in PBS solution at room temperature for 1h. Finally, the cultures were washed twice in PBS and slides were mounted with Vectashield containing DAPI (Vector Labs) and visualised by fluorescence microscopy. Immunohistochemistry controls for all antibodies were performed by omitting the primary antibodies. No positive labelling was observed in any of the controls. Images of TG cultures were acquired with a Zeiss Axioplan microscope with Qimaging Retiga 1300R camera and ImagePro® Image software (version 5; Media Cybernetics, Bethesda, MD). All positive cells in each coverslip were counted and expressed as percentage of the total number of cells present.

Table 2.6 Details of all primary antibodies and relevant secondary fluorescent labels employed in study.

Primary antibody	Supplier	Species raised in	Dilution	Appropriate secondary antibodies		
				Conjugate	Fluorochrome	Host species
β-tubulin III	Covant	Mouse monoclonal	1:1000	Anti-mouse	FITC	Donkey
	Abcam	Chicken polyclonal	1:1000	Anti-chicken	FITC	Donkey
GS	Abcam	Rabbit polyclonal	1:1000	Anti-rabbit	Cy3	Donkey
GFAP	Abcam	Rabbit polyclonal	1:750	Anti-rabbit	Cy3	Donkey
S-100	Dako	Rabbit polyclonal	1:250	Anti-rabbit	Cy3	Donkey
TLR4	NovusBio	Rabbit polyclonal	1:200	Anti-rabbit	Cy3	Donkey
TLR7	NovusBio	Rabbit polyclonal	1:1000	Anti-rabbit	Cy3	Donkey
TRPA1	ThermoFisher	Goat polyclonal	1:50	Anti-goat	Cy3	Donkey
TRPV1	Abcam	Rabbit polyclonal	1:750	Anti-rabbit	Cy3	Donkey
PAR2	NovusBio	Rabbit polyclonal	1:1000	Anti-rabbit	Cy3	Donkey
CGRP	Sigma	Mouse monoclonal	1:1000	Anti-mouse	Cy3	Donkey
				Anti-mouse	FITC	Donkey
p65 NF-κB	ThermoFisher	Rabbit polyclonal	1:200	Anti-rabbit	Cy3	Donkey
CD14	Strattech	Rabbit monoclonal	1:200	Anti-rabbit	Cy3	Donkey

2.11 Immunohistochemistry imaging analysis

To enable image analysis, fluorescent images were captured and displayed on a secondary monitor. All fluorescent images of cellular receptors such as TLR4, TLR7, TRPA1, and TRPV1 were taken with a 20× or 40× objective lens. The initial exposure time of each channel was chosen from optimal exposure and then it was kept constant between the experiments. In this study, we performed (1) analysis of cellular surface expression, (2) PAR2 expression, and (3) NF- κ B nuclear translocation.

2.11.1 Cellular surface expression

Positive protein receptor expression was classified as either present or not present with the relevant protein according to whether fluorescence could be seen by eye. Images were analysed for each of three independent experiments. An example of how cellular protein expression was quantified is illustrated in Figure 2.11.

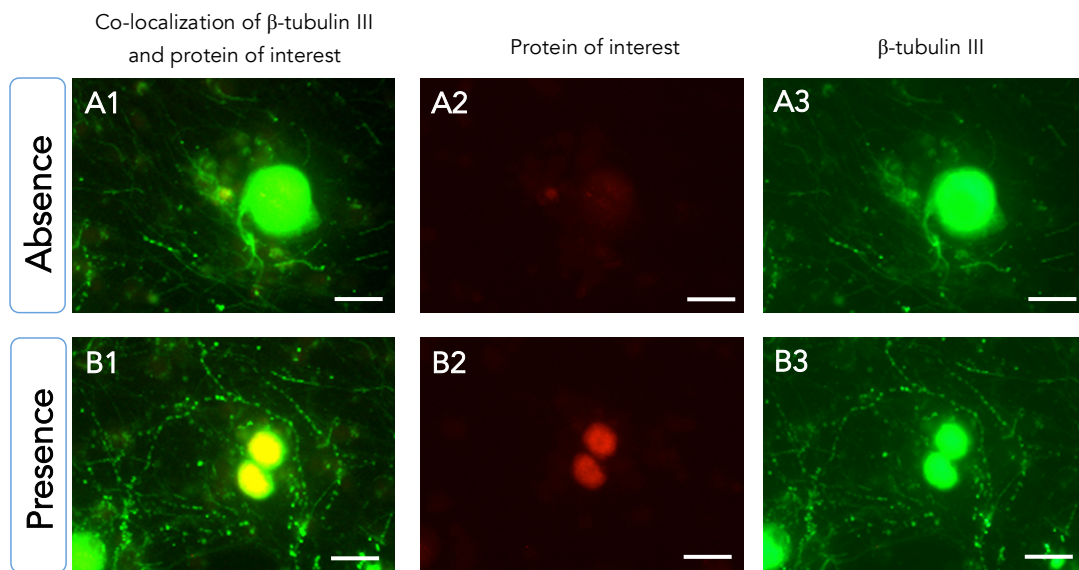


Figure 2.11 The principle of quantification of receptor occupancy.

Acquired images from fluorescent microscope were scored for receptor presence in TG culture by eye. The receptor of interest could be scored as either clearly absent (top panel) or present (bottom panel). Scale bar = 50 μ m.

2.11.2 PAR2 expression

As another approach that was applied to relative expression of PAR2, fluorescent intensities of cells were obtained using the 'statistic' facility within ImagePro® software. The area of interest (AOI) could be selected from cells by outlining and, for neurones, comparing that to the intensity of β -tubulin III staining (Figure 2.12).

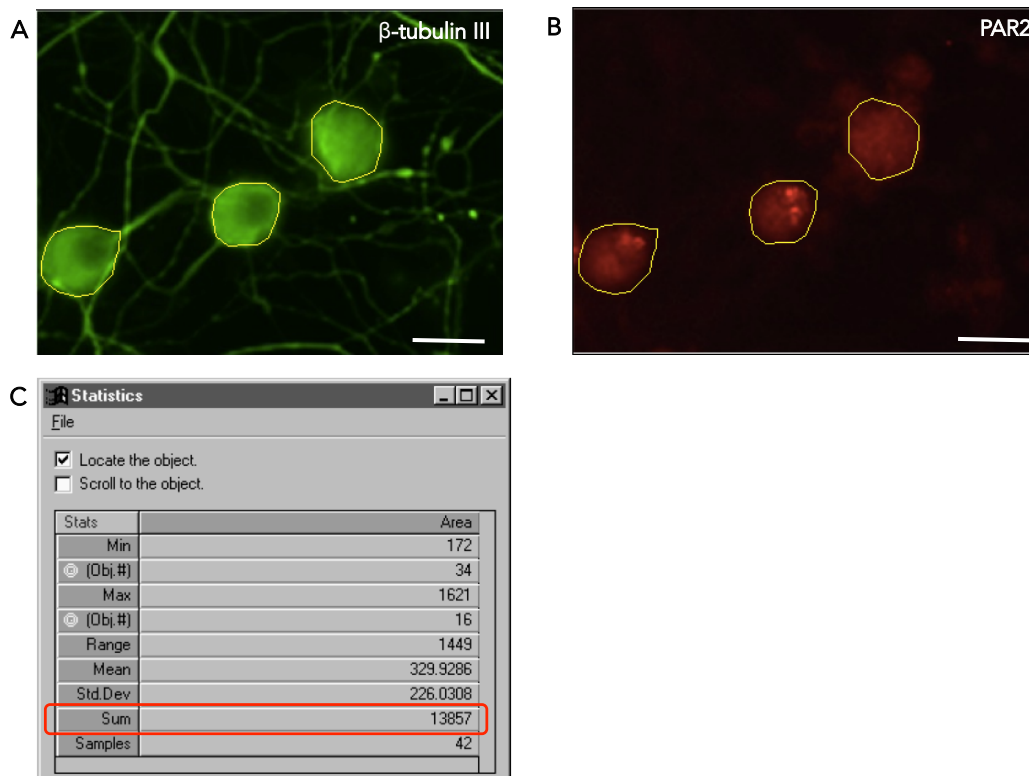


Figure 2.12 The principle of quantification of neuronal PAR2 expressions.

Neuronal outlines could be verified from β -tubulin III channel (A). Neuronal outlines were then replicated onto PAR panel to identify PAR2 area of common (B). Summary of area of labelling from either β -tubulin III or PAR2 could be obtained from 'Statistic' function within ImagePro® (C). Scale bar = 30 μ m.

Neuronal PAR2 expression was calculated as a percentage of PAR2/ β -tubulin III area of labelling as below and data were analysed from each of three independent experiments.

$$\% \text{ neuronal PAR2 expression} = \frac{\text{intensity of PAR2 labelling}}{\text{intensity of } \beta\text{-tubulin III labelling}} \times 100$$

2.11.3 Assessment of NF- κ B translocation

NF- κ B nuclear translocation was determined by observing NF- κ B in the cytoplasm shifting to the nucleus. Through immunohistochemistry, we analysed the relative intensity of NF- κ B staining in either the nucleus or cytoplasm by co-localization with DAPI (nuclear stain) which allowed determination of the proportion of NF- κ B in nuclear and cytoplasmic locations. The microscopic images were outlined, and the labelling was analysed as shown in Figure 2.13.

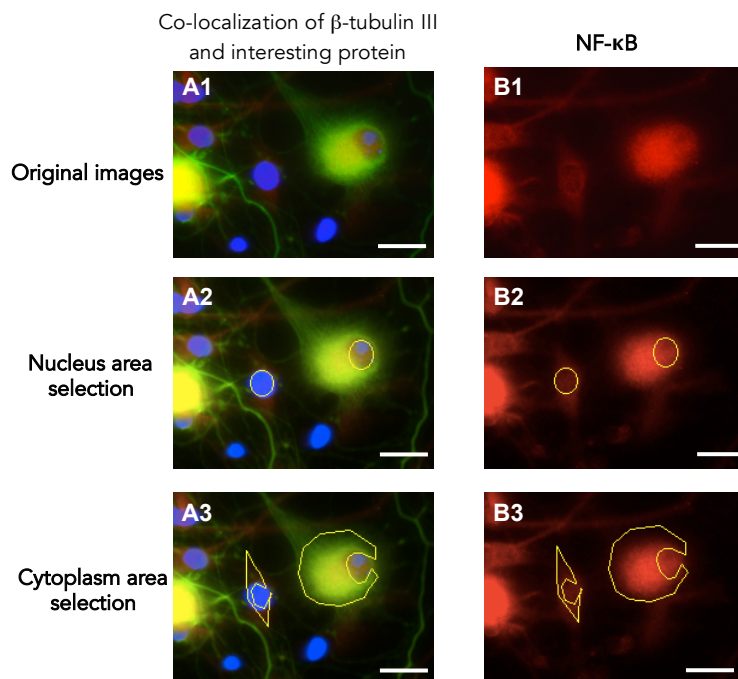


Figure 2.13 Analysis of immunolabelling of NF- κ B location.

Representative microscopic images of co-localisation of β -tubulin III, NF- κ B, and DAPI (A1-3) and NF- κ B image (B1-3). The figure is an example of a TG culture showing selection of labelling of the nucleus (A2, B2) and cytoplasm (A3, B3) compared with the original images (A1, B1). Scale bar = 50 μ m.

Positive cells that have NF- κ B located in the nucleus could also be classified as either translocated or not translocated according to whether fluorescence could be seen in the nucleus. Positive NF- κ B nuclear translocated cells were counted when proportion of NF- κ B labelling in nucleus/cytoplasm was greater than or equal to 1.

Positive NF- κ B nuclear translocated cell was;
$$\frac{\text{mean intensity in nucleus}}{\text{mean intensity in cytoplasm}} \geq 1$$

An example of how the NF- κ B nuclear translocated neurones and non-neuronal cells were quantified is illustrated in Figure 2.14, and Figure 2.15, respectively.

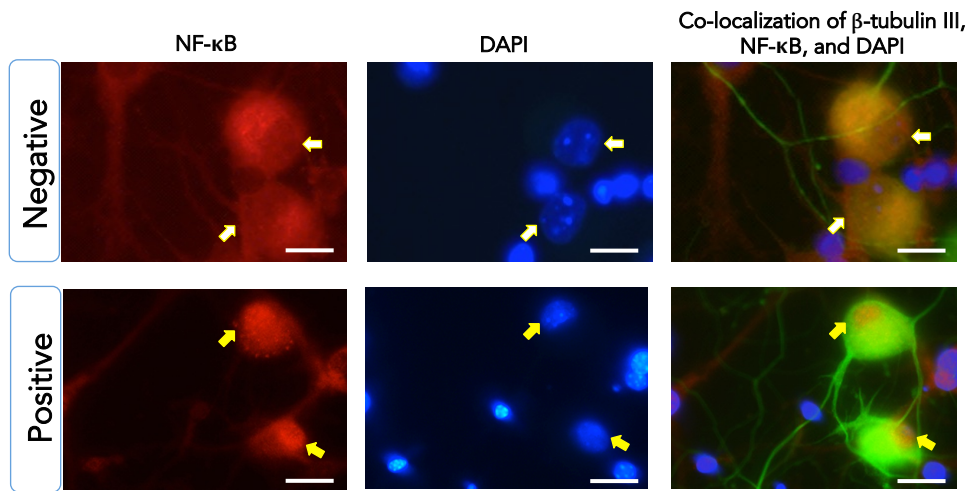


Figure 2.14 Principle of quantification of NF- κ B translocation in TG neurones.

Acquired images by fluorescent microscopy were scored for nuclear translocation of the NF- κ B protein in TG culture. NF- κ B could be scored as either negative when the NF- κ B panel show a hollow core in the nucleus area (top panel) or positive when the nucleus areas were filled with NF- κ B (bottom panel). Top panel is an example of proportion labelling of nucleus/cytoplasm that was less than one ($Nuc/Cyt < 1$). While the bottom panel is an example of proportion labelling of nucleus/cytoplasm that was greater than one ($Nuc/Cyt \geq 1$). Positive samples were exposed to *P. gingivalis* whole bacteria, while the negative samples were not exposed to a stimulus. Scale bar = 50 μ m.

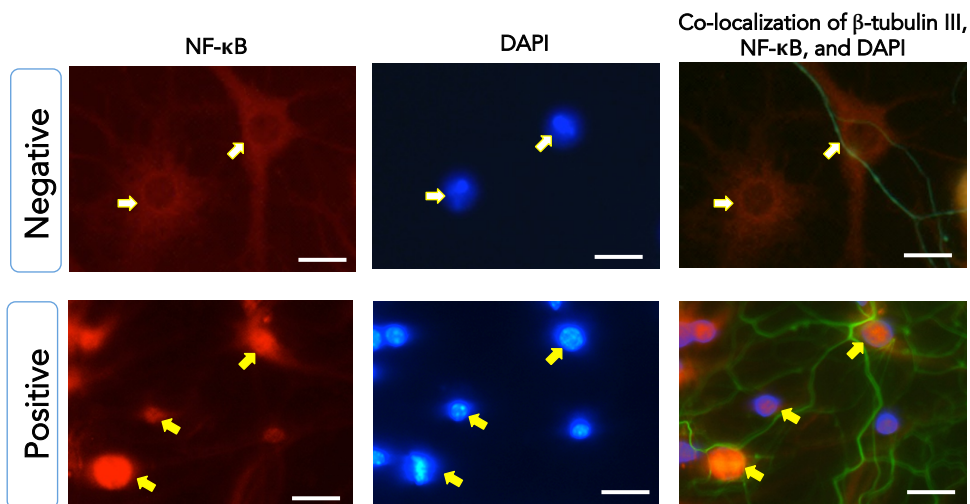


Figure 2.15 Principle of quantification of NF- κ B translocation in TG non-neuronal cells.

Acquired images by fluorescent microscopy were scored for nuclear translocation of the NF- κ B protein in TG culture. NF- κ B could be scored as either negative when the NF- κ B panel show a hollow core in the nucleus area (top panel) or positive when the nucleus area were filled with NF- κ B (bottom panel). Experimental conditions were as above (Figure 2.14). Scale bar = 50 μ m.

2.12 CGRP ELISA and the protocol development

In this study, we used primary cultures of trigeminal neurones as a tool to assess the effect of bacterial stimulation on the cells present as a model of infection. Several mechanisms of activation of neurones lead to CGRP release. This is a multifunctional neurotransmitter that is believed to play an important role in the underlying pathology of dental pain (Ceruti et al. 2011; Simonetti et al. 2008).

Here, we modified our culture model to detect the changes of calcitonin gene-related peptide (CGRP) levels in response to neuronal stimuli with a range of agonists (e.g. capsaicin). The supernatants of our TG cultures were collected following stimulation with agonists as described in section 2.8 and were analysed by ELISA for CGRP. For example the cultured cells were exposed to either vehicle or *P. gingivalis* LPS for 15 min and the supernatants collected and assayed by a competitive Enzyme-linked Immunosorbent Assay (ELISA) for CGRP (Figure 2.16). Briefly, the ELISA was performed by coating plates with 1:1000 anti-CGRP mouse monoclonal capture antibody (Sigma) in 0.05 M carbonate buffer, pH 9.5 overnight at 4° C to immobilise the capture antibody to the wells of microtitre plate. Plates were then washed 3 times with 0.05% PBS-Tween and blocked with 5% BSA in 0.05% PBS-Tween, pH 7.4, for 3 h at room temperature. After 3 washes, 50 µL standard CGRP and culture supernatant samples were added with 50 µL of 2 ng/mL biotin-conjugated CGRP (Biorbyt®) to the plate for 1 h at 37°C. After 6 washes, the plate was incubated with 1:400 streptavidin-horseradish peroxidase conjugate (strep-HRP) for 45 min. Tetramethylbenzidine/hydrogen peroxide substrate solution (TMB) (Sigma) was then added until colour developed, (10 – 20 min) and the reaction was stopped with 2N HCl. ELISA plate absorbance values were recorded using a spectrophotometer (Infinite 200 PRO, Tecan, Reading, UK) at 450 nm. Unknown CGRP concentrations were calculated by interpolation from a standard curve. In this system, the unlabelled CGRP from the supernatant samples competed with biotin-labelled CGRP for binding to the capture antibody, the more CGRP in the supernatant there was the less biotin-CGRP bound a reduced colour signal. The sensitivity range of the ELISA was 20 – 2,000 pg/mL.

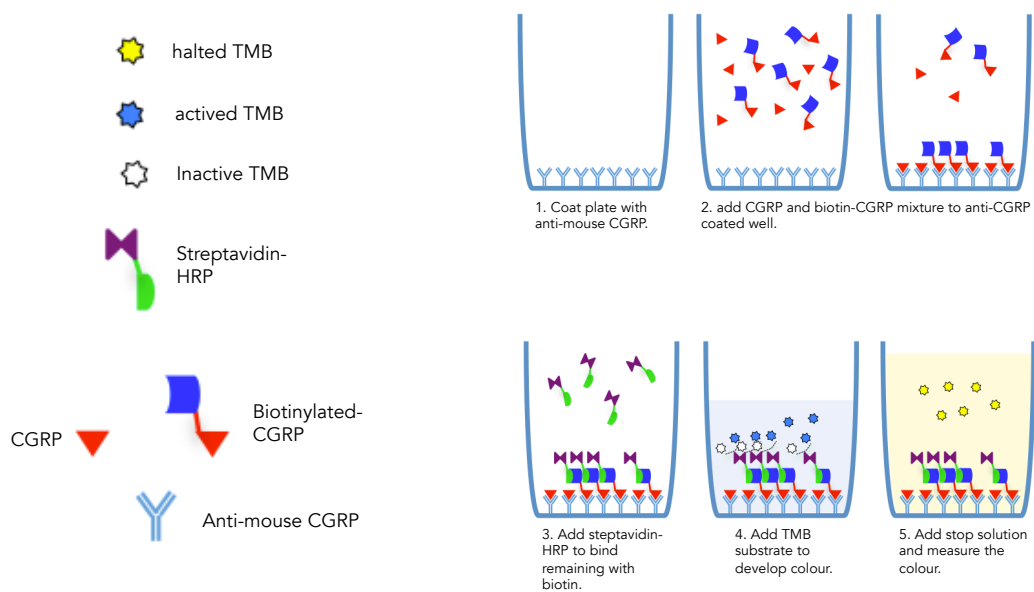


Figure 2.16 Competitive CGRP ELISA used in this study.

We performed competitive CGRP ELISA. Unlabelled CGRP from samples and the biotin-CGRP compete for binding to the capture CGRP antibody.

2.13 Total protein analysis

The culture supernatants were assayed for total protein so as to normalise the CGRP values to the biomass of the different TG cultures. Following the collection of the supernatant for CGRP ELISA, TG cells were lysed in HEPES lysis buffer (250 mM NaCl, 0.5% NP40, and 20 mM HEPES, pH 7.5) on ice for 15 min, and then scraped and collected to determine total protein level. This was analysed by bicinchoninic acid assay (BCA). Briefly, 25 μ L of protein standard or unknown sample was placed into a microplate well followed by 200 μ L of BCA working reagent. The resultant purple-colour developed within 30 min and its absorbance was recorded (Infinite 200 PRO, Tecan, Reading, UK) at 562 nm and plotted against the standard protein level.

2.14 Statistic analysis

Data were analysed by one-way ANOVA, and individual groups were compared by Bonferroni's post hoc test using Prism 6 (GraphPad Software, San Diego, CA, USA). Statistical significance was denoted as $p < 0.05$ (*), $p < 0.01$ (**) and $p < 0.001$ (***).



Chapter 3

*Culture system of
trigeminal ganglia*



3. Culture system of trigeminal ganglia

3.1 Introduction

There are various options for studying inflammatory pain, either using animal models, or cellular models. The aim of our study was to investigate mechanisms by which bacterial infection could cause pain generation through direct interaction with neurones, whilst excluding the effects of immune cells or other bystander cells. Therefore, in this study, we required an *in vitro* system of isolated trigeminal sensory neurones.

While we have considered the limitations of primary cultured cells, in that they share some characteristics with regenerating cells, such as the elevation of *trkA* in isolated cells in comparison to explant (whole ganglia) culture (Ma et al. 2010), the dissociated primary sensory neurones are still capable of maintaining the characteristics of those *in vivo* sensory nerve endings (Higginns and Banker 1998). Therefore, sensory neurone culture is still a powerful tool to study the basic mechanisms of sensory physiology and pain.

Our initial aim was to purify trigeminal neurones and establish a pure culture system. However, in trigeminal ganglia, the sensory neurones act in synergy with satellite glial cells (SGC). They are specialised cells that envelope neurones (Poulsen et al. 2014) and their physical proximities are believed to help establish a functional unit within the ganglia (Villa et al. 2010; Hanani 2015; Costa and Neto 2015). Nonetheless, we reasoned it might be possible to eliminate unwanted non-neuronal cells from a mixed culture employing antimetabolic agents, such as fluorodeoxyuridine (5-FDU), uridine, and cytosine arabinoside (AraC). These agents are toxic to any dividing cells so should have relatively little effect on cells that are not undergoing DNA synthesis, such as neurones (He and Baas 2003). Alternatively, such treatments might significantly enrich the population of neuronal cells in the culture even though the non-neuronal cells are still present since the molecular network of neurone-to-SGC interplay seems to have effects on the survival rate of isolated neurones (Wyatt et al. 1997).

Here, we have developed methods to isolate, culture, and purify sensory neurones from adult mice. We first have adopted a protocol used for dorsal root ganglia (DRG) in Professor John Haycock's group, KROTO Research Institute, Department of Material Science and Engineering, Sheffield University which we called the 'conventional protocol'. However, we then modified the procedures with a view to purifying trigeminal neurones by taking the advantage of antimetabolic agents. In order to verify the efficiency of each method, the cultured cells required characterisation in terms of:

- Development of extensive neurite outgrowth
- Identification of neurones or non-neuronal cells present under
 - Light microscopy
 - Immunostaining

In our study, trigeminal cultures were used as a model to study the mechanisms of peripheral sensitisation by various techniques such as calcium imaging and release of neuropeptide.

The aim of this part of our study was to,

- Obtain a healthy *in vitro* culture system of trigeminal ganglia neurones.
- Optimise the proportion of neurones to non-neuronal cells in the culture system.

3.2 Conventional protocol for neurone culture

3.2.1 Methods

The ganglia were obtained as described in section 2.2.2, Chapter 2: Materials and Methods. They were digested with collagenase type IV (1.25% w/v) twice in DMEM/F12 for 60 and 45 min at 37°C. Subsequently, 1.25% w/v of trypsin was used to digest for 30 min at 37°C. After digestion, the TG were dissociated by mechanical agitation by pipetting up and down until the TG became homogeneous. The mixtures were transferred to poly-L-lysine and laminin-coated 24-well tissue culture dishes. After 2 h incubation at 37°C, Bottenstain and Sato media (DMEM/F12 media, 1% w/v BSA, 1% N2 supplement, 1% PS) supplemented with 70 ng/mL of nerve growth factor (NGF) was added. The media were changed every 48 h. The experiments were terminated after 5 – 6 days of culture.

3.2.2 Results

At the beginning of the study, we focused solely on establishing a protocol to culture neurones *in vitro*. The early sets of the TG culture were unsuccessful because of bacterial infection. Moreover, insufficient attention was paid to the preparation of the cell-seeding surface which turned out to be highly critical in hindsight. The neuronal cells did not settle down and grow their neurite processes (data not shown).

The protocol was then modified by performing every step under sterile conditions and we strictly followed the manufacturer's protocol for coating the culture plates with the poly-L-lysine and laminin (Miljan and Fauvin 2007). Moreover, the speed of harvesting and processing the tissue sample proved to be crucial because of the short neuronal survival time *in vitro*. A harvesting time of not exceeding 15 min after animal death has been shown to increase in the success rate of neuronal cell cultures (Acosta and Davies 2007) and we would concur.

3.2.2.1 Microscopy images

After we had modified some steps as mentioned above, the processes of the trigeminal ganglia cells were well developed and formed the network after 24-h of seeding. The cell density also increased over time (see Figure 3.1). Trigeminal neurones could be defined as big, bright, round cell bodies and thin filopodia and they took around one day to develop neurite elongation. On the other hand, the morphology of glial cells was much more variable. In some cases, they were flattened and polygonal. The glial processes could be either one or two in number or showed a high degree of branching. Their size varied but they were normally smaller than neurones, so they could easily be overlooked when they were lying within a dense network. For a definite identification of neurones and glial cells, immunostaining methods proved to be exceptionally useful.

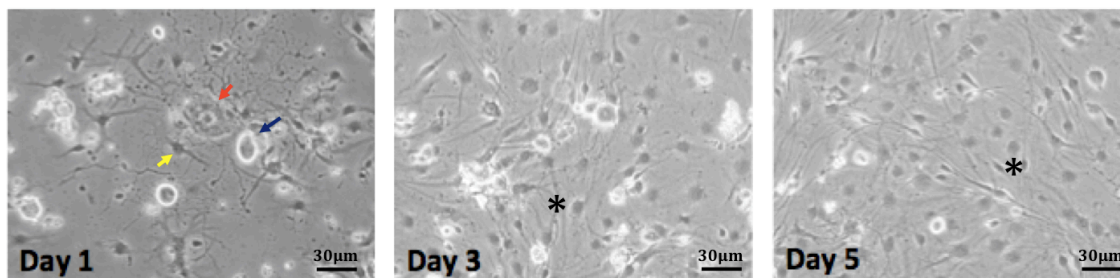


Figure 3.1 Day 1, 3 and 5 of TG cultures obtained by the 'conventional protocol' visualised under phase contrast microscopy.

On day 1 after dissociated trigeminal cells were plated, a mixture of cell types was observed. The bright round cell bodies (blue arrow) are neuronal cells, the smaller spindle-shaped cells (yellow arrow) are typical of satellite glial cells, and the large dark cells (red arrow) are fibroblasts. On day 3, the cellular lawn of non-neuronal cells (black asterisk) could be observed. On day 5, the non-neuronal cells were more crowded, while the axonal outgrowth of neurones were longer and more connected to the neighbouring cells. However, the non-neuronal cells ultimately outgrew and replaced the neuronal cells over the following few days (Scale bar = 30 μm).

3.2.2.2 Immunofluorescence

Non-neuronal cells could not always be easily distinguished from neurones. Therefore, to determine the proportion of neuronal-to-non-neuronal cells, immunofluorescence microscopy was conducted using the neuronal marker, β -tubulin III. Over time, neurones in the culture were decreased in number conversely, non-neuronal cells substantially increased and consequently replaced neurones. (Representative field shown in Figure 3.2)

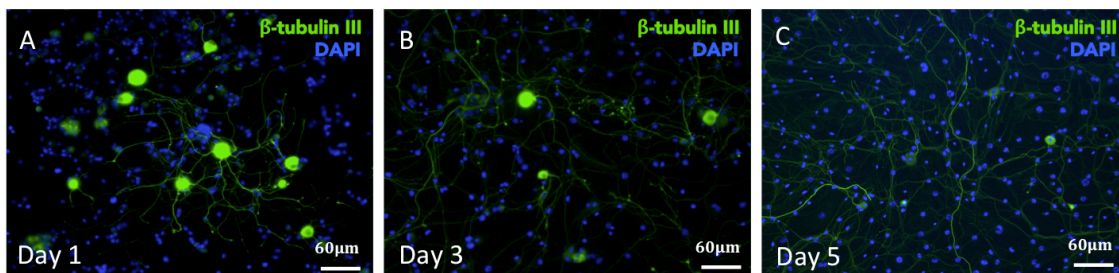


Figure 3.2 Day 1, 3, and 5 of TG cultures established using the 'convention protocol' visualised by immunofluorescence.

Representative immunofluorescence images of cultured TG on day 1, day 3, and day 5 are shown in panels A, B, and C respectively. The images show dual labelling of trigeminal cultures with the neuronal marker, β -tubulin III, along with DAPI (nuclei marker). They show the characteristic of trigeminal cultures over in 5 days. Over the 5 day period, the neurone number decreased, and was gradually replaced by the proliferating non-neuronal cells.

The immunocytochemistry of various protein markers i.e. β -tubulin III, GFAP, and S100 were employed in 5-day cultures to estimated percentages of cell types. They were counted as follows and representative data are shown in the Figure 3.3.

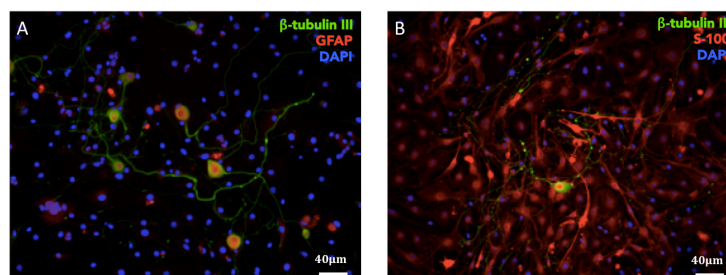


Figure 3.3 Day 5 of the 'conventional protocol' cultures of trigeminal ganglia visualised by immunofluorescence using three markers.

Representative immunofluorescence images as shown of cultured TG with dual labelling of GFAP and β -tubulin III (panel A), and dual labelling of S100 and β -tubulin III (panel B). The ratio of neurone-to-non-neuronal cells could be roughly shown here. β tubulin III is a specific neuronal marker; DAPI is marker for any nuclei, S100 is a marker of sensory neurone, satellite glial cell, and Schwann cells and GFAP is a marker for glial cells in the PNS.

β -tubulin III is a specific marker for neurones. GFAP is a protein expressed differently in CNS and PNS. In PNS, GFAP is specific marker for satellite glial cells. S100 is protein expressed in many cell in PNS including satellite glial cells, myelated and non-myelated Schwann cells, and neurones (Gonzalez-Martinez et al. 2003). In this study, we used S-100 antibody to identify any glial cells and peripheral neurones. GFAP antibody was used as the satellite glial cell marker, and β -tubulin III was used as the neuronal marker. Cells that were not stained with any of these markers were considered to be fibroblasts.

Using this method, by day 5 we characterised the proportion of each cell type in the TG cultures:

- Neurone 5 – 10%
- Satellite glial cells 40 – 45%
- Schwann cells 40 – 45%
- Fibroblasts 5 – 9%

3.3 Neuronal cell purification

Essentially, in the conventional TG cultures the non-neuronal cells were present in much greater numbers than neuronal cells. The culture protocols were therefore developed further to try maximising the neuronal cell proportion by using antimetabolic agents. The main effect of antimetabolic agents was to reduce the mitotic activity of non-neuronal cells, namely satellite glial cells, Schwann cells and fibroblasts. The antimetabolic agents affected these cells by the activation of NF- κ B and induction of programmed cell death. The agents used were, uridine, 5-FDU, and AraC which was found to reduce glial cells, Schwann cells and fibroblast, respectively (Anderson et al. 2003). We developed 2 methods for administering these 3 antimetabolic agents, firstly, by continual feeding (method 1) of the TG cultures; secondly, by providing a single high dose of antimetabolic agents (method 2); thirdly as method 2, but also employing a step to exclude small cells from the dissociated cell pellet (method 3).

3.3.1 Methods (1): Continual feeding with antimetabolic treatment

The ganglia were washed twice with phosphate buffered saline (PBS) containing 1% (w/v) penicillin, 1% (w/v) streptomycin (PS) and 1% Fungizone before being held in DMEM/F12 supplemented with 1% PS until they were ready to culture. TG were digested and dissociated as for the conventional protocol. The maintaining media were supplemented with 2 different concentrations of antimetabolic agents; firstly the recommended dose of 5-fluoro-2-deoxyuridine (5-FDU), uridine, and L- β -D-arabinofuranosyl cytosine (AraC) (10 μ M 5-FDU, 10 μ M uridine, 1 μ M AraC) and secondly, double the normal dosage (20 μ M 5-FDU, 20 μ M uridine, 2 μ M AraC).

The maintaining media supplemented with antimetabolic agents were changed every 48 h and the cells were quantified on day 1, 3, 5, 7, 10 and 14 of culturing.

3.3.2 Methods (2): Single high dose

This method only modified the maintaining phase by using high dose of anti-mitotic agents for single dose instead the continual low concentration of antimitotic supplementation. A final concentration of 20 μ M 5-FDU, 20 μ M uridine and 1 μ M AraC were added to the medium. Twenty-four hours after plating, these agents were left in place for 72 h. On day 3, the fresh media (without the antimitotic agents) were changed, and then fresh medium was applied and changed every 2 days.

3.3.3 Methods (3): Differential centrifugation to separate the cells by size

After the TG ganglia were dissociated by manually pipetting up and down, the mixture of cells were transferred to a 15 mL tube for gradient centrifugation in 15% BSA (1500 rpm, 10 minutes). We added this centrifugation step to reduce contaminating cells.

Large cells, expected to be the neurones and fibroblasts, should form a thin pellet at the bottom of the tube. Small cells and any debris were expected to form an upper layer, comprising satellite glial cells and Schwann cells. The gradient separation step is shown in Figure 3.4. The debris and small cell layer would be discarded. The large-cells layer was plated and fed with single high dose of antimitotic agents as described in the method 2.

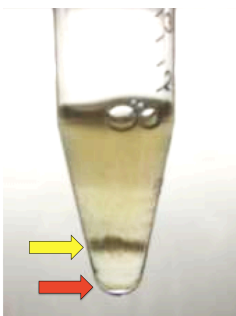


Figure 3.4 A mixture of dissociated cells was gradient separated into 2 layers of large and small cells.

The thin lower pellet (red arrow) proposed to contain only large cells such as neurones and fibroblasts. The upper thick layer (yellow arrow) proposed to contain small cells and debris — this layer would be discarded later.

3.3.4 Results

The effect of antimetabolic supplements on the trigeminal cell cultures was assessed over a time course by quantifying the double-labelled cells (β -tubulin III and DAPI) using Image J. The number of neuronal and whole trigeminal cells were plotted to study the effect of the antimetabolic agents at various time points. Two alternative administrations were examined, continual feeding, and single high dose.

3.3.4.1 *Continual feeding with antimetabolic treatment*

This method was tested with 2 concentrations of agents. It could be seen that the effect of the antimetabolic agents was to reduce the number of contaminating cells in the culture, but could not completely eliminate them. The major disadvantage appears to be that the antimetabolic agents affected the neuronal cell viability too. The effects of applying the antimetabolic agent are shown in comparison to the conventional method in terms of the cell numbers in the culture, from day 1 to day 14. In the conventional culture system, the total number of cells increased over time, but the neurone numbers declined to zero by day 14. Representative images of trigeminal cultures from day 1 to day 10 are shown in Figure 3.5. Representative data of the total cell count and the number of neurones in cultures from day 1 to day 14 are shown in Figure 3.6, and Figure 3.7, respectively

This method was tested with a range of concentrations of agents. Even though we showed only one set of independent samples, these represented the trends of both neuronal and non-neuronal cell survival found following treatment with antimetabolic agents. It could be seen that antimetabolic agents reduced the number of contaminating cells over time in the culture, but could not completely eliminate them. Moreover, the agents affected neuronal cell survival too.

Since continuous presence of antimetabolic agents during culture was deleterious for the neurones, we reasoned that it may be possible to reduce the number non-neuronal cells by using a combination of the antimetabolic agents but in a single high dose treatment.

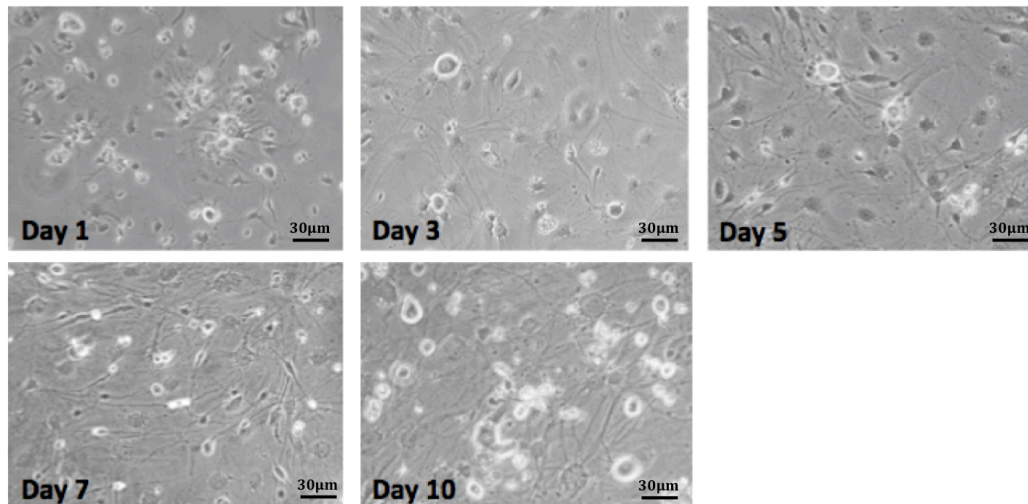


Figure 3.5 Trigeminal cultures from day 1 to day 10 in maintaining media supplemented with the recommended dose of antimetabolic agents.

From day 1, a mixture of cell types was observed. In the later stages, a lower density of non-neuronal cells was observed. The non-neuronal cells were less crowded, while the axonal outgrowth of neurones were longer and more connected to the neighbouring cells. However, the antimetabolic reagents could not completely eliminate non-neuronal cells (Scale bar = 30 μm).

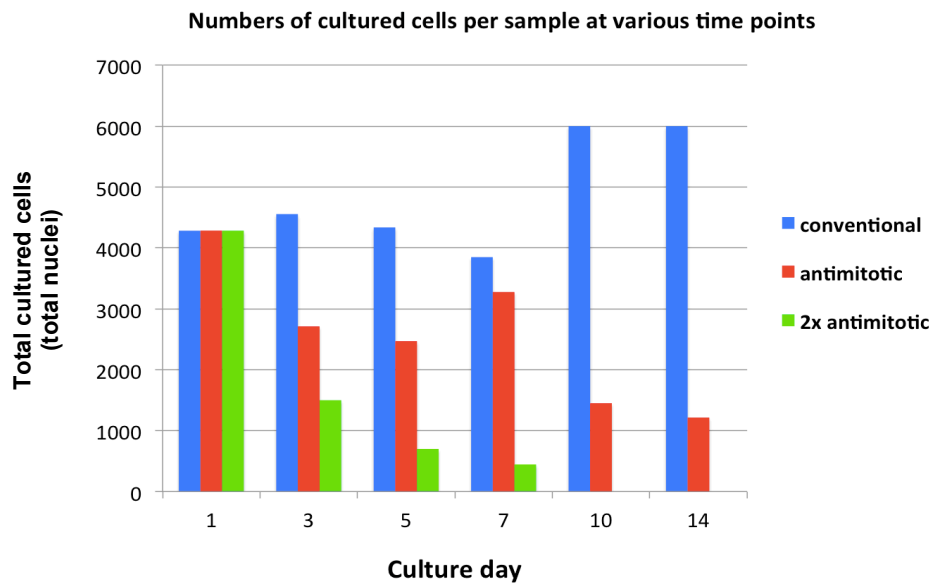


Figure 3.6 Graph showing the total cell count (stained by DAPI) of independent samples from day 1 to day 14.

This graph shows the trend of increasing total cells in conventional culture, but decreasing number of cells in the antimitotic — treated groups overtime. Data are the means from one experiment.

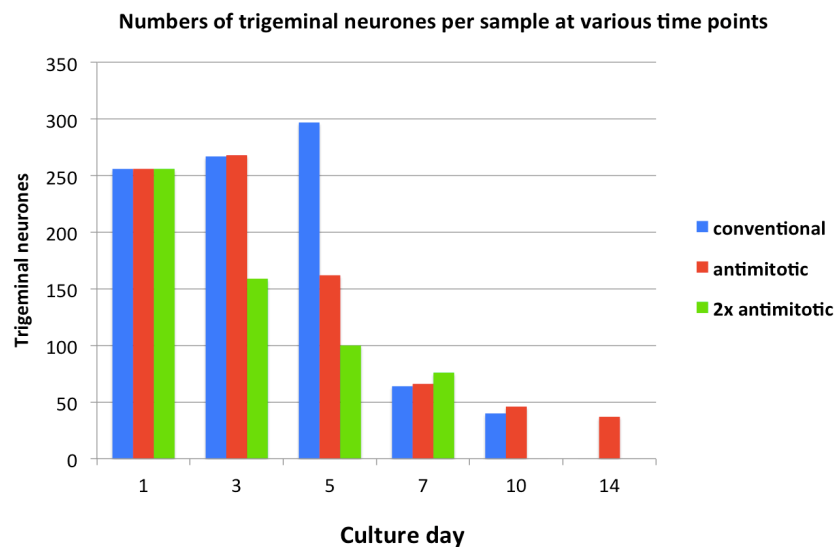


Figure 3.7 Graph showing the number of neurones from independent samples from day 1 to day 14.

This graph shows the trend of decreasing neuronal cells in culture overtime in all groups. The antimitotic agents seem to affect the neuronal survival rates in the high concentration group. Data are the means from only experiment.

3.3.4.2 Single high dose anti-mitotic agents

Using a protocol adapted from Liu et al. (2013) for the purification of embryonic rat dorsal root ganglia, a combination of antimetabolic agents was added to the medium to a final concentration of 20 μM uridine, 20 μM 5-FDU, and 1 μM AraC. Twenty-four hours after plating, these agents were left in place for 72 h. The media was changed every 2 days. The cultures were then fixed for the immunofluorescence on day 7.

By immunofluorescence, we found that approximately 30% of cells were neurones as shown in Figure 3.8. The proportion of neuronal cells had increased because the number of non-neuronal cells was depleted by the effect of the antimetabolic agents. By this method at day 7 of culture, we found the percentages of surviving cells were as follows:

- Neurones 25 – 30%
- Schwann cells 50 – 60%
- Satellite glial cells 8 – 10%
- Fibroblasts less than 5%

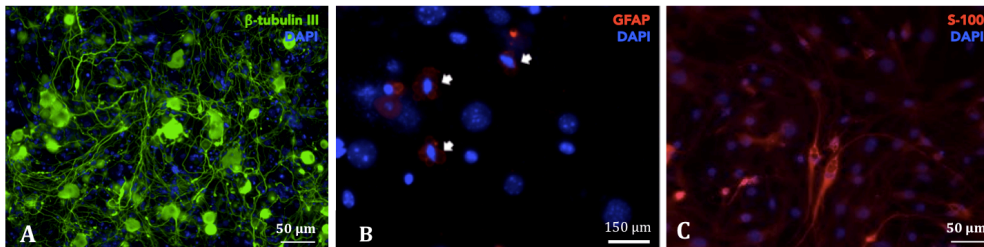


Figure 3.8 Day 7 of trigeminal cultured cells treated by single high dose of antimetabolic agents visualised by immunofluorescence.

The neuronal cells were identified by the immunocytochemistry. Each image was dual labelled by DAPI and either β -tubulin III, GFAP, or S-100. The proportion of neurones was around 25% of all cells in this sample (A), GFAP-stained cells (red) were $\sim 8 - 10\%$ of the total. The figures also show hollow clusters of the small cells, which had lost their spindle shape, which is a typical characteristic of glial cells (B), The S100-stained cells (red) were approximately 65 – 70% of the total. The hollow nuclei in the spindles cells are also found in non-neuronal cells (C). Scale bar = 30 μm .

3.3.4.3 Differential centrifugation to separate the cells by size

We employed this additional step to discard small non-neuronal cells. However, the lower pellet still consisted of neurones and a mixture of some intact satellite glial cells. These SGCs could potentially grow and proliferate in the culture systems as shown in Figure 3.9. Therefore, we opted to work with a mixed TG culture.

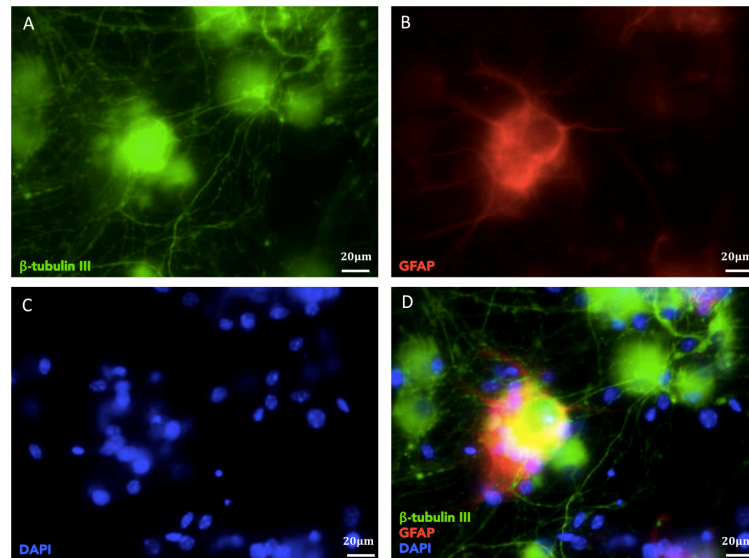


Figure 3.9 Images showing presence of SGCs in close proximity to neurones.

The images show the characteristics of the culture cells in early days. There were some tightly enwrapped neurones by the SGCs (identified by GFAP) to the neurones. Eventually, these non-neuronal cells could proliferate in the culture system. Trigeminal neurones, GFAP, nucleus, and triple labelling are demonstrated in panel A, B C, and D, respectively.

3.4 Characterisation of short-term TG cultures

3.4.1 Methods

We observed that the neurones exhibited healthy growth in first few days in culture, after which they would gradually be overgrown by non-neuronal cells. After trying to modify the 'conventional protocol' to obtain a high proportion of neurones, it became apparent that trigeminal neurones could not be sustained in long-term culture environments. Consequently, we eliminated any unnecessary steps in the protocol and increased the cell seeding. Subsequently immunofluorescence and further experiments were performed on 2-day cultures.

3.4.2 Results

By increasing the number of cells in the plating step, neurite networks were observed to be well established 2 days after plating. This demonstrated the healthy status of neurones. We also found that the ratio of neurone-to-non-neuronal cells was higher in these short-term cultures. Representative images of such short-term TG cultures are shown in Figure 3.10.

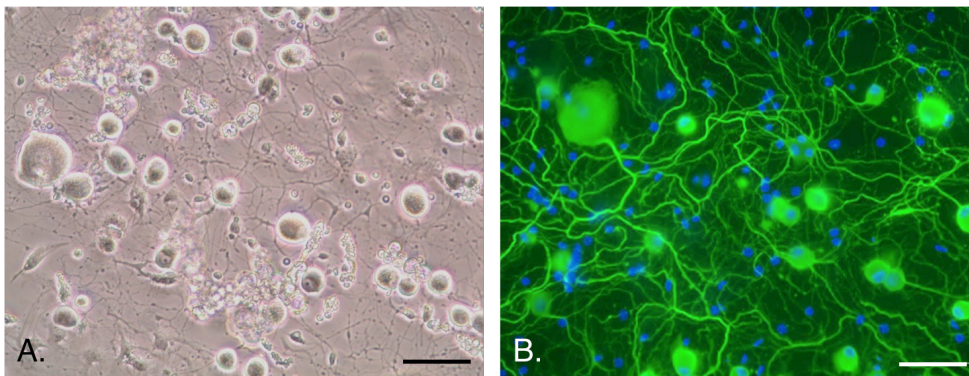


Figure 3.10 Day 2 of trigeminal cultures using the conventional method but with higher cell seeding

Neurite networks were well formed and the non-neuronal cell population was less dominant than in older cultures. The images show (A) phase contrast microscopy of typical cultures (B), the same cultures immune-stained for β -tubulin III (green) and DAPI (blue). Scale bar = 60 μ m.

The cultured cells were also characterised for their neuropeptide expression and presence of a number of cellular receptors including TLR4, TLR7, TRPA1, and TRPV1. For TLRs, and TRPs expressions, they are discussed further in Chapter 4, and 5, respectively. Here, we characterised our cultured cells to ensure that they displayed the expected phenotype in our *in vitro* cultures. We test neuronal cell viability by determining the calcium response to high potassium solutions using calcium imaging. The neuronal cells were found to have 100% response to high potassium (representative data are shown in Figure 3.11).

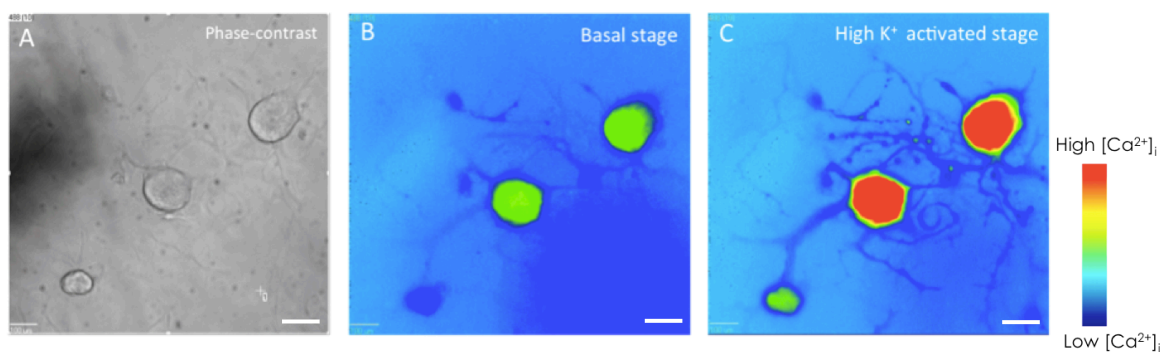


Figure 3.11 Confirmation of neuronal viability in culture by response to high potassium.

Neuronal viability was demonstrated by the calcium influx (using Cal-520 dye) into the neurones following treatment with high potassium. The phase-contrast image is shown on the left (A). Images B, and C show the calcium intensities at the basal and activated stages, respectively. Scale bar = 40 μm .

Also, we sought to determine whether the neuronal cell phenotype could express neuropeptides in culture. Immunocytochemistry of the neurones in the TG cultures also revealed the presence of peptidergic types of cells as demonstrated by accumulation of CGRP and SP at high level intracellularly. To visualise this we left the cells untreated in culture, so maximal levels of CGRP and SP are still being retained intracellularly (Figure 3.12 and Figure 3.13, respectively). CGRP and SP in the TG neurones were showing weak to high levels of CGRP-IR and SP-IR. As we expected, CGRP and SP expression was only seen in neurones, and they were present in nearly all of neurones.

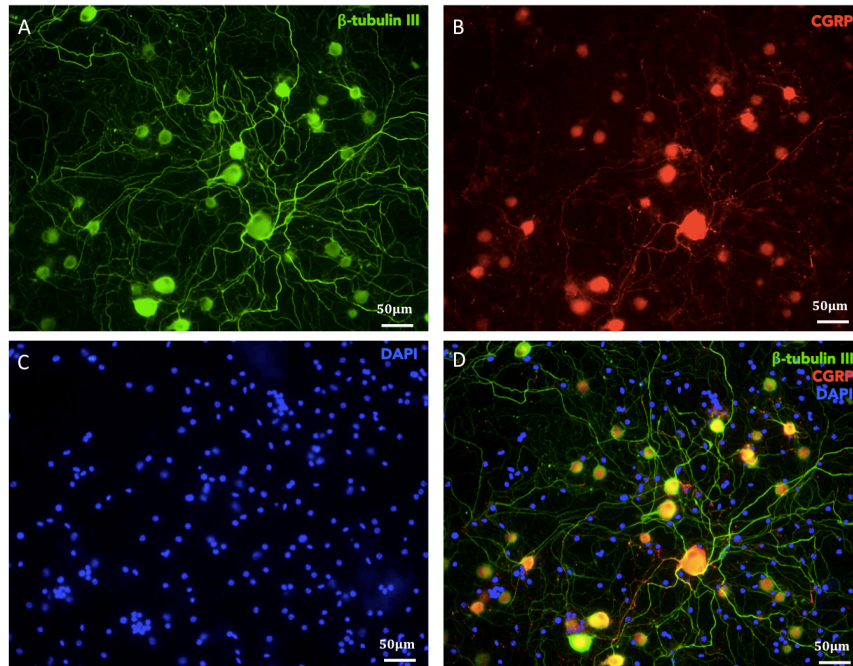


Figure 3.12 Trigeminal cultured neurones expressing intracellular CGRP.

These figures confirmed the characteristics of the culture cells and showed high levels of intracellular CGRP storage in the neurones. Trigeminal neurones, CGRP, nucleus, and triple labelling were demonstrated in panel A, B C, and D, respectively.

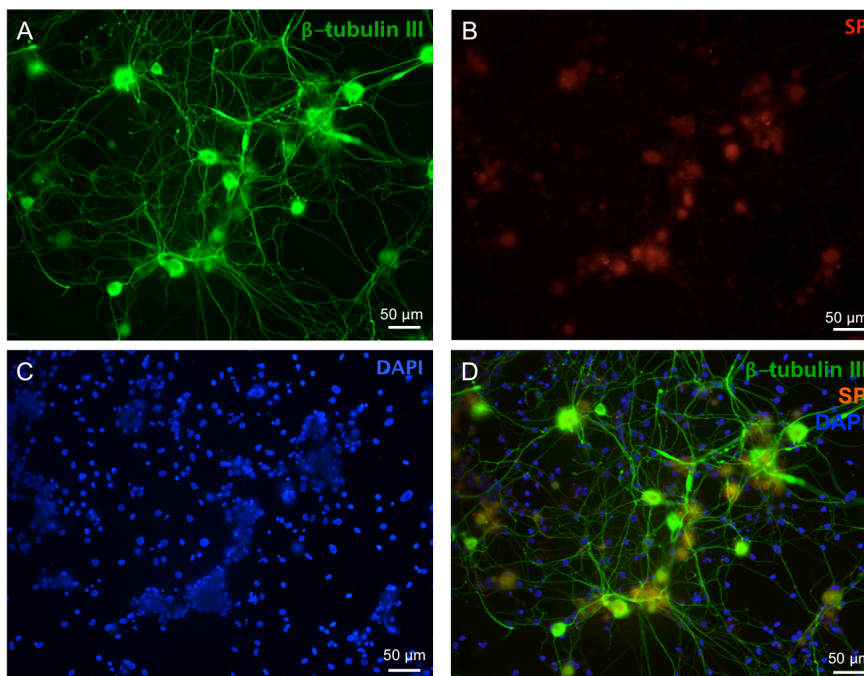


Figure 3.13 Trigeminal cultured neurones expressing intracellular SP.

These figures confirmed the characteristics of the culture cells that they could maintain intracellular SP storages in the neurones. Trigeminal neurones, SP, nucleus, and triple labelling were demonstrated in panel A, B C, and D, respectively.

3.5 Discussion

There are a range of possible methods that could be used for studying the effects of infection on neurones and inflammatory pain. In our study, we established cell culture models in order to study the direct effects of bacterial infection on neuronal physiology

3.5.1 Characterisation of trigeminal cell culture

The ultimate aim of this study was to establish a pure neuronal *in vitro* culture model for studying the direct effect of bacterial factors. However, this proved to be unachievable using the methods we tried and the presence of some support cells was required for good neuronal cell survival.

For the purification methods, we initially used an antimetabolic agent treatment. Even though the effect of antimetabolic agents could reduce the number of non-neuronal cells, it did not completely eliminate the contaminating cells (Acosta and Davies 2007, Ferraz et al. 2011, Goethal et al. 2010). Furthermore it was deleterious to the neurones.

Consequently a physical separation method was tried in which TG preparations were subjected to gradient centrifugation to try to separate the relatively large neurones from the other cells. However, the protocol using a 15% BSA suspending medium could not completely purify the neurones and this appeared to be because non-neuronal cells adhered tightly to the neurones.

In physiological conditions or *in vivo*, the peripheral neurones are surrounded by satellite glial cells. Schwann cells surround the axons, and accrue when the neurones age. So, the supporting cells are required for the healthy status of the neurones. An important reason why Schwann cells were fairly dominant in this culture method might be because we used adult mice, which have been reported to have more Schwann cells than the post-natal mice used in previous studies (Acosta and Davies, 2007).

Immunocytochemistry of the neurones in the TG cultures also revealed the presence of peptidergic types of cells as demonstrated by accumulation of CGRP at high level intracellularly. CGRP and SP expression was present found in nearly of all neurones in the cultures with varying levels of expression. However, *in vivo* trigeminal ganglia of rats have 30 – 40% of neurones expressing CGRP, and about 18 – 20% expressing SP (Tajti et al. 1999).

We found that the very act of culturing neurones *in vitro* enhanced the expression of the neuropeptides CGRP and SP. Perhaps this is not surprising since neuropeptide expression is known to vary with environmental conditions, e.g. pH (Zimmermann et al. 2002) and serum level in the medium and is altered by nerve injury. Moreover, it has been demonstrated that serum-free medium can increase activity of MAPK ERK1/2 and p38, which leads to the expression of CGRP (Kuris et al. 2007). Consequently, *in vitro* culture of neurones, especially in the presence of NGF – as is usually used in such culture systems – is likely to lead to higher CGRP levels even without specific stimulation.

3.5.2 Applications and limitations of the study

Advantages of primary neuronal cells.

Because the endings of sensory neurones have a very small diameter, they are currently not amenable to direct physiological and pharmacological investigations. Fortunately, it appears that the neuronal somata are similar in many ways to the endings. Therefore, investigation of the somata can yield essential information on the terminals. In addition, the accessibility of sensory ganglia, the simplicity of the neuronal morphology and the lack of synapses make cultured sensory ganglia an ideal tool to study general neuronal properties (He and Baas 2003).

The use of a variety of trigeminal or dorsal root ganglia neurones for the culturing of peripheral sensory models has been widely evaluated previously. Workers have used cultures of animal peripheral ganglia (either mouse, rat, or rabbit) to study the neurobiology of peripheral ganglion neurones, such as the mechanisms of nerve regeneration and physiology of ion channels. The procedures for preparing

dissociated cell cultures from mouse ganglia were well described by Malin et al. (2007).

A reason for the popularity of primary neuronal cell cultures for the study of pain is because they are simple and relatively inexpensive to prepare. Also, neurones are accessible for experimental manipulation, such as electrophysiological recording, and immunolabelling for microscopical assessment. However, the major limitations of this approach are the purity of the resultant neuronal cell population. Long-term culture has proven to be difficult and results in limited cell numbers.

3.5.3 Conclusion

A major aim of this part of the study was to isolate and sustain trigeminal neurones *in vitro*. Many modifications of the culture were employed but short-term culture appeared to provide the best method to produce a model resembling trigeminal ganglia *in vivo*. Purified neurones from primary cell culture have not yet been achieved by normal cultural techniques.

However, the major limitations of this approach are the purity of the neuronal cell population and differentiating the responses of these from those of other cells. Fortunately this can be at least partially negated by using calcium-imaging and immunofluorescence labelling to study individual cells in the culture system.

These models were optimised to ultimately study the neuronal activation effects in response to bacteria and their components. We have shown that the trigeminal cultures showed some of the physiologic characteristics expected of neurones *in vivo*, such as expression of CGRP and calcium influx following potassium application. The effect of bacteria and their components on the responses of trigeminal cultures using this culture system is the subject of later chapters (by using short-term TG cultures as describe in section 3.4).

Chapter 4

P. gingivalis infection and
environmental cues in
trigeminal cells



4. *P. gingivalis* infection and environmental cues in trigeminal cells

4.1 Introduction

Dental pulpal pain associated with infection is a complicated process involving various inflammatory mediators, several cell types and numerous bacteria. Previously, inflammatory pain was thought to be triggered merely by pro-inflammatory molecules such as bradykinin, cytokines, and growth factors. However, recently, there has been evidence to show that immune activation was not necessary for hyperalgesia during acute infection and that bacteria can directly activate nociceptors (Chiu et al. 2013). Therefore, it is possible that oral pathogenic bacteria in the pulp may directly sensitise trigeminal nociceptors, causing peripheral sensitisation and influencing inflammatory pain.

Bacteria that gain entry to the pulp are provided with a new environment that differs from that of dental plaque, the oral cavity and the dentinal tubule. This change in nutrition may lead to changes in the way that bacteria interact with the host nervous system. Moreover, noxious stimuli from bacteria could activate signal transduction pathways of the neuronal-inflammatory responses that involve NF- κ B, which is the pathway which induces the release of various inflammatory cytokines in response to stimuli and this could add to amplification of pain.

The hypothesis to be tested here is that Gram-negative oral pathogens, such as *P. gingivalis*, contribute to peripheral sensitisation by direct activation of neurones. The consequence of such neuronal activation should involve CGRP release and NF- κ B nuclear translocation. Furthermore, the environmental conditions of the root canal will provide a modified nutritional environment which consequently changes microbial virulence factors, which in turn affect neuronal activity.

The aims of this study are to:

1. Determine whether trigeminal nociceptors are activated directly by exposure to *P. gingivalis*.
2. Investigate the consequence of any neuronal activity in terms of neuropeptide release (CGRP) and NF- κ B nuclear translocation.
3. Measure any CGRP released in response to bacteria grown under different haemin conditions.

4.2 Results

4.2.1. *P. gingivalis* W50 activation of the calcium influx in TG neurones

The treatment of cells in TG cultures with whole *P. gingivalis* W50 bacteria is described in section 2.7.3, Chapter 2 and the resulting calcium imaging in section 2.7.4, Chapter 2. To study the mechanisms underlying dental pain directly caused by oral pathogens, we established, a *P. gingivalis* model using the mouse trigeminal neurone culture model described in Section 3.4, Chapter 3. TG neurone cultures were exposed to 100 µg/mL (wet weight) or approximately 10⁸ cells per mL of live *P. gingivalis*. Neuronal calcium levels were recorded over time from basal levels to that following *P. gingivalis* exposure followed by high potassium (KCl). The latter allowed assessment of neuronal viability and to help distinguish neuronal from non-neuronal cells.

We found that live *P. gingivalis* W50 cells induced a rapid calcium influx in 12.5% neurones (3/24), while every neurone responded to KCl. Representative data are shown in Figure 4.1.

4.2.2. Activation of CGRP release from neurone cultures by *P. gingivalis* W50

The above activation of neuronal calcium flux could also lead to neuropeptide release. Since CGRP was only seen to be stored in neuronal cells (Figure 3.12), it is assumed that the CGRP detected in the supernatant derived solely from neuronal cells. Consequently, we investigated whether *P. gingivalis* interaction with neurones led to CGRP release from neuronal cultures. The amount of secreted CGRP was measured by ELISA (see Section 2.12, Chapter 2) in cell culture supernatants after 15 min exposure to whole *P. gingivalis* cells. The results showed that CGRP was massively released on exposure to *P. gingivalis* compared with that obtained with application of the positive control, capsaicin, (Figure 4.2) ($p < 0.001$).

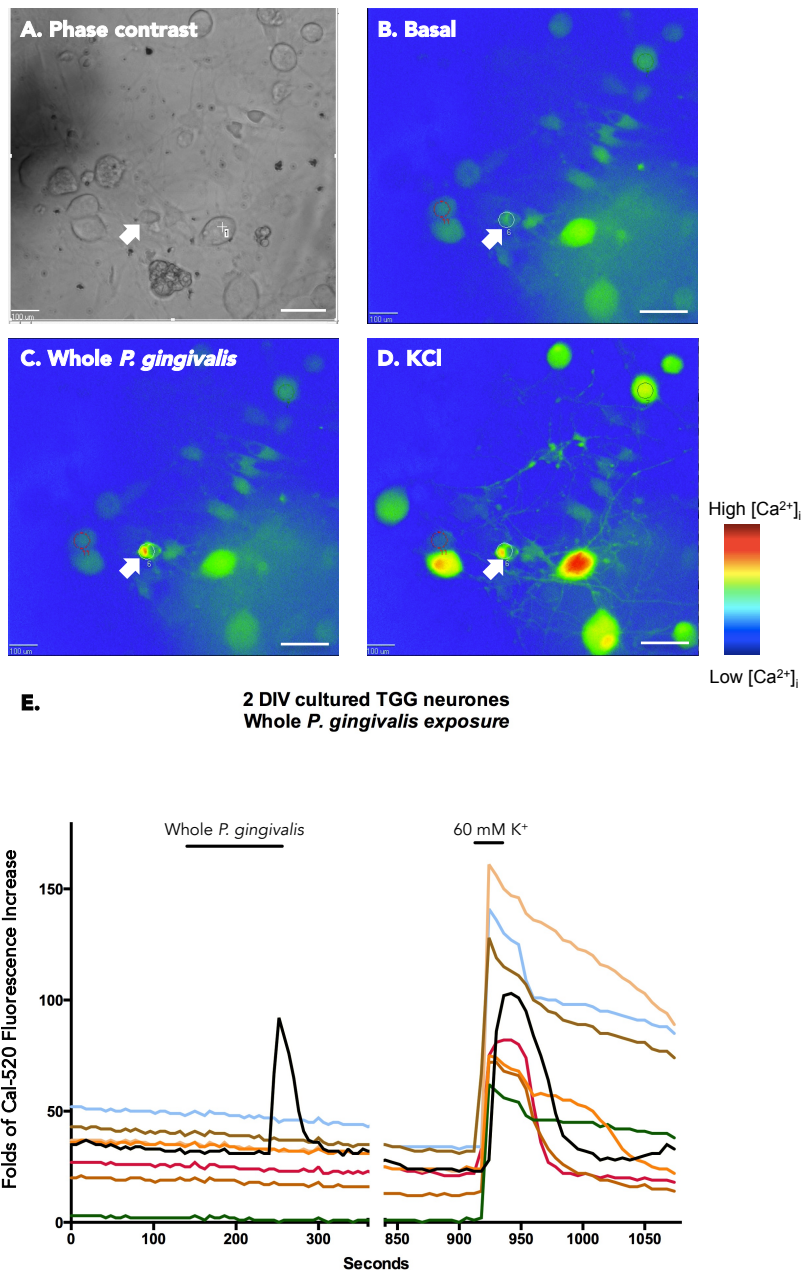


Figure 4.1 Analysis of intracellular calcium levels in primary trigeminal neurones in response to live *P. gingivalis* and high concentration of potassium chloride.

Ca^{2+} levels were measured by loading cells with the single wavelength fluorescent dye Cal 520-AM which were measured by time-lapse microscopy of TG neurone. Ca^{2+} levels are represented as the intensities of the fluorescence emitted at 520 nm after the excitation with 458 nm. After 2 min of optical fluorescence time-lapse acquisition, cells were treated with live *P. gingivalis* for 2 mins (120 sec – 240 sec) to induce the release of Ca^{2+} followed by 2 minutes wash out interval. (A) Phase-contrast image, (B) time-lapse calcium imaging during basal stage. (C) time-lapse calcium imaging during live *P. gingivalis* application. (D) The cells were consequently exposed to high KCl to distinguish healthy neurone from non-neuronal cells. (E) Ca^{2+} levels were demonstrated by Cal-520 intensities tracing of each neurone. The calcium image colour range is from blue of the baseline visual evoked response to red of the peak value. *P. gingivalis* could induce Ca^{2+} elevation in the representative neurone (white arrow). The calcium intensities tracing of responding neurone (white arrow in B, C, and D) is the black trace in Figure E. Scale bar is 60 μm .

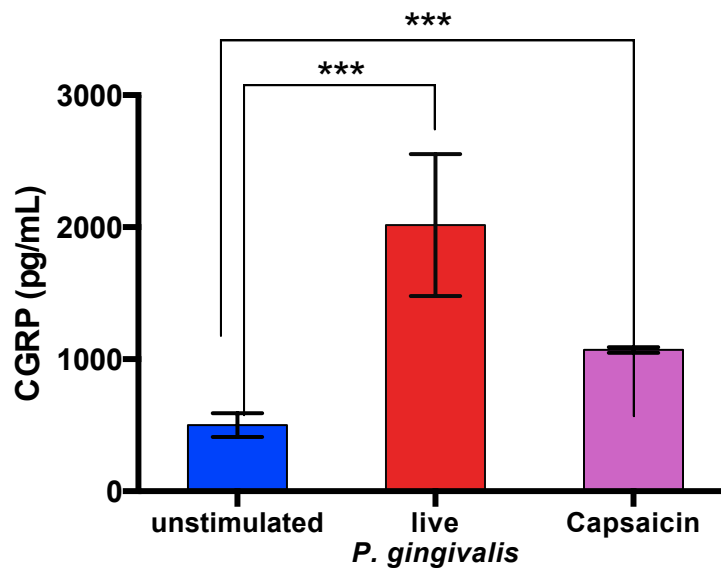


Figure 4.2 CGRP levels in live *P. gingivalis*-, and capsaicin-stimulated TG neurones from control.

The secreted CGRP response to LPS or capsaicin were determined by the incubation of TG cell for 15 minutes with live *P. gingivalis* (100 $\mu\text{g}/\text{mL}$ (from wet weight)) or capsaicin (5 μM) at 37°C with 5% CO_2 . Measurement of CGRP levels was performed using enzyme-linked immunosorbent assay. Data present the mean \pm SD. From two independent experiments. Bars are SD. *** $p < 0.001$.

4.2.3. *P. gingivalis* induces NF- κ B nuclear translocation.

P. gingivalis has been reported to stimulate production of inflammatory cytokines via pathways involving NF- κ B in cells such as monocytes, macrophages and other inflammatory cells. However, there are no reports describing activation of this pathway in neuronal cells following exposure to *P. gingivalis*. Thus we sought to investigate the effects *P. gingivalis* exposure on NF- κ B nuclear translocation in neuronal cells.

Figure 4.3 shows immunohistochemical analysis of a typical culture of TG neurones and non-neuronal cells stained for NF- κ B, β -tubulin and the nuclear stain DAPI. NF- κ B translocation was determined by measuring the nuclear/cytoplasm (nuc/cyt) ratio of NF- κ B fluorescence intensity as described in section 2.11.3, Chapter 2. Nuclear translocation was indicated by a nuc/cyt ratio of ≥ 1 . The results show NF- κ B nuclear translocation occurred in both neurones and non-neuronal cells over the time course of 30 min stimulation with *P. gingivalis*. There was a low level of NF- κ B observed associated with nuclei of neurones and non-neuronal cells even in unstimulated cultures and this may reflect an effect of the artificial culture environment.

For this, we used immunofluorescence and found that live *P. gingivalis* stimulation resulted in positive nuclear translocation of NF- κ B in TG neurones over a period of 30 min. The percentage of neuronal cells positive for NF- κ B translocation significantly increased from 18% to 52%. The percentage of NF- κ B translocation-positive non-neuronal cells also rose in response to live *P. gingivalis* from 37 to 61%. Quantitative analysis of neuronal nuclear translocation stimulated by *P. gingivalis* is shown in figure 4.3, E.

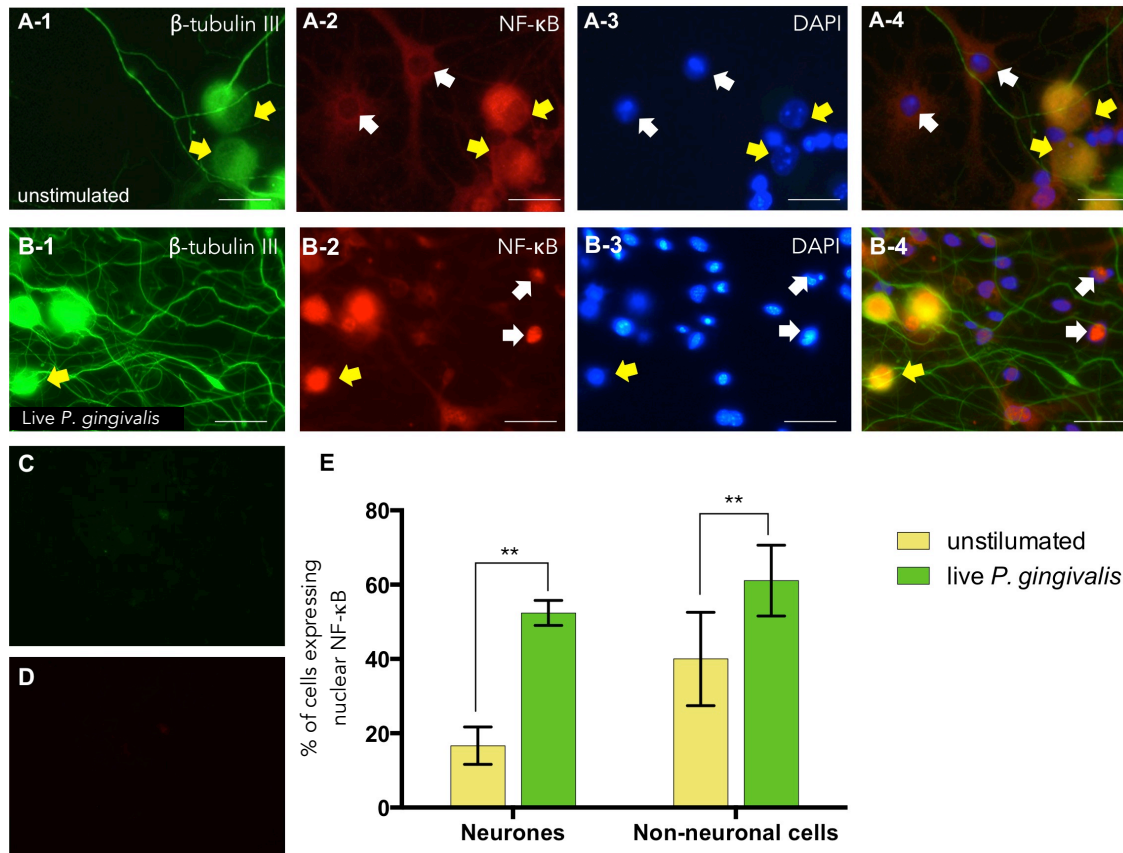


Figure 4.3 Photomicrographs of p65 NF-κB nuclear translocation in live *P. gingivalis*-treated TG neurones and non-neuronal cells.

The TG cultures were left untreated (panel A) or stimulated with 2.5×10^7 live *P. gingivalis* cells for 30 minutes (panel B). Cells were permeabilised with 0.1% Triton X-100 and subsequently stained with primary antibodies against anti-p65 NF-κB and the correspondent secondary antibodies. The negative control samples are also shown (C-D). The β-tubulin III is shown in green (A1-B1) and p65 NF-κB appears in red (A2-B2). Nuclear staining with DAPI (A3-B3) appears blue. The merged images show the combined p65 NF-κB, β-tubulin III and DAPI staining (A4-B4). Scale bars = 70 μm. Localisation of p65 NF-κB was visualised in neurones (yellow arrows) and non-neuronal cells (white arrows). The translocation of NF-κB was counted as positive when nuc/cyt ratio was ≥ 1 . Quantitative analysis of neuronal nuclear translocation stimulated by *P. gingivalis* LPS is shown in panel E. Neurones and non-neuronal cells positive for NF-κB nuclear translocation were quantified. Data present the mean \pm SD from three independent experiments. Error bars are \pm SD. ** $p < 0.01$. Scale bar is 80 μm.

4.2.4. Effect of haemin level on neuronal cell release of CGRP

The pulp environment is likely to be relatively rich in nutrients that *P. gingivalis* needs for growth compared with dental plaque and the availability of some essential nutrients is known to modulate virulence factors of *P. gingivalis*. One such essential nutrient is haemin, which has been reported to vary both the type of LPS synthesised and the expression of gingipain proteases. Consequently we studied the effect of high haemin vs low haemin growth conditions on the ability of *P. gingivalis* to stimulate neuronal CGRP release. High haemin growth conditions led to massive release of CGRP compared with low haemin conditions or unstimulated neuronal cultures (Figure 4.4).

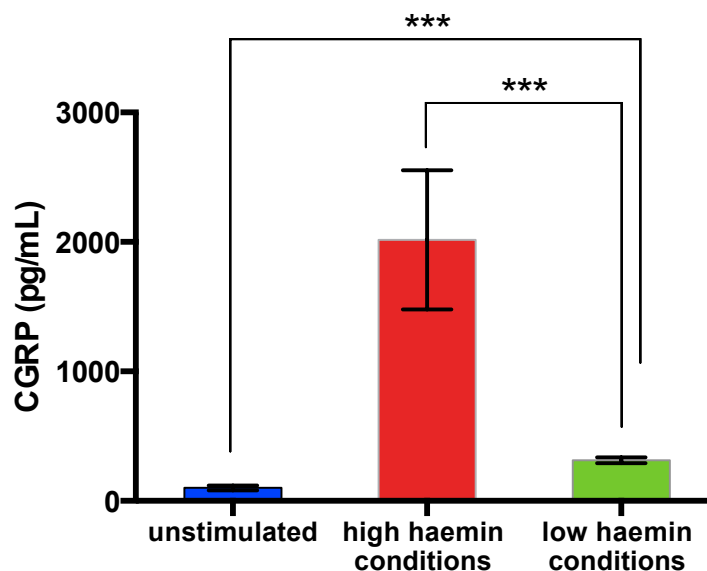


Figure 4.4 CGRP level in haemin modified *P. gingivalis*-stimulated TG neurones.

The secreted CGRP response to *P. gingivalis* grown in high and low haemin conditions. Secreted CGRP was determined in the supernatants of TG cell cultures after 15 minutes exposure to live *P. gingivalis* (100 $\mu\text{g}/\text{mL}$ wet weight) at 37°C with 5% CO_2 . Measurement of CGRP levels was performed using ELISA. Data are the mean from two independent experiments. Error bars are SD. *** $p < 0.001$.

4.3 Discussion

4.3.1 Overview

In the previous chapter, we described the development of an *in vitro* system from trigeminal ganglion neuronal culture to investigate individual cell responses, as well as the whole culture, to a range of stimuli. In this chapter, we describe the direct effects of *P. gingivalis* cells on trigeminal neurones (Figure 4.5). The value of using intracellular calcium imaging analysis to monitor the responses of individual cells to *P. gingivalis* is that calcium ion trafficking can control key functions in neurones and other cell types. Besides, by microscopical analysis is possible to distinguish the activities of neurones from the accompanying non-neuronal cells. Here we demonstrate that exposure to *P. gingivalis* results in significant neuronal activity as exemplified by calcium influx in neurones, and CGRP release and NF- κ B nuclear translocation in both neurones and non-neuronal cells.

These investigations raise questions on how *P. gingivalis* manipulates sensory neurones? The current study showed for the first time that neuronal calcium influx could be induced by live *P. gingivalis* cells. This supports work by others on more mainstream pathogens, such as *Staphylococcus aureus* (Ji et al. 2014; Chiu et al. 2013; Hansen et al. 2006; Minter et al. 2005). These could be viewed in relation to candidate cellular receptors and to *P. gingivalis* virulence factors. Example surface structures of *P. gingivalis* are shown in Figure 4.6 and it can be assumed that TG neuronal sensitisation would have been induced by molecules on the surface of the bacterial cells. The candidate surface molecules include LPS, gingipains, fimbriae, and haemagglutinins.

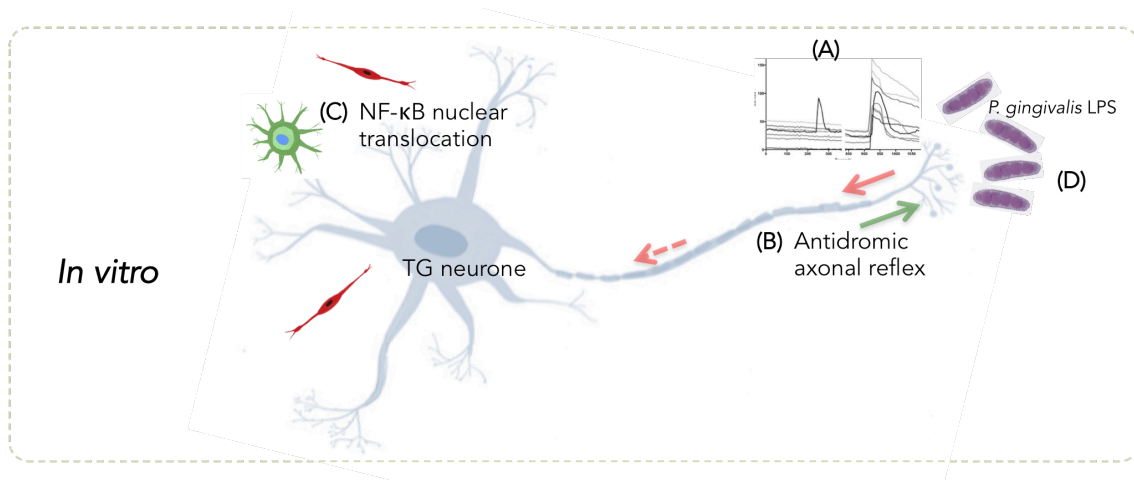


Figure 4.5 Overall TG responses in the exposure of live *P. gingivalis*.

In this study, we found the calcium influx of TG neurones (A). Subsequently, the TG neurones could release CGRP (B), and NF-κB locations also change to nucleus area of neurones and non-neuronal cells (C). Moreover, conditions of TG culture could also modify the neuronal activities.

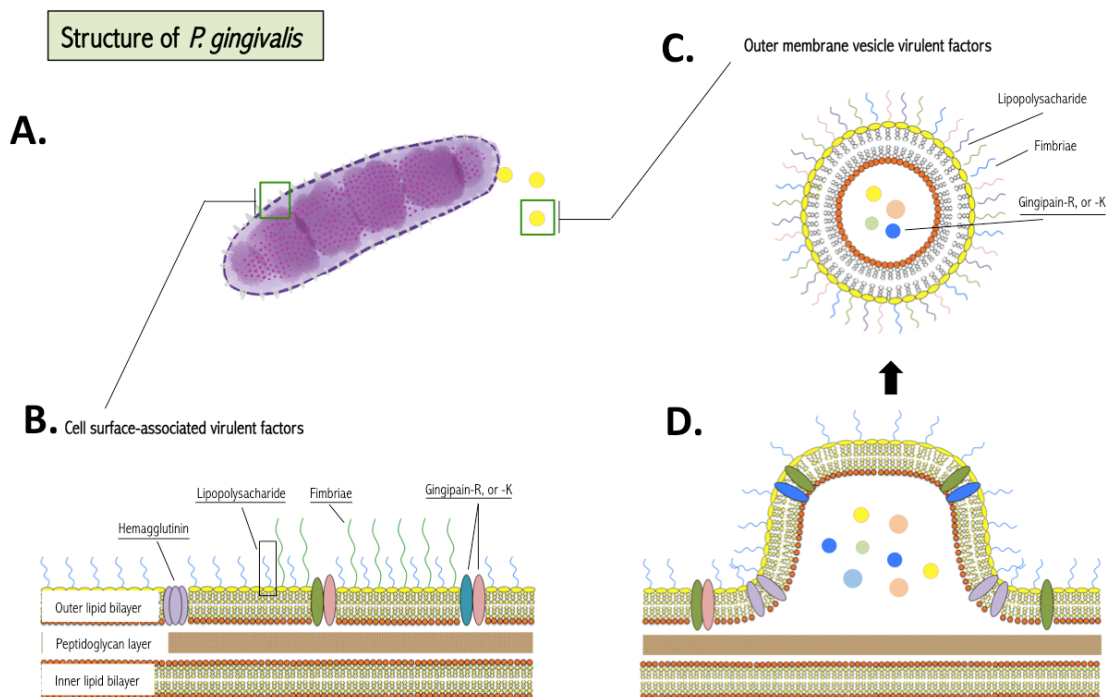


Figure 4.6 *P. gingivalis* virulence factors

(A) *P. gingivalis* is rod-shaped, Gram-negative, anaerobic bacteria. The virulence factors of *P. gingivalis* could be into 2 forms; cell surface-associated form (B), and outer-membrane vesicle (C). Both forms could contain LPS, gingipain, fimbriae, and etc. In the process of outer-membrane vesicle biogenesis of *P. gingivalis*, many virulence factors could be included in the vesicle as well (D). (Modified from Schwechheimer and Kuehn, 2015, copyright was granted to reproduce).

4.3.2 *P. gingivalis* strategies to manipulate host responses

A large number of Gram-negative bacteria have an ability to release outer-membrane membrane vesicles (OMVs). These vesicles contain the full components of bacterial membrane constituents of the cell wall such as LPS, fimbriae, hemagglutinin, and entrapped bacterial protease. The vesicles from the *P. gingivalis* likely to retain a full complement of the parent bacterial cells as shown in Figure 4.6 (Schwechheimer and Kuehn 2015; Nakao et al. 2011; Veith et al. 2014). There have been many studies to suggest that OMVs of *P. gingivalis* could cause the functional impairment of oral epithelial cells (Nakao et al. 2011; McKee et al. 1986). Taken together, the vesicles released from bacterial cells could be considered to be powerful projectile weapons to stimulate host cells, even without direct contact between bacterial cell and host cells. This remote mechanism is an important mechanism of Gram-negative bacteria to evade host defensive mechanisms.

However, in *in vitro* study, the pathogenicity of bacteria could possibly significantly reduce due to the loss of the OMVs as reported in the study of Nakao et al. (2011), who suggested that bacterial cell washing drastically reduced surface antigenicity caused by the loss of OMVs. So, it is possible that there are more vesicles likely to be made in a pulp environment than in a lab culture used in this study. It is possible that, in the laboratory set up, we need a higher concentration of bacterial components to mimic clinical injury sites.

There are many cellular receptors involved in direct activation of neurones, but we have selected to study LPS, and gingipains, in particular. These 2 components seem to have the most impact on the candidate receptors such as TRPV1, TRPA1, TLR4, and PAR2. Moreover, LPS, and gingipain have been studied extensively in the other cell types, mostly immune cell. Therefore, we can compare the mechanisms of a classic pathway with the neuronal activation pathway.

4.3.3 Control of peripheral sensitisation by integration of environmental cues

Haemin is a key microenvironmental component that is believed to vary depending on the state of local vascularity. There have been many studies which showed significant differences in the susceptibility of *P. gingivalis* cells grown under different concentration of haemin (McKee et al. 1986; Al-Qutub et al. 2006; Pike et al. 1994). Cells grown under haemin-excess conditions were always more virulent than haemin-limited cells (Marsh et al. 1994). This could be explained by the limited number of amino acids being metabolised during growth with limited nutrients (McKee et al. 1986). Haemin is known to be responsible for alterations in lipid A structure content (Al-Qutub et al. 2006). In addition, haemin levels influence enzyme activity, with haemin-excess conditions producing greater trypsin-like enzyme activity (Marsh et al. 1994).

However, for OMVs, cells grown under haemin excess conditions produce fewer extracellular vesicles — both surface-associated and secreted OMVs — when compared with cells grown under haemin limitation (McKee et al. 1986). Taken together, the availability of haemin for growth was one of the most significant factors to control virulence of *P. gingivalis*. In this study, we could support that haemin conditions could consequently changes microbial virulence factors, which in turn affect neuronal activity demonstrated by higher CGRP release following exposure of TG cultures to *P. gingivalis* grown in higher haemin conditions.

4.3.4 Trigeminal neuronal supporting cell

As well as direct effects on neurones, it is possible in our culture system that the neurones respond to stimulation by non-neuronal cells which themselves are responding to bacteria or their products. Indeed, we have demonstrated glial cell involvement in the neuronal responses to *P. gingivalis*. Recent reports have suggested that satellite glial cells could be a possible therapeutic target for the modulation of pain (Watkins and Maier 2002; Takeda et al. 2009). This is because neuronal excitability could be developed and maintained through the sensory neurone along with the surrounding satellite glial cells acting as a functional unit (Kushnir et al. 2011; Hanani 2015; Poulsen et al. 2014; Takeda et al. 2009; Villa et al. 2010; Costa and Neto 2015). In this study, we also demonstrated that TG neuronal supporting cells could be activated by *P. gingivalis* (e.g. through immunofluorescence of NF- κ B nuclear translocation). Taken together, the activation of neuronal supporting cells, such as satellite glial cells and/or Schwann cells, may be a crucial element in the generation and maintenance of orofacial pain. However, at this stage, it is not clear whether this activation of non-neuronal cells is involved the dental pain generation. A further study to characterise their contribution will be addressed in Chapter 7.

4.3.5 Limitation, and future prospects

In a model system like the trigeminal cultures developed here, it is difficult to estimate what concentration of bacteria should be used for challenge to be similar to that which occurs in an infected pulp. In a study of infected pulps the bacterial load was found to be, ranging from 1.68×10^4 to 3.3×10^7 with a median value of 3.02×10^5 (Siqueira et al. 2007). In our study, we used approximately 10^8 bacteria to stimulate a TG neurone culture, which was about 3-fold more than the highest number of bacteria found in an infected pulp. However, this number was distributed in 1 mL of culture medium, whereas in an infected pulp the bacteria present would be in a much smaller volume. Indeed the volume of the average adult pulp has been estimated to be only 0.02 mL (Avery 1990), which equates to approximately 2×10^6 bacteria/20 μ L i.e. within the range of bacterial load found in an infected pulp. *P. gingivalis* is known to be a poor inducer of some inflammatory cytokines (Liu et al. 2008). This could be the reason why a very high concentration of *P. gingivalis* is needed in our system before CGRP could be released from sensory neurones and the supporting cells.

This chapter demonstrates that *P. gingivalis* is able to directly activate TG neurones, and raises the question as to the mechanisms underlying this activation.


4.4 Conclusion

Dental pulp infection is a complicated process involving various molecules and interactions. To defend against the bacterial challenge, the nociceptive system seems to be a mechanism that responds with a latency of only seconds. Whereas aspects of the immune system would take longer to lead to an inflammatory response, which lends weight to the argument that the neurones may be acted upon directly by the bacteria and not only through products of the non-neuronal cells that surround them.

Direct activation of pain generation by bacteria has been less well studied than responses to inflammation, but by using an *in vitro* culture of trigeminal neurones we were able to study the response of individual neurones to *P. gingivalis*. Here, we have shown that nociceptive neurones respond directly to the presence of whole *P. gingivalis*. However, the molecular mechanisms involved require further study and we have addressed aspects of this in the following Chapters.

Chapter 5

*Possible roles of TLRs/TRPs
in generation of pain associated
with dental infection*





5. Possible role of TLRs, and TRPs in generation of pain associated with dental infection

5.1 Introduction

Infection of the dental pulp can activate a variety of pathophysiological mechanisms including the generation of pain. However, it remains unclear whether and how bacteria and/or their constituents and products can directly activate nociceptive sensory neurones (Ma et al. 2010; Vang et al. 2012; Lillesaar et al. 2003). There are two particularly potent stimulatory components of Gram-negative bacteria that may cause a direct activation of sensory neurones, which are lipopolysaccharide (LPS), and proteolytic enzymes. In this Chapter, we investigate the effects of LPS on TG neurones.

Although exposure to *E. coli* LPS and peptidoglycan components can increase neuronal excitability of dorsal root ganglion neurones (Meseguer et al. 2014), it is not known whether non-enterobacterial LPS found in pulpal infection, can directly affect neuronal responses. Such activation could be possible through Toll-like receptors (TLRs) or transient receptor potential cation channel members A1 and V1 (TRPA1, TRPV1).

These 2 categories of surface receptors are thought to be key participants in the rapid nociceptor response and neurogenic inflammatory responses to LPS. Firstly, it is known that LPS could trigger the pattern recognition property of TLRs. The innate immune system can react against invading microorganisms by relying on the presence of repetitive molecular patterns which are highly conserved throughout evolution (Santoni et al. 2015). There are 11 TLRs that have been identified in humans with varying ligand-binding specificities (Qi et al. 2011). For example, TLR4 is a receptor that specifically recognises LPS of Gram-negative bacteria (Coats et al. 2005).

Secondly, transient receptor potential channels (TRPs) are involved in sensitisation mechanisms associated with activation of nociceptors by inflammatory stimuli (Geppetti et al. 2008; Santoni et al. 2015; Veldhuis and Bunnett 2013). Sensitisation

of TRPV1 has been described to be initiated by LPS via a TLR4-mediated mechanism (Diogenes et al. 2011). On the other hand, TRPA1 activation relies on the general physico-chemical properties of an agonist. Given that the lipid A of LPS is anionic molecule which is reported to be a potential agonist to TRPA1, therefore it is possible that TRPA1 could play a mediating role in the interaction of nociceptors with LPS (Meseguer et al. 2014).

The aims of this study were to determine whether LPS from *P. gingivalis* could trigger cellular activity in neurones. Detecting and imaging calcium fluxes in the cells was used to assess neuronal responses because calcium ions act as intracellular signals to elicit cellular (neuronal and non-neuronal) responses such as altering gene expression, and regulating cytokine or neurotransmitter release (Fischer et al. 2010). In this part of the study, we tested the hypothesis that LPS directly activates TG sensory neurones via one or more of the cell receptors TLR4, TRPA1, or TRPV1. We suggest that one outcome of such activation would be release of the neuropeptide, calcitonin-gene related peptide (CGRP).

The objectives of the work in this Chapter were to:-

1. Determine the expression of TLRs, TRPs in TG culture
2. Extract LPS from *P. gingivalis*
3. Obtain calcium-imaging data following *P. gingivalis* LPS application
 - *P. gingivalis* W50 LPS
 - Ultrapure *P. gingivalis* LPS
4. Investigate the cellular receptors that are directly activated by LPS
5. Quantify levels of secreted CGRP in response to *P. gingivalis* LPS compared with the positive agonist, capsaicin
6. Observe intracellular changes of NF- κ B location following incubation with *P. gingivalis* LPS

5.2 Results

5.2.1 Expression of TLRs, TRPs in TG cultured cells

5.2.1.1 Presence of TLR4 and TLR7 demonstrated by immunofluorescence.

The mouse TG cultured neurones used in this study expressed both TLR4 and TLR7 receptors. Co-localisation studies indicated that TLR4 was expressed on both neurones and non-neuronal cells, as indicated by co-localisation of TLR4 with β -tubulin III antibodies. TLR4 was highly expressed in TG neurones with more than 70% (34/48) of neurones staining positively with anti-TLR4 antibody. However, the expression of TLR4 was also present on non-neuronal cells, although staining was much weaker (Figure 5.1).

We also found evidence for the presence of TLR7 on neurones. As shown in Figure 5.2, the majority of the TLR7-IR visible was observed on neurones whereas there was very little or weak immunofluorescence for TLR7-IR on non-neuronal cells. Quantitative analysis confirmed that TLR7 expression was also present on over 70% (65/87) of the neurones in the culture.

5.2.1.2 Presence of CD14 demonstrated by immunofluorescence.

Cluster of differentiation 14 (CD14) is a protein component of the innate immune system. It exists in two forms, either anchored to the cell membrane or in solution (Coats et al. 2005). CD14 is thought to act as a co-factor along with TLR4 to bind LPS (Watanabe et al. 2013; Court et al. 2011). In TG cultures, we could demonstrate weak expression of membrane-bound CD14 on nearly all of both the neurones and the non-neuronal cells, as shown in Figure 5.3.

5.2.1.3 Presence of TRPA1 and TRPV1 in TG cultures demonstrated by immunofluorescence.

Expressions of TRPV1, TRPA1 and TRPM8 have been demonstrated previously in TG sensory neurones innervating dental pulp (Gibbs et al. 2011; Huang et al. 2012). A range of methods have been used to demonstrate their presence including,

immunofluorescence, western blot, RT-PCR, and calcium flux functionality. Here we used immunofluorescence because it allowed us to observe expression in specific cell populations within the mixed cell culture. Triple labelling of either TRPV1 or TRPA1, β -tubulin III antibodies and DAPI was performed on 2 day-old TG cultures. TRPA1, and TRPV1 were clearly present on cells within the TG culture with approximately 40 % of TG neurones expressing TRPV1. This was particularly noticeable in the small-to-medium sized neurones (representative data is shown in Figure 5.4), while about 10-15% of TG neurones expressed TRPA1 and these were mainly in the small sized neurone population (representative data is shown in Figure 5.5).

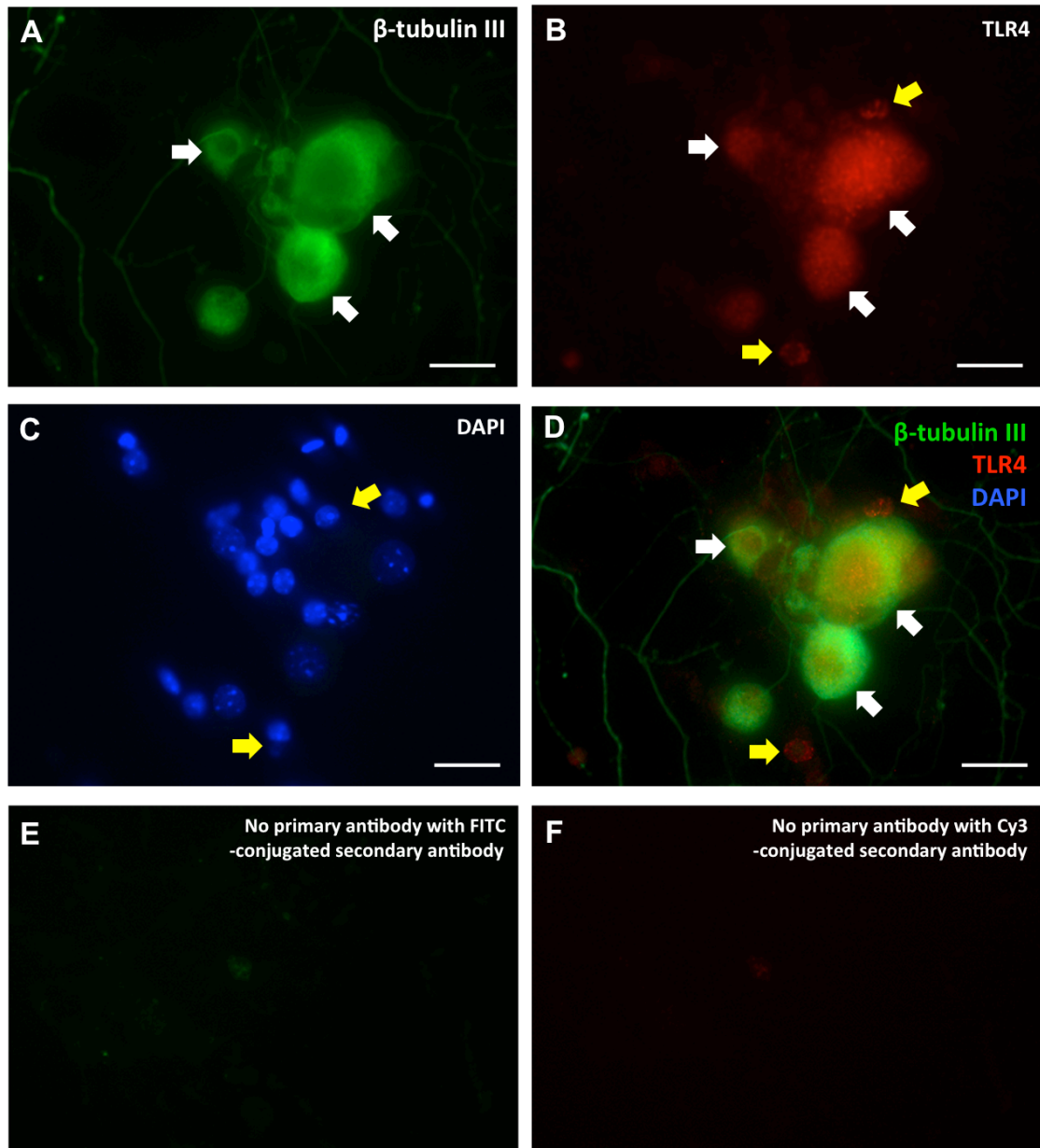


Figure 5.1 The expression of TLR4 in TG culture.

These figures show triple labelling of β -tubulin III (A), TLR4 (B), DAPI (C), and the co-localisation of all three molecules (D). White arrows depict example neurones that highly express TLR4. Some non-neuronal cells also express TLR4 as depicted by yellow arrows. The β -tubulin III, and TLR4 negative control samples showed no positive labelling in panel E and F, respectively. Scale bars are 70 μ m.

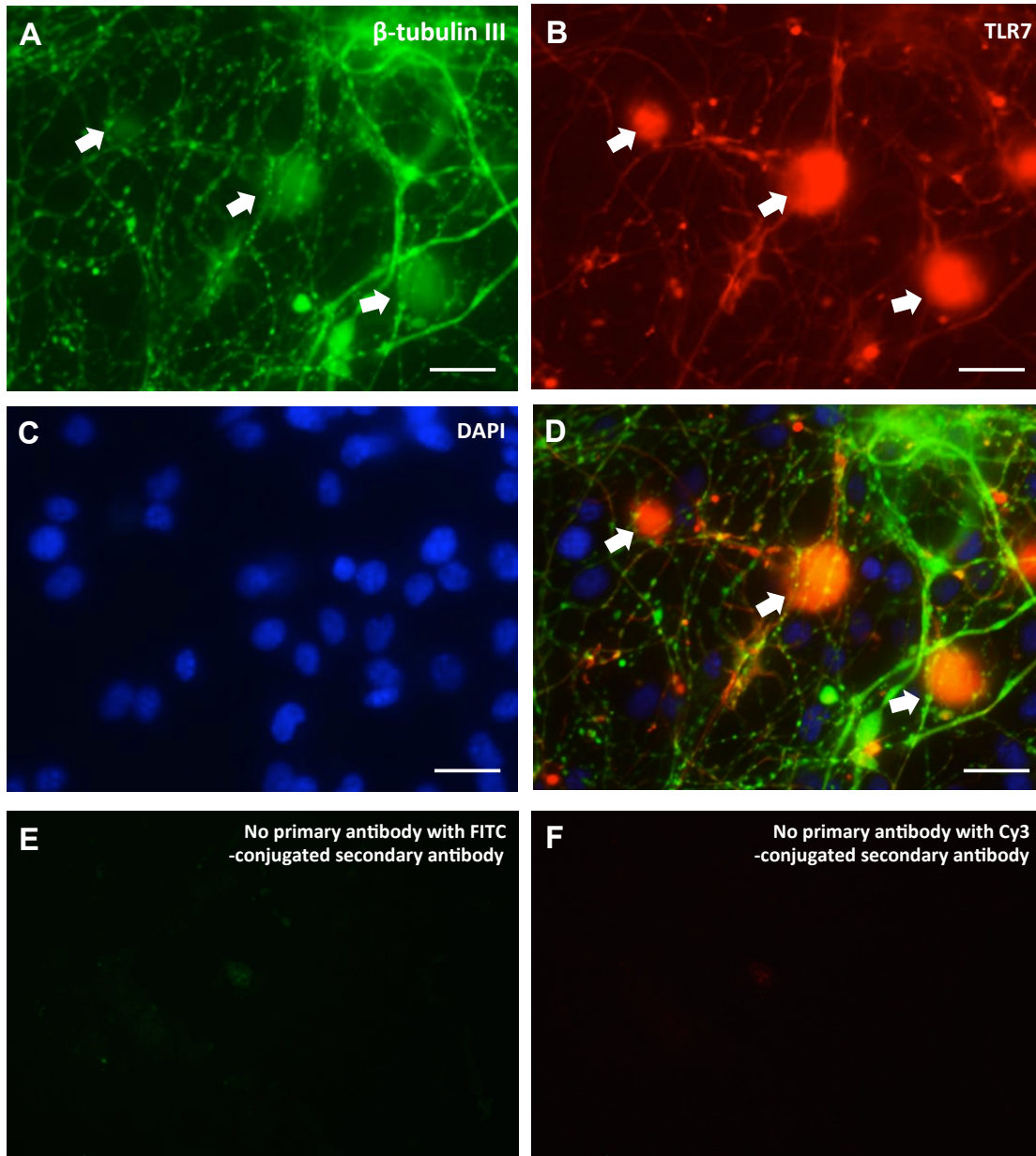


Figure 5.2 The expression of TLR7 in TG culture.

Representative images showing that TLR7 is expressed specifically on neurones. These figures show the triple labelling of β -tubulin III (A), TLR7 (B), DAPI (C), and the co-localised (D). Red arrows depict example neurones that express TLR7. Yellow arrows depict example neurones with lower expression of TLR7. Scale bars are 70 μ m.

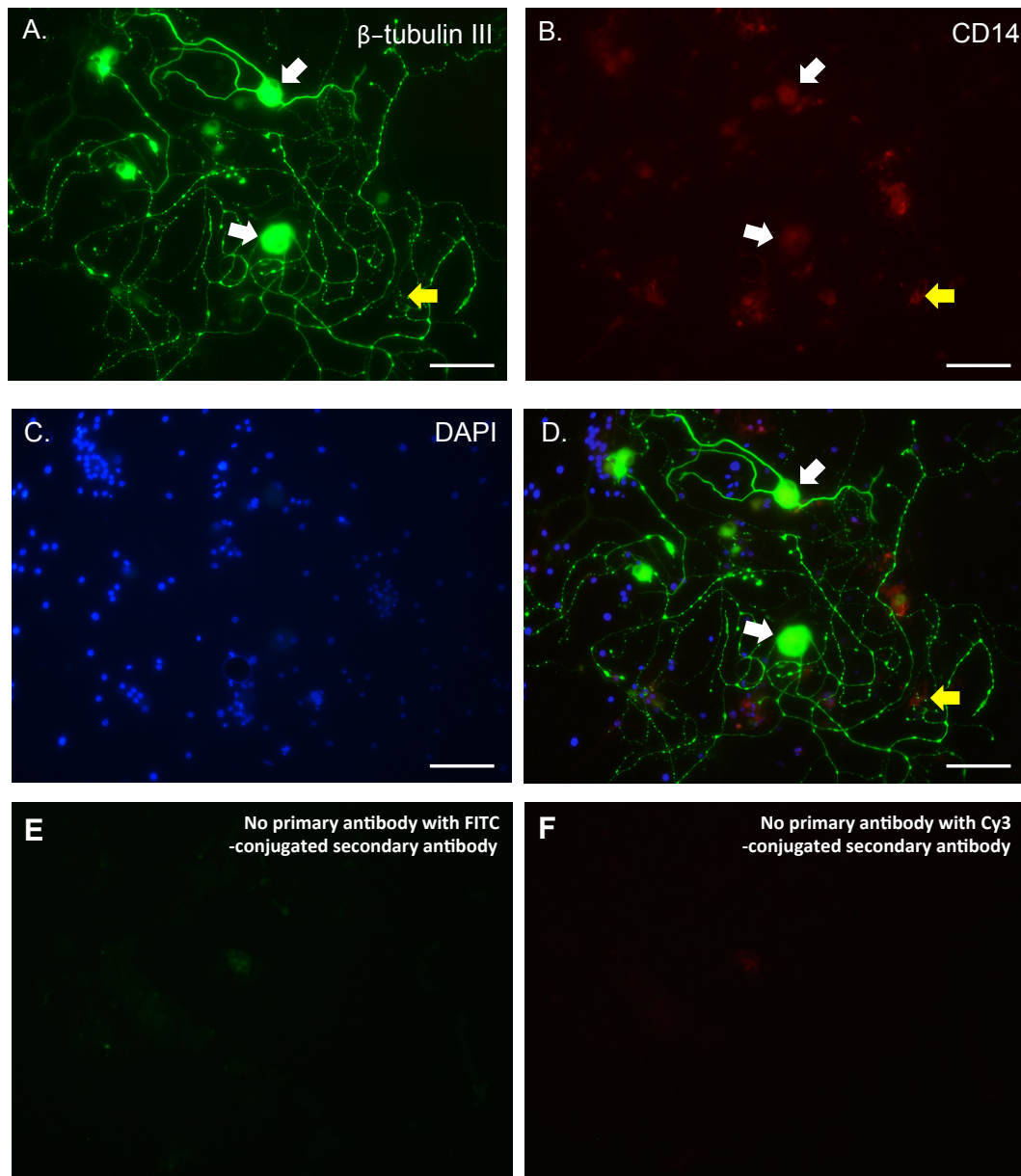


Figure 5.3 The expression of CD14 on cells of TG culture.

These figures show triple labelling of β -tubulin III (A), CD14 (B), DAPI (C), and the co-localisation of all three molecules (D). White arrows depict example neurons that weakly express CD14. Some non-neuronal cells also express CD14 as depicted by yellow arrows. Scale bars are 120 μ m.

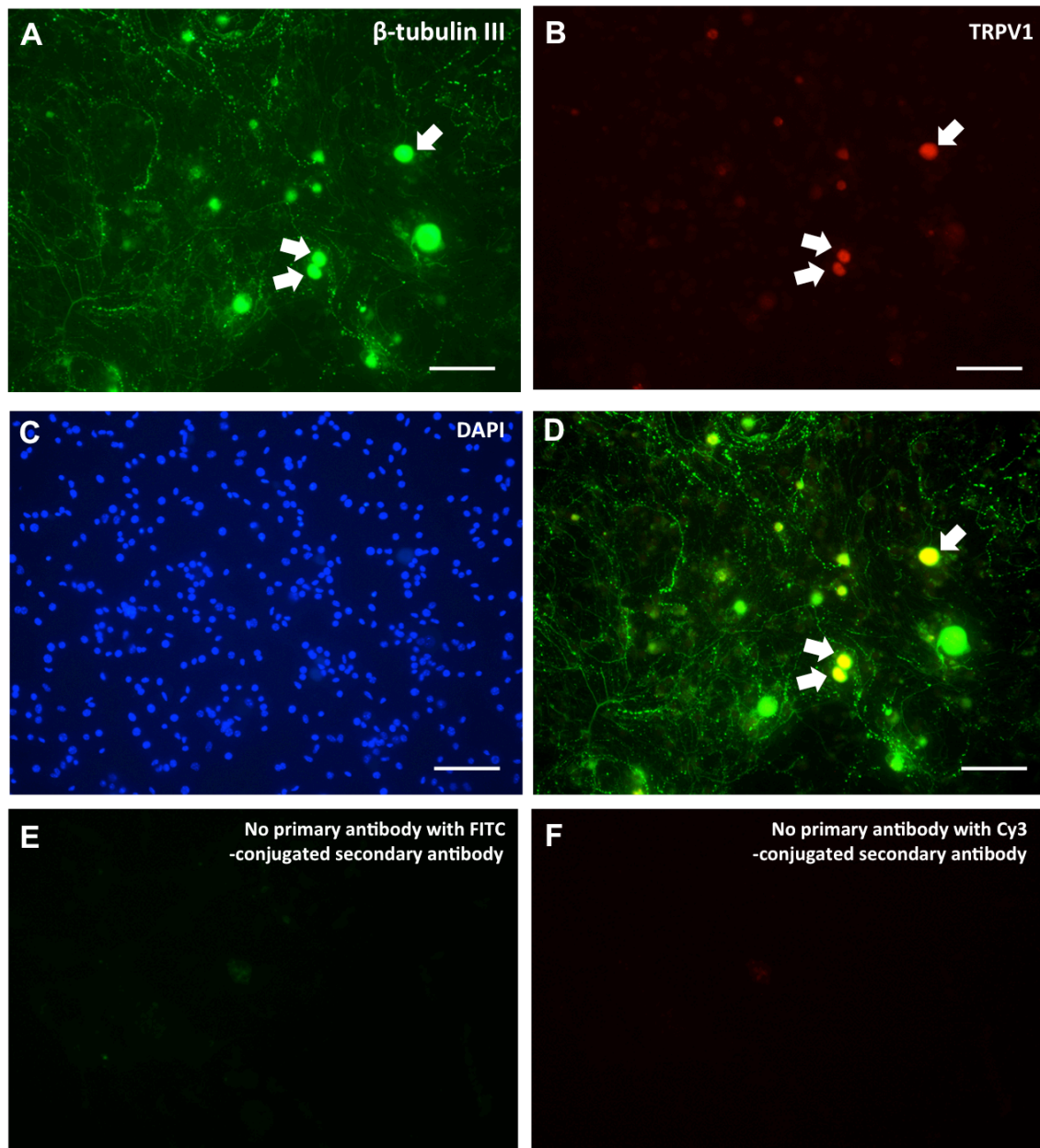


Figure 5.4 The expressions of TRPV1 on cells of TG culture.

These figures show the triple labelling of β -tubulin III (A), TRPV1 (B), DAPI (C), and the co-localisation of all three molecules (D). Arrows depict example neurons that express TRPV1. This representative data clearly showed that TRPV1 was expressed primarily on small-medium neurones. The β -tubulin III, and TRPV1 negative control samples showed no positive labelling in panel E and F, respectively. Scale bars are 150 μ m.

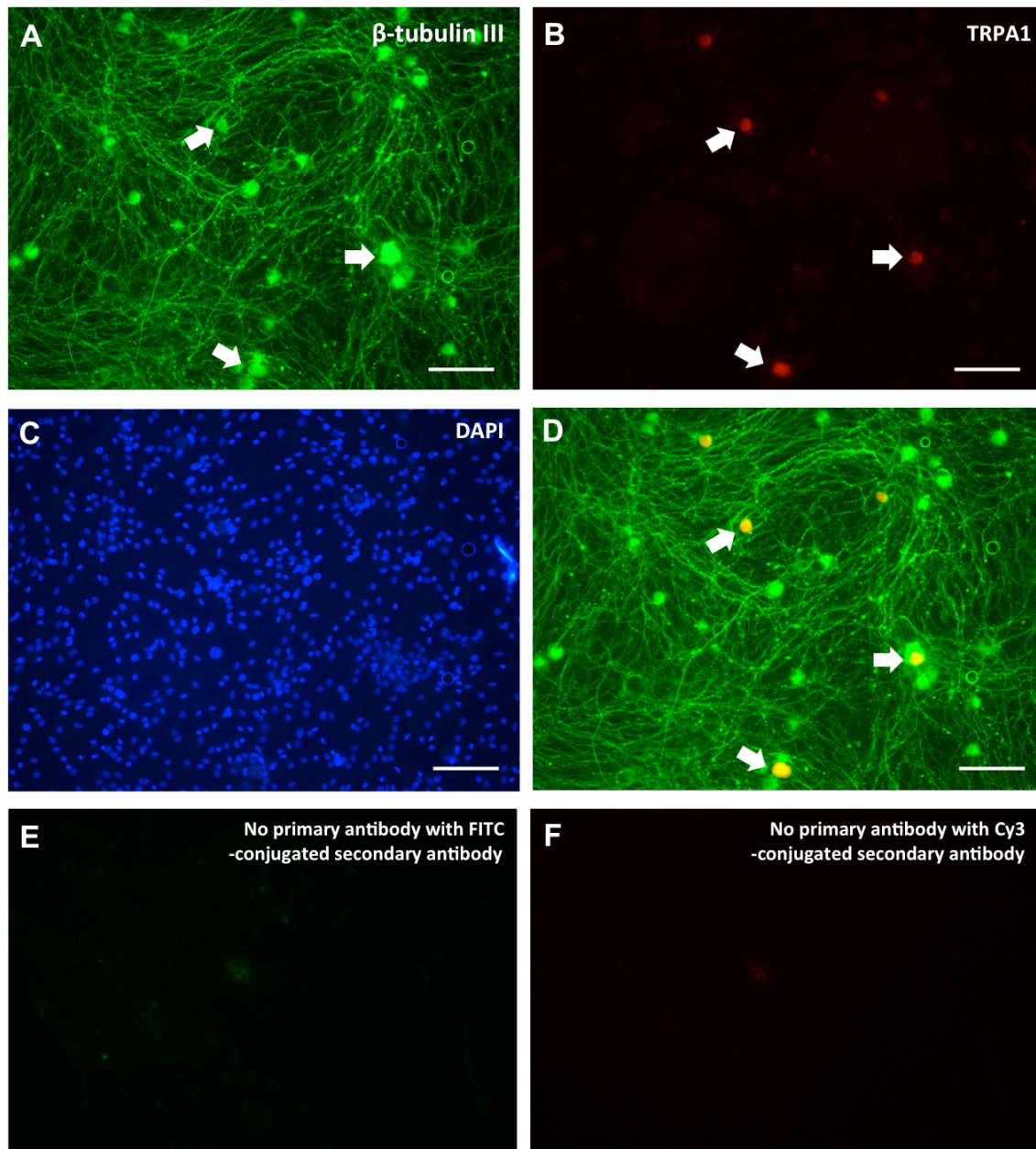


Figure 5.5 The expressions of TRPA1 on cells of TG culture.

These figures show the triple labelling of β -tubulin III (A), TRPA1 (B), DAPI (C), and the co-localisation of all three molecules (D). Arrows depict example neurones that express TRPV1. This representative data clearly showed that TRPV1 was expressed primarily on small neurones. The β -tubulin III, and TRPV1 negative control samples showed no positive labelling in panel E and F, respectively. Scale bars are 150 μ m.

5.2.2 Functional characterisation of TG cells in response LPS

5.2.2.1 Characterisation of LPS extraction from W50 *P. gingivalis*

5.2.2.1.1 Purification and qualitative analysis of LPS

LPS is a fundamental component of the outer membrane of the cell wall of Gram-negative bacteria. Here we report extraction and purification of LPS from *P. gingivalis* W50 using a commercial kit. Resultant *P. gingivalis* LPS samples (100 µg/mL; 20 µL/lane), and commercial *E. coli* LPS (50 µg/mL; 20 µL/lane) were loaded and run on 15% SDS-PAGE gels. The methods are described in section 2.4 in the Materials and Methods chapter.

To characterise the pattern of LPS, SDS-PAGE was used to observe the multiple repeating O-side chain, which produces a ladder on these gels. The gels contained 7 M urea and the profiles of extracted *P. gingivalis* LPS obtained are shown in Figure 5.6. No positive bands were found by coomassie blue staining suggesting low or no contamination with protein. In contrast silver staining showed a clear ladder and a smeared track of the polysaccharide components of LPS (Figure 5.6, lane 2). The *P. gingivalis* LPS obtained using the commercial extraction kit was similar in band pattern to that of the *E. coli* sample. To be sure that this was none of the bands were protein, the sample was treated with proteinase K (Rangarajan et al., 2008). No change to the band pattern was seen.

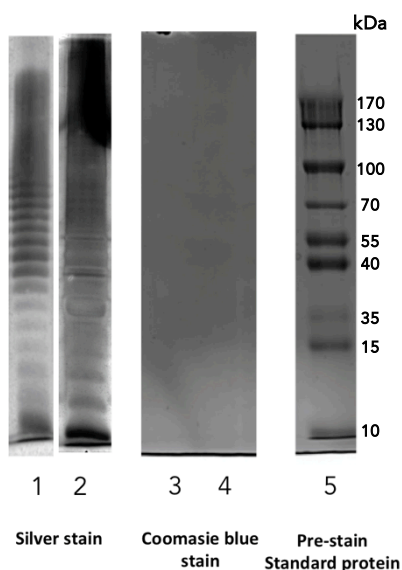


Figure 5.6 LPS loaded in SDS-PAGE with silver staining.

SDS-urea PAGE with silver staining and Coomassie blue staining of W50 *P. gingivalis* LPS. *E. coli* LPS (Lane 1) extracted *P. gingivalis* LPS (Lane 2) silver staining. Lanes 3-4 are Coomassie blue stained of the material in lanes 1-2. Lane 5 is protein molecular weight standards.

5.2.2.1.2 Biological evaluation of the LPS

THP-1 differentiated macrophages were used to evaluate the biological validity of the LPS preparations. Macrophages were exposed to various concentrations of *P. gingivalis* and *E. coli* LPS for 4 h and their TNF- α secretion response determined. All concentrations of the *P. gingivalis* LPS tested resulted in a dose-dependent release of TNF- α (Figure 5.7). Commercial *E. coli* LPS stimulated a maximal release of TNF- α at 2 $\mu\text{g}/\text{mL}$ or below and which was approximately fourfold greater than that obtained with the *P. gingivalis* preparation. Both the extracted *P. gingivalis* LPS and commercial *E. coli* LPS stimulated TNF- α secretion. The *E. coli* LPS resulted in higher levels of the TNF- α secretion, however the extracted *P. gingivalis* LPS significantly raised TNF- α secretion compared with negative control.

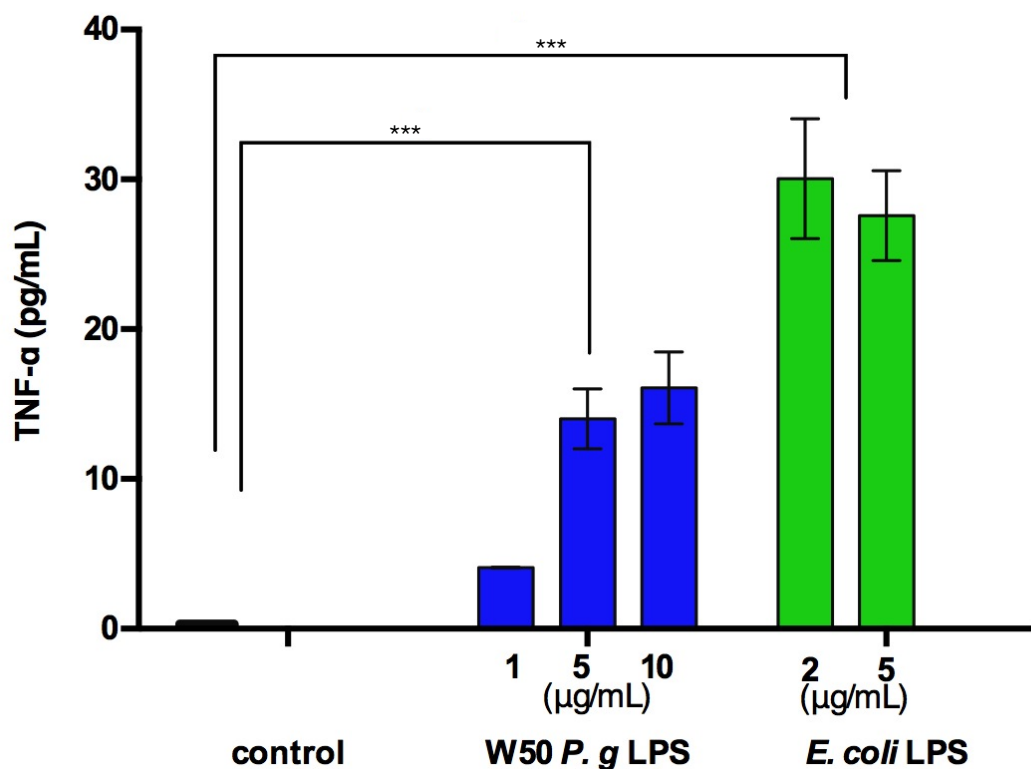


Figure 5.7 The secretion of TNF- α in response to *P. gingivalis* and *E. coli* LPS.

The secreted TNF- α response to *P. gingivalis* W50 and *E. coli* LPS were determined by the incubation of macrophage cells for 4 hours with their respective LPS (1, 5, and 10 $\mu\text{g}/\text{mL}$) or *E. coli* LPS (2, and 5 $\mu\text{g}/\text{mL}$) at 37°C with 5% CO₂. Measurement of TNF- α levels was performed using enzyme-linked immunosorbent assay. Data present the mean of two biological replicates. Bars are SD, *** $p < 0.001$.

5.2.2.2 LPS, TRPA1, and TRPV1 agonists can rapidly activate TG neurones.

5.2.2.2.1 *P. gingivalis* W50 LPS could activate TG neurones

In the initial stage of the study, we conducted experiments using LPS from *P. gingivalis* W50. The extracted LPS was shown to be biologically active by the stimulation of TNF- α secretion from macrophages (differentiated THP-1 cells). We then determined the biological effects of *P. gingivalis* on neurones by following calcium fluxes within those cells using an imaging method.

We found that 10, 20, and 50 $\mu\text{g}/\text{mL}$ of *P. gingivalis* LPS did cause a rise in calcium in TG neurones by Fura-2 AM. 50% of TG neurones responded to 50 $\mu\text{g}/\text{ml}$ *P. gingivalis* LPS compared to 15-20% of cells to 10-20 $\mu\text{g}/\text{mL}$. These data indicate that LPS from *P. gingivalis* could activate neuronal excitability which leads us to speculate that the activations of neurones may work through TLRs, such as TLR2 and TLR4 (Figure 5.8).

In this type of work, it is important to have a sufficient concentration of LPS to observe effects, as well as suitably pure material. It was decided, therefore, to study the activation of TG neurones using ultrapure *P. gingivalis* LPS and which is known to be able to interact with the TLR4 receptor (Ochoa-Cortes et al. 2010).

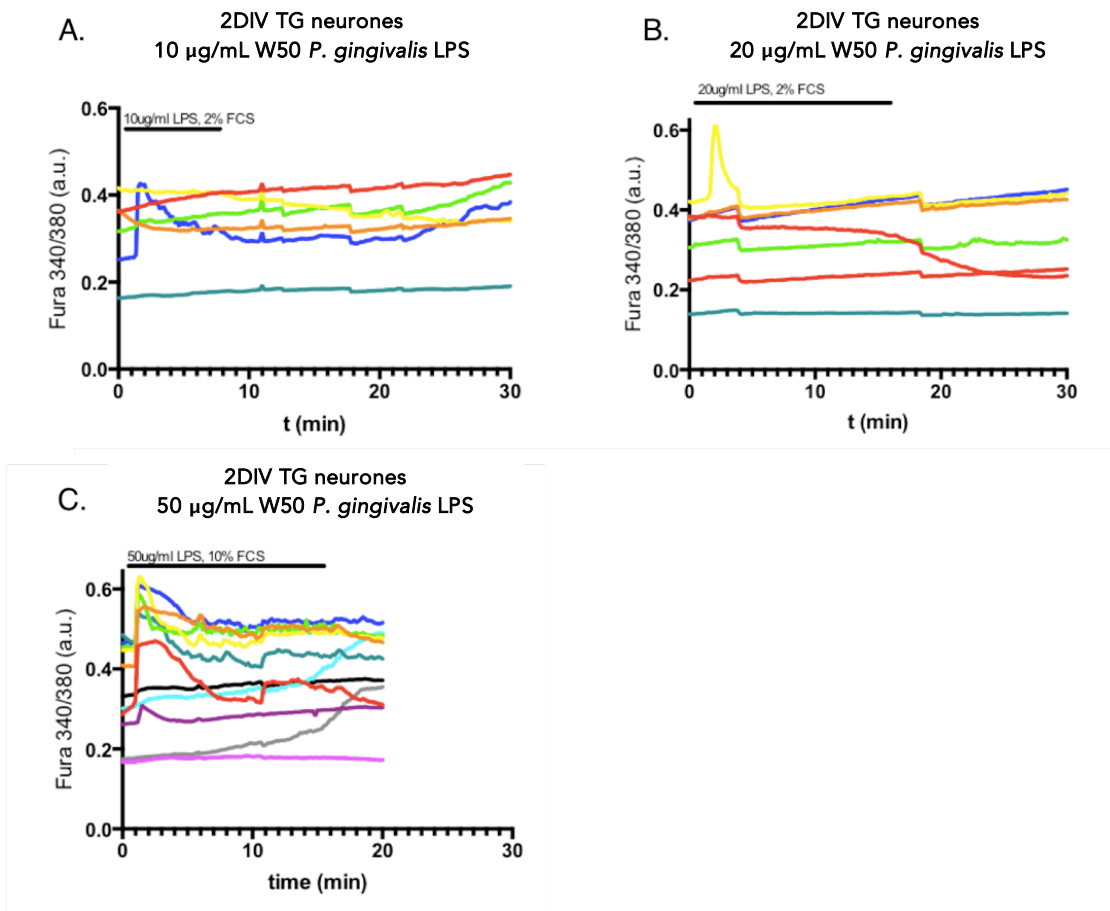


Figure 5.8 *P. gingivalis* W50 LPS-induced calcium signals in TG neurones.

Ca²⁺ levels were measured by loading cells with the ratiometric fluorescent dye Fura 2-AM which were measured by time-lapse microscopy of TG neurone. Coloured traces represent neuronal cell responses. Ca²⁺ levels are represented as the intensities of the fluorescence emitted at 340 and 380 nm after the excitation with 458 nm. Data represent the ratio of intensities of Fura 340/380 tracing of each neurones. After 2 min of optical fluorescence time-lapse acquisition (data not shown in the figure), cells were treated with *P. gingivalis* LPS for 8-15 min to induce the release of Ca²⁺. Traces in (A) and (B) show representative individual TG neurones responding to 10-20 µg/mL LPS over time. The traces show that 15-20% (n=37, from 2 independent experiments) of neurones responded to the LPS. Figure C shows that 50% (n=16, from 2 independent experiments) of representative individual TG neurones responded to 50 µg/mL LPS.

5.2.2.2.2 Ultrapure *P. gingivalis* LPS could activate TG neurones

Since the LPS preparation extracted from *P. gingivalis* W50 might have contained contaminants such as residual chemical reagents or protein debris that could possibly activate TG neurones, we confirmed the above results using commercial ultrapure *P. gingivalis* LPS. This ultrapure LPS from *P. gingivalis* ATCC 33277 is reported to be specifically recognised by TLR4.

Our study also demonstrated that about 13% (15/112), and 33% (37/112) of mouse TG neurones responded to cinnamaldehyde (CA) and capsaicin (CAP), respectively. Interestingly, there was 86.67% (13/15) overlap of neurone populations sensitive to LPS and CA, which was much higher than the overlap of LPS and CAP responsive population (13.5%; 5/37). Application of high potassium was performed to assess neurone viability and to help distinguish neuronal from non-neuronal cells.

Using Cal-520 AM for intracellular calcium imaging, the ultrapure 20 µg/mL *P. gingivalis* LPS directly activated more than 20% of TG neurones (24/90). Also, approximately 40% (18/57) of the non-neuronal cells present, such as satellite glial cells and Schwann cells, responded to the LPS (representative data are shown in Figure 5.9).

5.2.2.2.3 *E. coli* and ultrapure *P. gingivalis* LPS could both activate calcium influx

P. gingivalis LPS is thought to be a poor inducer when compared with *E. coli* LPS. This experiment were performed to determine the effects of *E. coli* and *P. gingivalis* LPS on transient calcium elevation. TG cultures were exposed to various concentrations of either *E. coli* LPS or *P. gingivalis* LPS. The data from 2 – 3 independent experiments showed that TG neurone intracellular calcium could be transiently elevated by lower concentrations of *E. coli* LPS (range from 2 – 20 µg/mL) but that higher concentrations of *P. gingivalis* LPS were needed to stimulate the TG neurones (20 µg/mL) (Table 5.1).

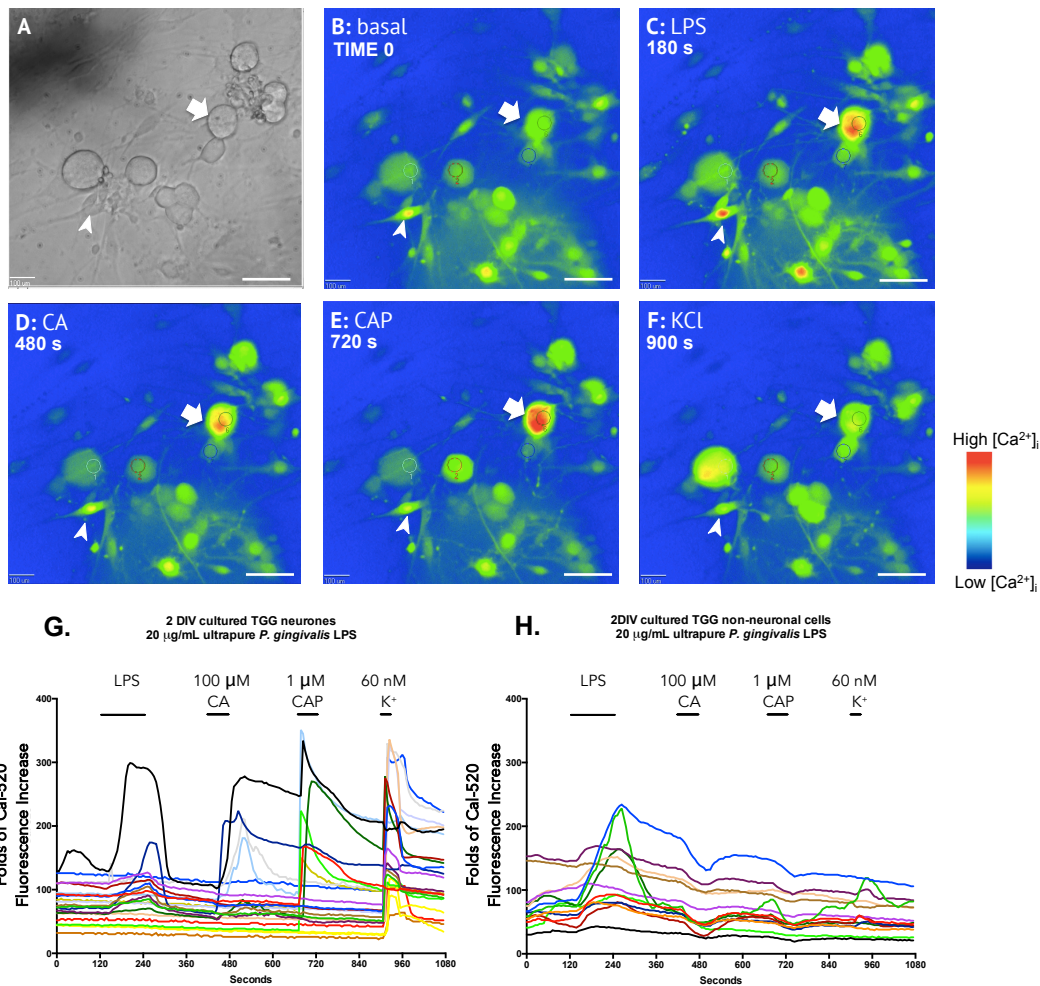


Figure 5.9 Analysis of intracellular calcium flux in primary TG cell cultures.

(A) Phase-contrast and (B-F) time-lapse calcium imaging in TG neurons (white arrow) and non-neuronal cells (white arrow head) loaded with Cal-520 AM during LPS, cinnamaldehyde (CA), capsaicin (CAP), and high potassium chloride (KCl) application. The high potassium application is to assess neurone viability and to help distinguish neuronal from non-neuronal cells. (G-H) Graphs tracing the transient change in calcium in individual cells over time after LPS and the agonist applications in neurons (G), and non-neuronal cells (H). Scale bar = 100 μ M.

Table 5.1 Percentages of neurones and non-neuronal cells that respond to *E. coli* LPS and *P. gingivalis* LPS

LPS and the concentrations		% of responded neurones (Numbers of responded neurones /Total presenting cells)	
<i>E. coli</i> LPS	0.2 µg/mL	0%	(0/16)
	0.5 µg/mL	0%	(0/14)
	2 µg/mL	6.25%	(1/16)
	5 µg/mL	4.76%	(1/21)
	10 µg/mL	6.67%	(1/15)
	20 µg/mL	8.33%	(1/12)
Ultrapure <i>P. gingivalis</i> LPS	10 µg/mL	0%	(0/13)
	20 µg/mL	26.67%	(24/90)

5.2.2.3 LPS effects can be abolished by TRPA1 blocker and modified by TLR4 antagonist.

We next investigated whether *P. gingivalis* LPS triggered calcium flux via TLRs or TRPs using the specific inhibitors; HC-030031 for TRPA1 and CLI-095 for TLR4. The TRPA1 antagonist HC-030031 (3 μ M) completely abolished the neurone response to LPS, whereas, pre-treatment of neurones with the TLR-4 signalling inhibitor, CLI-095, only partially inhibited the response (Figure 5.10 and Figure 5.12, B). Pre-treatment of cultures for 1 h with the novel TLR-4 signalling inhibitor CLI-095 reduced both the amplitude of responses and the proportion of neurones responding to LPS as shown in Figure 5.12, B and D. In contrast pre-treatment for 1 minute with the TRPA1 antagonist (3 μ M HC-030031) completely abolished the neurone response to LPS, and cinnamaldehyde (Figure 5.11 and Figure 5.12, C and D).

It also appeared that non-neuronal cells did not respond to ultrapure *P. gingivalis* LPS when pre-treated with HC-030031 (Figure 5.10, H). While, less than 10% (3/40) of non-neuronal cells responded to LPS in the presence of the TLR4 signalling inhibitor (Figure 5.9, F). However, accurate quantification of the proportion of responding non-neuronal cells is difficult to estimate because the low absorption of calcium dye into non-neuronal cells. In a similar manner to neuronal cells, non-neuronal cells did not respond to LPS in the presence of the TRPA1 blocker and responses were partially inhibited in the presence of the TLR4 signalling inhibitor. The summary of LPS effects in the presence and absence of TRPA1, and TLR4 signalling antagonists is shown in Figure 5.11.

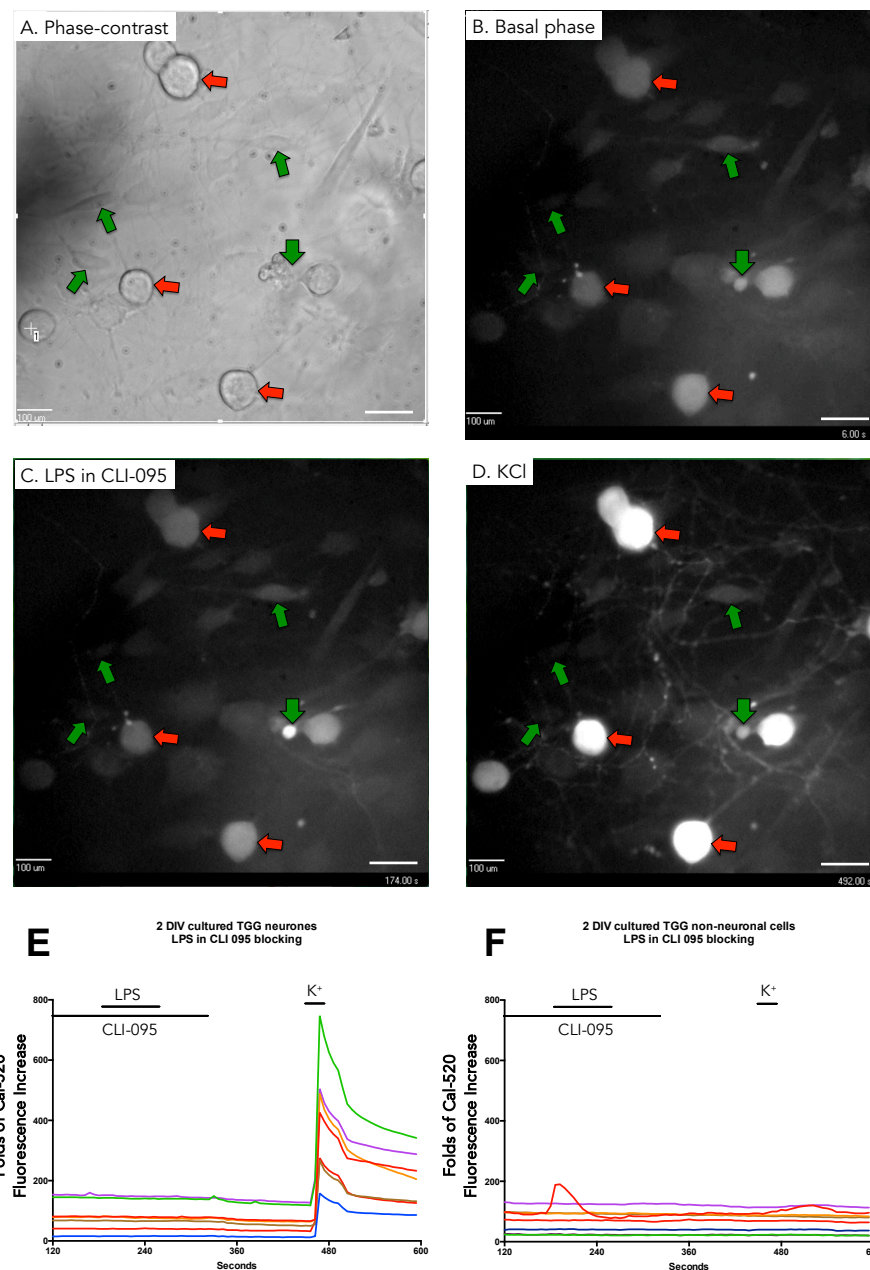


Figure 5.10 Analysis of intracellular calcium influx in primary TG cell cultures in the presence of CLI-095.

(A) Phase-contrast and (B-F) time-lapse calcium imaging in TG neurone (red arrows) and non-neuronal cells (green arrows) loaded with Cal-520 AM during application in the presence of CLI-095 LPS and high potassium (KCl) application. Graphs tracing the transient change in calcium in individual cells (E: neurones, F: non-neuronal cells) over time after application of LPS in the presence of CLI-095 and high potassium (KCl) application. This representative data shows that CLI-095 could partially inhibit calcium influx in both neuronal and non-neuronal cells in response to LPS. Scale bar = 80 μM.

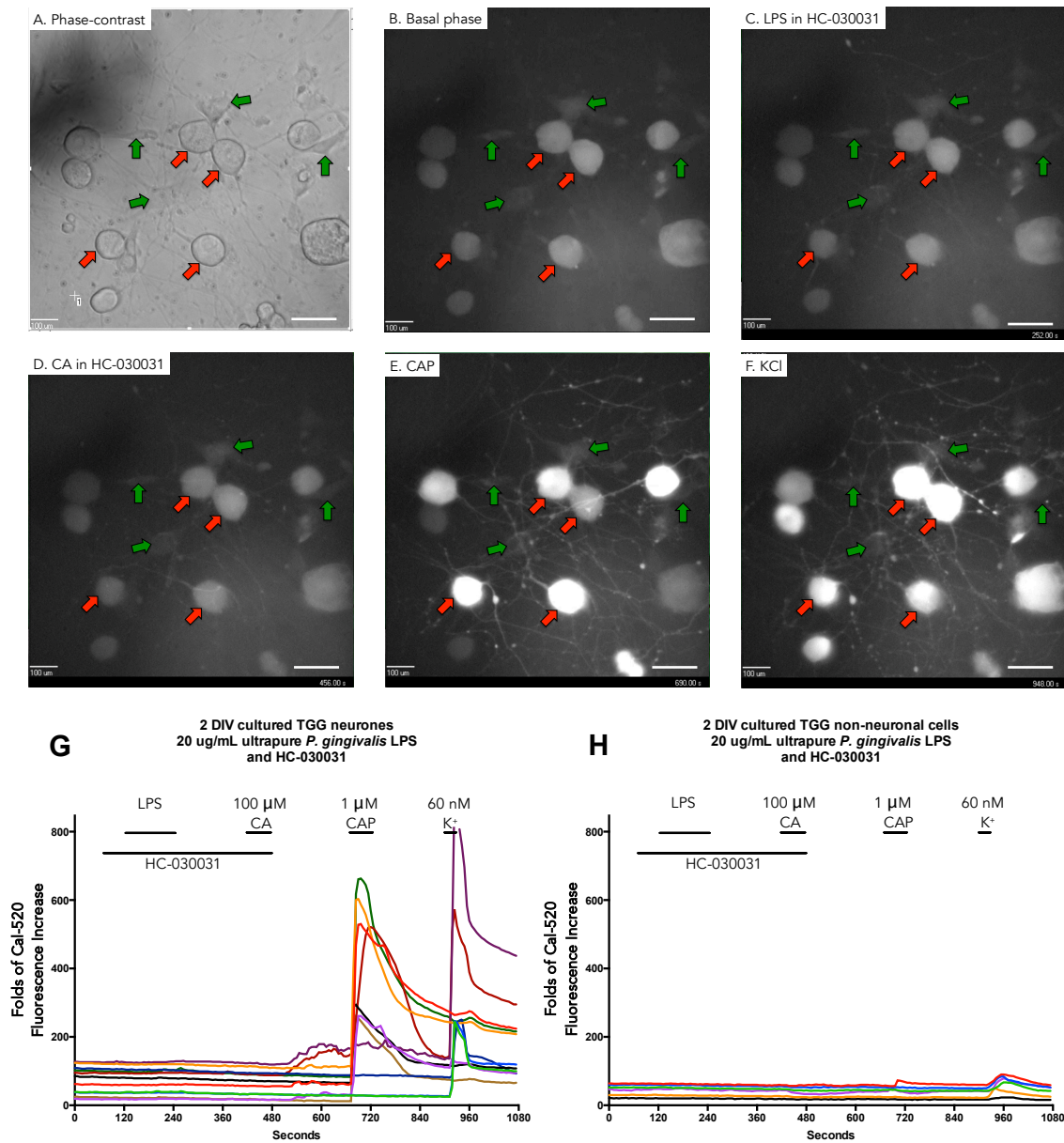


Figure 5.11 Analysis of intracellular calcium influx in primary TG cell cultures in the presence of HC-030031.

(A) Phase-contrast and (B-F) time-lapse calcium imaging in TG neurones (red arrows) and non-neuronal cells (green arrows) loaded with Cal-520 AM during HC-030031 co-exposed with LPS and cinnamaldehyde (CA), capsaicin (CAP), and high potassium (KCl) application. Graphs tracing the transient change in calcium in individual cells (G: neurones, H: non-neuronal cells) over time only after CAP and KCl applications in neurones. This representative data shows that HC-030031 could inhibit calcium influx in both neurone and non-neuronal cells in response to LPS. Scale bar = 100 μm.

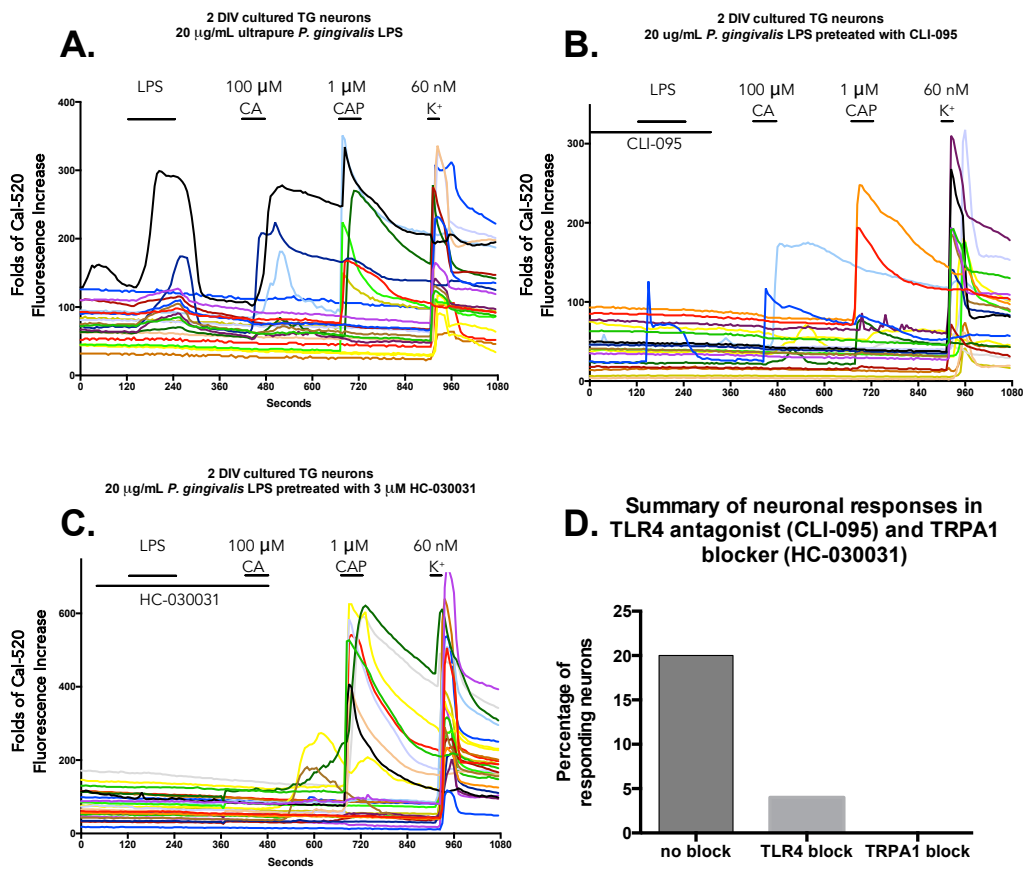


Figure 5.12 The effects of LPS and TRPA1 and TLR4 signalling.

Representative samples of responses to ultrapure *P. gingivalis* LPS in TG neurons following pre-incubation with no block (A), 1 μM CLI-095 (B), and 3 μM HC-030031 (C). Panel D shows the percentage of LPS-responding neurones in 3 groups; no block, TLR4 block, and TRPA1 block.

5.2.3 Consequent effects of LPS on TG neurones: CGRP release

5.2.3.1 *P. gingivalis* LPS caused significant release of CGRP in 15 mins

LPS is thought to be involved in the induction of neurogenic inflammation and the associated release of neuropeptides. We next evaluated, therefore, whether *P. gingivalis* LPS (20 µg/mL) could increase CGRP release from TG cell cultures.

CGRP release experiments were performed by collecting the supernatants of TG cultures exposed to LPS and quantifying CGRP using ELISA. Ultrapure *P. gingivalis* LPS significantly increased CGRP release from TG cultures (Figure 5.13, $p < 0.001$) and CGRP secretion following LPS application was similar to that obtained by stimulation with CAP.

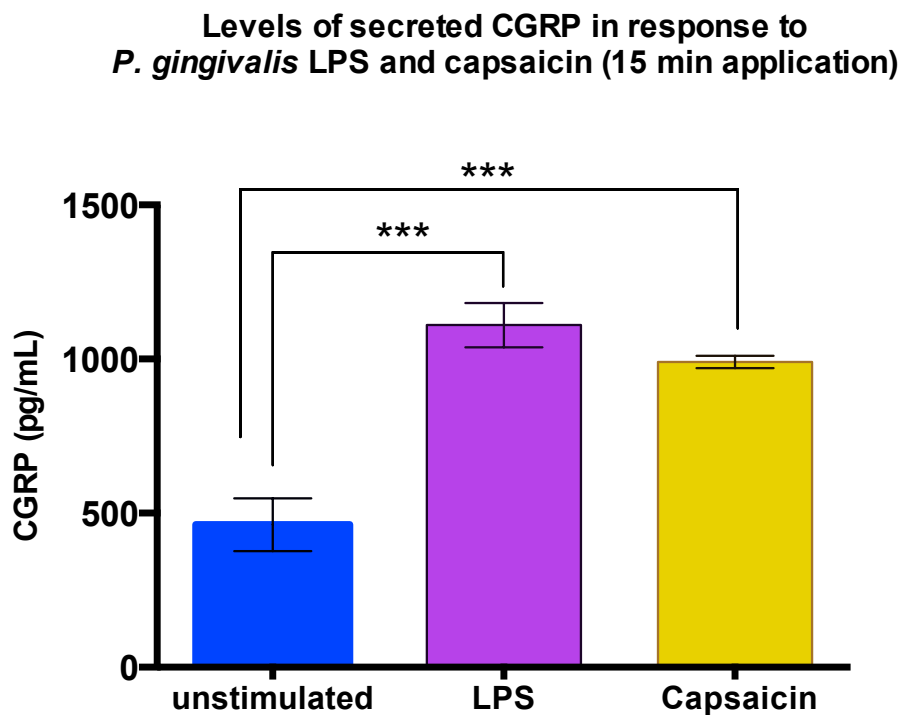


Figure 5.13 CGRP levels in LPS- and capsaicin-stimulated TG neurones.

The secreted CGRP response to *P. gingivalis* LPS or capsaicin were determined by the incubation of TG cells for 15 minutes with ultrapure *P. gingivalis* LPS (20 µg/mL) or capsaicin (1 µM) at 37°C in 5% CO₂. Measurement of CGRP levels was performed using enzyme-linked immunosorbent assay. Data present the mean ± SD from three independent experiments. Error bars are ± SD, *** $p < 0.001$.

5.2.3.2 HC-030031, CLI-095, and Capsazepine reduced the release of CGRP induced by *P. gingivalis* LPS.

Since the calcium influx in response to LPS could be abolished by the TRPA1 blocker, and partially removed by TLR4 signalling inhibition we next explored whether TLR4, TRPA1, and TRPV1 inhibitors could prevent CGRP secretion in response to LPS. CGRP release experiments were again performed by exposing TG cultures to LPS following pre-treatment with 3 μ M HC-030031, 1 μ M CLI-095, or 1 μ M Capsazepine (described in section 2.9 [Chapter Material and Methods]).

Ultrapure *P. gingivalis* LPS (20 μ g/mL) significantly increased CGRP release from TG cultures. However, this release could be prevented by all three inhibitors (Figure 5.13, $p < 0.001$). In the presence of inhibitors, CGRP secretion was similar to that obtained in unstimulated samples.

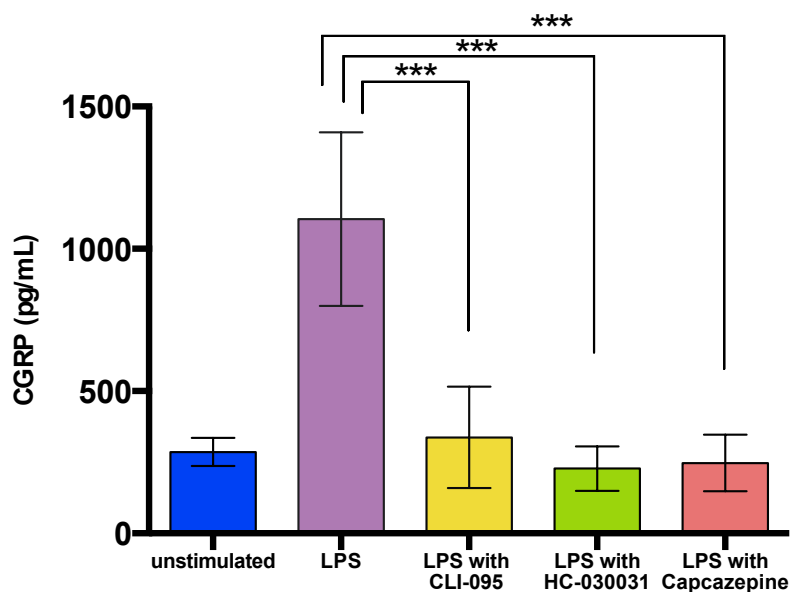


Figure 5.14 CGRP levels in TG neurone cultures in response to LPS in the presence of specific agonist inhibitors.

The secreted CGRP response to *P. gingivalis* LPS or LPS in the presence of TLR4, TRPA1, and TRPV1 blockers was determined by incubation of TG cells for 15 min with ultrapure *P. gingivalis* LPS (20 μ g/mL) without or with CLI-095 (1 μ M), or HC-030031 (3 μ M), or capsazepine (1 μ M) at 37°C in 5% CO₂. Measurement of CGRP levels was performed using enzyme-linked immunosorbent assay. Data presented are the means from two independent experiments. Error bars are \pm SD, *** $p < 0.001$.

5.2.4 Consequent effects of LPS on TG neurones: NF- κ B translocation.

5.2.4.1 *P. gingivalis* LPS could induce NF- κ B nuclear translocation in 30 mins.

Lipid A of *P. gingivalis* LPS has been reported to interact with both TLR2 and TLR4 depending upon the form of lipid A that is synthesised (e.g. degree of acylation), which in turn depends upon the growth environment of the bacteria (Herath et al. 2013; McKee et al. 1986). The lipid A moiety of the *P. gingivalis* LPS structure may also differentially activate signal transduction pathways of neuronal-inflammatory responses, in particular NF- κ B nuclear translocation. However, most of the previous studies on *P. gingivalis* LPS have investigated interactions with non-neuronal cells such as fibroblasts, endothelial cells, and monocytes.

Our findings demonstrated that *P. gingivalis* LPS stimulation could activate NF- κ B nuclear translocation in TG neurones over a period of 30 min. TG neuronal NF- κ B was visualised by co-localised immunofluorescence imaging as shown in Figure 5.15. Positive nuclear translocation was identified by the ratio of nuclear/cytoplasm NF- κ B fluorescence intensities (nuc/cyt ratio) being ≥ 1 as described in 2.11.3, Chapter 2. Quantification of NF- κ B nuclear translocation is shown in Figure 5.15 E. In response to *P. gingivalis* LPS, NF- κ B nuclear translocation increased significantly from 19 to 63 % in neurones and 40 to 68 % in non-neuronal cells that would be further described in Chapter 7.

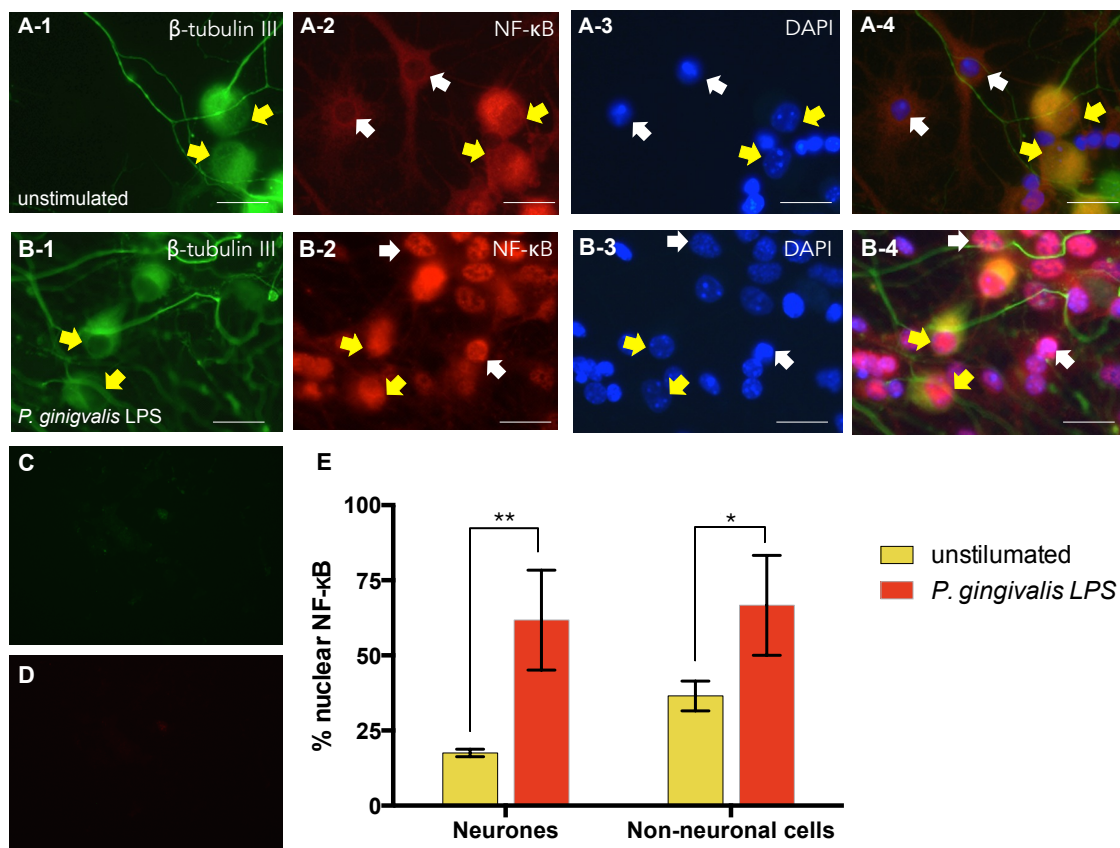


Figure 5.15 Photomicrographs of p65-NF- κ B nuclear translocation in *P. gingivalis* LPS-treated TG neurones and non-neuronal cells.

The TG cultures were left untreated (A) or stimulated with *P. gingivalis* LPS (B) for 30 min. Cells were permeabilized with 0.1% Triton X-100 and subsequently stained with primary antibodies against anti-p65 NF- κ B and the correspondent secondary antibodies. The β -tubulin III, and p65 NF- κ B control samples showed no positive labelling in panel C and D, respectively. The β -tubulin III is shown in green (A1-B1) and p65 NF- κ B appears in red (A2-B2). Nuclear staining with DAPI (A3-B3) appears blue. The merged images show the combined p65 NF- κ B, β -tubulin III and DAPI staining (A4-B4). Scale bars = 70 μ m. Localisation of p65 NF- κ B was visualised in neurones (yellow arrows) and non-neuronal cells (white arrows). Positive nuclear translocations were quantified by measuring the fluorescence intensity at each intracellular location. The translocation of NF- κ B was counted as positive when nuc/cyt ratio was > 1. Quantitative analysis of neuronal nuclear translocation stimulated by *P. gingivalis* LPS is shown in panel E. Neurones and non-neuronal cells positive for NF- κ B nuclear translocation were quantified. Data present the mean from 3 independent experiments. Error bars are \pm SD, * $p < 0.05$, ** $p < 0.01$. Scale bars are 80 μ m

5.2.4.2 Neuronal NF- κ B nuclear translocation could be partially prevented by CLI-095, or HC-030031, but not Capsazepine.

Since immunofluorescence analysis of TG cultures exposed to *P. gingivalis* LPS for 30 min showed increased NF- κ B nuclear translocation. We next explored whether TLR4, TRPA1, and TRPV1 inhibitors could prevent NF- κ B nuclear translocation in TG neurones. Again, TG neuronal NF- κ B was visualised by co-localised immunofluorescence imaging as shown in Figure 5.16. The positive neuronal and non-neuronal nuclear translocations were quantified as shown in Figure 5.17.

Using methods described in section 2.9, Chapter 2, we demonstrated that neuronal nuclear translocation activated by LPS could be inhibited by blocking TLR4 signalling (1 μ M CLI-095), or TRPA1 signalling (3 μ M HC-030031). The percentage of neurones showing nuclear translocation of NF- κ B significantly decreased from 65 % to about 30 % (Figure 5.17, A; $p < 0.05$) which is similar to that seen in unstimulated samples. However, this inhibition does not occur when TRPV1 signalling is blocked (10 μ M Capsazepine). Capsazepine did not modify the percentage of cell showing neuronal nuclear translocation. In the presence of Capsazepine, approximately 60 – 70 % of neurones displayed nuclear translocation in response to *P. gingivalis* LPS and this was similar to that seen in the absence of blockers.

The percentage of positive nuclear translocation of NF- κ B in non-neuronal cells activated by LPS decreased from 65 % to 25 % (Figure 5.17, B; $p < 0.05$) when cells were pre-treated with the TLR4 signalling inhibitor. However, this did not occur when TPRA1 or TRPV1 were inhibited using the specific blocking agents. Under these conditions approximately 70 – 80 % of cells responded to *P. gingivalis* LPS and this was similar to that which resulted from unblocked-LPS stimulation (67 %).

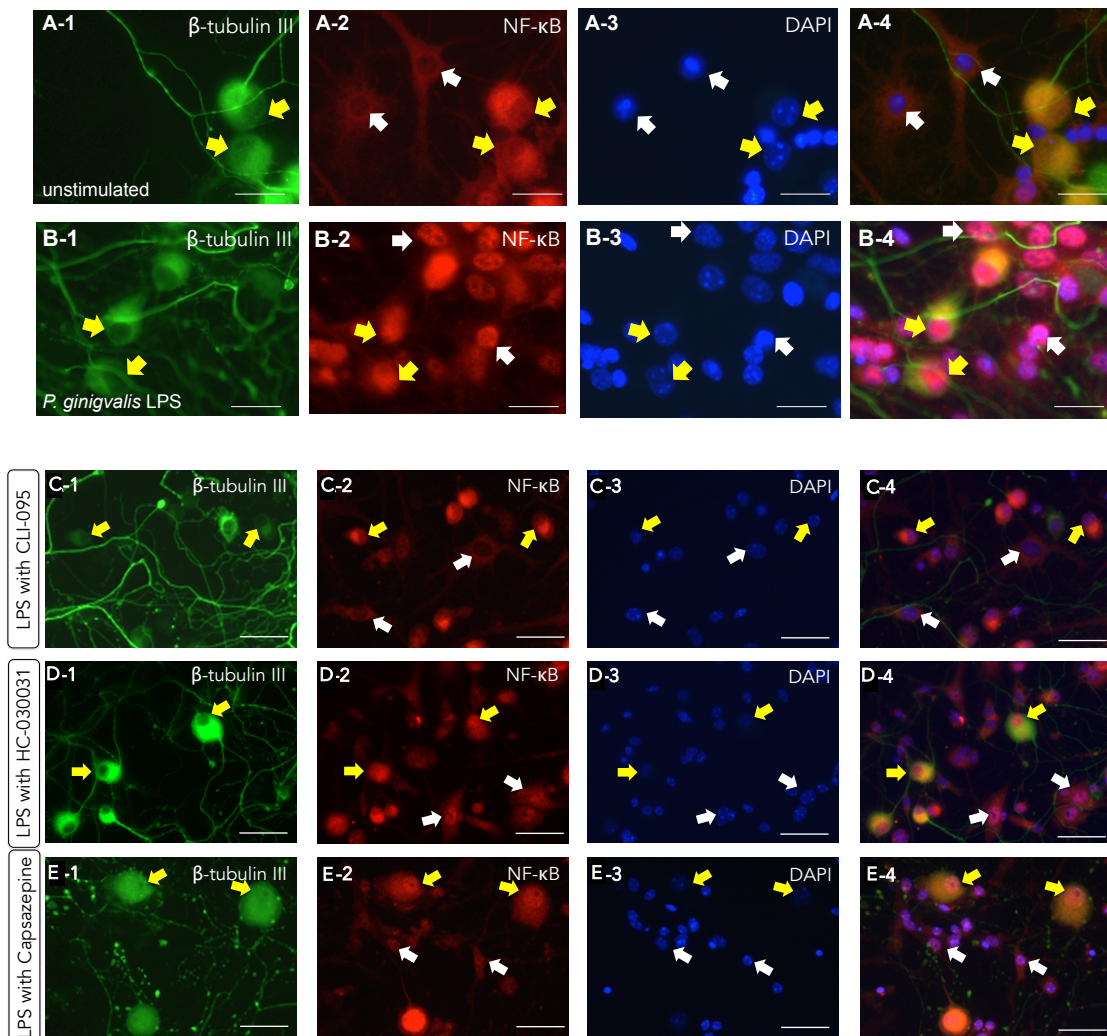
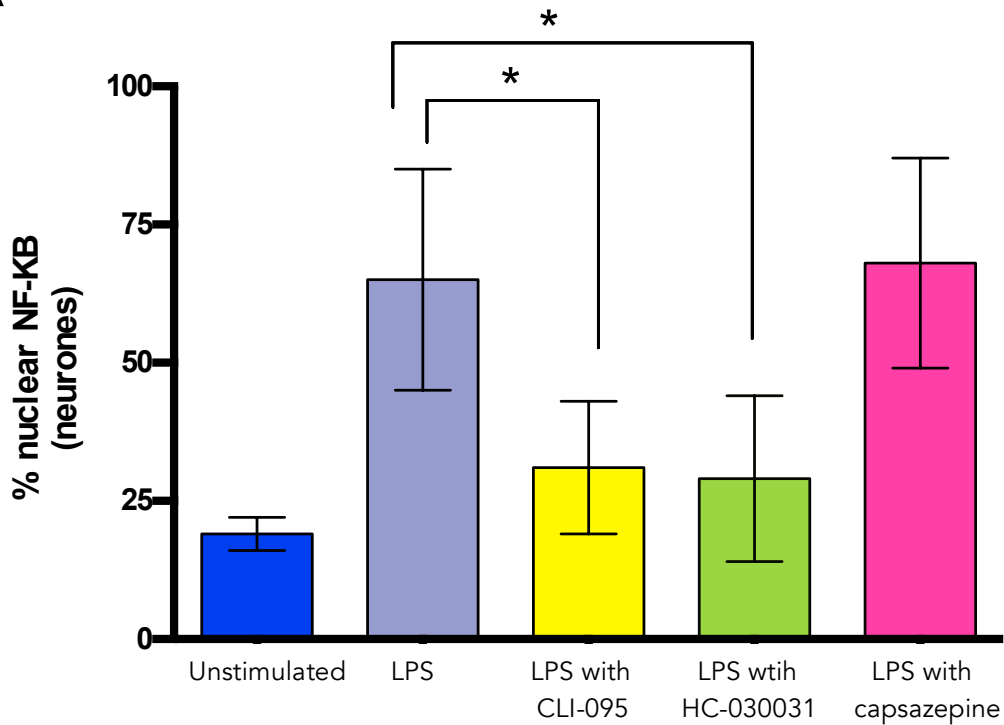


Figure 5.16 Photomicrographs of p5-NF- κ B nuclear translocation in *P. gingivalis* LPS-treated TG neurones in the presence of TLR4, TRPA1, and TRPV1 signalling inhibitors.

The TG cultures were left untreated (negative control; panel A) or stimulated with *P. gingivalis* LPS (positive control; panel B) for 30 min. The TG cultures were also stimulated with *P. gingivalis* LPS and CLI-095 (C), HC-030031 (D), and Capsazepine (E) for 30 min. Cells were permeabilized with 0.1% Triton X-100 and subsequently stained with primary antibodies against anti-p5 NF- κ B and the correspondent secondary antibodies. The β -tubulin III is shown in green (A1-E1) and p5 NF- κ B appears in red (A2-E2). Nuclear staining with DAPI (A3-E3) appears blue. The merged images show the combined p5 NF- κ B, β -tubulin III and DAPI staining (A4-E4). Localisation of p5 NF- κ B was visualised in neurones (yellow arrows) and non-neuronal cells (white arrows). This is representative data from 2 independent experiments. Scale bars = 70 μ m.

A



B

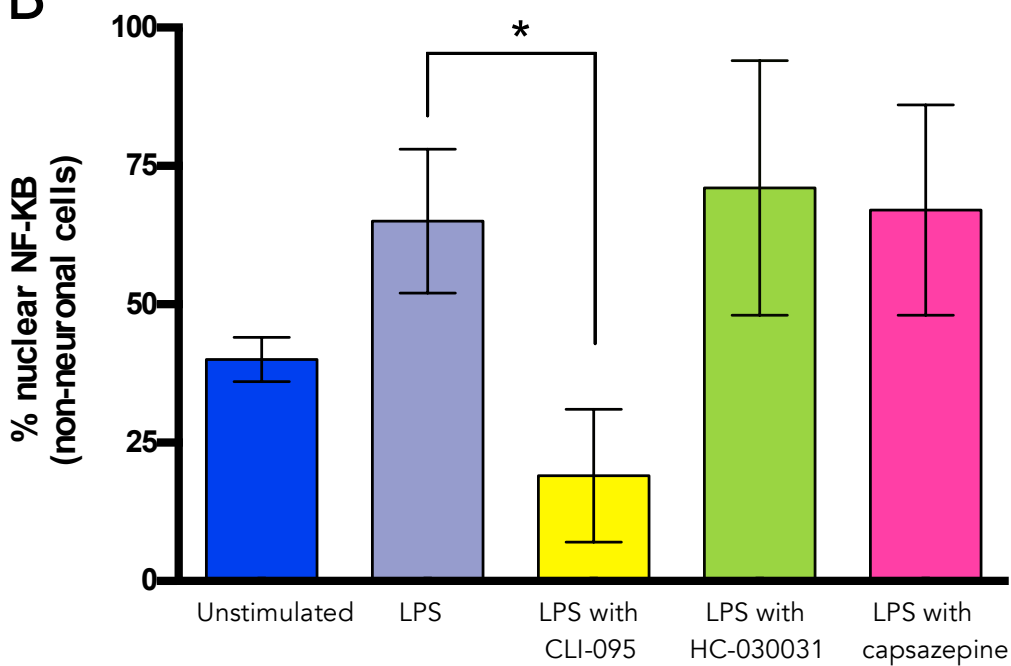


Figure 5.17 Percentages of p65-NF- κ B nuclear translocation in *P. gingivalis* LPS-treated neurones in the presence of TLR4, TRPA1, and TRPV1 signalling inhibitors

Positive nuclear translocations were quantified by measuring the fluorescence intensity at an intracellular location. The translocation of NF- κ B was counted as positive when nuc/cyt ratio was \geq 1. Quantitative analysis of neuronal nuclear translocation stimulated by *P. gingivalis* LPS alone and LPS in the presence of CLI-095, HC-030031, and Capsazepine. Neurones and non-neuronal cells positive for NF- κ B nuclear translocation were quantified. Data present the mean from 2 independent experiments. Error bars are \pm SD, * $p < 0.05$.

5.3 Discussions

5.3.1 Overview

Our initial hypothesis was that *P. gingivalis* LPS could directly activate sensory neurones and so contribute to dental pain. The experiments in the current chapter were performed to characterise TG neurones in culture system and to determine their functional characteristics as an altered neuronal activity occurring as a consequence of infection. To do this, protein expression of TG-associated receptors such as TLRs and TRPs were assessed by immunofluorescence microscopy. Further assessment of TG neuronal activation was performed by imaging of calcium flux (calcium imaging) to interrogate which cells within a culture respond to a stimulus and over what period of time. Moreover, we also investigated various responses of TG after a latent period of stimulation, which can vary in length such as release of neuropeptide, and NF- κ B nuclear translocation. A summary of the findings are shown in Figure 5.18.

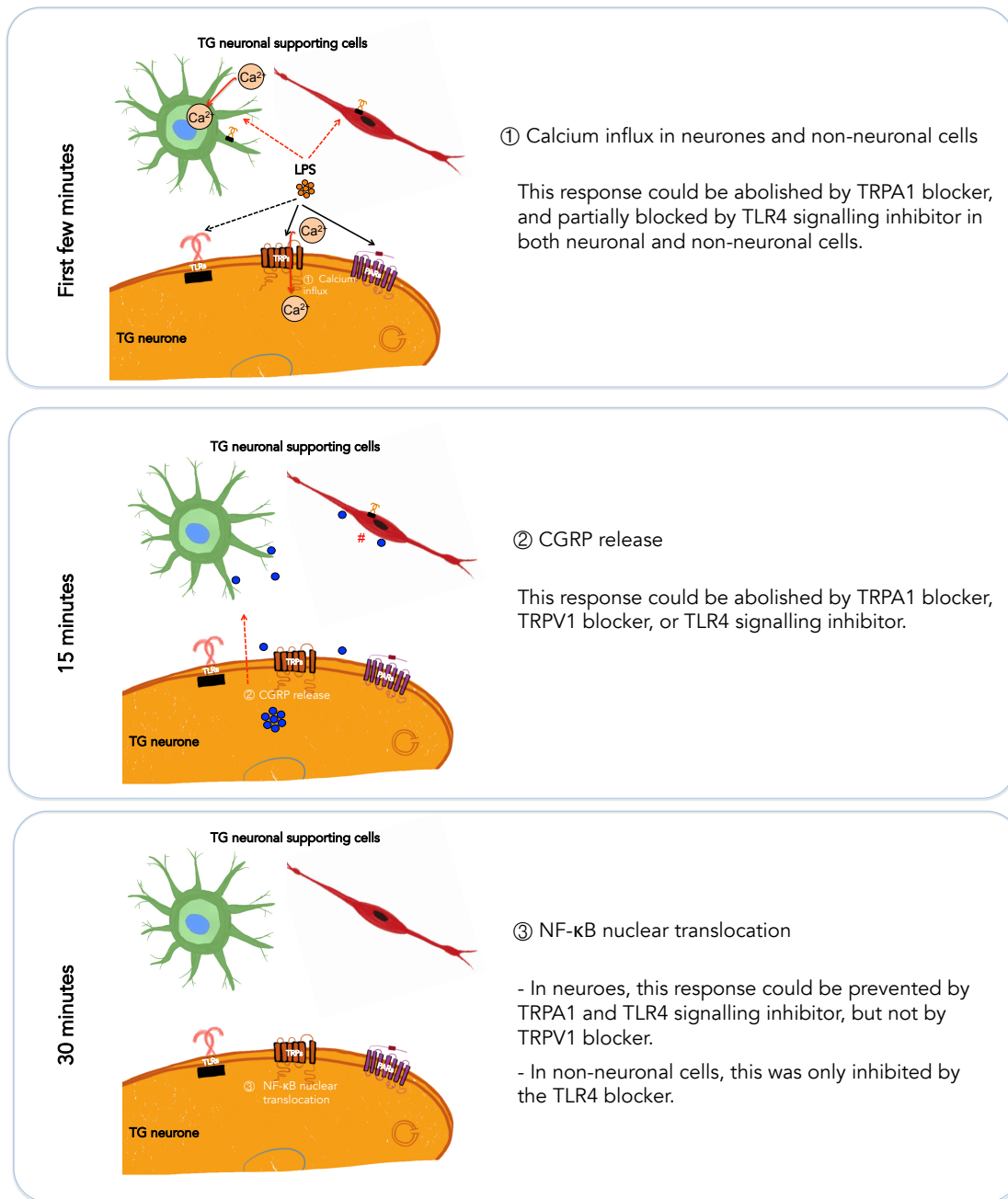


Figure 5.18 Summary of the findings from this chapter.

In the very first few minutes after LPS exposure, TG neurones responded to *P. gingivalis* LPS as we demonstrated by transient influx of Ca^{2+} in both neurones and non-neuronal cells. Subsequently, CGRP release could be observed. Lastly, NF-κB could be seen translocated to the nucleus of both types of cells. These neuronal activities could be prevented by TRPA1, TRPV1, and TLR4 signalling inhibitors.

5.3.2 Expression of potential LPS-interacting receptors in TG neurone cultures

Before embarking on this study, we knew the range of receptors that could potentially be involved in the responses to LPS and potentially in transduction of dental pain. There are 2 categories of cellular receptors that could potentially interact with LPS, namely TLRs and TRPs. TLRs have been thought to be the primary participants in the inflammatory response to LPS, but TRP receptors have emerged as playing critically important roles in peripheral nerve sensitisation.

Several authors have determined the expression of TLR4 in dental pulp. TLR4 is expressed by many types of cells including odontoblasts (Hong-Wei et al. 2006), fibroblasts (Hirao et al. 2009) but also nerve fibres have been reported to express TLR4 (Diogenes et al. 2011; Qi et al. 2011). This could support an important role of TLR4 in pulpal immune defence but its interactions with LPS could also lead to the development of pathological pain.

Previously, the presence and role of ligands stimulating the innate immune system had been rather overlooked in the nervous system. However, TLR3, and TLR4 have been found on TG ganglia cells (Goethals et al. 2010). This suggests an evolutionarily primitive function for these cellular receptors as a protective mechanism for peripheral nervous system in addition to their well known function on immune cells. TLRs were recently indicated to be expressed on rat TG neurones by Helley et al. (2015), they found TLR4 and TLR7 were expressed by 29.3% and 32.4%, respectively. However, in this study, we found that both TLR4 and TLR7 were expressed by more than 70% on our TG cultures. In addition, expression of CD14 in nearly all of neurones and non-neuronal cells is consistent with the study of Wadachi and Hargreaves (2006) that demonstrated CD14 from *post mortem* human trigeminal ganglia. Their findings also show co-localisation of TLR4 and CD14 and this provides evidence that the TLR4/CD14 complex is present in trigeminal neurones. Taken together, these data indicate that LPS stimulation may activate via TLR4/CD14 complex.

TLR7 has recently been thought to be related to the pain pathway of peripheral

nerves, especially in the dorsal root ganglion (Qi et al. 2011; Liu et al. 2012). TLR7 is another receptor that could detect pathogen-associated molecular patterns (PAMPs) and here we confirm its presence on TG neurones by immunofluorescence. TLR7 recognises imidazoquinoline derivatives, and elicits very rapid inward currents and action potentials (Goethals et al. 2010; Liu et al. 2013), however, in this thesis, we did not attempt to demonstrate the functional characteristics of neuronal TLR7 receptors.

Another category of potential receptors for LPS besides the TLRs are the transient receptor potential channel family (TRPs). Numerous studies have shown that TRP channels are a broad group of ion channels located on nociceptors (for the review see Guimaraes and Jordt 2007). TRPA1, and TRPV1 are thought to be related to bacterial infection in TG (Chung et al. 2011; Assas et al. 2014; Kunkler et al. 2011), however, the mechanisms underlying the generation of pain by TRP activation has not yet been established. TRPV1 is expressed in nerve fibres throughout the human tooth pulp, as demonstrated by TRPV1-immunoreactivity in small and medium diameter nerve fibres (Morgan et al. 2005; Chung et al. 2011) and there have been several reports that 20-35% of TG neurones in mice, ferrets and humans that were TRPV1 positive (Biggs et al. 2006; Chung et al. 2011; Gibbs et al. 2011). Compared with our study, we concur with this finding since we found 40% of the TG neurones in our cultures expressed TRPV1 and these were very largely in the small to medium sized neurones.

TRPA1 could act as a neuronal sensor for a broad spectrum of endogenous compounds and irritants. There has been a report of TRPA1 expression in TG and that TRPA1-immunoreactivity was distributed in only a very small population (6-10%) of TG neurones (Huang et al. 2012). Our finding concurs with this report also by our observation that the TRPA1 population is less than 15% of the total, and was distributed almost entirely within very small TG neurones.

It is therefore clear that TLR4, TRPA1, and TRPV1 are expressed on our TG culture system and so we sought to establish the functional characteristics of these receptors in relation to bacterial induction of dental pain.

5.3.3 Functional response of TG neurones to LPS

LPS varies in a number of ways between bacteria and with changes in the growth environment. For example the degree of LPS acylation can vary with temperature (Herath et al. 2013). Also, different species and strains have different glycan substitutions. Such variation leads to differences in the host responses and LPS obtained from Gram-negative oral anaerobic bacteria do not elicit the same responses that are observed with the classic *E. coli*-type endotoxin (Dixon and Darveau 2005; Herath et al. 2013; Darveau and Hancock 1983).

P. gingivalis LPS could be considered as having relatively low biological activity compared with *E. coli* LPS because of its lower phosphate content, altered length and position of fatty acids present in lipid A (Takada and Kotani 1989). However, *P. gingivalis* LPS is not without effect as it has been reported to induce an inflammatory response in mice that are non-responsive to conventional LPS (Kirikae et al. 1999). Moreover, there are many studies that have confirmed that *P. gingivalis* LPS triggers a different pattern of inflammatory mediator production from innate immune cells compared with the traditional pathway employed for *E. coli* LPS. The lipid A of *P. gingivalis* LPS was described as relatively nontoxic by Ogawa and Uchida (1996) because it induced both an up- and down-regulation of differential cytokine-producing activities following the activation through the common receptor sites of LPS on mononuclear cells. Therefore, it is possible that *P. gingivalis* LPS could have a range of effects on different cells according to the receptors and mechanisms involved.

In this study we aimed to investigate whether and by what mechanisms *P. gingivalis* LPS sensitises TG sensory neurones. We therefore assessed the calcium flux within neuronal cells and their response in terms of neuropeptide production, following *P. gingivalis* LPS application. We then tried to identify the receptors involved using inhibitors of the candidate receptors (CLI-095 for TLR4 and HC-030031 for TRPA1).

We isolated lipopolysaccharide LPS from *P. gingivalis* W50 and verified its biological effect on macrophages. Because we were uncertain of absolute purity and because our yield was lower than desired, we compared responses of neurones to this

preparation with that to a commercial, ultrapure preparation. We found that both *P. gingivalis* W50 LPS and the commercial ultrapure *P. gingivalis* ATCC 33277 LPS induced TG neurone calcium influx. A rapid response was obtained but using relatively high levels of *P. gingivalis* LPS (20-50 µg/mL) and the question arises as to how physiological this level is. While, *P. gingivalis* W50 and ATCC 33277 have been shown to have different abilities to induce a host response (Kesavalu et al. 1992), biological activity was however similar between these 2 strains (Kennell and Holt 1990).

The amount of *P. gingivalis* LPS required to elicit a response in another study (Liu et al. 2008) which was *in vivo* showed that a high dose (50 µg) could stimulate inflammatory cytokines production at a local level. However, that level was only minimally stimulatory when a systemic response was measured. Also an *in vitro* study reported by Yamagishi et al. (2011) showed that human dental pulp stem/progenitor cells (hDPSC) exhibited a response when challenged with 5 – 20 µg/mL of *P. gingivalis* LPS and that this was through the TLR2. Both studies mainly supported the notion that there is a lag period before the onset of response, which varied from 1 – 48 h. However, in the case of our study the response was more rapid, which we interpret as being consistent with a direct effect of *P. gingivalis* LPS on the sensory neurones.

It is difficult to absolutely relate LPS concentrations to numbers of bacteria because of the variability in types of LPS and the way in which it has been assayed. Nonetheless, Watson et al. (1977) estimated that in a log culture of *E. coli* there was approximately 50 fg of bound LPS per cell. If we assume that there are similar levels on *P. gingivalis*, then the LPS loading that we applied to our neuronal cultures would be equivalent to approximately 4×10^8 cells. In one study by Sunqvist et al. (1989), they estimated that infected pulps contained on average 2.8×10^5 bacteria of black-pigmented bacterioides species, whereas in another study (Khemaleelakul et al. 2002) the number of viable bacteria recovered from acute endodontic abscesses ranged from 10^4 to 10^8 . It is not known at what bacterial load pain would be initiated within an infected pulp and this will also depend upon the types of bacteria present,

but based upon the above calculation and bearing in mind the caveats, it is reasonable to conclude that the LPS load we employed is a little above that which might be expected in a pulp. In addition to this, in the infected pulp there could be OMVs that are composed of molecules derived from the outer membrane and contain outer membrane protein, lipids, and LPS (Veith et al. 2014). Having said that the amount we applied was in the bulk fluid and not all of that LPS would contact the neurones in the culture and the degree of occupancy of cell receptors by LPS that is needed to activate the neurone is unknown. Furthermore, when bacteria are residing very close to the neuronal membrane as could occur in an infected pulp, there could be a very high concentration of LPS within a few microns of the cell membrane.

We explored the involvement of two potential receptors for LPS on TG neurones, namely TRPA1 and TLR-4 (by calcium imaging). Approximately 20% of TG neurones responded to ultrapure *P. gingivalis* LPS and this response was completely blocked by the TRPA1 inhibitor HC-030031, and considerably reduced to less than 5% of neurones responding to LPS in the presence of the TLR4 antagonist, CLI-095. This suggests that both receptors can play a role in neuronal responses but that TRPA1 might be the 'high affinity high response' receptor. This is consistent with the findings by Meseguer et al (2014) that *E. coli* LPS exerts a fast excitatory action via TRPA1 in TG neurones. However, we can speculate that unlike *E. coli* LPS that is primarily dependent on TRPA1 channel for activation in neurones and develops independently of the TLR4 pathway (Meseguer et al. 2014), *P. gingivalis* LPS activation could occur via both TRPA1 and TLR4, with the former being a rapid-acting mechanism and the TLR4-mediated pathway being slower to develop. This could be explained by the different properties of *P. gingivalis* LPS and the classic *E. coli*-type endotoxin. Moreover, TLR4 could activate two major signalling pathways, as described in section 1.3.1 (Chapter 1 Introduction) namely the MyD88 and the TRIF pathways. It is possible that CLI-095 only blocked the MyD88 pathway, and therefore, the TRIF pathway could still partially interact with LPS as shown in Figure 5.19.

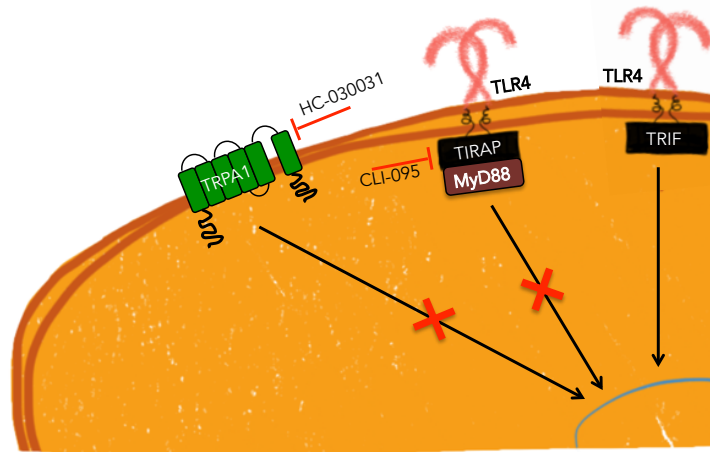


Figure 5.19 The mechanisms of CLI-095 and HC-030031.

This is the mechanism of CLI-095 that could inhibit MyD88 pathway of TLR4. While HC-030031 could be specifically induce pore-block of TRPA1.

Of course neuronal response to *P. gingivalis* LPS may not be limited to these two receptors and it is possible that multiple pathways could be triggered according to the local concentration of LPS. For example sensitisation by LPS may occur through a TRPV1-dependent pathway. Indeed there has been some limited evidence for this; Chung et al (2011) reported that TRPV1 could be up-regulated on stimulation with *E. coli* LPS, although the mechanisms involved were not identified. *P. gingivalis* LPS activation of sensory neurones could occur via the TLR4-mediated pathway which then potentiates the response of neurones to capsaicin via the TRPV1-mediated response (Diogenes et al. 2011). While our findings support the notion that *P. gingivalis* LPS could partly function through TLR4, our evidence indicates that it is the TRPA1-mediated pathway that is the most important in TG neuronal response to *P. gingivalis* LPS.

HC-030031 is thought to be able to specifically block TRPA1 activated by CA to induce calcium influx but that does not block TRPV1 activated by CAP *in vitro* (Eid et al. 2008). While, in an animal model, TRPA1 antagonists have been shown to inhibit pain associated with chemical effects (neuropathic pain and reduction of acute inflammatory responses to noxious chemical compound exposure, it is still quite possible that TRPA1 plays a crucial role in activation of neuronal inflammatory pain generation. Nonetheless, the cellular mechanisms involved are thought to be

complex and so are likely to involve more pathways in the sensory neuronal response (Mihara and Shibamoto 2015).

There are many studies which demonstrate functional interaction between TRPA1 and TRPV1. This is constructed on the basis that PIP_2 and intracellular Ca^{2+} release are PKC-dependent mechanisms, which activate TRPA1 downstream of inflammatory receptors (see Mihara and Shibamoto 2015 for review). The possible interactions of TRPA1 with other cellular receptors, such as TRPV1 and PAR2, via the PKC-independent pathway are shown in Figure 5.20. However, the involvement of PAR2 is discussed in more detail in a later chapter (Chapter 6).

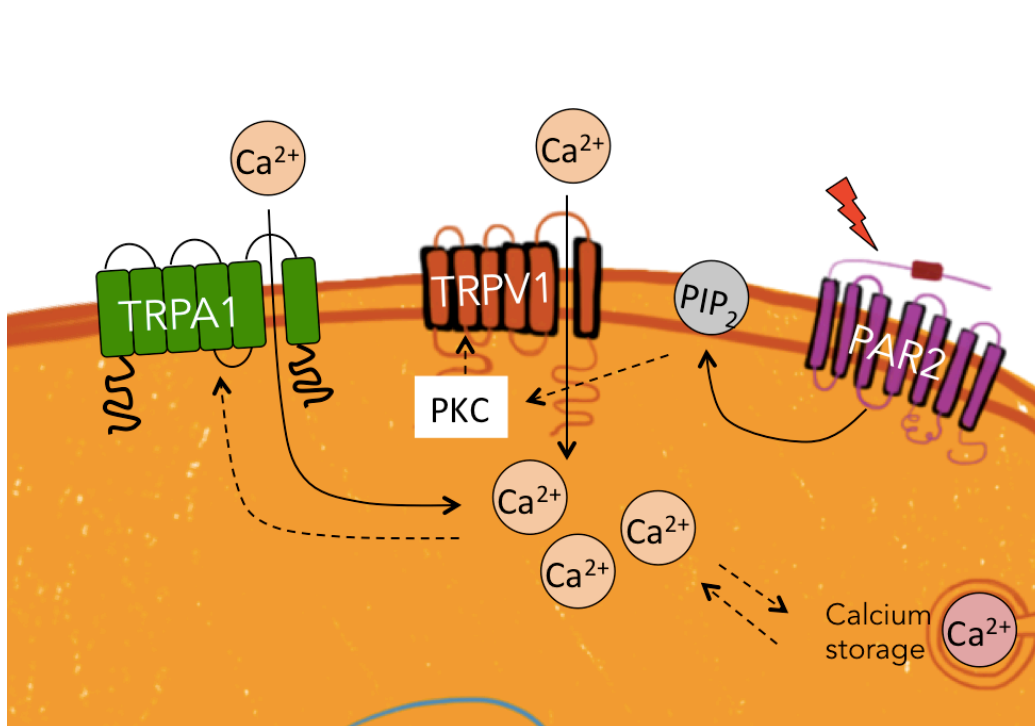


Figure 5.20 Model of functional interactions involving PAR2, TRPA1, and TRPV1.

This diagram depicts functional interactions of TRPA1 with TRPV1 and other potential receptors. This is constructed on the basis that PIP_2 and the intracellular Ca^{2+} release are PKC-dependent mechanisms, which activate TRPA1 downstream of inflammatory receptors. (Modified from Mihara and Shibamoto 2015).

5.3.3.1 Consequences of neuronal activation following exposure to *P. gingivalis* LPS.

5.3.3.2 Acute CGRP release by LPS

We found that low concentration of *P. gingivalis* LPS (2 µg/mL) did not directly alter the neuronal activities, which is in accordance with the findings of Ferraz et al (2011). However, here we report that higher concentrations of *P. gingivalis* LPS (20 µg/mL) could enhance neuronal activation and produce a significant increased release of CGRP.

Moreover, we found that effect of LPS on the release of CGRP could be reversed by not only TRPA1 or TLR4 signalling blockers, but also by a TRPV1 blocker. This finding may support the notion that *P. gingivalis* LPS somehow induces a TRPV1-dependent release of CGRP, which would be consistent with the findings of Diogenes et al. 2011. They showed that TLR4 could enhance TRPV1 activation leading to the release of CGRP. Even though, there has been very limited evidence to show how LPS modulates peripheral sensitisation. It has been thought that Ca²⁺ permeation through TRPV1 leads to exocytosis, which underlies CGRP and SP release (Henrich and Buckler 2009) which is a rapid neuronal response. While, it is possible that CGRP release may also be influenced by the triggering of PKC/PLC pathways (Vellani et al. 2010), which may underlie CGRP and SP release as a latent consequence. Taken together, our data cannot rule out the possibility that LPS sensitivity of TG neurones requires TRPV1 to release CGRP.

5.3.3.3 NF-κB translocation following incubation with *P. gingivalis* LPS

In order to have the further effects on neurones, LPS would be expected to result in activation of the NF-κB pathway because this is the major transcription factor responsible for modulating gene expression in response to LPS (Arias-salvatierra et al. 2011). Also, both TRPA1 and TLR4 mediate the production of inflammatory mediators through the NF-κB pathway and the NF-κB pathway is thought to be related to voltage-gated channel (e.g. Ca²⁺, Na⁺ channels) over-expression, which could induce allodynia, thermal hyperplasia, or chronic pain (Huang et al. 2014).

Immunofluorescence analysis of TG cultures exposed to *P. gingivalis* LPS for 30 min showed increased NF- κ B nuclear translocation. In TG neurones, this did not occur when TLR4 or TRPA1 were inhibited. We also found that LPS activated calcium movement through TLR4 and TRPA1. This could explain the rapid responses of TG neurones.

Thus, the secretion of CGRP may relate to both these two receptors, though secretion of CGRP also seems to involve TRPV1-dependent pathway because CGRP release could also be prevented by the TRPV1 blocker. The involvement of TLR4 and TRPA1 in direct response leads us to propose a possible model for LPS stimulation of TG cells as shown below in Figure 5.21.

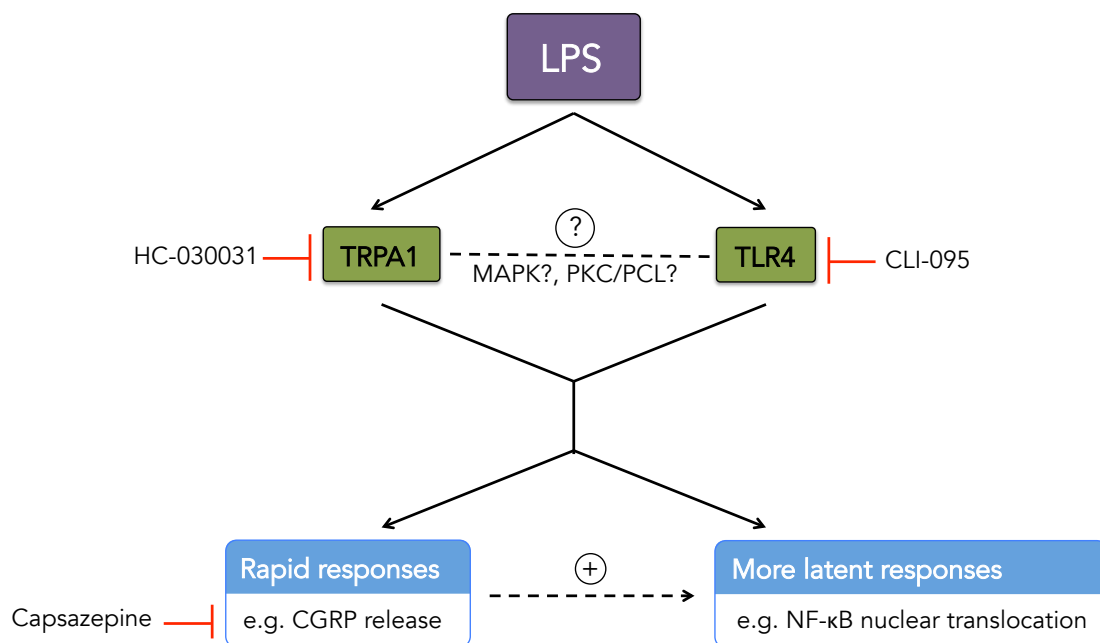


Figure 5.21 Proposed model for LPS stimulation of TG neurones.

LPS could activate TG neurones via TRPA1 and TLR4 which could be blocked by their specific antagonist HC-030031 and CLI-095, respectively. The neuronal activation can result in rapid and more latent responses such as CGRP release and NF- κ B nuclear translocations.

5.3.4 Limitations and future prospects

Until recently, there have been very few reports in the literature regarding the direct effects of *P. gingivalis* LPS on TG neurone. This is partly due to the difficulties of establishing pure cultures of neurones since they appear to need proximity of various support cell lineages for survival. Consequently the limited work that has been done, including that reported here, has involved use of mixed cultures of TG neurones and non-neuronal cells. The result is that analyses have to be done imaging of single cells or by assaying products that are thought to only derive from neurones.

In relation to the amount of LPS needed to invoke the response we observed, the question is what level of LPS is pathophysiological. We demonstrated only high concentration of *P. gingivalis* LPS have an effect, which might be supraphysiological but perhaps not by much. Also, in classical LPS receptor complexing with TLR4, MD2 and CD14 are required as co-factors. However, in supraphysiological LPS concentrations, LPS signalling could occur by CD14-independent mechanisms (Ulevitch and Tobias 1995). So, the mechanisms in this study may not completely represent the canonical pathway of TLR4-LPS interaction. Also, it is possible that supraphysiological LPS could have cytotoxic effects on cells in the culture. Consequently, future experiments could include assaying reduction of Methyl tetrazolium (MTT) to confirm the viability of the cells.

Our calcium-imaging data showed that some TG neurones could respond to both CA and CAP. This could show that TRPA1 is highly expressed in TG but perhaps only in a specific subpopulation of neurones that co-express TRPV1. It is believed that TRPV1 and TRPA1 could play an integral role in pain (Bevan and Winter 1995; Fernandes et al. 2012) and neurogenic inflammation (see review in Geppetti et al. 2008). Therefore, we cannot exclude TRPV1 effect on pain generation associated with dental infection.

TRPV1 seems to play a role in LPS-TG activation as we demonstrated that TRPV1 was involved in CGRP release. However, in this thesis, we did not investigate the effects of a TRPV1 antagonist e.g. Capzasepine on TG calcium influx.

5.3.5 Clinical relevance

P. gingivalis LPS was shown to be able to modulate rapid peripheral sensitisation via TLR4 and mainly TRPA1-dependent pathways. A specific TRPA1 antagonist, HC-030031 might be useful analgesic tool. However, the adverse effects of this antagonist should be further investigated and confirmed.

5.4 Conclusion

This study has explored the mechanisms of dental pain that could be directly caused by LPS, a component of the Gram-negative cell envelope. The consequences of TG neuronal exposure to *P. gingivalis* LPS have been demonstrated to involve calcium movement via TRPA1- and/or TLR4-mediated pathways that leads to the release of CGRP which can induce neurogenic inflammation. Moreover, NF- κ B nuclear translocation within the neurones and non-neuronal cells was demonstrated as a more latent response. These findings could shed light on the mechanisms of inflammatory pain activated by bacterial infection.

Chapter 6

*Possible roles of P. gingivalis
protease in dental infection pain:
potential for involvement of PARs*



6. Possible role of *P. gingivalis* protease in dental infection pain: potential for involvement of PARs

6.1 Introduction

In the former chapters, we demonstrated the neuronal responses to live *P. gingivalis* and LPS. However, *P. gingivalis* and neuronal cell interactions could be more complex because bacteria possess a range of virulence factors and neurones also possess a wide range of cellular receptors that could be targets for these factors. Amongst the virulence factors of *P.gingivalis* are a group of cysteine proteases called gingipains; Arg-gingipain (HRpgA, RgpB), and Lys-gingipain (Kgp). These three gingipain enzymes could mediate cellular responses through interaction with the proteinase-activated receptor 2 (PAR2) (Rothmeier and Ruf 2012), which is expressed on trigeminal nociceptor neurones, including human tooth pulp afferents (Morgan et al. 2009).

Proteinase-activated receptors belong to a subfamily of G-protein-coupled receptors (GPCRs) activated via proteolytic cleavage by serine proteinases (Steinhoff et al. 2005; Ossovskaya and Bunnett 2004). These receptors have been thought to be highly active in response to diverse biological activities. For example the important activating protease, thrombin, can activate PAR 1, 3, and 4 (Vellani et al. 2010; Steinhoff et al. 2005; Soh et al. 2010). Serine proteases, such as trypsin and Rgp, have been shown to activate any of the four receptors, PAR1-4 (Lourbakos et al. 2001; Giacaman et al. 2009) and in particular trypsin and Rgp have been shown to be able to cleave the neuronal PAR1, 2, 4 (Ossovskaya and Bunnett 2004). In addition, protease activation of neuronal PARs may derive from inflammatory cells (Vergnolle et al. 2001) as part of the concerted response to infection.

PARs play roles in many mammalian systems, however it is PAR1 and 2 that are expressed throughout the nervous systems and they are expressed at low levels in glial cells in the peripheral nervous system. Neuronal PAR1 and PAR2 activation can signal to the neurones in peripheral and perhaps central nervous tissues to influence inflammation and pain (Vellani et al. 2010; Phillippe et al. 2011; Dai et al. 2007) but

only PAR2 has been extensively investigated in sensory neurones (in rat and mouse). The activation of PAR2 in C-fibres and nociceptive primary afferent neurones could induce pro-inflammatory effects, such as increase in neuropeptide level, up-regulation of Fos, leukocyte recruitment, etc (Dinh et al. 2005; Press 2013; Wang et al. 2012; Dai et al. 2007; Patwardhan et al. 2006, Vellani et al. 2010) However, PAR3 is also expressed in a significant population of trigeminal neurones and satellite glial cells, but the functional role of PAR3 remains unclear (Press 2013).

The literature contains very few studies on the role of PARs in trigeminal ganglia. There is some evidence indicating that the expression of PAR2 in trigeminal neurones is associated with neurogenic inflammation (Patwardhan et al. 2006; Dai et al. 2004; Dinh et al. 2005) and previous work from our lab has shown that neuronal PAR2 expression was significantly less in human painful carious teeth than in carious asymptomatic teeth (Morgan et al. 2009). Taken together, bacteria proteinases may be key modulators of trigeminal neuronal PAR2 function and consequently it is possible that gingipains may directly effect the generation of pain through a PAR2-mediated pathway.

The aims of this part of the study were to:

- Determine the expression of PARs in trigeminal ganglion culture
- Investigate the cellular calcium concentrations that are directly effected by
 - Trypsin
 - *P. gingivalis* arg-gingipain
- Investigate the cellular receptors that are directly activated by gingipains
- Quantify levels of secreted CGRP in response to gingipains

6.2 Results

6.2.1 Presence of PAR2 in TG cultured cells

Before the TG neurones were exposed to gingipains, the PAR2 protein had to be clearly demonstrated. Figure 6.1 (A1-A4) shows the expression of PAR2 on cultured trigeminal neurones using immunofluorescence. The mouse TG-cultures expressed PAR2 on both neurones and non-neuronal cells. The granules of PAR2 could be observed on the cell surface, particularly of neuronal cells and some granules were also superimposed within the cytoplasmic area. Quantitative analysis [see section 2.11.2, Chapter 2 Material and Methods] confirmed that neuronal PAR2 expression was present on 91.71% (SD±15.65) of neuronal cell surface in the culture. Considerably lower PAR2 expression was observed on non-neuronal cells.

6.2.2 The reduction of PAR expression following exposure to gingipain

The intensity of PAR2 expression was high on the surface of TG cultured cells. Surprisingly, these surface receptors virtually completely disappeared after 5 minutes exposure to either 2 μ M Rgp (protease activity equal to 100 μ g/mL trypsin) or 2 μ M Kgp (or protease activity equal 100 μ g/mL trypsin). To estimate the degree of PAR2 reduction following gingipain treatment, the area of PAR2 expression were again analysed compared with unstimulated cultures. The % neuronal PAR2 area decreased from 91.71% (SD±15.65) of the control to 70.65% (SD±13.42) by Rgp and 50.11% (SD±10.46) by Kgp within 5 minutes (2 independent experiments, $p < 0.05$). The reduction of non-neuronal PAR2 was also apparent. Representative data are shown in Figure 6.1, F.

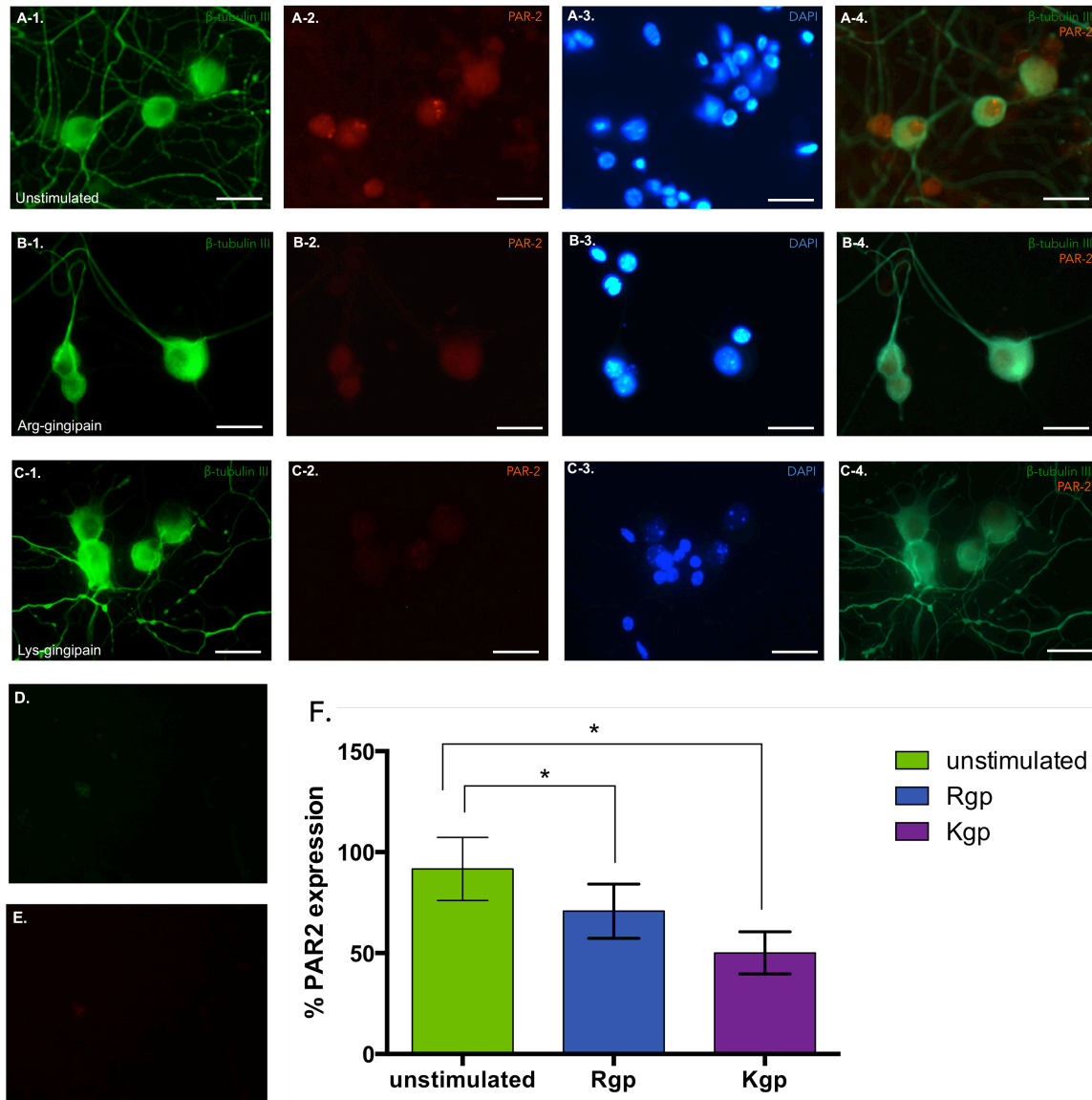


Figure 6.1 The reduction of PAR2 in trigeminal cells after stimulation with Rgp and Kgp.

Representative images of TG cultures that were either untreated (A-1 to A-4) or stimulated with *P. gingivalis* 2 μ M Arg-gingipain (Rgp) (B-1 to B-4) or 2 μ M Lys-gingipain (Kgp) (C-1 to C-4) for 5 minutes. Cells were permeabilised with 0.1% Triton X-100 and subsequently stained with anti-PAR2 primary antibody and the correspondent secondary antibodies. The PAR2 appears in red and β -tubulin III in green in the above images. TG cultures were counterstained with DAPI. The merged images (panels numbered 4) show the combined PAR2, and β -tubulin III. The β -tubulin III, and PAR2 control samples showed no labelling (panels C and D respectively). The merged images demonstrate the reduction of surface PAR2 after the treatment with Rgp or Kgp. The experiments were performed 3 times. Quantitative analysis of % neuronal PAR2 expression stimulated by gingipains is shown in figure E. Data are the mean \pm SD from three independent experiments. Error bars are \pm SD, * $p < 0.05$. Scale bar = 70 μ m.

6.2.3 Effect of proteolytic enzymes on the functional response of TG cells

Trypsin and Rgp stimulation of calcium influx in TG

Since the gingipains could reduce the expression of neuronal PAR2, we sought to determine whether activation of PAR2 affected cellular calcium concentration using calcium imaging techniques. In the initial stage of this experimental set up, we conducted experiments using trypsin that has been shown to activate neuronal PAR2 in TG culture system (Dai et al. 2007; Miike et al. 2001). We determined the biological effects of Rgp on calcium fluxes in TG neurones and non-neuronal cells.

A transient increase of intracellular calcium occurred following activation with trypsin and *P. gingivalis* Rgp, which are both PAR agonists. Representative data are shown in Figure 6.2 and Figure 6.3. Surprisingly, 2 μ M Rgp which cleaves proteins after arginine residues in a similar manner to trypsin, stimulated higher levels of intracellular calcium both in terms of the number of cells responding and in their average amplitude (Figure 6.3). Approximately 15.38% (8/42) of TG neurones responded to 100 μ g/mL of trypsin exposure, while about 63.16% (48/76) of TG neurone responded to Rgp (activity equal 100 μ g/mL trypsin). In addition, nearly all of the non-neuronal cells present in the samples also responded to both trypsin (Figure 6.2, H) and Rgp (Figure 6.3, G). Interestingly, the calcium movement in response to Rgp is in an oscillatory manner in both neurones (Figure 6.3, F) and non-neuronal cells (Figure 6.3, G).

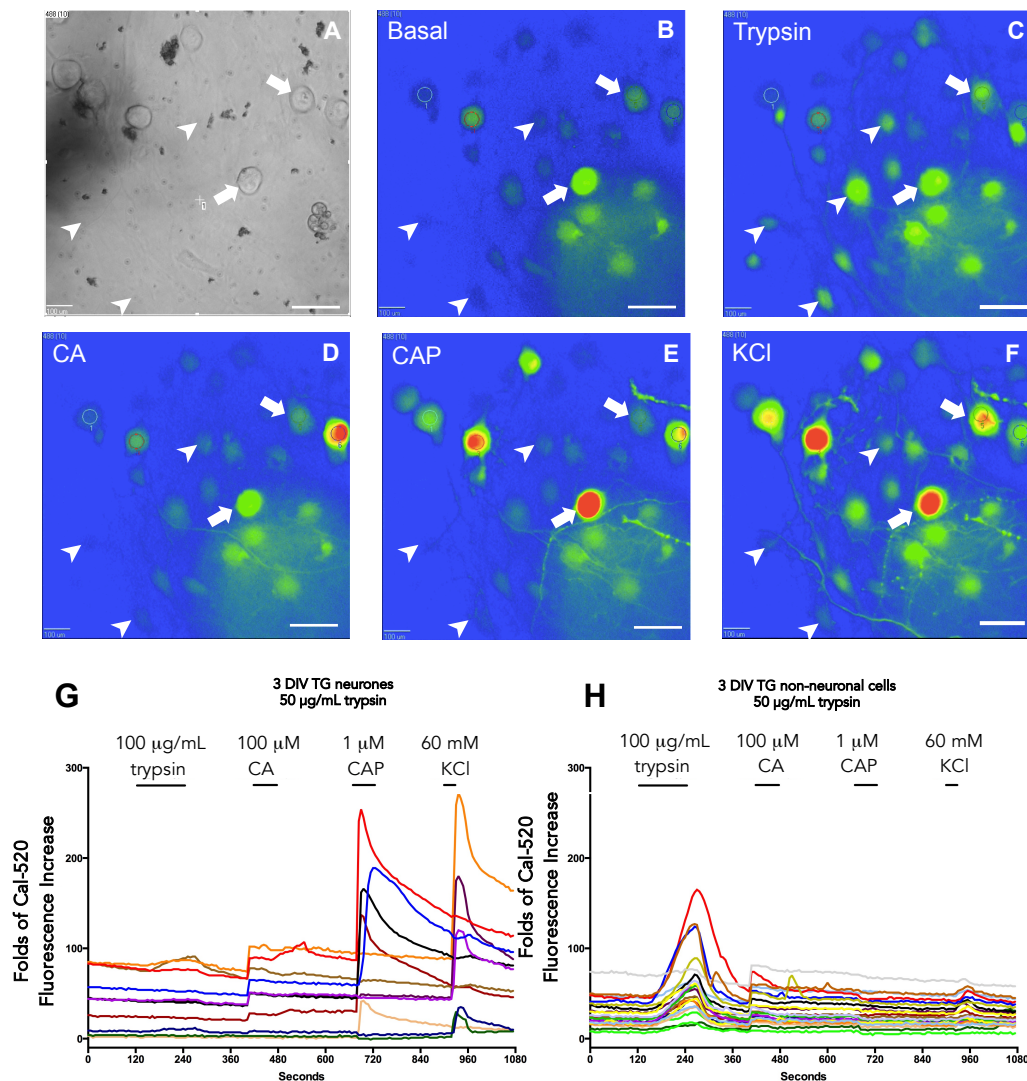


Figure 6.2 Analysis of intracellular calcium in primary trigeminal cell culture – effect of trypsin.

(A) Phase-contrast and (B-F) time-lapse calcium imaging in trigeminal ganglion neurones (white arrow) and non-neuronal cells (white arrow head) loaded with Cal-520 AM during trypsin, cinnamaldehyde (CA), capsaicin (CAP), and high potassium chloride (KCl) application. The high potassium application was to assess neurone viability and to help distinguish neuronal from non-neuronal cells. (G-H) Graphs tracing the transient change in calcium in individual cells over time after trypsin and the agonist applications in neurones are shown in G, and non-neuronal cells in H. Scale bar = 100 µM.

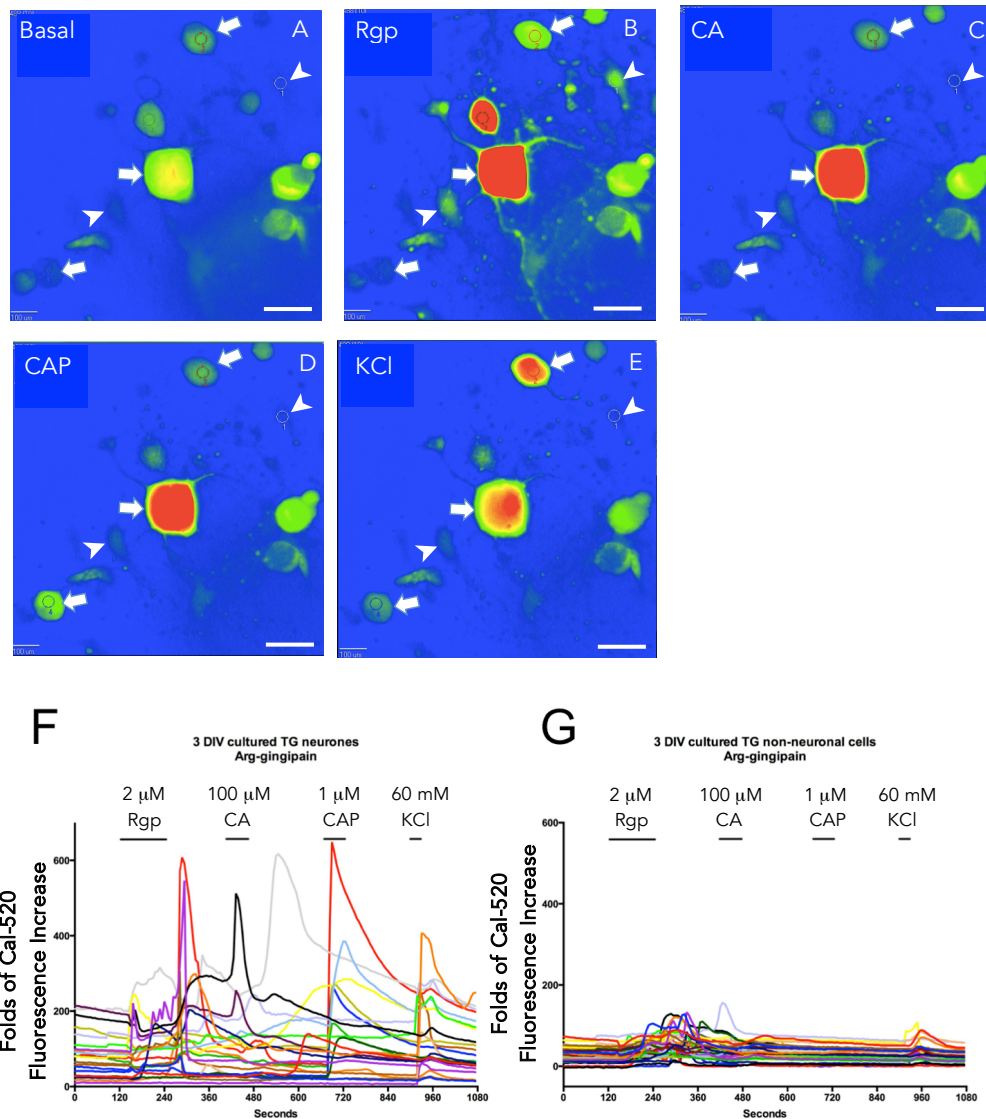


Figure 6.3 Effects of Rgp on trigeminal cell response.

(A–E) time-lapse calcium imaging in trigeminal ganglion neurones (white arrow) and non-neuronal cells (white arrow head) during basal stage (A), Rgp (B), CA (C), CAP (D), and KCl (E) applications. Figure F and G are traces of the transient change in calcium in individual cells over time after Rgp and the agonist applications in neurones (F), and non-neuronal cells (G). Scale bar = 100 μM.

6.2.4 Rgp and Kgp caused significant release of CGRP

PAR2 is a receptor for inflammatory protease that is thought to be related to neurogenic inflammation, involving neuropeptide release (Henderson et al. 1996). Therefore we next evaluated, whether high proteolytic activity of Rgp and Kgp (proteolytic activity equal 100 $\mu\text{g}/\text{mL}$ of trypsin) could alter the neuronal neuropeptide response of trigeminal cell cultures. CGRP release experiments were performed by collecting the supernatants of TG cultures after exposure to the gingipains and quantifying the neuropeptide by ELISA. Both Rgp, and Kgp significantly increased CGRP release from trigeminal neurones (Figure 6.4, $p < 0.001$) and they were slightly higher than quantity to that obtained by stimulation with CAP.

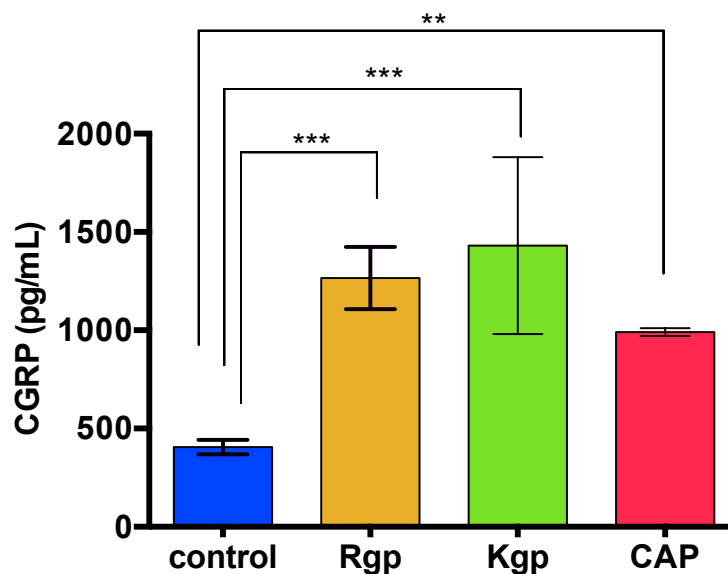


Figure 6.4 CGRP levels in Rgp, Kgp, and capsaicin-stimulated TG neurones from control.

The secreted CGRP response to gingipains or capsaicin were determined by the incubation of TG cultures for 15 minutes with Rgp, and Kgp (enzymatic activity equal 100 $\mu\text{g}/\text{mL}$ trypsin) or capsaicin (5 μM) at 37°C with 5% CO_2 . Measurement of CGRP levels was performed using enzyme-linked immunosorbent assay. Data are the mean \pm SD of two independent experiments. Bars are \pm SD, ** $p < 0.01$, *** $p < 0.001$.

6.2.5 The ability of *P. gingivalis* gingipain mutants to stimulate CGRP release

To confirm the effects of free enzyme on CGRP release from cells in TG cultures, we compared the effect of mutants that lacked each type of gingipain with that of wild type cells. Three gingipain-knock out mutant strains were employed; (Δ -*rgpA:B*-, Δ -*kgp*-, and Δ -*rgpA:B:kgp*).

We found that the Δ -*rgpA:B*- and Δ -*rgpA:B:kgp* mutants stimulated a lower secretion of CGRP levels from the TG cultures (Figure 6.5, $p < 0.05$), which were two-fold in quantity to that obtained from unstimulated cultures. In contrast the Δ -*kgp* strain stimulated similarly high levels of CGRP as the wild-type *P. gingivalis* W50. This suggests that the Rgp is involved in neural sensitisation.

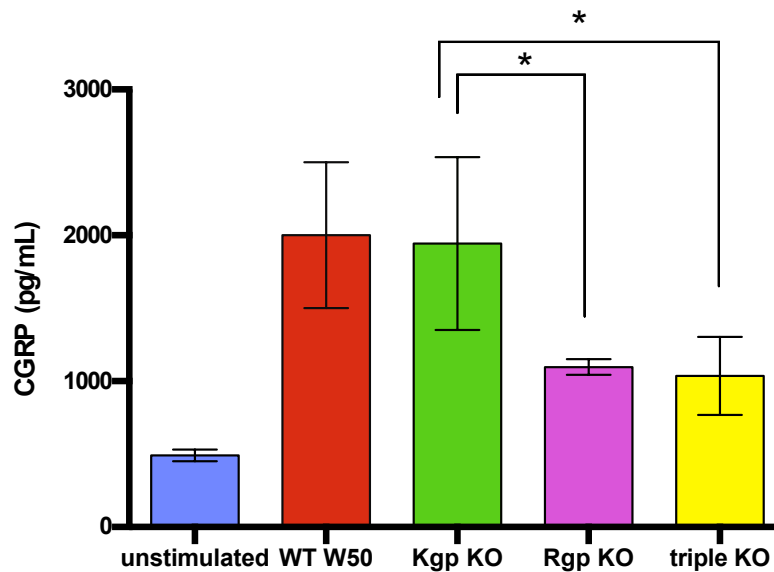


Figure 6.5 Release CGRP in response to various *P. gingivalis* strains.

The secreted CGRP response to various strains of *P. gingivalis*. Secreted CGRP was determined by the incubation of TG cultures for 15 minutes with live *P. gingivalis* (2.5×10^7 bacteria) at 37°C with 5% CO₂. Measurement of CGRP levels was performed using enzyme-linked immunosorbent assay. Data are the mean \pm SD from two independent experiments. Bars are \pm SD, * $p < 0.05$.

6.2.6 The reduction of CGRP against Rgp and Kgp

The primary structure of CGRP contains a number of potential lysine and arginine cleavage sites for the gingipains so it is possible that CGRP could be being degraded in the assay rather than secretion of the peptide being affected. To investigate this we directly compared the amount of mouse CGRP peptide that was detectable in the presence and absence of pure Kgp and Rgp. We found little effect of Rgp on detectability of CGRP but there was an effect of Kgp (Figure 6.6). The amount of CGRP 'destroyed' was approximately 50% by the Kgp treatment.

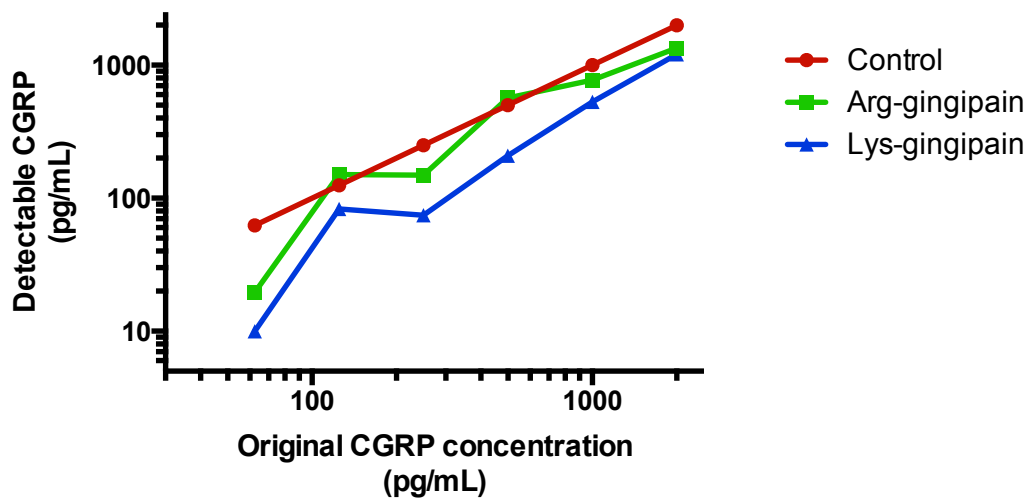


Figure 6.6 CGRP concentration plots in the present of Rgp, and Kgp against no treatment CGRP in various concentrations.

The various concentrations of CGRP in the presence of Arg-gingipain (Rgp), and Lys-gingipain (Kgp) that the proteolytic activity equal 100 $\mu\text{g/mL}$ of trypsin. It could be seen the little effect of Rgp on detectability of CGRP but there was an effect of Kgp.

6.3 Discussion

6.3.1 Overview

The rationale for this part of the study comes from the evidence that *P. gingivalis* constituents interact directly with neuronal cells (LPS in Chapter 5) and that it is likely that other pathogenic features of the organism are likely to impact on neuronal function as well, either directly or indirectly (Laarman et al. 2010; Potempa et al. 2000; Rangarajan et al. 2008). Also, there is ample evidence in the literature that gingipains can stimulate pro-inflammatory mediators through PARs in gingival fibroblasts (Uehara et al. 2005; Stathopoulou et al. 2009; Joseph et al. 2000; Giacaman et al. 2009). So, in this chapter, we explored whether protease from *P. gingivalis* could also directly activate sensory neurones. It is known that the ability of gingipains is to activate and/or deregulate a wide range of host proteins (Rangarajan et al. 1997; Uehara et al. 2005) is important in other disease process, most notably periodontitis, and so it could be an important virulence factor in mediating dental pain through PAR2.

PAR2 is a potential receptor that could transduce inflammatory pain (Veldhuis and Bunnett 2013; Wang et al. 2012; Dai et al. 2007; Rothmeier and Ruf 2012). Although, until recently, there have been very few reports regarding the direct effects of bacteria protease on trigeminal ganglion neurones.

In this study, experiments were initially performed to establish the presence and degree of PAR2 on cells in the trigeminal ganglia cultures. PAR2 was indeed found and exposure of the cultures to gingipains, both Rgp and Kgp, resulted in a reduction in surface PAR2. This was mirrored by changes in calcium flux and greater level of CGRP in the culture supernatant.

6.3.2 Both Rgp and Kgp could cleave PAR2

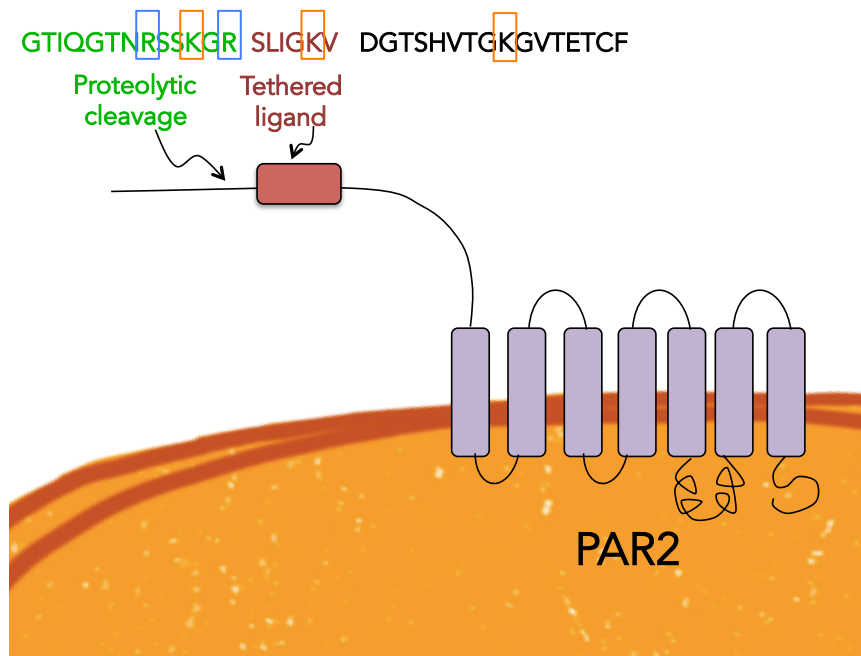
Morgan et al. (2009) demonstrated the expression of PAR2 in dental pulp that could be found in vascular tissue, pulpal fibroblasts, and dental pulp nerve fibres. Besides, PAR2 is expressed by 65% of neurones in the DRG of the rat (Wang et al. 2012; Dai et al. 2004). In this study, we found that neuronal PAR2 of TG was expressed on the cell surface of both neurones and non-neuronal cells. However, we could not quantify the number of TG neuronal cells that expressed PAR2 because PAR2 was seen to be present on most neurones. Consequently in our system we quantified the percentage of surface expression of PAR2, which we showed was about 92% TG neurones expressing PAR2.

After activation of PAR2 on the cell surface by the agonists, it is internalised into early endosomes and lysosomes (Matsushima et al. 2006). We also found that neuronal PAR2 expression was reduced following Rgp and Kgp exposures, from 91.71% to 70.65% and 50.11% respectively but that could be due either to internalisation of the receptor or to its cleavage. To our knowledge, this is the first time it has been demonstrated that Rgp and Kgp directly affect neuronal PAR2 in trigeminal ganglion cultures.

This could be explained by reference to the primary structure of PAR2 studies have showed that PAR2 has both proteolytic cleavage and tethered ligands (Figure 6.7) and that it contains cleavage sequences that could be targeted by gingipains (Vergnolle et al. 1998). Arg (R) and Lys (K) amino acids are located in many positions of the functional domain and it is known that PAR2 contains a putative Rgp cleavage site SKGR³⁴↓S³⁵ LIGKV (Ossovskaia and Bunnett 2004). According to the amino acid sequences previously published, we could also observe at least 3 lysine amino acid groups that are the possible cleavage sites for Kgp. So, it is possible that both Rgp, and Kgp can cleave both of functional domain and the antigen epitope recognised by the anti-PAR2 antibody.

Full amino acid sequence of PAR2:

MRSPSAAWLLGAAILLAASLSCS GTIQGTNRSSKGRSLIGKVDGTSHVTGKGVTETCF
 VDEFSASVLTGKLTTVFLPIVYTIVFVVGLPSNGMALWVFLFRTKKKHPAVIYMANLALAD
 LLSVIWFPLKIAYHIHGNNWIYGEALCNVLIGFFYGNMYCSILFMTCLSVQRYWVIVNPM
 GHSRKKANIAIGISLAIWLLILLVTIPLYVVKQTIFIPALNITTCHDV LPEQLLVGDMFNYFL
SLAIGVFLFPAFLTASAYVLMIRMLRSSAMDENSEKKRKRAIKLIVTVLAMYLICFTPSNLL
LVVHYFLIKSQGQSHVYALYIVALCLSTLNSCIDPFVYFVSHDFRDHAKNALLCRSVRTV
 KQMQLVSLTSKKHSRKSSTSSSTTVKTSY

Functional domain of PAR2:**Figure 6.7 Functional domain of PAR2.**

The schematic shows the structure and functional domains of PAR2. The figure shows the important domains, which are proteolytic cleavage, and tethered ligand. Potential cleavage sites of Rgp and Kgp are highlighted in blue boxes for Rgp cleavages, and red boxes for Kgp cleavages. The full amino acid sequence is shown in the box above. The functional domain is highlighted in blue and the domain to indicate the antibody binds is highlighted in yellow. Potential cleavage sites with both domains are underlined.

6.3.3 Possible neuronal PAR2 mechanisms

There have been extensive studies of the roles of PAR2 in inflammatory processes. PAR2 is widely distributed in various tissues. Recently, there has been particular interest in peripheral nociception because PAR2 is expressed on nociceptive afferents (Steinhoff et al. 2005). Previous work from our group suggests that a decrease in neuronal PAR2 expression levels was only found within carious painful samples and not in association with caries alone (Morgan et al. 2009), which may suggest a relation between activation of PAR2 and pain symptoms.

In DRG, PAR2 activation has been studied and shown to be involved in neuronal elevation of $[Ca^{2+}]_i$ (Vergnolle et al. 1998; Vellani et al. 2010; Liu et al. 2014). Also, according to this study we show evidence to support the premise that PAR2 activation by Rgp is involved in neuronal and non-neuronal cell activities represented by calcium influx. However, non-neuronal responses were lower than that seen in neurones. This discussed more extensively in section 7.3.3 (Chapter 7).

Although, the molecular mechanisms of PAR2-mediated inflammation and hyperalgesia are unclear, it is likely to involve signalling events that regulate activity or expression of ion channels such as TRPV1 (Vellani et al. 2010). Activation of PAR2 has been shown to enhance TRPV1-induced Ca^{2+} signalling and TRPV1 currents in cell lines and neurones by a PKC-dependent mechanism and also potentiates capsaicin-induced release of CGRP. These results may suggest that activated PAR2 couples PKC, which may phosphorylate and activate TRPV1, thereby inducing hyperalgesia (Veldhuis and Bunnett 2013; Dai et al. 2004). Besides, oscillatory patterns of calcium movement in response to stimuli are reported to be highly related to the complex interplay of many receptors and ion channels (Feske et al. 2012). This could support the idea that the mechanisms by which gingipains activate TG cells involve multiple cellular receptors. A summary of such a mechanism is shown in Figure 6.8.

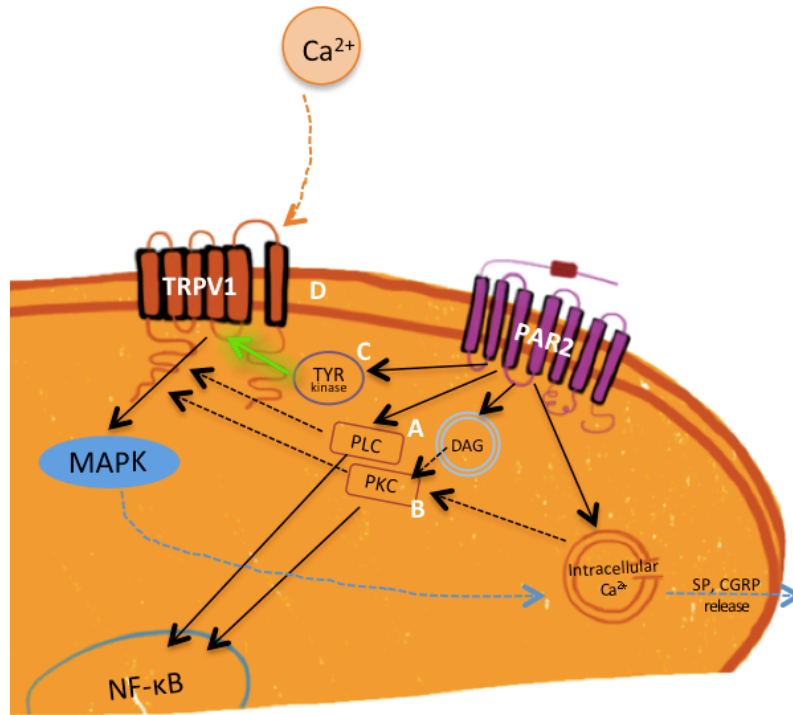


Figure 6.8 PAR2 could internally sensitise TRPV1.

After PAR2 activation (A), PLC hydrolysis induces PKC activation (B), and TYR kinase (C), and then leads to TRPV1 phosphorylation and sensitisation (D).

6.3.4 Consequences of neuronal activation following exposure to gingipains

PAR2 cleavage could indicate that there is direct activation of trigeminal sensory neurones and subsequent induction of CGRP release. There are similar data from another study which suggested that a 2 hour stimulation by RgpB could induce human tooth pulp to release SP and CGRP via p38 MAPK pathway (Tancharoen et al. 2005). It was indicated that dental pulp tissue could release the neuropeptide. However, the present study suggests that Rgp and Kgp could activate neuronal PAR2 and rapidly release CGRP from sensory nerves in response to an infection.

The results of our study could support a role for PAR2 in pain sensation because we could demonstrate that the peripheral sensitisation by gingipains subsequently activated calcium mobilisation and release of CGRP. This is consistent with the finding of Dai et al. (2004) who showed that trypsin and mast cell tryptase could cleave PAR2 on DRG sensory nerve and cause neurogenic inflammation. Taken together, this could suggest that direct activation of trigeminal neurones by either Rgp or Kgp can occur via a PAR2-dependent pathway, and that this is another rapid mechanism for *P. gingivalis* to activate TG neurones.

It needs to be noted that less CGRP could be detected in the presence of gingipain, especially Kgp (Figure 6.6). This might be because the primary structure of CGRP is ACNTATCVTHRLAGLLSRSGGVVKNNFVPTNVGSKAF-NH₂ (Hökfelt et al. 2000) which reveals a number of potential cleavage sites for Rgp and Kgp, although it seems to be more susceptible to bacteria that are not expressing Rgp. Interestingly this leads to a possible 'dampening' of the effect of Rgp on neurones, since cleavage of PAR2 by Rgp would result in elevated level of CGRP release but that peptide can also be at least partially degraded by Rgp which would ameliorate its inflammatory and pain-promoting effect.

Since the ideal gingipain inhibitor has yet to be discovered (Olsen and Potempa 2014), we inhibited the effects of either Rgp, and/or Kgp in *in vitro* models of bacterial infection by using gingipain knock-out strains. This could confirm that

gingipains play multi-functional roles for the development of neurogenic inflammation. This study also shows that Kgp can dampen down CGRP which is consistent to the study of Stathopoulou et al. 2009 that Kgp can degrade cytokine. So, it could be considered that *P. gingivalis* can subvert the protective host response by direct CGRP degradation through gingipains, especially Kgp.

6.3.5 Limitations and future prospects

There have been very few reports in the literature regarding the direct effects of gingipain on TG neurones. It may be because of difficulties to obtain pure neurones in culture (as discussed in the previous Chapters).

In this study, we could not demonstrate the effects of NF- κ B in response to gingipains, because long treatment of cultured cells with proteases tended to damage the culture system (Pike et al. 1994; Gee et al. 2000). Therefore, in this study, we could only challenge the cultures for a short period and we were observing the rapid effects of the gingipains. Also, it is possible that gingipains could have cytotoxic effects on cells in the culture. Consequently, future experiments could include assaying reduction of MTT to confirm the viability of the cells.

It would be useful to study in future co-localisation of PAR2 with TRPA1 or TRPV1 to determine whether these 2 categories of receptors could interact with each other in response to bacterial components. As shown in the study of Dai et al., 2007 that trypsin and tryptase could trigger TRPA1 activation. Besides, Chen et al., 2011 also supported that PAR2 activation could sensitise TRPV1, TRPV4, and TRPA1. These findings may support the idea that these signalling receptors could have inter-crosstalk to response to bacterial infection. Moreover, the activation of neuronal supporting cells may be a crucial element in dental pain generation, which is addressed in the next Chapter (7).

6.3.6 Clinical relevance

PAR2 may constitute an important target for modulating the effects of an infectious pathology such as periodontal inflammatory disease. A specific PAR2 antagonist might be a useful analgesic tool. However, the loss of a functional PAR2 may lead to adverse effects such as tissue repair. So this has to be confirmed, as there are currently very little data on specific PAR2 antagonists.

6.4 Conclusion

This study has shown that gingipains are another significant virulence factor of *P. gingivalis* that can directly interact with trigeminal neurones and this appears to be through the PAR2 receptor.

Chapter 7

*Neuronal-glia! behaviour in
response to sensory
nerve activation*





7. Neuronal-glia behaviour in response to sensory nerve activation

7.1 Introduction

In the previous chapters, we demonstrated the neuronal responses to *P. gingivalis* components. Both LPS and gingipains apparently interact with TLR4 and PAR2. However, dental pain is a perceptive complex that is a multidimensional phenomena involving multiple cellular and molecular mechanisms with both central and peripheral nervous systems. In the central nervous system, supporting cells such as microglial and astrocytes have been shown to be very important in pain pathway signalling (Guillot et al. 2012; Scemes and Giaume 2006). Recently, there is more evidence to indicate that the supporting cells in the peripheral nervous system, such as satellite glial cells (SGCs) and Schwann cells, also play a role in communicating with the neurones and modulating the neuronal-glia activities could modulate neuronal activities.

In TG, glial cells and neurones also establish this relationship. Interaction between non-neuronal cells and neurones in the peripheral nervous system is a relatively recent research field to focus in pain generation (Villa et al. 2010; Poulsen et al. 2014; Hanani 2015). In the previous 2 chapters, we demonstrated the expression of TLR4 and PAR2 receptors on satellite glial cells, as well as, functional characteristics of some non-neuronal cells in response to the *P. gingivalis* components.

Therefore, it might be suggested that non-neuronal cells in the TG culture could represent pathways that modulate pain signalling in the peripheral nervous system itself. The aim of this work was to investigate the possible roles of non-neuronal cells in neuronal sensation. We began by characterising the phenotypic changes of glial cells from TG of adult mice in tissue culture. We subsequently followed these cells for up to 4 days and observed profound morphological and immunohistochemical changes in them. Furthermore, by using live cell calcium imaging, we could study TG neuronal networks and sensory processing by both neurones and non-neuronal cells independently in the mixed culture system.

In the Chapters 4 – 6, we demonstrated that the release of CGRP is a rapid response mechanism and suggested that this could play a part in neurogenic inflammation in TG induced by *P. gingivalis* and its components. Meanwhile, minocycline is thought to be one of the reagents that could inhibit cytokine release such as TNF- α (Ledeboer et al. 2005) mainly by blocking the up-regulation of SGCs (Gong et al. 2015). Here, we also sought to verify whether the inhibitory effect of minocycline could inhibit neurogenic inflammation and NF- κ B nuclear translocation mediated through glial cells.

In summary, the aim of this study is to

1. Demonstrate TG non-neuronal cell characteristics in ganglia and *in vitro*
2. Demonstrate the sensitivities of non-neuronal cells to bacterial components
3. Consider the scheme of neuronal-glia responses to LPS and gingipain from *P. gingivalis*
4. Explore the overall effects of bacterial components on non-neuronal cells, such as CGRP release and NF- κ B activation, and the effects of pre-treatment with minocycline

7.2 Results

7.2.1 Characteristics of non-neuronal cells in TG

7.2.1.1 Close Interaction of neurones and non-neuronal cells in TG

Neurones and satellite glia cells are close neighbours inside the sensory ganglion such as TG and DRG. While, β -tubulin III is specifically expressed on neurones, the glial cells can be identified using immunohistochemistry for various types of proteins such as S100, glial fibrillary acidic protein (GFAP), and glutamine synthetase (GS). Figure 7.1 shows β -tubulin III, S100, and DAPI labelling that label neurones and non-neuronal cells such as satellite glial cells and Schwann cells. This image shows the TG sensory neurones that are surrounded by glial cells showing the close contact between these two types of cells.

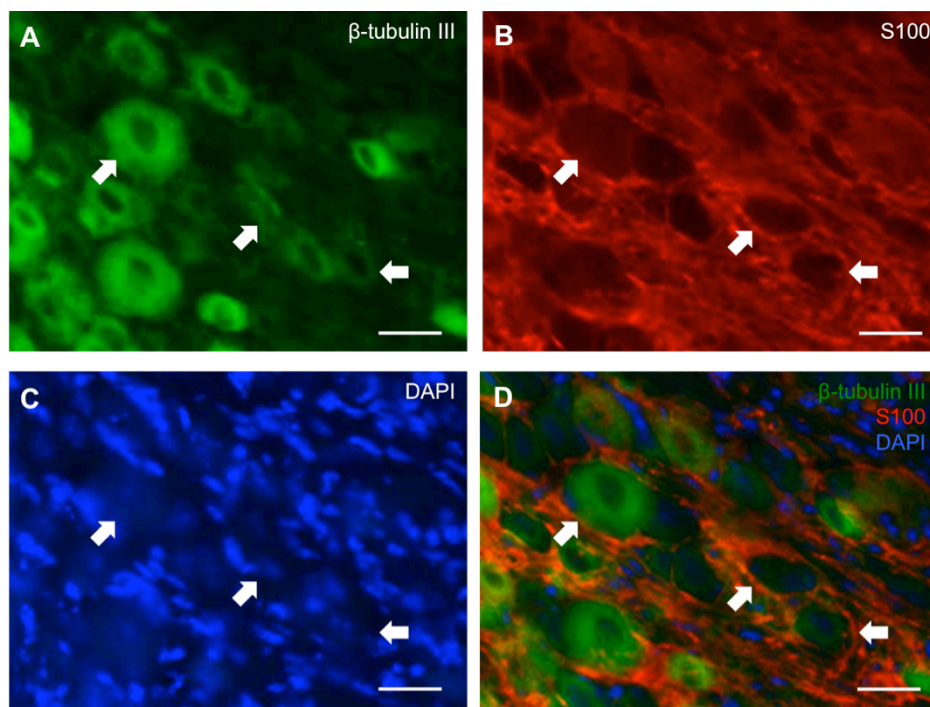


Figure 7.1 Cross section of TG showing the close contact of neurones (green), and satellite glial cells (red).

Representative images showing that TG neurones are surrounded by glial cells. These figures show the triple labelling of β -tubulin III (A), GFAP (B), DAPI (C), and their co-localisation (D). White arrows depict example SGCs that surround the TG neurones showing the close contact between these two types of cells. Scale bars are 70 μ m.

7.2.1.2 TG non-neuronal cell growth *in vitro*

In this culture system, the TG cultures were incubated for 2 and 4 days to determine the optimum length of time to culture TG cells, as shown in Chapter 3. At the early stages (2 DIV) in the culture (Figure 7.2), some glial cells still attach to neurones. Subsequently, the glial cells exhibited proliferation and moved away from the neurones and lost some of their cellular characteristics e.g. in the latter days (4 DIV) *in vitro* (Figure 7.3).

More than half of the non-neuronal cells present appeared to be Schwann cells, which could be identified by the expression of S100, but only in the early days of culture (data was shown in Chapter 3). However, the differentiated cells in later cultures do not express much protein S100 or GS. So, the optimal length of time to culture the TG models was identified to be 2 days. Indeed 2 day *in vitro* (2 DIV) culture resulted in minimal non-neuronal cells without significant loss of their characteristics.

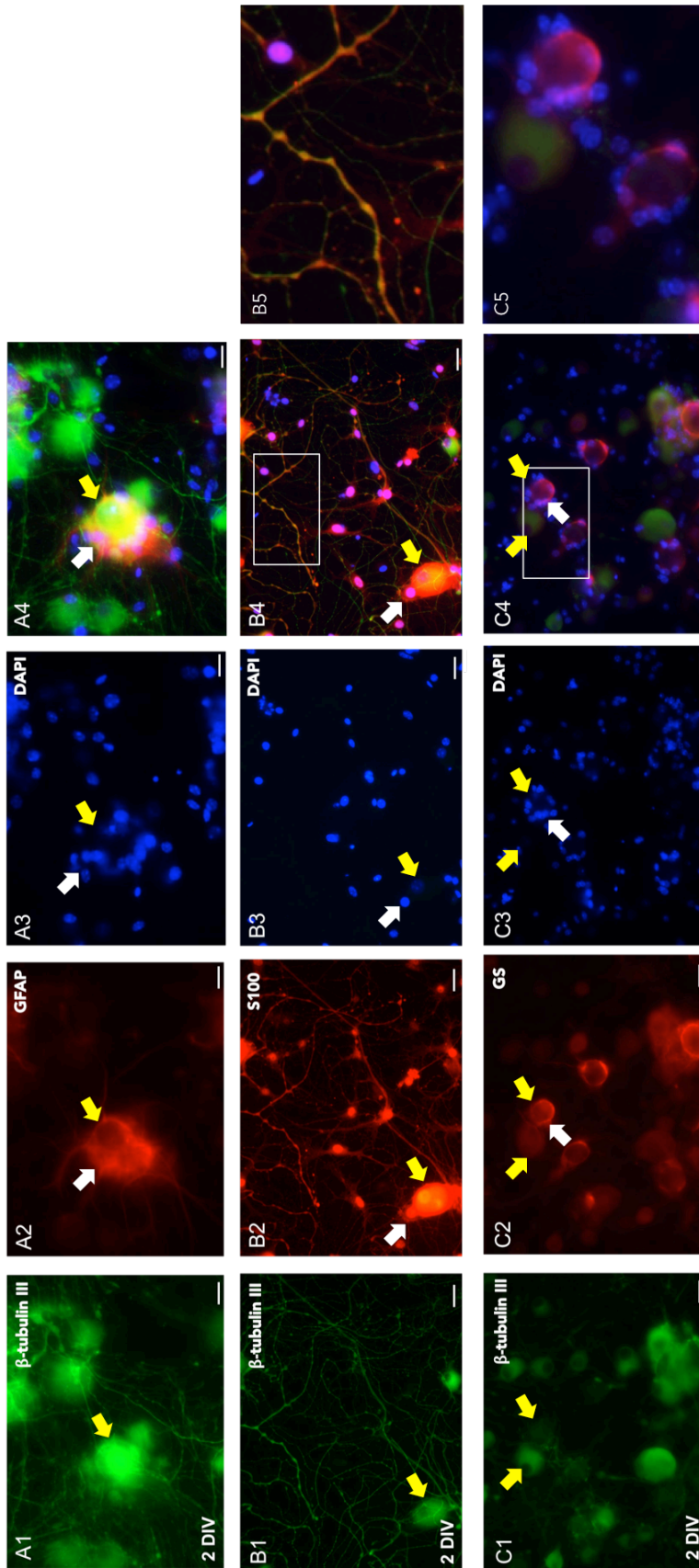


Figure 7.2 Non-neuronal cells characterised by satellite glial cell marker, GFAP, co-localisation with β -tubulin III, and DAPI in the early days of the cultures.

Representative images of TG cell mixtures of neurones and non-neuronal cells. The TG cultures were left untreated in culture for 2 day (2DIV) to study their general characteristics. Cells were permeabilised with 0.1% Triton X-100 and subsequently stained with primary antibodies against various types of non-neuronal cell marker (A2-C2) and the correspondent secondary antibodies. The β -tubulin III is shown in green (A1-C1) and non-neuronal cell markers are shown in red (A2-B2). Non-neuronal cells were characterised by GFAP (A2), S100 (B2), and GS (C2). Nuclear staining with DAPI (A3-B3) appears blue. The merged images show the combined β -tubulin III and DAPI with GFAP or S100 or GS staining (A4-C4). Localisation of neurones and SGCs are indicated by yellow arrows (neurones) and white arrows (SGCs). The characteristics of non-neuronal cells were very similar to *in vivo* in early day (day 2) that neurones are enwrapped by non-neuronal cells such as SGCs. B5 is the magnification area of the white squared box shown in B4 (double plus S100 labelled). This is thought to show Schwann cells attached to neurone's axons. C5 is the magnification area of the white squared box shown in C4 (double plus GS labelled). This staining pattern surrounding the cell body of neuronal cells is typical of SGCs. Scale bars = 30 μ m.

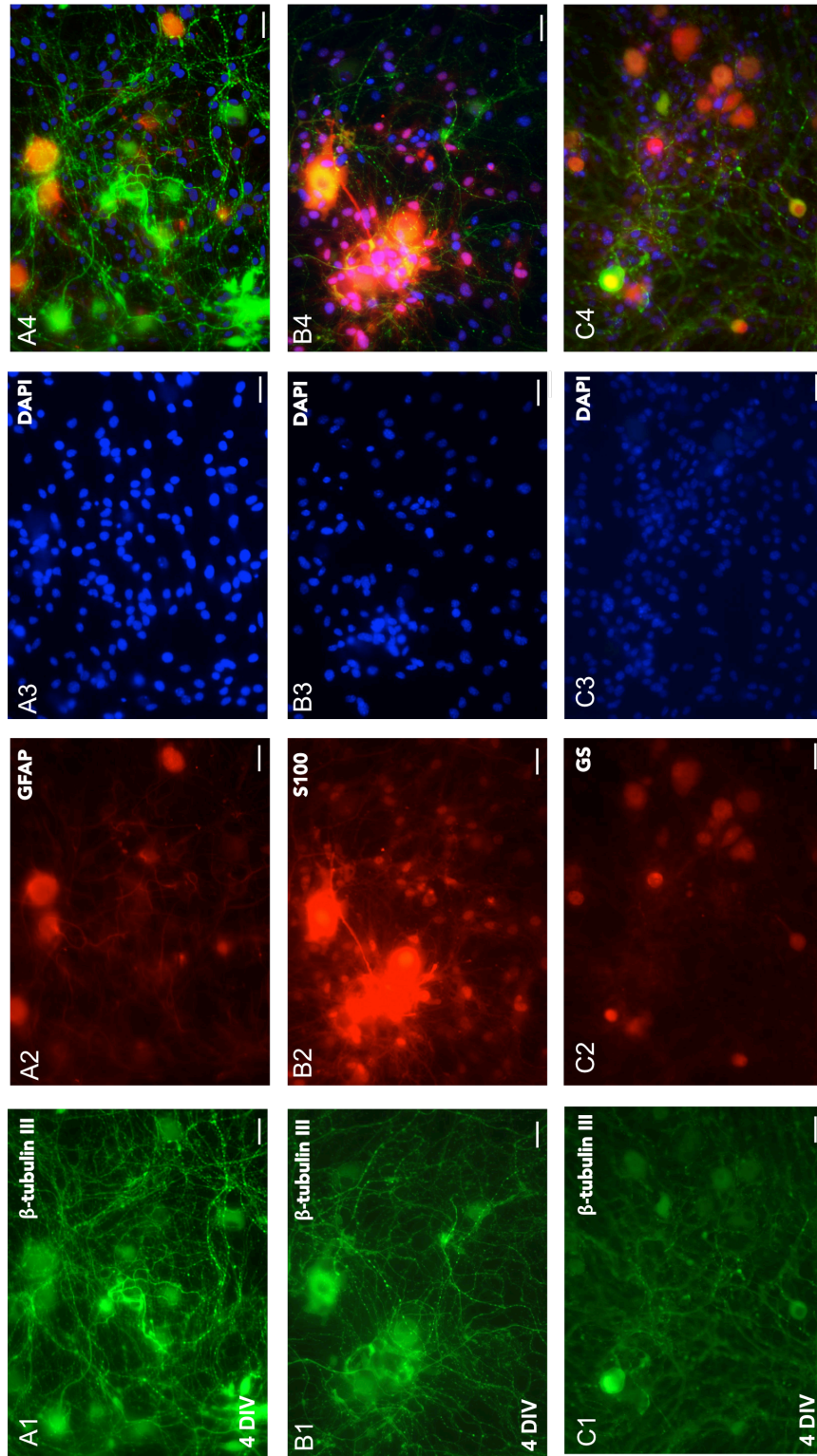


Figure 7.3 Satellite glial cells characterised by glutamine synthetase (GS), co-localised with β -tubulin III, and DAPI in older cultures.

Representative images of TG cell mixture of neurones and non-neuronal cells. The TG cultures were left untreated in culture for 2 days (2DIV) to study their general characteristics. Cells were permeabilised with 0.1% Triton X-100 and subsequently stained with primary antibodies against various types of neuronal cell marker (A2-C2) and the correspondent secondary antibodies. The β -tubulin III is shown in green (A1-C1) and non-neuronal cell markers are shown in red (A2-B2). Non-neuronal cells were characterised by GFAP (A2), S100 (B2), and GS (C2). Nuclear staining with DAPI (A3-B3) appears blue. The merged images show the combined β -tubulin III and DAPI with GFAP or S100 or GS staining (A4-C4). The characteristics of non-neuronal cells were difficult to distinguish from neurones in the older cultures (day 4). Because the non-neuronal cells have lost their characteristics of GFAP, and GS expressions which are SGCs. Such non-neuronal cells were seen to proliferate and split away from neurones in the later days of cultures. Scale bars = 30 μ m.

7.2.2 Non-neuronal cells respond to whole *P. gingivalis* W50 cells

In the Chapter 4, we discussed the direct effects of whole wild-type *P. gingivalis* W50 cells on TG neurones. Moreover, non-neuronal cells have been reported to be part of the peripheral sensitisation mechanisms (Ceruti et al. 2008; Austin and Gila 2010; Poulsen et al. 2014). In this chapter, we have focussed on the non-neuronal cells in the TG culture system.

From the work reported in Chapter 4, we have direct evidence that whole *P. gingivalis* could directly activate TG SGCs or Schwann cells. We also demonstrate that there was significant NF- κ B nuclear translocation within non-neuronal cells in response to 30 min exposure to whole *P. gingivalis* cells. NF- κ B nuclear translocation in non-neuronal cells increased from 40% of unstimulated cells to 63% when stimulated by whole *P. gingivalis* cells. This is similar to neuronal NF- κ B nuclear translocations that increased from 17% to 56% in Chapter 4. The summary of NF- κ B nuclear translocation is shown again in Figure 7.8.

7.2.3 Non-neuronal cells respond to *P. gingivalis* LPS

7.2.3.1 Non-neuronal cells respond to LPS as much as or more than neurones

Non-neuronal cell intracellular calcium was transiently elevated by lower concentrations of *E. coli* LPS, range from 200 ng/mL to 20 µg/mL of *E. coli* LPS and 10 – 20 µg/mL of *P. gingivalis* LPS, compared to those required % of activation to achieve the same from TG neurones as shown in Table 7.1.

Table 7.1 Percentages of neurones and non-neuronal cells that respond to *E. coli* LPS and *P. gingivalis* LPS

LPS and the concentrations		% of cells responding (Numbers of responding cells /Total presenting cells)			
		Neurones		Non-neuronal cells	
Ultrapure <i>E. coli</i> LPS	0.2 µg/mL	0%	(0/16)	12.5%	(2/16)
	0.5 µg/mL	0%	(0/14)	0%	(0/10)
	2 µg/mL	6.25%	(1/16)	7.14%	(1/14)
	5 µg/mL	4.76%	(1/21)	57.1%	(8/14)
	10 µg/mL	6.67%	(1/15)	20%	(3/15)
	20 µg/mL	8.33%	(1/12)	31.58%	(6/19)
Ultrapure <i>P. gingivalis</i> LPS	10 µg/mL	0%	(0/13)	14.29%	(1/7)
	20 µg/mL	26.67%	(24/90)	31.58%	(18/57)

7.2.3.2 Non-neuronal cells responded to *P. gingivalis* LPS rapidly

Exposure of TG cultures to *P. gingivalis* LPS resulted in more than 20% of neurones (24/90) responding by change in calcium flux, (shown in section 5.2.3 [Chapter 5]), however, approximately 40% (18/57) of the non-neuronal cells present also responded. Figure 7.4 shows a representative example of neuronal and non-neuronal cell calcium responses on exposure to *P. gingivalis* LPS. This method also allows the duration and the latency of the responses to be observed and it can be seen that non-neuronal cells were activated before the neuronal cells, by between 10 and 30 seconds (median 20 seconds).

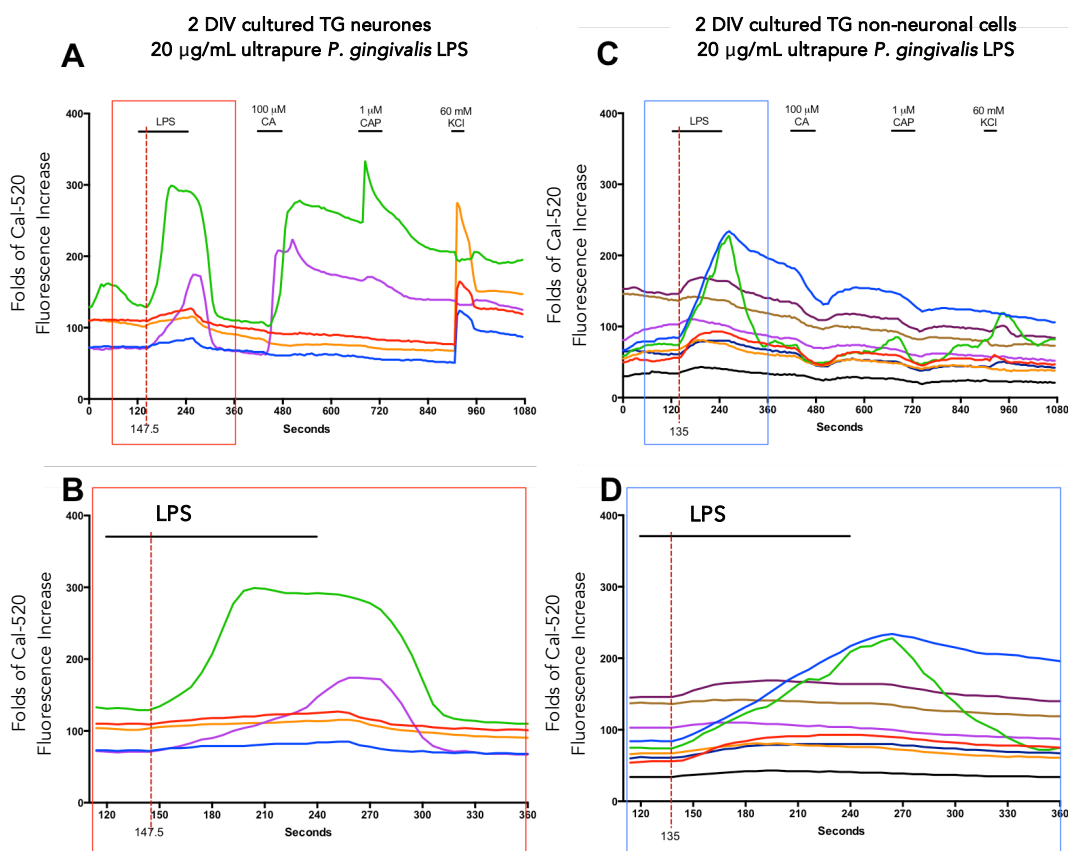


Figure 7.4 Graphs tracing the transient changes in calcium in individual cells over time following LPS application to TG 2-day *in vitro* cultures.

Optical fluorescence time-lapse acquisition of Ca^{2+} levels of TG neurones (A) and TG non-neuronal cells (C) measured by loading cells with the single wavelength fluorescent dye Cal 520-AM. The magnification data of the neurones (red squared box) and non-neuronal cells (blue squared box) are in figure B and D, respectively (at 110 – 360 s; LPS treatment). Data represent the fluorescent intensities of each cell over time as measured ($458 \text{ nm}_{\text{ext}}$ $520 \text{ nm}_{\text{emm}}$). After 2 min, cells were treated sequentially with *P. gingivalis* LPS for 2 min, CA, and CAP for 1 min to induce the release of Ca^{2+} with 2 min wash out intervals. The cultured cells were then treated with high KCl to distinguish healthy neurones from non-neuronal cells. The images and traces are representative data from 3 independent experiments. For TG neurones, the Ca^{2+} levels started to increase at 40 s after LPS application, while non-neuronal cells started to increase at 20 s after LPS exposure.

7.2.3.3 Some LPS-responding non-neuronal cells might be satellite glial cells.

The identity of the non-neuronal cells that responded to LPS was determined by the cytological features of the cells. Satellite glial cells were identified on the basis of (1) their smaller size, (2) by their location in close contact with the neurones, and (3) by immunostaining for the satellite glial cell marker, glutamine synthetase (GS). GS-positive cells were found to display a Ca^{2+} response when exposed to *P. gingivalis* LPS. This suggests that satellite glial cells in the TG cultures are part of the responsive cell population to *P. gingivalis* LPS (see Figure 7.5).

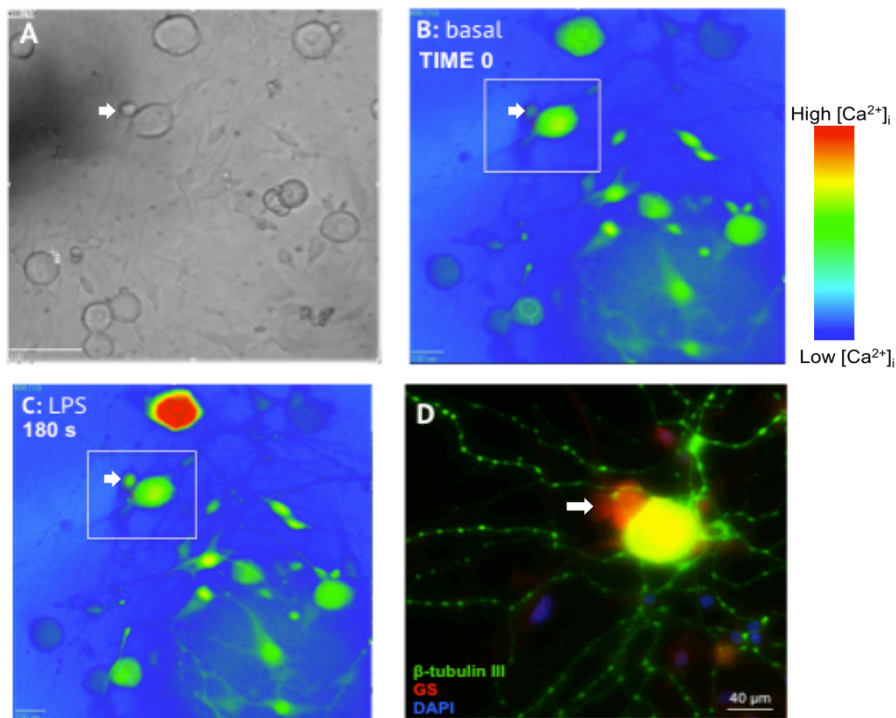


Figure 7.5 Identification of responding SGCs to LPS in culture.

Calcium imaging of TG cells in response to *P. gingivalis* LPS exposure were recorded. (A) Phase-contrast image, (B) time-lapse calcium imaging during basal stage, and (C) time-lapse calcium image during LPS application. (D) The cells were subsequently stained with primary antibodies to the SGC cell marker, glutamine synthetase (red), the neuronal marker β -tubulin III (green), and nuclear marker DAPI (blue). Ca^{2+} levels were demonstrated by time-lapse microscopy of mixed TG neurones and non-neuronal cells in culture. The calcium image colour range (B and C) is from blue representing the baseline to the peak response value shown as red. *P. gingivalis* could induce Ca^{2+} elevation in the representative non-neuronal cells (arrow). This sample coverslip was subsequently studied for their characteristics by IHC. The responding non-neuronal cells could be identified as SGCs because of the GS-IR. Scale bar = 40 μm .

7.2.4 Non-neuronal cells respond to gingipains

7.2.4.1 Non-neuronal cells responded to arg-gingipain.

Stimulation of TG cultures with arginine-gingipain (Rgp) isolated from *P. gingivalis* resulted in more than 50% of TG neurones showing a calcium flux response (shown in section 6.2.3 [Chapter 6]). However, nearly all of the non-neuronal cells present also showed a calcium flux response to Rgp. Representative data are shown in Figure 7.6 which indicate that the amplitudes of the intracellular calcium influx of non-neuronal responses were lower compared to those of the neuronal calcium influx level. It was observed that the non-neuronal cells present were showed a response 40 - 60 s (median 50 s) after that of the neuronal cells.

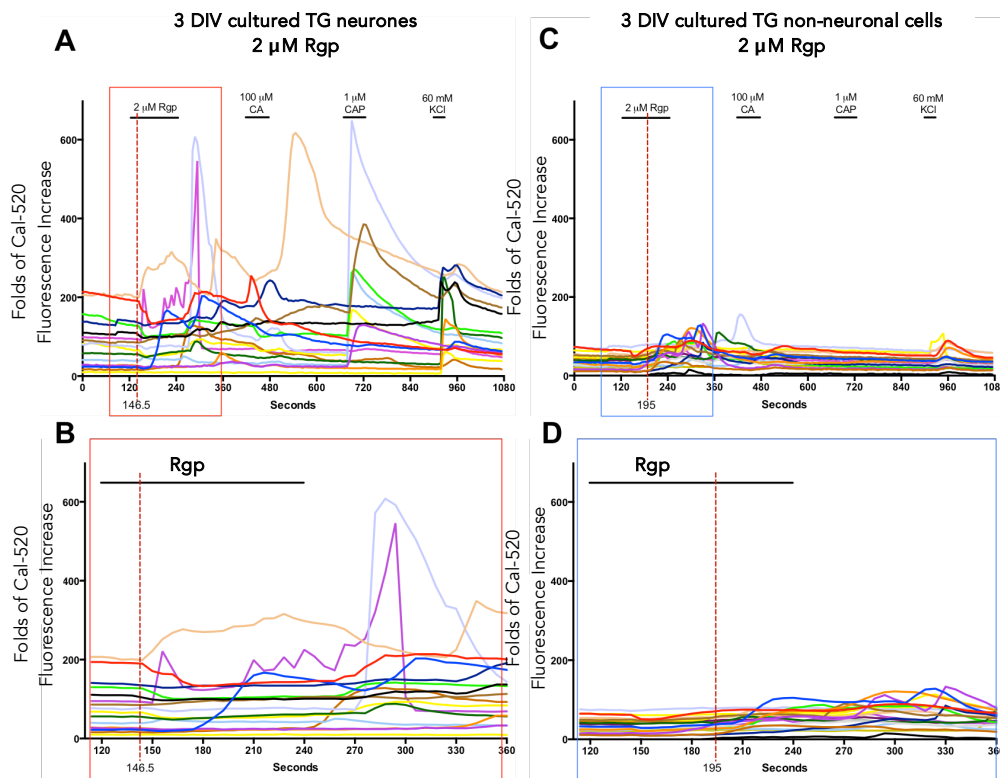


Figure 7.6 Graphs tracing the transient changes in calcium in individual cells over time following Rgp application to TG 3-day *in vitro* cultures

Calcium imaging of TG cells in response to *P. gingivalis* LPS exposure were recorded as described above in Fig 7.5. Time-lapse microscopy of TG neurones in panel A and TG non-neuronal cells are shown in panel C. The magnification data of the neurones (red squared box) and non-neuronal cells (blue squared box) are in figure B and D, respectively (at 110 – 360 s; LPS treatment). Data represent the fluorescent intensities of each cell over time as measured (458 nm_{ext} 520 nm_{emm}). After 2 min, cells were treated sequentially with *P. gingivalis* LPS for 2 min, CA, and CAP for 1 min to induce the release of Ca²⁺ with 2 min wash out intervals. The cultured cells were then treated with high KCl to distinguish healthy neurones from non-neuronal cells. The images and traces are representative data from 3 independent experiments. For TG neurones, the Ca²⁺ levels were started to increase at 26.5 s after Rgp application, while non-neuronal cells started to increase at 75 s after Rgp application.

7.2.5 Minocycline reduced the release of CGRP in response *P. gingivalis* and its constituents.

In the previous sections we demonstrated that intracellular calcium of non-neuronal cell activities elevated and NF- κ B translocated to the nucleus following exposure to *P. gingivalis* LPS and gingipain. We also found that TLR4 and PAR2 were expressed on non-neuronal cells, which could indicate that non-neuronal cells might also be activated in response to bacterial infection. However, it is also interesting to consider whether activated non-neuronal cells could regulate the neurones? In order to test this idea, we had to suppress the non-neuronal cell activities independent of neuronal activity and to do this we blocked glial cell activities with minocycline, which is a non-selective microglial inhibitor (Garrido-Mesa et al. 2013).

To begin, we assessed CGRP release from cells in response to *P. gingivalis* and its components (LPS and gingipains) by collecting supernatants of the TG cultures after exposure to *P. gingivalis*, in a similar way to that described in Chapter 4 and section 2.12, Chapter 2. The data showed that blockage of TG cultures with minocycline reduced the release of CGRP in response to the bacteria and their components. The release of CGRP was significantly increased on exposure to *P. gingivalis* LPS or gingipain (as similar as data shown in the Chapters 4 – 6), while it was reduced to less than unstimulated group when cultures were treated with 30 μ M minocycline ($p < 0.01$, Figure 7.7).

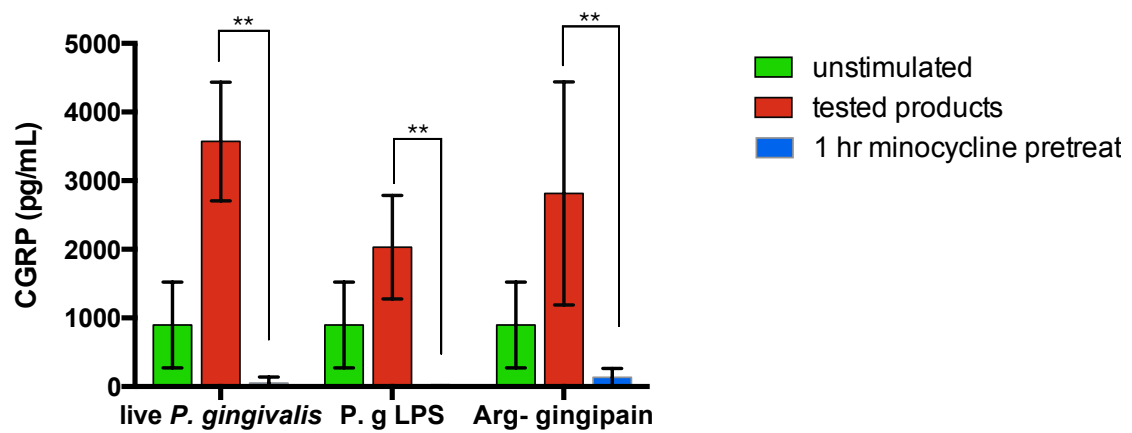


Figure 7.7 Effects of *P. gingivalis*, LPS and arg-gingipain in the presence and absence of minocycline.

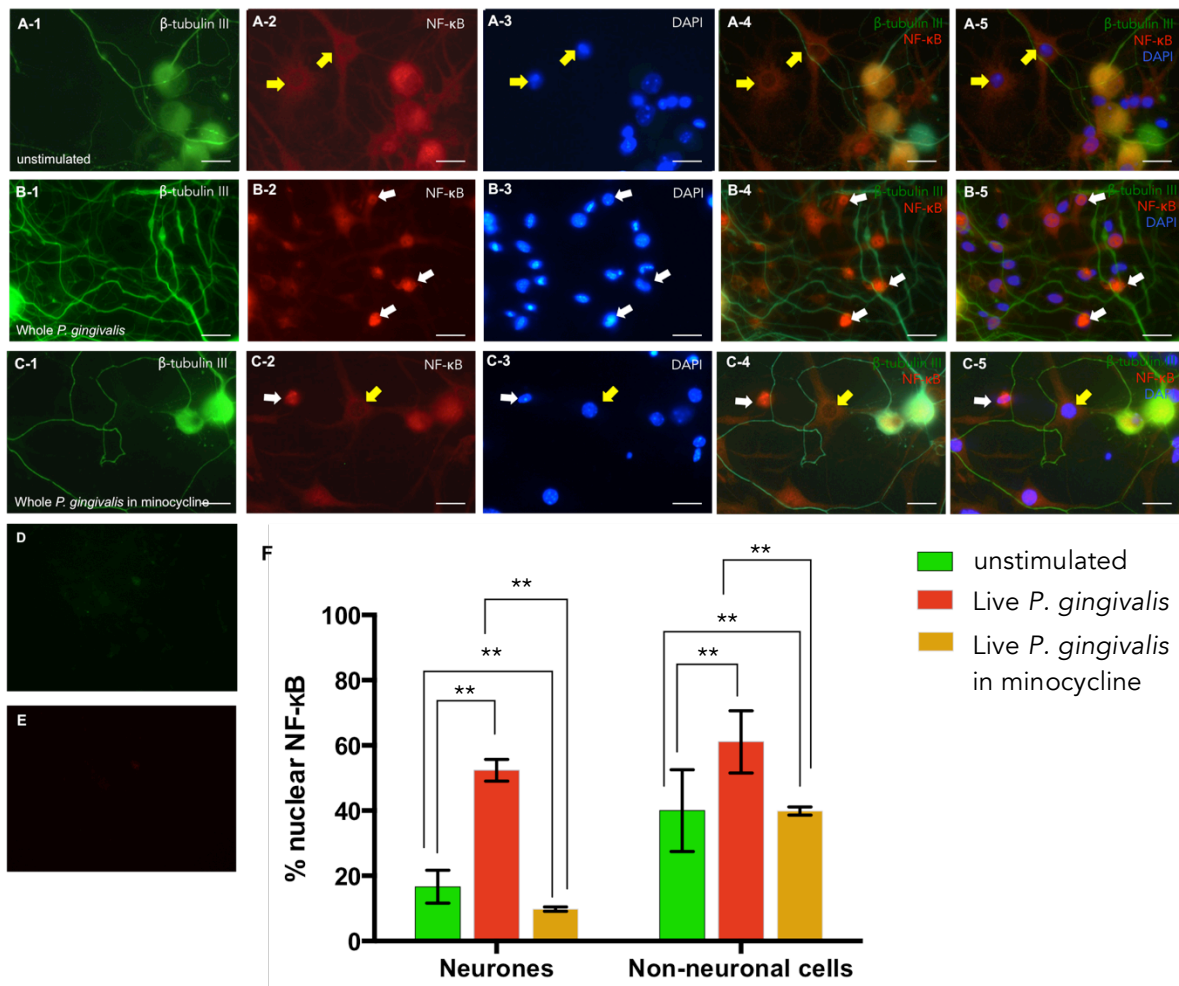
CGRP release experiment was measured by ELISA as described in section 2.12, [Chapter 2 Material and Methods]. Supernatants of TG cultures exposed to *P. gingivalis*, LPS and gingipains were collected for 15 minutes and subsequently secreted CGRP were quantified by ELISA. The release of CGRP was significantly increased by *P. gingivalis*, LPS or gingipain, but was significantly decreased by pretreatment of cultures with 30 μ M minocycline. Error bars are \pm SD, ** $p < 0.01$.

7.2.6 Minocycline inhibited the nuclear translocation of NF- κ B in both neurones and non-neuronal cells in response to *P. gingivalis*.

We showed earlier that exposure of TG neurones to *P. gingivalis* LPS resulted in NF- κ B nuclear translocations in both neurones and non-neuronal cells by *P. gingivalis* and the LPS. Here we sought to establish whether NF- κ B nuclear translocation triggered by *P. gingivalis* LPS was affected by pre-treatment with minocycline (see section 2.9, [Chapter 2 Material and Methods])

Representative images of NF- κ B nuclear translocations in cells of TG cultures and the quantitative data in response to *P. gingivalis* and its LPS are shown in Figure 7.8 and Figure 7.9, respectively. There was detectable translocation of NF- κ B from cytoplasm to nucleus in neurones in response to whole *P. gingivalis* cells from 19% to 53%. However, by pretreating with minocycline, the NF- κ B nuclear translocation was significantly reduced by more than 40% compared to the unstimulated group.

Figure 7.9 also showed an increase of neuronal NF- κ B nuclear translocation in response to *P. gingivalis* LPS from 19% to 63%. However, by pretreatment with minocycline, the NF- κ B nuclear translocations was much lower with only 5% of cells being positive and which was less than unstimulated cells. In a similar way NF- κ B nuclear translocations in non-neuronal cells increased from 40% to 68% by *P. gingivalis* LPS stimulation, but showed only 35% in the minocycline blocked group which was almost the same as the unstimulated group.



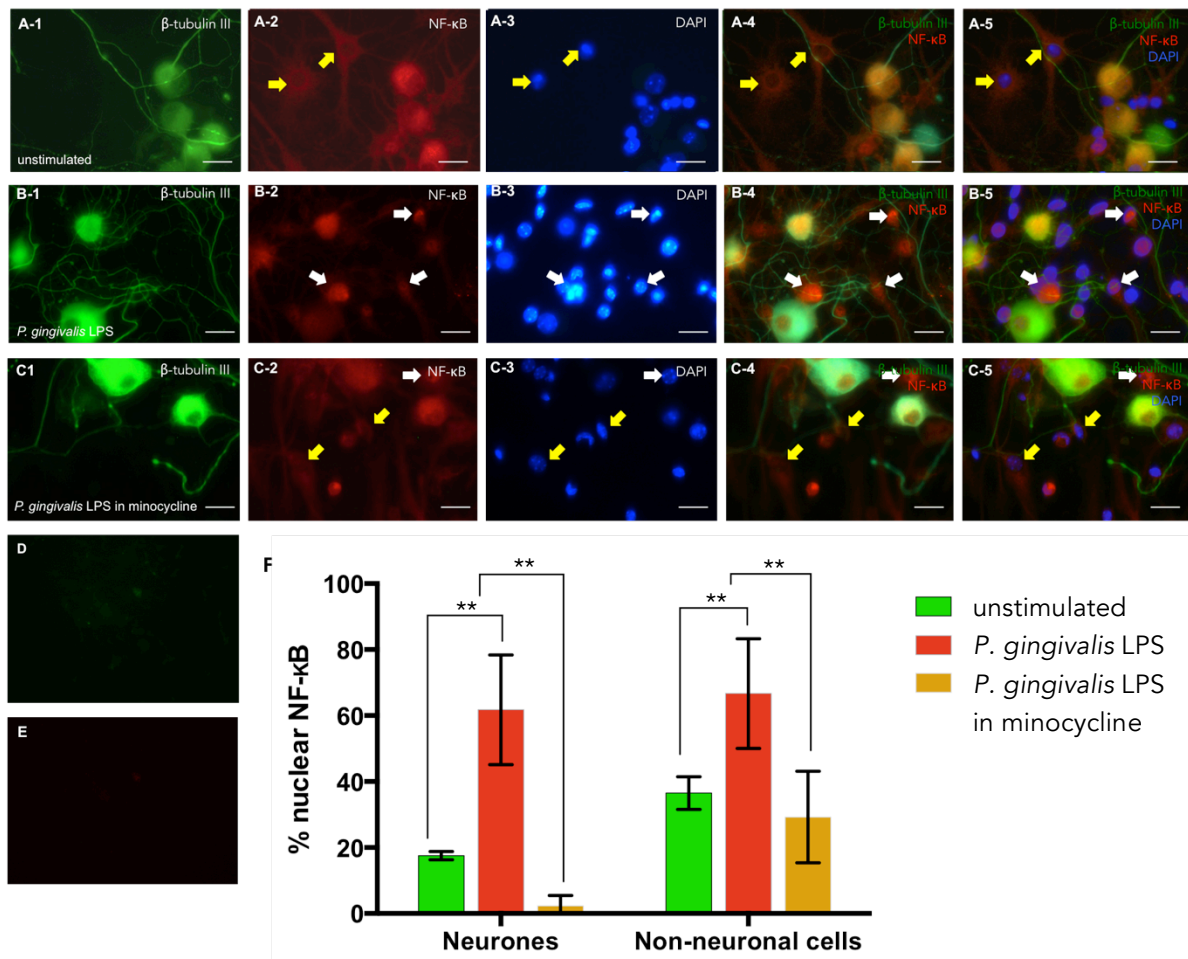


Figure 7.9 NF- κ B nuclear translocation of non-neuronal cells in TG cultures induced by *P. gingivalis* LPS and the effect of minocycline.

Representative images of TG cultures either left untreated (A-1 to A-5) or stimulated with *P. gingivalis* LPS (B-1 to B-5) and *P. gingivalis* LPS following 60 min minocycline treatment (C-1 to C-5). Cells were permeabilised with 0.1% Triton X-100 and subsequently stained with primary antibodies against anti-p65 NF- κ B and the corresponding secondary antibodies. The β -tubulin III, and p65 NF- κ B control samples showed no positive labelling in figure D and E, respectively. The β -tubulin III is shown in green (A1-C1) and p65 NF- κ B appears in red (A2-C2). Nuclear staining with DAPI (A3-C3) appears blue. The merged images of all three stains are shown in A4-B4. The translocation of NF- κ B was counted as positive when nuc/cyt ratio was > 1 (white arrows); examples of negative cells are shown by the yellow arrows. Data are the means from three independent experiments. Error bars are \pm SD, ** $p < 0.01$. Scale bars = 70 μ m.

7.3 Discussion

7.3.1 Overview

We demonstrated in Chapter 4 – 6 that neuronal activities could be stimulated by *P. gingivalis* and their components. The purpose of this chapter was to study the other cell types in our TG culture system, non-neuronal cells. The aim of this work was to gather knowledge about the morphological and functional characteristics of neuronal supporting cells and their interactions with the primary afferent neurones. Again, by studying their individual responses by calcium movements and expression of key markers in each cell by IHC, we could study non-neuronal cells in the TG cultures in response to *P. gingivalis* and their components independently of the neurones. We also observed the impact of non-neuronal cells on neuronal activity by using the glial cell activity inhibitor, minocycline.

Summary of the findings of non-neuronal cells

1. Characteristics of *in vitro* are different to inside sensory ganglia.
2. Non-neuronal cells responded to whole *P. gingivalis*
 - Demonstrated by NF- κ B nuclear translocation.
3. Non-neuronal cells responded to *P. gingivalis* LPS.
 - Demonstrated by calcium imaging i.e. non-neuronal cells showed the response to LPS but slightly more rapid, and the responding non-neuronal cells were GS-IR.
 - Showing by NF- κ B nuclear translocation.
4. Non-neuronal cells responded to gingipains.
 - Demonstrated by calcium imaging i.e. non-neuronal cells showed the showed delayed response to gingipain ompared with neurones.
5. Minocycline
 - CGRP in response *P. gingivalis* and its constituents could be prevented by minocycline.
 - NF- κ B nuclear translocation could be reduced by minocycline.

7.3.2 Characteristics of TG non-neuronal cell *in vitro*

As the first step of this thesis, we have characterised TG cultures in many aspects including morphological features of TG *in vitro*. In this chapter, we have shown that the non-neuronal cells show morphological changes following cell maintenance *in vitro*. In the first 48 hours in cultures, some glial cells still attach to neurones. This was consistent with the study of Ceruti et al. 2008 that demonstrated the clusters of neurones surrounded by SGCs in culture resembling the morphological and functional unit observed in intact ganglia within 2 days of maintenance in culture. However, SGCs could retain the physical relationships with sensory neurones, most of the non-neuronal cells population were seen to proliferate and split away from neurones in the later days of cultures.

TLR4 is thought to be primarily expressed by DRG neurones and not by SGCs. However, in the absence of neurones TLR4-IR is upregulated in the intracellular compartment of DRG glial cells (Tse et al. 2014). While, expression of TLR4 on Schwann cells in the PNS could play critical role in sensing tissue damage. Our data show weak immunofluorescence of TLR4 on non-neuronal cells could suggest that TLR4-IR cells could be either satellite glial cells or Schwann cells.

PAR2 is known to be widely expressed in the CNS in neurones and astrocytes (Bushell et al., 2006). PAR2 is also expressed throughout the PNS, but neuronal PAR2 has been the focus of many inflammatory pain studies (Vellani et al. 2010; Phillippe et al. 2011; Dai et al. 2004). To our knowledge, this is the first time that PAR2 in non-neuronal cells has been studied in the TG.

In the Chapter 5 and 6, we demonstrated expression of TLR4 and PAR2 on non-neuronal cells and this seems to correspond to their functional characteristics in their response to LPS and gingipains. The non-neuronal cell functional characteristics are discussed in the next sections.

7.3.3 Different patterns of neurone-glia interaction responded to LPS and gingipain exposures.

7.3.3.1 *P. gingivalis* LPS

Austin and Gila (2010) described glial cells surrounding neurones that could play immune-like responses. In PNS, glial are represented by Schwann and satellite cells that could play role to modulate neuronal activity. In this study, we demonstrated that TG neuronal supporting cells could be also activated by *P. gingivalis* LPS (e.g. through calcium influx and NF- κ B nuclear translocations). Moreover, Kushnir et al. (2011) demonstrated by calcium imaging that *E. coli* LPS caused increased sensitivity of TG SGCs to ATP by upregulation of P2X receptors. There is little data available for TG non-neuronal cells, and this study is the first time the functional characteristics of TG non-neuronal cells have been studied in relation to TLR4-signalling agonist.

In this study, we also showed the time course between neurones and non-neuronal cells in response to *P. gingivalis* LPS and demonstrated that TG non-neuronal cells respond approximately 20s before neurones. There is no previous evidence to describing responses of non-neuronal cell occurring prior to neuronal activity, this may indicate that the non-neuronal cells are more sensitive to LPS.

7.3.3.2 gingipains

In this study, we also demonstrated that TG neuronal supporting cells could be directly activated by gingipains by virtue of calcium flux responses and CGRP release. This is consistent with the finding of Fan et al. (2014) who showed that the receptor PAR2 was involved in the release of neuronal inflammatory mediators and brain-derived neurotrophic factor (BDNF) by microglia and that this could be partially blocked by PAR2 antagonists.

In Chapter 6, we demonstrated that non-neuronal PAR2-IR could also be reduced after 5 min gingipain exposures. However, there is very limited data on PAR2 in TG non-neuronal cells. This could suggest that non-neuronal PAR2 could be directly

cleaved or internalised by gingipains.

Interestingly, we observed a different pattern in the time course between neurones and non-neuronal cells in response to gingipains. Unlikely their responses to LPS which were more rapid than neuronal responses, TG non-neuronal cells respond to gingipains approximately 50s later than neurones. This could be explained by the study of Boesmans et al. (2013) that neurones typically show an immediate Ca^{2+} influx in response the stimuli, while glial cells only respond with delay. This indicates neurone-to-glia communication.

7.3.4 Mechanisms of minocycline

Recent reports have suggested that satellite glial cells could be a possible therapeutic target for the modulation of pain (Watkins and Maier 2002; Takeda et al. 2009). This is because neuronal excitability could be developed and maintained in the sensory neurone through the actions of the surrounding satellite glial cells acting as a functional unit (Kushnir et al. 2011; Hanani 2015; Poulsen et al. 2014; Takeda et al. 2009; Villa et al. 2010; Costa and Neto 2015)

Minocycline is known as microglial activation inhibitor, it is thought to act by specifically blocking p38 MAPK of SGC in the PNS (Ju et al 2009; Ikeda et al. 2012; Ledebøer et al. 2005). In *Ex vivo* studies, minocycline could prevent development of hypersensitivity following spinal nerve ligation (Raghavendra et al. 2003), supporting the idea that glial cells could be an effective therapeutic target for chronic pain or neuropathic pain.

In this study, pre-treatment of TG cultures with 30 μM minocycline apparently blocked the release of CGRP to less than that of the unstimulated culture. This would support the study of Seo-Yeon et al. (2012) which showed that minocycline inhibits spinal microglia release of cytokines and which subsequently blocks the LPS-induced hyperalgesia. This could be explained if minocycline inhibits not only the spinal p38 signalling cascade but also the release of pro-inflammatory mediators (Ikeda et al. 2012; Ledebøer et al. 2005).

The data has shown that reduction of glial NF- κ B nuclear translocations is coincident with neuronal NF- κ B nuclear translocations suggesting that the two events may be associated. Indeed, according to the study of Diya Zhang et al. (2008) minocycline can also suppress NF- κ B signalling of glial cells in response to nerve injury. However, we do not have any direct evidence to confirm that glial cell activities could induce the neuronal sensitisation.

There is no evidence that glial cells could directly release CGRP. However, there is evidence that other cell types, such as oral epithelial or fibroblasts (not present in our neuronal cell cultures) can release CGRP following noxious stimulations. Despite this, data from our culture system show that CGRP production was limited to neurones (section 3.4.2) and so it is unlikely that minocycline is affecting CGRP release by the non-neuronal cells present. We propose that therefore suppression of glial cell activity could in turn affect neuronal release of CGRP.

Other workers have suggested mechanisms by which minocycline could influence glial cells (Daehyun et al 2009; Ikeda et al. 2012; Ledebor et al. 2005) such as, through for example suppressive of p38 of microglial phosphorylated p-38 MAPK, and down regulation of microglial production of pro-inflammatory cytokines such as IL-1 β , TNF- α , and prostaglandin. Gong et al (2010) suggested that minocycline could change the behaviour of the dorsal root reflex in *in vivo* study. However, this could also be explained by the phenomenon being affected by glial cells.

7.3.5 Possible roles of non-neuronal cell in PNS

The physiology of non-neuronal cells in responding to *P. gingivalis* and its constituents were established by measuring the intercellular calcium wave, CGRP release (which has a paracrine function on neurones and non-neuronal cells) and translocation of a key regulator of inflammatory processes, NF- κ B. Taken together, the activation of neuronal supporting cells such as satellite glial cells and/or Schwann cells may be a crucial element in generation and maintenance of orofacial pain.

The possible roles for non-neuronal cells in this context will be discussed under the 2 headings: (1) paracrine function, and (2) NF- κ B roles.

7.3.5.1 Paracrine functions of neurone and non-neuronal cell

SGCs and neurones communicate through transmission of calcium wave (Scemes and Giaume 2006; Kristiansen and Edvinsson 2010) and so by calcium-imaging, we were able to demonstrate intracellular calcium mobilisation in both neurones and non-neuronal cells in response to *P. gingivalis* cells and LPS. It is possible that non-neuronal cells are also involved in mediating neuronal responses in response to *P. gingivalis*. Kushnir et al. (2011) showed that supporting glial cells do not always respond to the stimuli directly, but they show delayed responses that could be modulated *via* ATP signalling pathways.

Paracrine-like response to various products is another way in which neurones and SGCs could influence each other. There are some potential candidates to mediate the paracrine signalling such as neuropeptides, nitrous oxide, and ATP (Matsuka et al. 2001). Moreover, substance P released in response to orofacial inflammation was accompanied by the expression of NK1 receptors on surrounding non-neuronal cells. It is possible that cross-communication between neurones and non-neuronal cells can occur through many molecules including SP and CGRP.

These could possibly suggest that activations of non-neuronal cell to *P. gingivalis* LPS and Rgp maybe because the non-neuronal cells were modulated *via* ATP signalling from neurones. Alternatively they maybe being directly activated by the

agonists and in either it is possible that neuropeptides released from neurones could play an important role in paracrine signalling in inflammation. However, relying on calcium imaging as a means to detect which type of cell was driving a response for the other was difficult and could only be inferred from their speed of response to the agonist.

7.3.5.2 NF- κ B

NF- κ B is known as a key regulator of inflammatory processes in reactivate glial cells. It has been shown that this transcription factor regulates the expression of many genes such as inflammatory mediators (cytokines, chemokines, iNOS), CNS injury, and neuropathic pain (Fu et al. 2010; Ochoa-Cortes et al. 2010; Arias-salvatierra et al. 2011). In this study, we observed the nuclear translocation of NF- κ B in both neurones and non-neuronal cells in response to whole *P. gingivalis* cells and its LPS. We also showed that the suppression of glial activities by minocycline could lead to reduction of NF- κ B in both types of cells. It is possible then that reductions of glial NF- κ B nuclear translocation was associated with neuronal NF- κ B nuclear translocation and subsequent gene regulation. This could support the bidirectional neurone-glia signalling system to modulate peripheral sensitisation in the PNS.

7.3.6 Limitation and future prospects

A major limitation of the study was the characterisation of satellite glial cells and Schwann cells in the *in vitro* cultures. We have mentioned in the first section that the characteristics of glial cells could not be completely retained in the culture system especially when the cultures become older. Moreover, the 'reconnection' of neurones and the supporting cells may not be identical to that as it was *in vivo* and so may not ideally represent the functional unit neurones and satellite glial cells. However, it would be useful to study the calcium movement of neurones and non-neuronal cells in the presence of LPS and gingipain in minocycline pre-treatment.

7.3.7 Clinical relevance

This study has shown that TG non-neuronal cells could participate in cellular responses to *P. gingivalis* that are commensurate with pain generation. Therefore, the effect of minocycline to suppress glial activity might be a useful analgesic tool. However, as previously mentioned, minocycline could have adverse effects on other systems as well which operate through the MAPK pathways. However, this has yet to be confirmed, as there are currently very little data on minocycline and the PNS.

7.4 Conclusion

We demonstrated direct effects of bacteria on TG neurone in previous chapters but here we show that non-neuronal cells could also potentially contribute to pain responses to *P. gingivalis*. We showed by immunofluorescence that suppression of glial activities could reduce CGRP release from neurones and the nuclear translocation of NF- κ B in both neurones and non-neuronal cells. However, it was not possible to establish with certainty whether non-neuronal cells were responding primarily or secondarily to *P. gingivalis*. Nonetheless, these data could help shed light on the significant roles of supporting cells in pain generation.

Chapter 8

General discussion



8. General discussion

8.1 Rationale for study

The primary rationale for this study was to investigate whether there is any evidence for the generation of dental pain by direct action of bacteria on sensory neurones. The majority of symptomatic infected dental pulps (inflammatory pain) has been shown to contain at least one species of black-pigmented anaerobe (Jacinto et al. 2006; Galhotra et al. 2015; Rôças et al. 2002). Therefore, we selected *P. gingivalis* which has been extensively studied and which possesses a variety of virulence factors that could potentially impact on TG cells.

We sought to answer these 2 questions:

1. Does *P. gingivalis* LPS sensitise TG sensory neurones, if so, is the sensitisation acts through TLRs or TRPs?
2. Do *P. gingivalis* proteases sensitise TG sensory neurones, if so, is the sensitisation acts through PAR?

To investigate bacterial-neuronal interactions *in vitro*, a model of TG was required. Although having failed to purify TG neurones (Chapter 3), we could study individual cells in the cultures by calcium imaging and immunohistochemistry. Also, we looked for neuronal-specific peptide responses to bacterial challenge, namely CGRP release.

We began the study by establishing the direct effects of *P. gingivalis* on TG peripheral sensitisation (Chapter 4). We found that live *P. gingivalis* could activate neuronal responses and reasoned that this could be due to direct contact of surface located bacterial molecules, such as LPS and gingipains, and/or from soluble gingipains released into the medium. Such a notion could then involve three categories of cellular receptors: Transient receptor potential channels, Toll-like receptors, and Proteinase-activated receptors.

There is divergent evidence in the literature for neuronal sensitisation mediated by LPS. For example, LPS is thought to be a key initiator of innate immune responses on sensory neurones through interaction with TLR4 (Acosta and Davies 2008). LPS

can be a complement to TRPV1 activation, however, it seems that LPS does not directly activate TRPV1 itself (Ferraz et al. 2011). Therefore, activation of sensory neuronal responses by LPS has been thought to be linked to either LPS/TLR4 or LPS/TRPV1 interactions or a combination of the two. However, a more recent study by Meseguer et al. (2014) has demonstrated that TRPA1 could act as a molecular determinant for direct LPS effects.

Interestingly, each receptor apparently plays a role at different time points and varies with the experimental approach being employed. LPS exerted excitatory action via TRPA1 in only a few seconds, as demonstrated by calcium imaging (Meseguer et al. 2014). Another study showed that response to LPS involved TRPV1 as shown by CGRP release but this was over the much longer period of 15 minutes (Ferraz et al. 2011). The protein named 'nociceptin/orphanin FQ' which is a marker of peripheral inflammation was shown to be up-regulated by 30 mins of LPS exposure and this was thought to involve TLR4 (in Acosta and Davies (2008) study). These pieces of evidence imply that each of the receptors could play a role in the different events of pain physiology, and it seems to show divergent interpretation because of different methods and time scales employed in the experiments.

Another important virulence factor of *P. gingivalis*, is the group of gingipain proteases. Some are retained on the cell surface while some are released into the culture medium. However, irrespective of whether the gingipain is cell-surface located or released, contact of gingipains with neurones could be via the neuronal PAR2-dependent pathway (Joseph et al. 2000). Indeed we have demonstrated rapid movement of calcium and reduction of cellular PAR2 expression following exposure to gingipains. We have also shown CGRP release following a 15 min exposure to gingipains. This along with the reports that PAR2 activation can enhance activation of TRP channels (Vellani et al. 2010) leads to the suggestion that lys-gingipain may initially activate PAR2, which in turn activates the TRPA1/V1-mediated responses.

There are several other factors that are thought to modify the influence of bacterial virulence factors on the dental pulpal response, such as number of microbial cells present (Hahn and Liewehr 2007; Chiu et al. 2013), variation between strains (Marsh

et al. 1994; Enersen et al. 2013), and between different bacterial growth environments.

Using the TG neurone cultures, it was found that *P. gingivalis* could produce at least two potential molecules that directly interact with neuronal cellular receptors. The overall picture of our findings could therefore be summarised as shown in Figure 8.1.

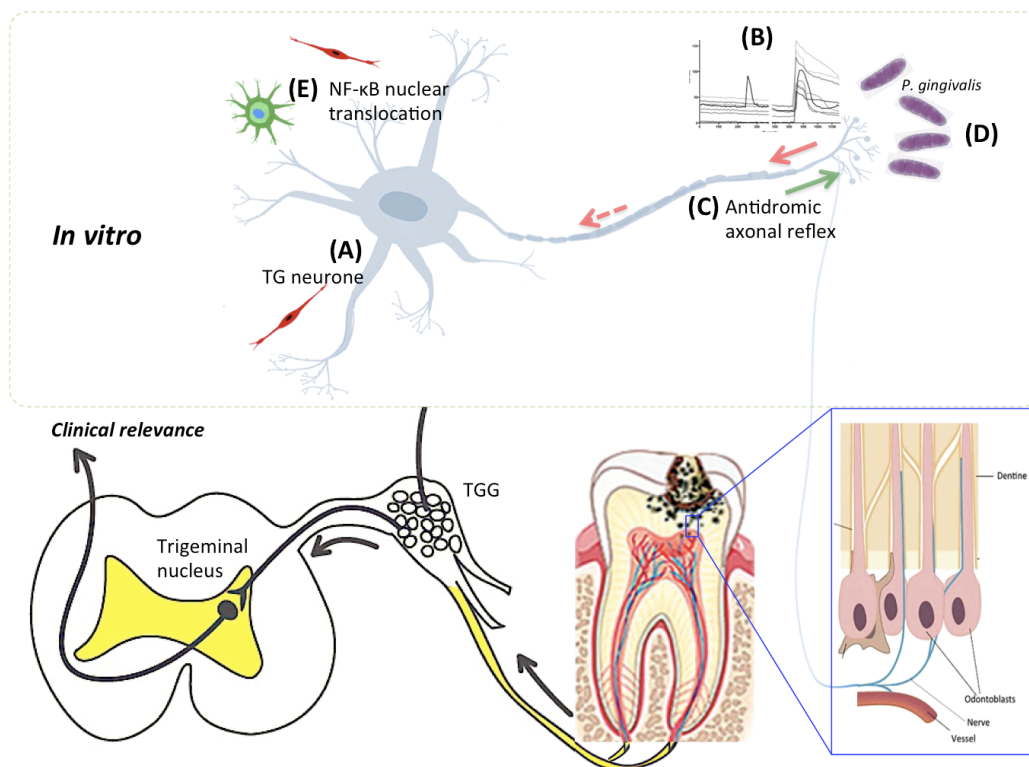


Figure 8.1 Schematic of TG sensitisation by *P. gingivalis* arising from this thesis.

The diagram shows TG neurones (A) that could be directly activated by *P. gingivalis* as demonstrated by transient calcium influx (B). This could activate antidromic axonal reflex (green arrow) of TG neurones to secrete CGRP (C). NF- κ B translocation could be demonstrated in both neurones and non-neuronal cells following *P. gingivalis* exposure (E). This model, obtained from *in vitro* data, could be a representative of the clinical manifestation of various levels of dental pulpal response to the direct interaction of bacteria with sensory neurones. The noxious signal could then be transmitted via afferent sensory nerve to the TG which contains TG neurones and their supporting cells. The signal would then be transmitted to be interpreted in the higher brain. The activation by *P. gingivalis* could change TG reflex that contributes to the mechanism of TG-mediated neurogenic inflammation, which can partly be explained by CGRP release.

8.2 The empirical findings and theoretical implication

We have demonstrated rapid responses of TG cultures to *P. gingivalis*. The evidence for this came from demonstration of intracellular Ca^{2+} signalling following exposure of the cultures to *P. gingivalis* and its components and the resultant release of CGRP. These findings are in accordance with the findings of Steinhoff et al. (2000) who showed changes in intracellular Ca^{2+} flux resulted in the release of neuropeptides from nerve endings. This neuropeptide release could in turn interact with other TG neurones and the endothelium to increase vascular permeability and cause vasodilation.

In this thesis, we also demonstrate TG neuronal changes over time, from the very rapid, within a few seconds, to changes that occur over 30 mins. We demonstrated that both neurones, and non-neuronal cells responded to *P. gingivalis*. The effects have been summarised within the respective chapters, however, this section will synthesise the empirical findings into three events namely; (1) synergistic effects of LPS and gingipains on neurones, (2) environmental cues that control neuronal changes, and (3) neuronal-glia interactions that could modulate pain generation.

8.2.1 Synergistic effects of LPS and gingipains

We hypothesise that two important virulence factors of *P. gingivalis*, LPS and gingipain proteases, together modulate neuronal signalling via PARs and TLRs. (Uehara et al. 2008). We showed that very high CGRP release occurs within 15 minutes of exposure to whole *P. gingivalis* cells and that this was greater than obtained from LPS or gingipains alone. This suggests that the two virulence factors could act in concert on the neurones, first through activation of neuronal PAR2 (gingipain) which is augmented by LPS acting via TRPA1 and TLR4 together (Figure 8.2).

However, it has been reported recently (Wilensky et al. 2015) that gingipains degrade CD14 (but not TLR2, and TLR4) on macrophages causing reduced response to the bacterial challenge. This effect was greater with lys-gingipain than with arg-

gingipain. This could show that the effects of LPS and gingipains could vary with different cell types.

Consequently, the first effect of *P. gingivalis* invasion into the pulp could involve secreted gingipains influencing host cells. Further effects may then occur when the neurones encounter bacterial cell surface LPS. Since the calcium-imaging demonstrated that both LPS and gingipain could begin to activate TG neurone in about 6 – 7s.

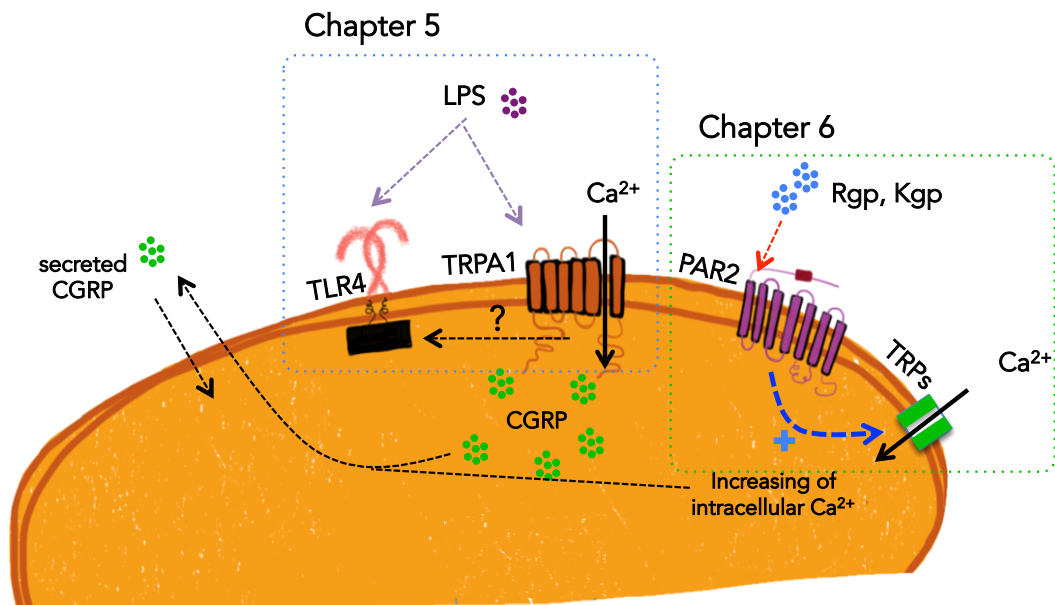


Figure 8.2 Summary of the response of a TG nerve ending following encounter with *P. gingivalis* LPS and gingipains.

The diagram shows a TG neurone being directly activated by *P. gingivalis* LPS and gingipains. The potential mechanisms have been discussed in Chapters 5, and 6. However, here the suggestion of the synergistic effects of LPS and gingipains is shown, i.e. that both virulence factors could trigger TG through the activation of neuronal PAR2 by gingipains and augmented by LPS via TRPA1 and TLR4. The effects of this synergistic mechanism could induce massive release of CGRP.

8.2.2 Environmental cues control neuronal changes

An additional hypothesis arising from the work reported here is that '*bacteria growing under different growth conditions can affect the neuronal pain pathway differently*'. This is based on our finding that *P. gingivalis* grown in high haemin conditions led to massive release of CGRP from TG cells compared with low haemin conditions or unstimulated neuronal cultures (Chapter 4) and the fact that bacterial culture conditions can modify the expression and composition of certain virulence factors of *P. gingivalis* (McKee et al. 1986). For example, growth of *P. gingivalis* in conditions of haemin-excess (such as when there is bleeding) were more virulent in a mouse skin infection model than when haemin was limited. Also, gingipain (trypsin-like) activity also increased in high haemin (Marsh et al. 1994). However, high levels of haemin also result in a modification to the lipid A structure of *P. gingivalis* (transitions from penta-acylated to tetra-acylated form) which could in turn reduce the TLR4 reactivity to *P. gingivalis* (Herath et al. 2013), although not change TLR2 responsiveness (Jain et al. 2013). Hence, under low-haemin conditions, the *P. gingivalis* adopts a more immune-evading, lower neuronal stimulating phenotype, while in a high-haemin environment, the bacterium is immunosuppressive and more highly 'neuroactive'.

In our study we show that *P. gingivalis* W50 grown in haemin-excess conditions stimulated higher levels of CGRP secretion from TG cultured cells compared with that released in response to haemin-limited *P. gingivalis* cells. This could be taken to indicate that high bacterial proteolytic activity (haemin excess) could stimulate high neuronal activity, irrespective of a possibly weaker TLR4-mediated response. Consequently, it is tempting to speculate that under certain environmental conditions TLR4 is not the pivotal neuronal receptor modulating CGRP release in response to Gram-negative challenge and under those conditions the effect of proteases may be more influential than LPS. Against such a hypothesis, however, is the report that gingipains are downregulated at elevated temperature, conditions that would be expected in the inflammatory microenvironment (Konkel and Tilly 2000), although temperature-induced changes in LPS results in (tetra-acylated to

penta-acylated transition) a more potent agonist of TLR4, than when growing at lower temperatures (Curtis et al. 2011). Clearly then, there are complex effects of the environmental conditions on the expression and relative make up of *P. gingivalis* virulence factors and we acknowledged that their interaction with nociceptor neurones could involve other receptors as well (e.g. TLR7) but we have demonstrated a more marked response of neurones to *P. gingivalis* grown under conditions that could well prevail in an inflamed dental pulp.

8.2.3 Neuronal-glia interaction

The culture system in this study was a mixture of neurones and non-neuronal cells although both were activated by *P. gingivalis* and its components. So far, however, we have only considered the possible direct interactions with neuronal receptors but it is suspected that the non-neuronal cells could release inflammatory mediators in response to *P. gingivalis*, which could also influence nociceptor responses. Evidence for this comes from our demonstration here of nuclear translocation of NF- κ B in both the neurones and non-neuronal cells in response to *P. gingivalis* (Chapters 4 and 5), which is crucial transcription factor for production of inflammatory cytokines. Furthermore, the glia activity blocking agent, minocycline, inhibited release of CGRP in response to *P. gingivalis* within the TG cultures. This possible 'glial to neurone' interaction could shed light on the importance of the neuronal supporting cells in peripheral sensitisation mechanisms during the inflammatory process.

8.3 Limitations of the study

8.3.1 Primary TG culture

In order to demonstrate the neuronal activity in response to bacterial components, we attempted to create conditions that simulated bacterial infection. In this study, we investigate neuronal-bacterial interaction by using primary cell culture from mouse TG which allowed us to study individual cell behaviour. However, we could not dissociate the neurones from their supporting cells nor could it be assumed that reconnections of nerve cells with their supporting cells would be identical to that within the original ganglia. This may affect their properties as neurone-SGC functional units such as the intracellular calcium wave, and the paracrine function.

However, primary trigeminal cell culture has been thought by others too to be a good representative model for the study of sensory afferent neurones, because cell morphology and cellular molecules are preserved (Poulsen et al. 2014; Passmore 2005). Indeed, we could demonstrate the presences of candidate receptors TPRA1, TRPV1, TLR4, and PAR2 (Chapters 5 and 6) and showed that the TG neurones were apparently healthy, as judged by their calcium flux response to high potassium.

In this thesis, three different techniques were employed to analyse neuronal activities following exposure to bacterial components: calcium-imaging, CGRP ELISA, and immunohistochemistry to analyse receptor proteins and NF- κ B location is crucial transcription factor to produce inflammatory cytokine. These are the advantages and limitations of each technique.

8.3.1.1 Calcium-imaging assay for TG *in vitro*

There are a number of reasons why calcium imaging was used for this study. It is considered a very useful technique to directly visualise and quantify intracellular calcium signals of any cell type. The regulation of calcium concentrations in neurones is fundamental in the control of neuronal excitability because its influx triggers exocytosis from neurotransmitter-containing synaptic vesicles. The nature of the response depends on the duration of the stimulus: brief exposure triggers a rapid, transient increase in $[Ca^{2+}]_i$, whereas continued exposure induces an influx of extracellular Ca^{2+} . The influx of extracellular Ca^{2+} and the refilling of internal stores of Ca^{2+} are both essential for oscillations in $[Ca^{2+}]_i$.

Limitations

- Monitoring TG activities in this study could only be made over relatively short periods because the perfusion system needed to flow LPS and gingipains while TG were recording which made the process expensive.
- The protocol was difficult to develop requiring optimisation of the exposure of the emitted light and taking account of the fact that the calcium dye could be photo-bleached.
- It is difficult to measurement calcium concentrations by a single wavelength dye such as Cal-520 AM. Because unlike ratiometric dyes that allow for correction of dye leakage from the cells, single wavelength dyes do not allow for this (Heusinkveld and Westerink 2011). Therefore, in this study, we could only quantify the response of cells by determining the peak of calcium flux, but we could not quantify the response in term of calcium concentration changes.
- Inclusion of serum in the system, in order to simulate the *in vivo* situation, was not possible because of the disturbance it caused to the osmolality of the buffer. Consequently, it is acknowledged that co-factors for cellular response, such as CD-14, were lacking.

8.3.1.2 CGRP release quantification by ELISA

Pros

We could demonstrate TG neuronal responses such as CGRP release following calcium movement, (Figure 8.2). Intracellular calcium signals are thought to induce neuropeptide stored in large dense-cored vesicles (LDCVs) to be released via a synaptic TRPV1 or TRPA1 mechanism. ELISA is a valuable technique to measure the level of secreted CGRP because of its high sensitivity, low cost of equipment, high throughput capacity and ability to quantify the peptide.

Cons

- Since this was not a commercial kit, it took time to develop and optimise the protocol.

8.3.1.3 Immunohistochemistry of primary TG cultures

Pros

Immunohistochemistry (IHC) was considered as a very reliable technique and indirect immunofluorescence is an established method used for studying primary neurone cultures in a number of other studies (Passmore 2005; Powell et al. 2014; Pazyra-Murphy and Segal 2008; Malin et al. 2007; Tucker et al. 2005). A major advantage of IHC is that it can be used to determine the presence and location of cellular proteins and receptors. In addition, using appropriate image analysis it was possible to quantify, or semi-quantify. Besides, we could demonstrate protein expression in response to the tested materials.

Cons

The quantitative analysis performed using image analysis is relatively subjective. This relies on the operator and their consistency in selecting the image threshold. However, there have been a number of studies that investigated the reliability and validity of this method and which have shown that quantitative analysis and observer reliability were excellent.

8.3.2 Bacterial aspects

8.3.2.1 Bacterial components

In this study, we challenged the TG cultures with 5×10^7 bacteria per millilitre which is equivalent to approximately 10^6 bacteria per 20 μl of average dental pulp volume. Even though, this bacteria load is relatively high, the range of bacteria load found in an infected pulp is from 1.68×10^4 to 3.3×10^7 (median 3×10^5) (Siqueira et al. 2007). From this, we could calculate the approximate amount of LPS that might be found in an infected dental pulp. Example calculation is shown in Figure 8.3.

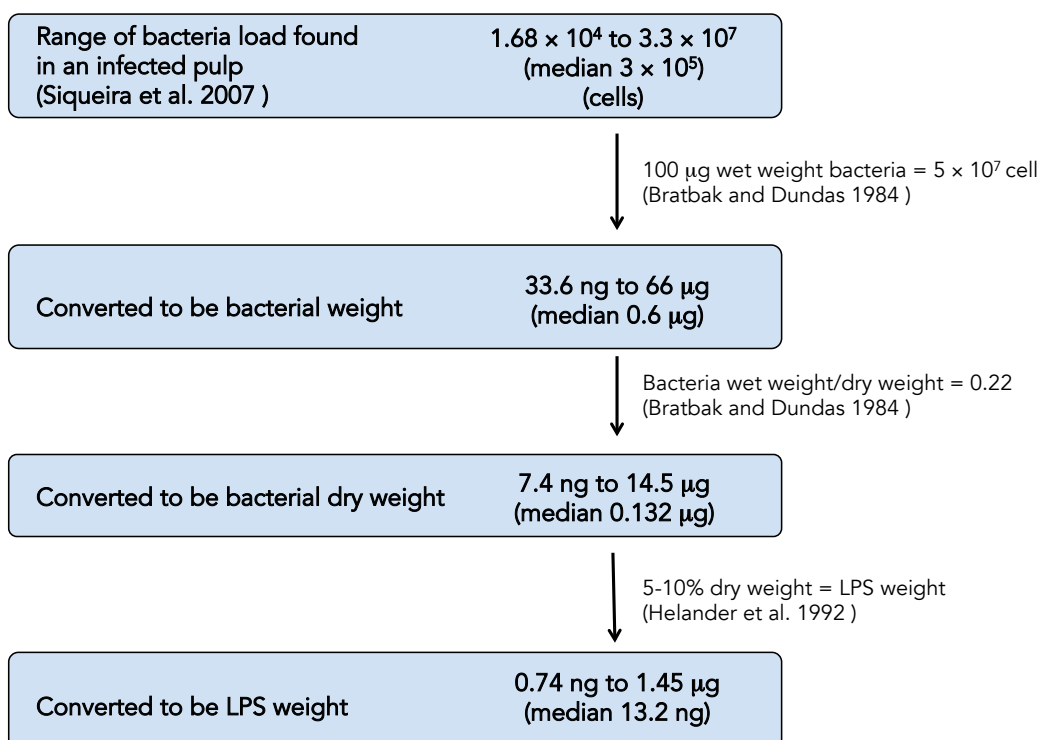


Figure 8.3 Approximate concentration of LPS calculated from average bacterial load found in infected teeth.

The average volume of dental pulp is 20 μl (Avery 1990), so to convert them to concentration for experimental design; it should range from 35 ng/mL to 72.5 $\mu\text{g/mL}$ (median 660 ng/mL). In addition, if we consider OMVs that carry some virulence factors of the parental bacterium, the concentration of LPS in this study (20 $\mu\text{g/mL}$ of *P. gingivalis* W50 LPS or 20 $\mu\text{g/mL}$ ultrapure *P. gingivalis* LPS) seems to be within the range found in dental infection.

However, similar estimates for the range of gingipain concentrations that might be expected were more difficult because unlike LPS, of the enzymes are both secreted and cell-associated. We therefore challenged the TG cultures with a wide range of protease concentrations. In this thesis, we also expressed the gingipain concentrations as a factor of trypsin enzymatic activity so as to enable a direct comparison with the results of the previous studies.

8.4 Future investigations arising from studies in this thesis

In order to build on the findings described here, the following studies are proposed.

Firstly, since non-neuronal cells seem to play an important role in activating sensory neurones. It would be useful to investigate whether calcium movement within neurones and non-neuronal cells following application of LPS and/or gingipain is affected by minocycline.

Secondly, *P. gingivalis* components seem to directly interact with TG neurones via TRPA1, TLR4, and PAR2. LPS activation could be inhibited by HC-030031, and CLI-095. However, gingipains seem to interact with PAR2 which can play a major role in regulating pain signalling mechanisms. TRPA1, TLR4 or PAR2 antagonists could be potential reagents to treat pain associated with bacterial infection. However, suitable trials and *in vivo* models would be needed to catalogue any adverse effects of the antagonists.

Thirdly, the functional unit of neurone and its supporting cells is the unit that should be studied to more fully understand neuronal responses. It would be interesting to study the neurone-SGC mechanism in an animal model, as it would preserve the morphology and characteristics of cells better compared to TG culture.

Finally, future experiments should focus on other potential virulence factors of Gram-negative bacteria such as fimbriae, heamagglutins, or the invasive property of *P. gingivalis*. We believe that the high level of CGRP release seen in response to whole *P. gingivalis* cells could be because the TG neurones were triggered by many mechanisms at once. It is also possible that whole *P. gingivalis* cells possess other potential virulence factors that could contribute to neuronal activity and which were not studied here.

Bibliography



- Acosta C, Davies A. Bacterial lipopolysaccharide regulates nociceptin expression in sensory neurons. *J Neurosci Res*. 2008; 86(5): 1077-1086.
- Aksoy E, Goldman M, Willems F. Protein kinase C epsilon: A new target to control inflammation and immune-mediated disorders. *Int J Biochem Cell Biol*. 2004; 36(2): 183-188.
- Al-Qutub MN, Braham PH, Karimi-Naser LM, Liu X, Genco CA., Darveau RP. Hemin dependent modulation of the lipid A structure of *Porphyromonas gingivalis* lipopolysaccharide. *Infect Immun*. 2006; 74(8): 4474-4485.
- Andersen PL, Ronald Doucette J, Nazarali AJ. A novel method of eliminating nonneuronal proliferating cells from cultures of mouse dorsal root ganglia. *Cell Mol Neurobiol*. 2003; 23(2): 205-210.
- Arias-salvatierra D, Silbergeld EK, Acosta-saavedra LC, Calderon-aranda ES. Role of nitric oxide produced by iNOS through NF- κ B pathway in migration of cerebellar granule neurons induced by Lipopolysaccharide. *Cell Signal*. 2011; 23(2): 425-435.
- Aruni W, Vanterpool E, Osbourne D, Roy F, Muthiah A, Dou Y, and Fletcher HM. Sialidase and sialoglycoproteases can modulate virulence in *Porphyromonas gingivalis*. *Infect Immun*. 2011; 79(7): 2779-2791.
- Assas BM, Miyan JA, Pennock JL. Cross-talk between neural and immune receptors provides a potential mechanism of homeostatic regulation in the gut mucosa. *Mucosal Immunol*. 2014; 7(6): 1283-1289.
- Austin PJ, Gila M-T. The neuro-immune balance in neuropathic pain: Involvement of inflammatory immune cells, immune-like glial cells and cytokines. *J Neuroimmunol*. 2010; 229(1-2): 26-50.
- Avery JK. Foreword. In: Inoki R, Kudo T, Olgart LM, eds. *Dynamic Aspects of Dental Pulp; Molecular Biology, Pharmacology and Pathophysiology* .Vol 11. 2nd ed. London: Chapman and Hall; 1990: XV.
- Barreto-Chang OL, Dolmetsch RE. Calcium imaging of cortical neurons using Fura-2AM. *J Vis Exp*. 2009; 23: 3-5.
- Basbaum AI, Bautista DM, Scherrer G, Julius D. Cellular and Molecular Mechanisms of Pain. *Cell*. 2009; 139(2): 267-284.
- Bratbak G, Dundas IAN. Bacterial Dry Matter Content and Biomass Estimations. 1984; 48(4):

755-757.

Belzer V, Shraer N, Hanani M. Phenotypic changes in satellite glial cells in cultured trigeminal ganglia. *Neuron Glia Biol.* 2010; 6(04): 237-243.

Bergenholtz G. Inflammatory response of the dental pulp to bacterial irritation. *J Endod.* 1981; 7(3): 100-104.

Bevan S, Winter J. Nerve growth factor (NGF) differentially regulates the chemosensitivity of adult rat cultured sensory neurons. *J Neurosci.* 1995; 15(7 Pt1): 4918-4926.

Bhave G, Hu HJ, Glauner KS, Zhu W, Wang H, Brasier DJ, Oxford GS, Gereau IV RW. Protein kinase C phosphorylation sensitizes but does not activate the capsaicin receptor transient receptor potential vanilloid 1 (TRPV1). *Proc Natl Acad Sci U S A.* 2003; 100(21): 12480-12485.

Biggs JE, Yates JM, Loescher AR, Clayton NM, Boissonade FM, Robinson PP. Changes in vanilloid receptor 1 (TRPV1) expression following lingual nerve injury. *Eur J Pain.* 2007; 11: 192-201

Boesmans W, Martens MA, Weltens N, Hao MH, Tack J, Cirillo C, Berghe PV. Imaging neuron-glia interactions in the enteric nervous system. *Front Cell Neurosci.* 2013; 7(October): 183.

Brogden KA, Guthmiller JM, Salzet M, Zasloff M. The nervous system and innate immunity: the neuropeptide connection. *Nat Immunol.* 2005; 6(6): 558-564.

Byers MR, Suzuki H, Maeda T. Dental neuroplasticity, neuro-pulpal interactions, and nerve regeneration. *Microsc Res Tech.* 2003; 60(5): 503-515.

Campos Lopes P, Barros M, Correia MJ. Gingipains as a virulence factor in the oral cavity. *Rev Port Estomatol Med Dent e Cir Maxilofac.* 2012; 53(4): 240-245.

Caviedes-Bucheli J, Lombana N, Azuero-Holguín MM, Muñoz HR. Quantification of neuropeptides (calcitonin gene-related peptide, substance P, neurokinin A, neuropeptide Y and vasoactive intestinal polypeptide) expressed in healthy and inflamed human dental pulp. *Int Endod J.* 2006; 39(5): 394-400.

Ceruti S, Fumagalli M, Villa G, Verderio C, Abbracchio MP. Purinoceptor-mediated calcium signaling in primary neuron-glia trigeminal cultures. *Cell Calcium.* 2008; 43(6): 576-590.

Chen Y, Yang C, Wang ZJ. Proteinase-activated receptor 2 sensitizes transient receptor

- potential vanilloid 1, transient receptor potential vanilloid 4, and transient receptor potential ankyrin 1 in paclitaxel-induced neuropathic pain. *Neuroscience*. 2011; 193: 440-451.
- Chung MK, Lee J, Duraes G, Ro JY. Lipopolysaccharide-induced Pulpitis Upregulates TRPV1 in Trigeminal Ganglia. *J Dent Res*. 2011; 90(9): 1103-1107.
- Coats SR, Pham TT, Bainbridge BW, Reife RA, Darveau RP. MD-2 mediates the ability of tetra-acylated and penta-acylated lipopolysaccharides to antagonize *Escherichia coli* lipopolysaccharide at the TLR4 signaling complex. *J Immunol*. 2005; 175(7): 4490-4498.
- Costa FAL, Neto FLM. Satellite glial cells in sensory ganglia: its role in pain. *Brazilian J Anesthesiol (English Ed)*. 2015; 65(1): 73-81.
- Chiu IM, Heesters BA, Ghasemlou N, Von Hehn CA, Zhao F, Tran J, Wainger B, Strominger A, Muralidharan S, Horswill AR, et al. Bacteria activate sensory neurons that modulate pain and inflammation. *Nature*. 2013; 501(7465): 52-57.
- Clavelou P, Pajot J, Dallel R, Raboisson P. Application of the formalin test to the study of orofacial pain in the rat. *Neurosci Lett*. 1989;103(3):349-53.
- Court N, Rose S, Bourigault ML, Front S, Martin OR, Dowling JK, et al. Mycobacterial PIMs inhibit host inflammatory responses through CD14-dependent and CD14-independent mechanisms. *PLoS One*. 2011;6(9).
- Curtis MA, Percival RS, Devine D, Darveau RP, Coats SR, Rangarajan M, Tarelli E, Marsh PD. Temperature-Dependent Modulation of *Porphyromonas gingivalis* Lipid A Structure and Interaction with the Innate Host Defenses. *Infect. Immun*. 2011; 79: 1187-1193.
- Dai Y, Moriyama T, Higashi T, Togashi K, Kobayashi K, Yamanaka H, Tominaga M, Noguchi K. Proteinase-activated receptor 2-mediated potentiation of transient receptor potential vanilloid subfamily 1 activity reveals a mechanism for proteinase-induced inflammatory pain. *J Neurosci*. 2004; 24(18): 4293-4299.
- Dai Y, Wang S, Tominaga M, Yamamoto S, Fukuoka T, Higashi T, Kobayashi K, Obata K, Yamanaka H, Noguchi K. Sensitization of TRPA1 by PAR2 contributes to the sensation of inflammatory pain. *J Clin Invest*. 2007; 117(7): 1979-1987.
- Darveau RP, Hancock RE. Procedure for isolation of bacterial lipopolysaccharides from both smooth and rough *Pseudomonas aeruginosa* Procedure for Isolation of Bacterial Lipopolysaccharides from Both Smooth and Rough *Pseudomonas aeruginosa* and

- Salmonella typhimurium strains. *J Bacteriol.* 1983; 155(2): 831-838.
- Dinh QT, Cryer A, Dinh S, Trevisani M, Georgiewa P, Chung F, Geppetti e, Werner Hept P, Klapp BF, Fischer A. Protease-activated receptor 2 expression in trigeminal neurons innervating the rat nasal mucosa. *Neuropeptides.* 2005; 39: 461-466.
- Diogenes A, Ferraz CCR, Akopian AN, Henry MA, Hargreaves KM. LPS sensitizes TRPV1 via activation of TLR4 in trigeminal sensory neurons. *J Dent Res.* 2011; 90(6): 759-764.
- Diogenes A, Patwardhan AM, Jeske N a, Ruparel NB, Goffin V, Akopian AN, et al. Prolactin modulates TRPV1 in female rat trigeminal sensory neurons. *J Neurosci.* 2006;26(31):8126–36.
- Diya Z, Lili C, Shenglai Li, Zhiyuan G, Jie Y. Lipopolysaccharide (LPS) of Porphyromonas gingivalis induces IL-1beta, TNF-alpha and IL-6 production by THP-1 cells in a way different from that of Escherichia coli LPS. *Innate Immun.* 2008; 14(2): 99-107.
- Dixon DR, Darveau RP. Lipopolysaccharide heterogeneity: innate host responses to bacterial modification of lipid a structure. *J Dent Res.* 2005; 84(7): 584-595.
- Donovan J, Grundy D. Endocannabinoid modulation of jejunal afferent responses to LPS. *Neurogastroenterol Motil [Internet].* 2012;24(10):956–e465.
- Eid SR, Crown ED, Moore EL, Moore EL, Liang HA, Choong K, Dima S, Henze DA, Kane SA, Urban MA. HC-030031, a TRPA1 selective antagonist, attenuates inflammatory- and neuropathy-induced mechanical hypersensitivity. *Mol Pain.* 2008; 4: 48.
- Eklind S, Mallard C, Leverin AL, Gilland E, Blomgren K, Mattsby-Baltzer I, Hagberg H. Bacterial endotoxin sensitizes the immature brain to hypoxic--ischaemic injury. *Eur J Neurosci.* 2001;13(6):1101-6.
- El Karim IA, Lamey PJ, Linden GJ, Awawdeh LA LF. Caries induced changes in the expression of pulpal neuropeptide Y. *Eur J Oral Sci.* 2006; 14: 133-137.
- Ellis A, Bennett DLH. Neuroinflammation and the generation of neuropathic pain. *Br J Anaesth.* 2013; 1: 26-37.
- Enersen M, Nakano K, Amano A. Porphyromonas gingivalis fimbriae. *J Oral Microbiol.* 2013;5(2013):1–10.
- Fan Y, Chen J, Ye J, Yan H, Cai Y. Proteinase-activated receptor 2 modulates corticotropin releasing hormone-induced brain-derived neurotrophic factor release from microglial

- cells. *Cell Biol Int*. 2014; 38(1): 92-96.
- Fehder WP, Ho WZ, Campbell DE, Tourtellotte WW, Michaels L, Cutilli JR, Uvaydova M, Douglas SD. Development and evaluation of a chromatographic procedure for partial purification of substance P with quantitation by an enzyme immunoassay. *Clin Diagn Lab Immunol*. 1998; 5(3): 303-307.
- Fehrenbacher JC, Sun XX, Locke EE, Henry MA, Hargreaves M. Capsaicin-evoked iCGRP release from human dental pulp: a model system for study of peripheral neuropeptide secretion in Normal Healthy Tissue. *Pain*. 2009; 144(3): 253-261.
- Fernandes ES, Fernandes MA., Keeble JE. The functions of TRPA1 and TRPV1: Moving away from sensory nerves. *Br J Pharmacol* . 2012; 166(2): 510-521.
- Ferraz CCR, Diogenes A, Henry M a, Hargreaves KM. LPS from *Prophyromonas gingivalis* Sensitizes Capsaicin-Sensitive Nociceptors. *J Endodontology*. 2011; 37(1): 45-48.
- Feske S, Skolnik EY, Prakriya M. Ion channels and transporters in lymphocyte function and immunity. *Nat Rev Immunol*. 2012; 12(7): 532-547.
- Fischer MJM, Mak SWY, McNaughton PA. Sensitisation of Nociceptors—What are Ion Channels Doing? *Open Pain J*. 2010; 3: 82-96.
- Fouad AF. The microbial challenge to pulp regeneration. *Adv Dent Res*. 2011; 23(3): 285-289.
- Frenkel D, Trudler D, Farfara D. Toll-like receptors expression and signaling in glia cells in neuro-amyloidogenic diseases: Towards future therapeutic application. *Mediators Inflamm*. 2010; 45: 345-356.
- Friso G, Kaiser L, Raud J, Wikström L. Differential protein expression in rat trigeminal ganglia during inflammation. *Proteomics*. 2001; 1(3): 397-408.
- Fu ES, Zhang YP, Sagen J, Candiotti KA, Morton PD, Liebl JD, Bethea JR, Brambilla R, Transgenic Inhibition of Glial NF-kappa B reduces pain behavior and Inflammation after Peripheral Nerve Injury. *Pain*. 2010; 148(3): 509-518.
- Galhotra V, Dey S, Priyank H, Paranjape T, Sharma N, Singh I. Prevalence of Microorganisms in Root Canals of Human Permanent Teeth with Symptomatic Nonvital Pulp and Chronic Periapical Lesions: A Microbiological Study. *J Int Oral Heal*. 2015; 7(September): 70-73.
- Garrido-Mesa N, Zarzuelo A, and Gálvez J. Minocycline: far beyond an antibiotic. *Br J*

- Pharmacol. 2013;169(2):337–352.
- Gee KR, Brown KA, Chen W-NU, Bishop-Stewart J, Gray D, Johnson I. Chemical and physiological characterization of fluo-4 Ca²⁺-indicator dyes. *Cell Calcium*. 2000; 27(2): 97-106.
- Geppetti P, Nassini R, Materazzi S, Benemei S. The concept of neurogenic inflammation. *BJU Int Suppl*. 2008; 101(SUPPL. 3): 2-6.
- Giacaman RA, Asrani AC, Ross KF, Herzberg MC. Cleavage of protease-activated receptors on an immortalized oral epithelial cell line by *Porphyromonas gingivalis* gingipains. *Microbiology*. 2009; 155(10): 3238-3246.
- Gibbs JL, Melnyk JL, Basbaum AI. Differential TRPV1 and TRPV2 channel expression in dental pulp. *J Dent Res*. 2011; 90(6): 765-770.
- Goethals S, Ydens E, Timmerman V, Janssens S. Toll-like receptor expression in the peripheral nerve. *Glia*. 2010; 58(14): 1701-1709.
- Gong K, Zou X, Fuchs PN, Lin Q. Minocycline inhibits neurogenic inflammation by blocking the effects of tumor necrosis factor- α . *Clin Exp Pharmacol Physiol*. 2015; 42(9): 940-949.
- Gonzalez-Martinez T, Perez-Piñera P, Díaz-Esnal B, Vega J a. S-100 proteins in the human peripheral nervous system. *Microsc Res Tech*. 2003;60(6):633–8.
- Gonzalez-Rey E, Ganea D, Delgado M. Neuropeptides: Keeping the balance between pathogen immunity and immune tolerance. *Curr Opin Pharmacol*. 2010; 10(4): 473-481.
- Grayson R, Douglas CW, Heath J, Rawlinson A, Evans GS. Activation of human matrix metalloproteinase 2 by gingival crevicular fluid and *Porphyromonas gingivalis*. *J Clin Periodontol*. 2003; 30(6): 542-50.
- Grimm S, Baeuerle PA. The inducible transcription factor NF- κ B: structure-function relationship of its protein subunits. *Biochem J*. 1993;290:297-308.
- Guillot X, Semerano L, Decker P, Falgarone G, Boissier MC. Pain and immunity. *Jt Bone Spine*. 2012; 79(3): 228-236.
- Guimaraes MZP, Jordt SE. TRPA1 : TRP Ion Channel Function in Sensory Transduction and Cellular Signaling Cascades. In: Liedtke WB HS, ed. TRP Ion Channel Function in Sensory Transduction and Cellular Signaling Cascades. CRC Press/Taylor & Francis; 2007.

- Hagains CE, Trevino L a., He J-W, Liu H, Peng YB. Contributions of dorsal root reflex and axonal reflex to formalin-induced inflammation. *Brain Res.* 2010; 1359: 90-97.
- Hahn CL, Liewehr FR. Relationships between Caries Bacteria, Host Responses, and Clinical Signs and Symptoms of Pulpitis. *J Endod.* 2007; 33(3): 213-219.
- Hajishengallis G, Lamont RJ. Breaking bad: Manipulation of the host response by *Porphyromonas gingivalis*. *Eur J Immunol.* 2014; 44(2): 328-338.
- Hanani M. Role of satellite glial cells in gastrointestinal pain. *Front Cell Neurosci.* 2015; 9(October): 1-10.
- Hansen CJ, Burnell KK, Brogden K a. Antimicrobial activity of Substance P and Neuropeptide Y against laboratory strains of bacteria and oral microorganisms. *J Neuroimmunol.* 2006; 177(1-2): 215-218.
- Hashimoto M, Asai Y, Ogawa T. Separation and structural analysis of lipoprotein in a lipopolysaccharide preparation from *Porphyromonas gingivalis*. *Int Immunol.* 2004; 16(10): 1431-1437.
- He Y, Baas PW. Growing and working with peripheral neurons. *Methods Cell Biol.* 2003; 71: 17-35.
- Hedge V. *Enterococcus faecalis*; clinical significance and treatment considerations. *Endodontology [Internet].* 2009;48–54.
- Henrich M, Buckler KJ. Acid-evoked Ca²⁺ signalling in rat sensory neurones: Effects of anoxia and aglycaemia. *Pflugers Arch Eur J Physiol.* 2009; 459(1): 159-181.
- Herath TDK, Darveau RP, Seneviratne CJ, Wang CY, Wang Y, Jin L. Tetra- and Penta-Acylated Lipid A Structures of *Porphyromonas gingivalis* LPS Differentially Activate TLR4-Mediated NF- κ B Signal Transduction Cascade and Immuno-Inflammatory Response in Human Gingival Fibroblasts. *PLoS One.* 2013; 8(3).
- Heusinkveld HJ, Westerink RH. Caveats and limitations of plate reader-based high-throughput kinetic measurements of intracellular calcium levels. *Toxicology and applied pharmacology.* 2011; 255: 1-8.
- Helander IM, Hurme R, Haikara A, Moran AP. Separation and characterization of two chemically distinct lipopolysaccharides in two *Pectinatus* species. *J Bacteriol.* 1992;174(10):3348–54.

- Helley MP, Abate W, Jackson SK, Bennett JH, Thompson SWN. The expression of Toll-like receptor 4, 7 and co-receptors in neurochemical sub-populations of rat trigeminal ganglion sensory neurons. *Neuroscience*. 2015;310:686–98.
- Henderson B, Poole S, Wilson M. Bacterial modulins: a novel class of virulence factors which cause host tissue pathology by inducing cytokine synthesis. *Microbiol Rev*. 1996;60(2):316–41.
- Higginns D, Banker G. Primary dissociated cell cultures. In: Stevens CF, ed. *Culturing Nerve Cells*. 2nd ed. The MIT Press; 1998: 37-78.
- Hirao K, Yumoto H, Takahashi K, Mukai K, Nakanishi T, Matsuo T. Roles of TLR2, TLR4, NOD2, and NOD1 in Pulp Fibroblasts. *J Dent Res*. 2009; 88(8): 762-767.
- Hiruma H, Saito a, Ichikawa T, Kiriyama Y, Hoka S, Kusakabe T, Kobayashi H, Kawakami T. Effects of substance P and calcitonin generelated peptide on axonal transport in isolated and cultured adult mouse dorsal root ganglion neurons. *Brain Res*. 2000; 883(2): 184-191.
- Hökfelt T, Broberger C, Xu ZQ, Sergejev V, Ubink R, Diez M. Neuropeptides—an overview. *Neuropharmacology*. 2000; 39(8): 1337-1356.
- Hong-Wei J, Zhang W, Ren B-P, Zeng J-F, Ling J-Q. Expression of toll like receptor 4 in normal human odontoblasts and dental pulp tissue. *J Endod*. 2006;32(8):747–51.
- Hou L, Li W, Wang X. Mechanism of interleukin-1 beta-induced calcitonin generelated peptide production from dorsal root ganglion neurons of neonatal rats. *J Neurosci Res*. 2003; 73(2): 188-197.
- Huang D, Li S, Dhaka A, Story GM, Cao Y. Expression of the transient receptor potential channels TRPV1, TRPA1 and TRPM8 in mouse trigeminal primary afferent neurons innervating the dura. *Mol Pain*. 2012; 8(1): 1.
- Huang J, Zhang X, McNaughton PA. Inflammatory pain: the cellular basis of heat hyperalgesia. *Curr Neuropharmacol*. 2006; 4(3): 197-206.
- Igwe OJ. c-Src kinase activation regulates preprotachykinin gene expression and substance P secretion in rat sensory ganglia. *Eur J Neurosci*. 2003;18(7):1719–30.
- Ikeda H, Kiritoshi T, Murase K. Contribution of microglia and astrocytes to the central sensitization, inflammatory and neuropathic pain in the juvenile rat. *Mol Pain*. 2012; 8(1): 43.

- Ingmer H, Brøndsted L. Proteases in bacterial pathogenesis. *Res Microbiol.* 2009; 160(9): 704-710.
- Jacinto RC, Gomes BPFA, Shah HN, Ferraz CC, Zaia AA, Souza-Filho FJ. Quantification of endotoxins in necrotic root canals from symptomatic and asymptomatic teeth. *J Med Microbiol.* 2005; 54(8): 777-783.
- Jacinto RC, Gomes BP, Shah HN, Ferraz CC, Zaia AA, Souza-Filho FJ. Incidence and antimicrobial susceptibility of *Porphyromonas gingivalis* isolated from mixed endodontic infections. *Int Endod J.* 2006; 39(1): 62-70.
- Jain S, Coats SR, Chang AM, Darveau RP. A novel class of lipoprotein lipase-sensitive molecules mediates Toll-like receptor 2 activation by *Porphyromonas gingivalis*. *Infect Immun.* 2013; 81: pp.1277–1286.
- Ji RR, Xu ZZ, Gao YJ. Emerging targets in neuroinflammation-driven chronic pain. *Nat Rev Drug Discov.* 2014; 13(7): 533-548.
- Jiang HW, Zhang W, Ren BP, Zeng JF, Ling JQ. Expression of Toll Like Receptor 4 in Normal Human Odontoblasts and Dental Pulp Tissue. *J Endod.* 2006; 32(8): 747-751.
- Jo D, Chapman CR, Light AR. Glial Mechanisms of Neuropathic Pain and Emerging Interventions. *Korean J Pain.* 2009; 22(1): 1-15.
- Joseph A-O, Nyama N D, Alex G, Hashim A, Evans HE, Rangarajan M, Slaney JM, Curtis MA. Generation of Lys-gingipain protease activity in *Porphyromonas gingivalis* W50 is independent of Arg-gingipain protease activities. *Microbiology.* 2000; 146(8): 1933-1940.
- Kansal RG, Nizet V, Jeng A, Chuang W-J, Kotb M. Selective modulation of superantigen-induced responses by streptococcal cysteine protease. *J Infect Dis.* 2003;187(3):398–407.
- Kayaoglu G, Ørstavik D. Virulence factors of *Enterococcus faecalis*: relationship to endodontic disease. *Crit Rev Oral Biol Med.* 2004; 15(5): 308-320.
- Kennell W, Holt SC. Comparative studies of the outer membranes of *Bacteroides gingivalis*, strains ATCC 33277, W50, W83, 381. *Oral Microbiol Immunol.* 1990; 5(3): 121-130.
- Kesavalu L, Ebersole JL, Machen RL, Holt SC. *Porphyromonas gingivalis*-virulence in mice: Induction of immunity to bacterial components. *Infect Immun.* 1992; 60(4): 1455-1464.

- Khemaleelakul S, Baumgartner JC, DDS, Pruksakorn S. Identification of bacteria in acute endodontic infections and their antimicrobial susceptibility. *Oral Surg Oral Med Oral Path Oral Radiol Endodontology* 2002; 94: 746-755.
- Kim YS, Son JY, Kim TH, Paik SK, Dai Y, Noguchi K, Ahn DK, Bae YC. Expression of transient receptor potential ankyrin 1 (TRPA1) in the rat trigeminal sensory afferents and spinal dorsal horn. *J Comp Neurol*. 2010; 518(5): 687-698.
- Kim S. Neurovascular interactions in the dental pulp in health and inflammation. *J Endod*. 1990; 16(2): 48-53.
- Kirikae T, Nitta T, Kirikae F, Suda Y, Kusumoto S, Qureshi N, Nakano M. Lipopolysaccharides (LPS) of oral black-pigmented bacteria induce tumor necrosis factor production by LPS-refractory C3H/HeJ macrophages in a way different from that of Salmonella LPS. *Infect Immun*. 1999; 67(4): 1736-1742.
- Klein DCG, Skjesol A, Kers-Rebel ED, Sherstova T, Bjørnar Sporsheim1, Kjartan W. Egeberg1, Bjørn T. Stokke4, Terje Espevik1† and Harald Husebye1. CD14, TLR4 and TRAM Show Different Trafficking Dynamics During LPS Stimulation. *Traffic*. 2015: 1-14.
- Konkel M.E., and Tilly K., Temperature-regulated expression of bacterial virulence genes. *Microbes and Infection*. 2000; 2(2): pp.157-166.
- Kristiansen KA, Edvinsson L. Neurogenic inflammation: a study of rat trigeminal ganglion. *J Headache Pain*. 2010; 11(6): 485-495.
- Krysko DV, Kaczmarek A, Krysko O, Woznicki J, Bogaert P, Cauwels A, Takahashi N, Magez S, Bachert C, Vandenabeele P. TLR-2 and TLR-9 are sensors of apoptosis in a mouse model of doxorubicin-induced acute inflammation. *Cell Death Differ*. 2011; 18(8): 1316-1325.
- Kunkler PE, Ballard CJ, Oxford GS, Harts J. TRPA1 receptors mediate environmental irritant-induced meningeal vasodilation. *Pain*. 2011; 152(1): 38-44.
- Kuris A, Xu C-B, Zhou MF, Tajti J, Uddman R, Edvinsson L. Enhanced expression of CGRP in rat trigeminal ganglion neurons during cell and organ culture. *Brain Res*. 2007; 1173: 6-13.
- Kushnir R, Cherkas PS, Hanani M. Peripheral inflammation upregulates P2X receptor expression in satellite glial cells of mouse trigeminal ganglia: A calcium imaging study. *Neuropharmacology*. 2011; 61(4): 739-746.

- Laarman A, Milder F, Van Strijp J, Rooijackers S. Complement inhibition by grampositive pathogens: Molecular mechanisms and therapeutic implications. *J Mol Med*. 2010; 88(2): 115-120.
- Lapointe TK, Altier C. The role of TRPA1 in visceral inflammation and pain. *Channels*. 2011; 5(6): 525-529.
- Ledeboer A, Sloane EM, Milligan ED, Frank MG, Mahony JH, Maier SF, Watkins LR. Minocycline attenuates mechanical allodynia and proinflammatory cytokine expression in rat models of pain facilitation. *Pain*. 2005; 115(1-2): 71-83.
- Lee CC, Avalos AM, Ploegh HL. Accessory molecules for Toll-like receptors and their function. *Nat Rev Immunol*. 2012; 12(3): 168-179.
- Leow-dyke S, Allen C, Denes A, Nilsson O, Maysami S, Bowie AG, Rothwell NJ, Pinteaux E. Neuronal toll-like receptor 4 signaling induces brain endothelial activation and neutrophil transmigration in vitro. *J Neuroinflammation*. 2012; 230(9): 1-11.
- Li D, Ren Y, Xu X, Zou X, Fang L, Lin Q. Sensitization of Primary Afferent Nociceptors Induced by Intradermal Capsaicin Involves the Peripheral Release of Calcitonin Gene-Related Peptide Driven by Dorsal Root Reflexes. *J Pain*. 2008; 9(12): 1155-1168.
- Liaunardy-jopeace A, Gay NJ. Molecular and cellular regulation of Toll-like receptor-4 activity induced by lipopolysaccharide ligands. *Front Immunol*. 2014; 5: 1-5.
- Lin J-J, Du Y, Cai W-K, Kuang R, Chang T, Zhang Z, Yang Y, Sun C, Li Z, Kuang F. Toll-like receptor 4 signaling in neurons of trigeminal ganglion contributes to nociception induced by acute pulpitis in rats. *Sci Rep*. 2015; 5(January): 12549.
- Lillesaar C, Arenas E, Hildebrand C, Fried K. Responses of rat trigeminal neurones to dental pulp cells or fibroblasts overexpressing neurotrophic factors in vitro. *Neuroscience*. 2003; 119(2): 443-451.
- Liu H-Y, Hong Y-F, Huang C-M, Chen C-Y, Huang T-N, Hsueh Y-P. TLR7 negatively regulates dendrite outgrowth through the Myd88-c-Fos-IL-6 pathway. *J Neurosci*. 2013; 33(28): 11479-11493.
- Liu R, Desta T, Raptis M, Darveau RP, T. Dana Graves. Porphyromonas gingivalis and E. coli Lipopolysaccharide Exhibit Different Systemic but Similar Local Induction of Inflammatory Markers. *J Periodontol*. 2008; 79(7): 1241-1247.
- Liu S, Liu YP, Yue DM, Liu GJ. Protease-activated receptor 2 in dorsal root ganglion

- contributes to peripheral sensitization of bone cancer pain. *Eur J pain*. 2014; 18: 326-337.
- Liu T, Gao YJ, Ji RR. Emerging role of toll-like receptors in the control of pain and itch. *Neurosci Bull*. 2012; 28(2): 131-144.
- Lourbakos A, Chinni C, Thompson P, Potempa J, Travis J, MacKie EJ, Pike, RN. Cleavage and activation of proteinase-activated receptor-2 on human neutrophils by gingipain-R from *Porphyromonas gingivalis*. *FEBS Lett* . 1998; 435(1): 45-48.
- Lourbakos A, Potempa J, Travis J, D'Andrea MR, Andrade-Gordon P, Santulli S, Mackie EJ, Pike RN. Arginine-Specific Protease from *Porphyromonas gingivalis* Activates Protease-Activated Receptors on Human Oral Epithelial Cells and Induces Interleukin-6 Secretion Arginine-Specific Protease from *Porphyromonas gingivalis* Activates Protease-Activated Recept. *Infect Immun*. 2001; 69(8): 5121-1530.
- Lundy FT, Linden GJ. Neuropeptides and Neurogenic Mechanisms in Oral and Periodontal Inflammation. *Crit Rev Oral Biol Med*. 2004; 15(2): 82-98.
- Ma W, Dumont Y, Vercauteren F, Quirion R. Lipopolysaccharide induces calcitonin gene-related peptide in the RAW264.7 macrophage cell line. *Immunology*. 2010; 130(3): 399-409.
- Macfarlane SR, Seatter MJ, Kanke T, Hunter GD, Plevin R. Proteinase-Activated Receptors. *Pharmacological Rev* . 2001; 53(2): 245-282.
- Malin SA, Davis BM, Molliver DC. Production of dissociated sensory neuron cultures and considerations for their use in studying neuronal function and plasticity. *Nat Protoc*. 2007; 2(1): 152-160.
- Maltos KLM, Menezes GB, Caliaro M V., Rocha O a., Santos JMM, Alves DLF, et al. Vascular and cellular responses to pro-inflammatory stimuli in rat dental pulp. *Arch Oral Biol*. 2004;49(6):443–50.
- Marsh PD, McDermid AS, McKee AS, Baskerville A. The effect of growth rate and haemin on the virulence and proteolytic activity of *Porphyromonas gingivalis* W50. *Microbiology-Sgm*. 1994; 140(4): 861-865.
- Martin VV., Beierlein M, Morgan JL, Rothe A, Gee KR. Novel fluo-4 analogs for fluorescent calcium measurements. *Cell Calcium*. 2004; 36(6): 509-514.
- Matsuka Y, Neubert JK, Maidment NT, Spigelman I. Concurrent release of ATP and

- substance P within guinea pig trigeminal ganglia in vivo. *Brain Res.* 2001; 915(2): 248-255.
- Matsushima R, Takahashi A, Nakaya Y, Maezawa H, Miki M, Nakamura Y, Ohgushi F, Yasuoka S. Human airway trypsin-like protease stimulates human bronchial fibroblast proliferation in a protease-activated receptor-2-dependent pathway. *Am J Physiol Lung Cell Mol Physiol.* 2006; 290(2): L385-L395.
- McKee AS, McDermid AS, Baskerville A, Dowsett AB, Ellwood DC, Marsh PD. Effect of hemin on the physiology and virulence of *Bacteroides gingivalis* W50. *Infect Immun.* 1986; 52(2): 349-355.
- Meng J, Wang J, Lawrence G, Dolly JO. Synaptobrevin I mediates exocytosis of CGRP from sensory neurons and inhibition by botulinum toxins reflects their antinociceptive potential. *J Cell Sci.* 2007; 120(Pt 16): 2864-2874.
- Meseguer V, Alpizar YA, Luis E, Tajada S, Denlinger B, Fajardo O, Manenschijn J, Fernandez-Pena C, Talavera A, Kichko T, et al. TRPA1 channels mediate acute neurogenic inflammation and pain produced by bacterial endotoxins. *Nat Commun.* 2014; 5: 3125.
- Metz-Boutigue MH, Kieffer a. E, Goumon Y, Aunis D. Innate immunity: Involvement of new neuropeptides. *Trends Microbiol.* 2003; 11(12): 585-592.
- Michaelson PL, Holland GR. Is pulpitis painful? *Int Endod J.* 2002; 35(10): 829-832.
- Mihara S, Shibamoto T. The role of flavor and fragrance chemicals in TRPA1 (transient receptor potential cation channel, member A1) activity associated with allergies. *Allergy Asthma Clin Immunol.* 2015; 11(1): 11.
- Miike S, McWilliam AS, Kita H. Trypsin induces activation and inflammatory mediator release from human eosinophils through protease-activated receptor-2. *J Immunol.* 2001; 167(11): 6615-6622.
- Miller RJ, Jung H, Bhangoo SK, Fletcher A. White. Cytokine and Chemokine Regulation of Sensory Neuron Function. *Handb Exp Pharmacol.* 2009; 194: 417-449.
- Minter LM, Turley DM, Das P, Shin HM, Joshi I, Lawlor RG, et al. Inhibitors of gamma-secretase block in vivo and in vitro T helper type 1 polarization by preventing Notch upregulation of Tbx21. *Nat Immunol.* 2005;6(7):680-8.
- Moretti S, Bellocchio S, Bonifazi P, Bozza S, Zelante T, Bistoni F, Romani L. The contribution

- of PARs to inflammation and immunity to fungi. *Mucosal Immunol.* 2008; 1(2): 156-168.
- Morgan CR, Rodd HD, Clayton N, Boissonade FM. Changes in proteinase-activated receptor 2 expression in the human tooth pulp in relation to caries and pain. *J Orofac Pain.* 2009; 23(3): 265-274.
- Morgan CR, Rodd HD, Clayton N, Davis JB. Vanilloid receptor 1 expression in human tooth pulp in relation to caries and pain. *J Orofac Pain.* 2005; 19(3): 248-260.
- Nadkarni MA, Simonian MR, Harty DWS, Zoellner H, Jacques N a., Hunter N. Lactobacilli are prominent in the initial stages of polymicrobial infection of dental pulp. *J Clin Microbiol.* 2010; 48(5): 1732-1740.
- Nakao R, Hasegawa H, Ochiai K, Takashiba S, Ainai A, Ohnishi M, Watanabe H, Senpuku H. Outer membrane vesicles of porphyromonas gingivalis elicit a mucosal immune response. *PLoS One.* 2011; 6(10).
- Nguyen MD1, Julien JP, Rivest S. Innate immunity: the missing link in neuroprotection and neurodegeneration? *Nat Rev Neurosci.* 2002;3(3):216-27.
- Nhu Q, Shirey K, Teijaro J, Farber DL, Netzel-Arnett S, Antalis M, Fasano A, Vogel SN. Novel signalling interactions between proteinase activated receptor 2 and Toll-like receptors in vitro and in vivo. *Mucosal Immunol.* 2010; 3(1): 29-39.
- Nisapakultorn K, Ross K, Herzberg M. Calprotectin expression in vitro by oral epithelial cells confers resistance to infection by Porphyromonas gingivalis. *Infect Immun.* 2001; 69(7): 4242-4247.
- Nishimura E, Eto A, Kato M, Hashizume S, Imai S, Nisizawa T, et al. Oral Streptococci Exhibit Diverse Susceptibility to Human-Defensin-2: Antimicrobial Effects of hBD-2 on Oral Streptococci. *Curr Microbiol.* 2004;48(2):85–7.
- Obata K, Noguchi K. MAPK activation in nociceptive neurons and pain hypersensitivity. *Life Sci.* 2004; 74(21): 2643-2653.
- Ochoa-Cortes F, Ramos-Lomas T, Miranda-Morales M, Spreadbury I, Ibeakanma C, Barajas-Lopez C, Vanner S. Bacterial cell products signal to mouse colonic nociceptive dorsal root ganglia neurons. *Am J Physiol Gastrointest Liver Physiol.* 2010; 299(3): G723-G732.
- Ogawa T, Uchida H. Differential induction of IL-1B and IL-6 production by the nontoxic lipid A from Porphyromonas gingivalis in comparison with synthetic Escherichia coli lipid A in human peripheral blood mononuclear cells. *Immunol Med Microbiol.* 1996;14:1–13.

- Okuda T, Sakamoto S, Deguchi T, Misawa S, Kashima K, Yoshihara T, Ikushima S, Hibi S, Imashuku S. Hemophagocytic syndrome associated with aggressive natural killer cell leukemia. *Am J Hematol.* 1991;38(4):321-3.
- Okun E, Griffioen KJ, Mark P, Mattson. Toll-like receptor signalling in Neural Plasticity and Disease. *Trends Neurosci.* 2011; 34(5): 269-281.
- Olsen I, Potempa J. Strategies for the inhibition of gingipains for the potential treatment of periodontitis and associated systemic diseases. *J Oral Microbiol.* 2014; 6: 1-12.
- Ossovskaya VS, Bunnett NW. Protease-activated receptors: contribution to physiology and disease. *Physiol Rev.* 2004; 84(2): 579-621.
- Pääkkönen V, Bleicher F, Carrouel F, Vuoristo JT, Salo T, Wappler I, Couble M, Magloire H, Peters H, Tjaderhane L. General expression profiles of human native odontoblasts and pulp-derived cultured odontoblast-like cells are similar but reveal differential neuropeptide expression levels. *Arch Oral Biol.* 2009; 54(1): 55-62.
- Pandit N, Changela R, Bali D, Tikoo P, Gugnani S. *Porphyromonas gingivalis* : Its virulence and vaccine. *J ICDRO.* 2015; 7(1): 51-58.
- Passmore GM. Dorsal root ganglion neurones in culture: A model system for identifying novel analgesic targets? *J Pharmacol Toxicol Methods.* 2005; 51(3 SPEC.ISS.): 201-208.
- Patwardhan AM, Berg KA, Akopian AN, Jeske NA, Gamper N, Clarke WP, and Hargreaves KM. Departments. Bradykinin-induced functional competence and trafficking of the delta-opioid receptor in trigeminal nociceptors. *J Neurosci.* 2005; 25(39): 8825-8832.
- Patwardhan AM, Diogenes A, Berg KA, Fehrenbacher JC, Clarke WP, Akopian AN, Hargreaves KM. PAR-2 agonists activate trigeminal nociceptors and induce functional competence in the delta opioid receptor. *Pain.* 2006; 125(1-2): 114-124.
- Pazyra-Murphy MF, Segal RA. Preparation and maintenance of dorsal root ganglia neurons in compartmented cultures. *J Vis Exp.* 2008; (20): 1-4.
- Phillippe M, Diamond AK, Sweet LM, Oppenheimer KH, Bradley DF. Expression of coagulation-related protein genes during LPS-induced preterm delivery in the pregnant mouse. *Reprod Sci.* 2011; 18(11): 1071-1079.
- Pike R, McGraw W, Potempa J, Travis J. Lysine- and arginine-specific proteinases from *Porphyromonas gingivalis*: Isolation, characterization, and evidence for the existence of complexes with hemagglutinins. *J Biol Chem.* 1994; 269(1): 406-411.

- Plutzer B. Comparative Efficacy Of Endodontic Medicaments Against *Enterococcus Faecalis* Biofilms. 2009.
- Popadiak K, Potempa J, Riesbeck K, Blom AM. Biphasic effect of gingipains from *Porphyromonas gingivalis* on the human complement system. *J Immunol.* 2007; 178(11): 7242-7250.
- Potempa J, Banbula a, Travis J. Role of bacterial proteinases in matrix destruction and modulation of host responses. *Periodontol.* 2000; 24: 153-192.
- Potempa M, Potempa J, Kantyka T, Nguyen KA, Wawrzonek K, Manandhar SP, et al. Interpain A, a cysteine proteinase from *Prevotella intermedia*, inhibits complement by degrading complement factor C3. *PLoS Pathog.* 2009;5(2).
- Poulsen JN, Larsen F, Duroux M, Gazerani P. Primary culture of trigeminal satellite glial cells: A cell-based platform to study morphology and function of peripheral glia. *Int J Physiol Pathophysiol Pharmacol.* 2014; 6(1): 1-12.
- Powell S, Vinod A, Lemons ML. Isolation and Culture of Dissociated Sensory Neurons From Chick Embryos. *J Vis Exp.* 2014; (91): 1-8.
- Press J. Expression of Protease-Activated Receptor 3 in the Trigeminal and Dorsal Root Ganglion of adult rats using immunohistochemistry. *Plymouth Student Sci.* 2013; 6(1): 72-85.
- Price TJ, Louria MD, Candelario-Soto D, Dussor GO, Jeske NA, Patwardhan AM, Diogenes A, Trott AA, Hargreaves KM, Flores CM. Treatment of trigeminal ganglion neurons in vitro with NGF, GDNF or BDNF: effects on neuronal survival, neurochemical properties and TRPV1-mediated neuropeptide secretion. *BMC Neurosci.* 2005; 6: 4.
- Qi J, Buzas K, Fan H, Cohen JI, Wang K, Mont E, Klinman D, Oppenheim JJ, Howard OMZ. Painful pathways induced by TLR stimulation of dorsal root ganglion neurons. *J Immunol.* 2011; 186(11): 6417-6426.
- Raghavendra V, Tanga F, DeLeo JA. Inhibition of microglial activation attenuates the development but not existing hypersensitivity in a rat model of neuropathy. *J Pharmacol Exp Ther.* 2003; 306(2): 624-630.
- Rang HP, Bevan S, Dray a. Chemical activation of nociceptive peripheral neurones. *Br Med Bull.* 1991;47(3):534-48.
- Rangarajan M, Aduse-Opoku J, Paramonov N, Hashim A, Bostanci N, Fraser OP, Tarelli E,

- Curtis MA. Identification of a second lipopolysaccharide in *Porphyromonas gingivalis* W50. *J Bacteriol.* 2008; 190(8): 2920-2932.
- Rangarajan M, Smith SJ, Curtis MA. Biochemical characterization of the arginine-specific proteases of *Porphyromonas gingivalis* W50 suggests a common precursor. *Biochem J.* 1997; 323 (Pt 3):701-709.
- Ren K, Dubner R. Neuron-glia crosstalk gets serious: role in pain hypersensitivity. *Curr Opin Anaesthesiol.* 2008; 21(5): 570-579.
- Rôças IN, Siqueira JF, Andrade AF, Uzeda M. Identification of Selected Putative Oral Pathogens in Primary Root Canal Infections Associated with Symptoms. *Anaerobe.* 2002; 8(4): 200-208.
- Rodd HD, Boissonade FM. Substance P in human tooth pulp in relation to caries and pain experience. *Eur J Oral Sci.* 2000; 108(6): 467-74.
- Roosterman D, Goerge T, Schneider SW, Bunnett NW, Mu I, Goerge T, et al. Neuronal Control of Skin Function: The Skin as a Neuroimmunoendocrine Organ. *Physiol Rev.* 2006;86:1309-79.
- Rothmeier AS, Ruf W. Protease-activated receptor 2 signaling in inflammation. *Semin Immunopathol.* 2012; 34(1): 133-149.
- Sanghavi TH, Shah N, Shah RR, Sanghavi A. Investigate the correlation between clinical sign and symptoms and the presence of *P. gingivalis*, *T. denticola*, and *T. forsythia* individually or as a "Red complex" by a multiplex PCR method. *J Conserv Dent.* 2014; Nov-Dec; 17(6): 555-560.
- Santoni G, Cardinali C, Morelli MB, Santoni M, Nabissi M, Amantini C. Danger- and pathogen-associated molecular patterns recognition by pattern-recognition receptors and ion channels of the transient receptor potential family triggers the inflammasome activation in immune cells and sensory neurons. *J Neuroinflammation.* 2015; 12(1): 21.
- Scemes E, Giaume C. Astrocyte calcium waves: What they are and what they do. *Glia.* 2006; 54(7): 716-725.
- Schwechheimer C, Kuehn MJ. Outer-membrane vesicles from Gram-negative bacteria: biogenesis and functions. *Nat Rev Microbiol.* 2015; 13(10): 605-619.
- Seo-Yeon Y, Patel D, Dougherty PM. Minocycline blocks lipopolysaccharide induced hyperalgesia by suppression of microglia but not astrocytes. *Neuroscience.* 2012;

27(221): 214-224.

Simonetti M, Giniatullin R, Fabbretti E. Mechanisms mediating the enhanced gene transcription of P2X3 receptor by calcitonin gene-related peptide in trigeminal sensory neurons. *J Biol Chem*. 2008; 283(27): 18742-18752.

Siqueira JF, Magalhaes KM, Rocas IN. Bacterial Reduction in Infected Root Canals Treated With 2.5% NaOCl as an Irrigant and Calcium Hydroxide/Camphorated Paramonochlorophenol Paste as an Intracanal Dressing. *J Endod*. 2007; 33(6): 667-672.

Smith ESJ, Lewin GR. Nociceptors: a phylogenetic view. *J Comp Physiol A*. 2009; 195(12): 1089-1106.

Sobota JA, Mohler WA, Cowan AE, Eipper BA, Mains RE. Dynamics of peptidergic secretory granule transport are regulated by neuronal stimulation. *BMC Neurosci*. 2010; 11: 32.

Socransky SS, Haffajee AD, Cugini MA, Smith C, Kent RL Jr. Microbial complexes in subgingival plaque. *J Clin Periodontol*. 1998; Feb; 25(2): 134-44.

Soh UJ, Dores MR, Chen B, Trejo J. Signal transduction by protease-activated receptors. *Br J Pharmacol*. 2010; 160(2): 191-203.

Stathopoulou PG, Benakanakere MR, Galicia JC, Kinane DF. The host cytokine response to *Porphyromonas gingivalis* is modified by gingipains. *Oral Microbiol Immunol*. 2009; 24(1): 11-17.

Steinhoff M, Buddenkotte J, Shpacovitch V, Rattenholl A, Moormann C, Vergnolle N, Luger TA, Hollenberg MD. Proteinase-activated receptors: Transducers of proteinase-mediated signaling in inflammation and immune response. *Endocr Rev*. 2005; 26(1): 1-43.

Steinman L. Elaborate interactions between the immune and nervous systems. *Nat Immunol*. 2004;5(6):575-81.

Stuart CH, Schwartz S A., Beeson TJ, Owatz CB. *Enterococcus faecalis*: Its role in root canal treatment failure and current concepts in retreatment. *J Endod*. 2006; 32(2): 93-98.

Suadicani SO, Cherkas PS, Zuckerman J, Smith DN, Spray C, Hanani M. Bidirectional calcium signalling between satellite glial cells and neurons in cultured mouse trigeminal ganglia. *Neuron*. 2010; 6(1): 43-51.

Sundqvist G, Johansson E, Sjögren U. Prevalence of black-pigmented bacteroides species in

- root canal infections. *J Endodont* 1989; 15: 13-19
- Tada M, Takeuchi A, Hashizume M, Kitamura K, Kano M. A highly sensitive fluorescent indicator dye for calcium imaging of neural activity in vitro and in vivo. *Eur J Neurosci*. 2014; 39(11): 1720-1728.
- Takada H, Kotani S. Structural Requirements of Lipid a for Endotoxicity and Other Biological Activities. *Crit Rev Microbiol*. 1989; 16(6): 477-523.
- Tajti J, Kuris A, Vécsei L, Xu C-B, Edvinsson L. Organ culture of the trigeminal ganglion induces enhanced expression of calcitonin gene-related peptide via activation of extracellular signal-regulated protein kinase 1/2. *Cephalalgia*. 2011; 31(1): 95-105.
- Takeda M, Takahashi M, Matsumoto S. Contribution of the activation of satellite glia in sensory ganglia to pathological pain. *Neurosci Biobehav Rev*. 2009; 33: 784-792.
- Tancharoen S, Sarker KP, Biswas KK, Biswas KK, Matsushita K, Tatsuyama S, Travis J, Potempa J, Torii M, Maruyama I. Neuropeptide Release from Dental Pulp Cells by RgpB via Proteinase-Activated Receptor-2 Signaling. *J Immunol*. 2005; 174: 5796-5804.
- Thakur M, Crow M, Richards N, Davey GI, Levine E, Kelleher JH, Agle CC, Denk F, Harridge SD, McMahan SB. Defining the nociceptor transcriptome. *Front Mol Neurosci*. 2014; 7(November): 1-11.
- Tóth DM, Szoke E, Bölcskei K, Kvell K, Bender B, Bosze Z, Szolcsanyi J, Sandor J. Nociception, neurogenic inflammation and thermoregulation in TRPV1 knockdown transgenic mice. *Cell Mol Life Sci*. 2011; 68(15): 2589-2601.
- Tsan F, Gao B. Endogenous ligands of Toll-like receptors. *J Leukoc Biol*. 2004; 76(3): 514-519.
- Tse K, Chow KBS, Leung WK, Wong YH, Wise H. Lipopolysaccharide differentially modulates expression of cytokines and cyclooxygenases in dorsal root ganglion cells via Toll-like receptor-4 dependent pathways. *Neuroscience*. 2014; 267: 241-251.
- Tucker BA., Rahimtula M, Mearow KM. A procedure for selecting and culturing subpopulations of neurons from rat dorsal root ganglia using magnetic beads. *Brain Res Protoc*. 2005; 16(1-3): 50-57.
- Uehara A, Imamura T, Potempa J, Travis J, Takada H. Gingipains from *Porphyromonas gingivalis* synergistically induce the production of proinflammatory cytokines through protease-activated receptors with Toll-like receptor and NOD1/2 ligands in human

- monocytic cells. *Cell Microbiol.* 2008; 10(5): 1181-1189.
- Uehara A, Muramoto K, Imamura T, Nakayama K, Potempa J, Travis J, Sugawara S, Takada H. Arginine-specific gingipains from *Porphyromonas gingivalis* stimulate production of hepatocyte growth factor (scatter factor) through protease-activated receptors in human gingival fibroblasts in culture. *J Immunol.* 2005; 175(9): 6076-6084.
- Ulevitch RJ, Tobias PS. Receptor-dependent mechanisms of cell stimulation by bacterial endotoxin. *Annu Rev Immunol.* 1995; 13: 437-457.
- Vaisid T, Kosower NS. Calpastatin is upregulated in non-immune neuronal cells via toll-like receptor 2 (TLR2) pathways by lipid-containing agonists. *Biochim Biophys Acta - Mol Cell Res.* 2013; 1833(10): 2369-2377.
- Vang H, Chung G, Kim HY, Park S, Jung SJ, Kim J, Oh SB. Neurochemical Properties of Dental Primary Afferent Neurons. *Exp Neurobiol.* 2012; 21(2): 68-74.
- Veith PD, Chen YY, Gorasia DG, Chen D, Glew MD, O'Brien-Simpson NM, Cecil JD, Holden JA, Reynolds EC. *Porphyromonas gingivalis* outer membrane vesicles exclusively contain outer membrane and periplasmic proteins and carry a cargo enriched with virulence factors. *J Proteome Res.* 2014; 13(5): 2420-2432.
- Veldhuis N a, Bunnett NW. Proteolytic regulation of TRP channels: Implications for pain and neurogenic inflammation. *Proc Aust Physiol Soc.* 2013; 44: 1-8.
- Vellani V, Kinsey AM, Prandini M, Hechtfisher SC, Reeh P, Magherini PC, Giacomoni C, McNaughton PA. Protease activated receptors 1 and 4 sensitize TRPV1 in nociceptive neurones. *Mol Pain.* 2010.
- Vergnolle N, Macnaughton WK, Al-Ani B, Saifeddine M, Wallace JL, Hollenberg MD. Proteinase-activated receptor 2 (PAR2)-activating peptides: identification of a receptor distinct from PAR2 that regulates intestinal transport. *Proc Natl Acad Sci U S A.* 1998; 95(13): 7766-7771.
- Vergnolle N, Wallace JL, Bunnett NW, Hollenberg MD. Protease-activated receptors in inflammation, neuronal signaling and pain. *Trends Pharmacol Sci.* 2001; 22(3): 146-152.
- Villa G, Fumagalli M, Verderio C, Abbracchio MP, Ceruti S. Expression and contribution of satellite glial cells purinoceptors to pain transmission in sensory ganglia: an update. *Neuron Glia Biol.* 2010; 6(1): 31-42.
- Wadachi R, Hargreaves KM. Trigeminal nociceptors express TLR-4 and CD14: a mechanism

- for pain due to infection. *J Dent Res*. 2006; 85(1): 49-53.
- Wang S, Dai Y, Kobayashi K, Zhu W, Kogure Y, Yamanaka H, Wan Y, Zhang W, Noguchi K. Potentiation of the P2X3 ATP receptor by PAR-2 in rat dorsal root ganglia neurons, through protein kinase-dependent mechanisms, contributes to inflammatory pain. *Eur J Neurosci*. 2012; 36(3): 2293-2301.
- Watanabe S, Kumazawa Y, Inoue J. Liposomal Lipopolysaccharide Initiates TRIF Dependent Signaling Pathway Independent of CD14. *PLoS One*. 2013; 8(4): 2-8.
- Watkins LR, Maier SF. Beyond neurons: evidence that immune and glial cells contribute to pathological pain states. *Physiol Rev*. 2002; 82(4): 981-1011.
- Watson, S. W., T. J. Novitsky, H. L. Quinby, and F. W. Valois. 1977. Determination of bacterial number and biomass in the marine environment. *Appl. Environ. Microbiol*. 33: 940-946.
- White JPM, Cibelli M, Fidalgo AR, Nagy I. Extracellular signal-regulated kinases in pain of peripheral origin. *Eur J Pharmacol*. 2011; 650(1): 8-17.
- Wilensky A, Tzach-Nahman R, Potempa J, Shapira L, Nussbaum G. *Porphyromonas gingivalis* gingipains selectively reduce CD14 expression, leading to macrophage hyporesponsiveness to bacterial infection. *J Innate Immun*. 2015; 7(2): 127-135.
- Wyatt S, Pinon LG, Ernfors P, Davies AM. Sympathetic neuron survival and TrkA expression in NT3-deficient mouse embryos. *EMBO Journal*. 1997; 16(11): 3115-3123.
- Yoon S, Patel D, Dougherty PM. Minocycline Blocks Lipopolysaccharide Induced Hyperalgesia By Suppression Of Microglia But Not. *Neuroscience*. 2012; 221: 214-224.
- Zhang Y, Wolfert MA, Boons GJ. Modulation of Innate Immune Responses with Synthetic Lipid A Derivatives. *JACS Artic*. 2007; (10): 5200-5216.
- Zhao P, Metcalf M, Bunnett NW. Biased signaling of protease-activated receptors. *Front Endocrinol (Lausanne)*. 2014; 5(MAY): 1-16.
- Zheng J. Molecular Mechanism of TRP Channels. *Compr Physiol*. 2013; 3(1): 221-242.